



Norwegian University of
Science and Technology

Flow Behaviour of Fine-Grained Soils

Matthew Adamson

Geotechnics and Geohazards

Submission date: June 2017

Supervisor: Vikas Kumar Thakur, IBM

Norwegian University of Science and Technology
Department of Civil and Environmental Engineering



Report Title: Flow Behaviour of Fine-Grained Soils	Date: 10.06.2017
	Number of pages (incl. appendices): 165
	Master Thesis X
Name: Matthew Adamson	
Professor in charge/supervisor: Professor Vikas Thakur	
Other external professional contacts/supervisors: N/A	

Abstract:

Estimating the propagation and run-out distances of a landslide is a crucial part of risk assessment and mitigation for infrastructure development in Norway. Computational and numerical models are currently being developed to model sensitive clay slides in three dimensions, and aim to integrate geotechnical design calculations with in-situ and laboratory geotechnical data. These models rely on accurate input parameters for analysis, and therefore, the flow behaviour of sensitive clays is required.

Previous studies have applied the Herschel-Bulkley rheological model to Canadian and Norwegian clays in order to investigate their flow behaviour.

Expanding on past studies, the flow behaviour of fine-grained soils has been investigated in this thesis. This was achieved by conducting quickness tests and viscometric experiments on quick clay samples from Tiller, Norway and Perniö, Finland. An artificial clayey silt and silt were also produced and tested. The Herschel-Bulkley model was used to find rheological parameters, which have been verified by past results.

A total of 35 quickness tests and 24 viscometer tests were performed on fine-grained soils. The viscometer tests were done using a coaxial cylinder viscometer in a temperature controlled environment of 7°C to replicate ground temperature. The salinity and liquidity index were varied for different samples to study how these parameters influence a soils rheological properties.

The fine-grained soils tested show a shear thinning behaviour when subjected to shear. The rheological parameters show a dependency on liquidity index and salinity. An increase in liquidity index gives a decrease in yield stress and consistency parameter, and an increase in Herschel-Bulkley exponent. An increase in salinity results in the opposite effect. Relationships between the Herschel-Bulkley parameters and liquidity index are found for the Tiller clay, Perniö clay as well as the clayey silt. These are valid for salinity in the range of 1.56-2.30 g/L and liquidity index 1.74-5.31. Quickness and viscometer tests can not be conducted accurately on silt soils due to high levels of segregation.

The set of Herschel-Bulkley parameters found for a flow curve are not unique. Large variations in the consistency parameter and Herschel-Bulkley exponent are observed for minor variations in yield stress. The Herschel-Bulkley yield stress, however, is a good approximation of a soil's real yield stress.

This study has verified proposed limits between quickness and remoulded shear strength. A number of relationships and limits between geotechnical and rheological parameters have also been proposed as a result of the laboratory test outcomes.

Keywords:

1. Sensitive clay
2. Quickness
3. Rheology
4. Herschel-Bulkley model

(sign.)

MASTER DEGREE THESIS

Spring 2017

for

Student: Matthew Adamson

Flow Behaviour of Fine-Grained Soils

BACKGROUND

The knowledge and understanding of the flow behaviour of sensitive clays is critical when predicting retrogressive landslides and assessing future infrastructure planning in Norway. Commercial tools such as GeoSuite Toolbox is being developed further to estimate the run-out of sensitive clay slides debris. This is done through the GeoFuture II project. The numerical models require the input of geotechnical and rheological behaviour parameters. The current knowledge of sensitive clays flow behaviour is from research on Canadian clays, with limited information on Norwegian clays. However, Canadian sensitive clays are generally more plastic and more over-consolidated than the Norwegian sensitive clays. The flow behaviour of fine-grained soils can be measured using liquidity index, remoulded shear strength, quickness and viscosity. Therefore, it is desirable to establish the parameters indicating flow behaviour for Norwegian clays and fine-grained soils, as well as establishing relationships between the parameters.

TASK

The aims of this master thesis are to investigate the flow behaviour of fine-grained soils by quickness and viscometric testing, and to verify that the Herschel-Bulkley rheology can suit Norwegian sensitive clays and the tested fine-grained soils.

Task Description:

- Literature review on the rheological and flow behaviour of sensitive clays
- Quickness testing and viscometric testing to investigate the flow behaviour of fine-grained soils (sensitive clays, clayey silts and silts)
- Establish a procedure for extraction and assessment of the test results
- Verify uniqueness of the quickness test
- Interpretation of fine-grained soil viscometric laboratory results with the Herschel-Bulkley rheology
- Determine relationships between the yield stress, consistency parameter and Hershel-Bulkley exponent and geotechnical properties
- Compare findings with Finnish and Canadian sensitive clays
- Determine a recommendation, if any, regarding the flow properties of fine-grained soils for Norwegian applications



VIKAS THAKUR

Professor

Geotechnical Division, NTNU

Preface

This master thesis is written as part of the Master of Science degree in Geotechnics and Geohazards at the Norwegian University of Science and Technology (NTNU) in Trondheim. The thesis has been written during the spring semester, 2017, between January and June.

The thesis contains a literary review of the significance and historical developments into research on the flow behaviour of quick clays and fine-grained soils. The testing program and experimental procedures are described, along with the results and critical discussion. This report is intended for readers with a basic knowledge in geotechnics and rheology.

The concept for this thesis was developed by my supervisor, Vikas Thakur, as a further study into the flow behaviour of fine-grained soils. This study forms the basis for using key geotechnical parameters in three dimensional computational modelling of landslides and run-outs. A portion of this study is also an extension of previous work done by Ragnhild Grue in 2015, by which viscometer tests were conducted on Norwegian quick clays.

Trondheim, 2017-06-10



Matthew Adamson

Acknowledgment

I am very thankful to my supervisor Vikas Thakur (NTNU) for his constant support, motivation and encouragement over the duration of the thesis. I am grateful for the tutelage and help provided by Helene A. Amundsen during the laboratory work, to Petter Fornes for his technical guidance, and to Erik Larsen at the Department of Geology and Mineral Resources Engineering at NTNU for providing the viscometer and support needed for the laboratory work.

I wish to acknowledge the efforts of Ragnhild Grue and Jean-Sebastian L'Heureux for their previous research on the thesis topic and for allowing me the use of their laboratory data and results.

I would also like to thank my fellow students for their discussions, feedback and assistance with laboratory testing. Finally I would like to thank my family and friends, both in Australia and Norway, for their continual support and reassurance.

M.A.

Summary and Conclusions

Estimating the propagation and run-out distances of a landslide is a crucial part of risk assessment and mitigation for infrastructure development in Norway. Computational and numerical models are currently being developed to model sensitive clay slides in three dimensions, and aim to integrate geotechnical design calculations with in-situ and laboratory geotechnical data. These models rely on accurate input parameters for analysis, and therefore, the flow behaviour of sensitive clays is required.

Previous studies have applied the Herschel-Bulkley rheological model to Canadian and Norwegian clays in order to investigate their flow behaviour. Expanding on past studies, the flow behaviour of fine-grained soils has been investigated in this thesis. This was achieved by conducting quickness tests and viscometric experiments on quick clay samples from Tiller, Norway and Perniö, Finland. An artificial clayey silt and silt were also produced and tested. The Herschel-Bulkley model was used to find rheological parameters, which have been verified by past results.

A total of 35 quickness tests and 24 viscometer tests were performed on fine-grained soils. The viscometer tests were done using a coaxial cylinder viscometer in a temperature controlled environment of 7°C to replicate ground temperature. The salinity and liquidity index were varied to study how these parameters influence a soils rheological properties.

The fine-grained soils tested show a shear thinning behaviour when subjected to shear. The rheological parameters show a dependency on liquidity index and salinity. An increase in liquidity index gives a decrease in yield stress and consistency parameter, and an increase in Herschel-Bulkley exponent. An increase in salinity results in the opposite effect. Relationships between the Herschel-Bulkley parameters and liquidity index are found for the Tiller clay, Perniö clay as well as the clayey silt. These are valid for salinity in the range of 1.56-2.30 g/L and liquidity index 1.74-5.31. Quickness and viscometer tests can not be conducted accurately on silt soils due to high levels of segregation.

The set of Herschel-Bulkley parameters found for a flow curve are not unique. Large variations in the consistency parameter and Herschel-Bulkley exponent are observed for minor variations in yield stress. The Herschel-Bulkley yield stress, however, is a good approximation of a soil's real yield stress .

This study has verified the proposed limits between quickness and remoulded shear strength. A number of relationships and limits between geotechnical and rheological parameters have also been proposed as a result of the laboratory test outcomes.

Contents

- Preface i
- Acknowledgment iii
- Summary and Conclusions v

- 1 Introduction 1**

 - 1.1 Background 1
 - 1.2 Objective 3
 - 1.3 Limitations and Approach 3
 - 1.4 Structure of the Thesis 4

- 2 Literature Study on the Characteristics and Flow Behaviour of Fine-Grained Soils 5**

 - 2.1 Fine-Grained Soils 5
 - 2.1.1 Sensitive Clays 5
 - 2.1.2 Quick Clays 6
 - 2.2 Geotechnical Parameters 7
 - 2.2.1 Water Content and Atterberg Limits 7
 - 2.2.2 Salinity 8
 - 2.2.3 Grain Size Distribution (or Molecular/Grain Structure) 9
 - 2.2.4 Clay Activity 10
 - 2.3 Flow Behaviour of Fine-grained Soils 10
 - 2.4 Remoulded Shear Strength 11
 - 2.5 Quickness 13
 - 2.6 Rheology 15
 - 2.6.1 Viscosity 15
 - 2.6.2 Herschel-Bulkley Model 18

2.6.3	Use of Viscometers For Geotechnical Applications	18
2.7	Previous Studies	21
2.7.1	Quickness Tests	21
2.7.2	Viscometer Tests on Canadian Clays	23
2.7.3	Viscometer Tests on Norwegian Clays	26
2.8	Expected Findings	28
3	Laboratory Experiments	29
3.1	Materials	29
3.1.1	Material Description	30
3.2	Test Program	30
3.3	Preparation of Samples	31
3.4	Index Tests	33
3.4.1	Water Content	33
3.4.2	Salinity	33
3.4.3	Atterberg Limits	33
3.4.4	Remoulded Shear Strength	33
3.5	Quickness Tests	34
3.5.1	Test Setup and Procedure	34
3.5.2	Sample Preparation	36
3.5.3	Basic Assumptions	36
3.6	Viscometer Tests	37
3.6.1	Instrument	37
3.6.2	Sample Preparation and Steady State Conditions	39
3.6.3	Dynamic Response Test	39
3.6.4	Basic Assumptions	40
4	Data Processing	41
4.1	Quickness Test Data	41
4.2	Viscometer Test Data	41

5	Results and Discussion	45
5.1	Index Tests	45
5.2	Quickness Tests	50
5.2.1	Effect of Remoulded Shear Strength on Quickness	51
5.2.2	Effect of Water Content on Quickness	52
5.2.3	Effect of Salinity on Quickness	55
5.2.4	Limitations and Experimental Problems	56
5.3	Viscometric Tests	58
5.3.1	Dynamic Response Test	58
5.3.2	Data Processing	59
5.3.3	Best Fit Herschel-Bulkley Parameters for all Tests	61
5.3.4	Observed Errors in Tests and Experimental Problems	62
5.4	Influence of Liquidity Index, Salinity and Temperature	66
5.4.1	Effect of Liquidity Index	66
5.4.2	Effect of Salinity	67
5.4.3	Effect of temperature	68
5.5	Herschel-Bulkley Parameters for Tiller Clay	70
5.5.1	Yield Stress	70
5.5.2	Consistency Parameter	72
5.5.3	Herschel-Bulkley Exponent	74
5.6	Herschel-Bulkley Parameters for Perniö Clay	76
5.6.1	Yield Stress	76
5.6.2	Consistency Parameter	78
5.6.3	Herschel-Bulkley Exponent	79
5.7	Herschel-Bulkley Parameters for Clayey Silt	81
5.7.1	Yield Stress	81
5.7.2	Consistency Parameter	83
5.7.3	Herschel-Bulkley Exponent	84
5.8	Comparing All Results	86
5.8.1	Yield Stress	86

5.8.2	Consistency Parameter and Herschel-Bulkley Exponent	87
5.9	Relationship Between Quickness and Flow Behaviour	90
5.10	Use of Data for Norwegian Applications	91
6	Conclusions and Further Work	93
6.1	Conclusions	93
6.2	Further Work	95
	Bibliography	96
A	Quickness Test Results	101
B	Previous Viscometer Test Results	107
C	Viscometer Test Data	111
D	Viscometer Test Results	133

List of Tables

- 2.1 Proposed relationships between I_L and c_{ur} 12
- 2.2 Soil characteristics for Norwegian sensitive clays 21
- 2.3 Rheological properties of Jonquiere clay 25
- 2.4 Soil characteristics for Norwegian and Canadian clays 26

- 3.1 Soil characteristics for tested clays 29
- 3.2 Material and sample descriptions 30
- 3.3 Rotation speed options for the Bohlin Visco 88 BV 38
- 3.4 Viscometer Cylinder Properties 38

- 5.1 Results from index testing on fine-grained soils 46
- 5.2 Results of quickness tests 50
- 5.3 Relationship between c_{ur} and Q 51
- 5.4 Relationship between c_{ur} and Q with constant power 52
- 5.5 Relationship between w/w_L and Q 54
- 5.6 Results for curve fitting for Tiller Clay 2 - $c_{ur} = 0.2\text{kPa}$ 60
- 5.7 Results for curve fitting for Tiller Clay 2 - $c_{ur} = 0.29\text{kPa}$ 61
- 5.8 Best fit Herschel-Bulkley parameters for all samples 62
- 5.9 Regression lines between τ_y and I_L for Tiller clays 71
- 5.10 Regression lines between K^* and I_L for Tiller clays 72
- 5.11 Regression lines between n and I_L for Tiller clays 74

- B.1 Best fit Herschel-Bulkley parameters for all samples 108

List of Figures

1.1	Retorgression flow slides in sensitive clays	1
1.2	Relationship between retrogression length, c_{ur} and S_t	2
2.1	Change in marine clay structure due to fresh water leaching	6
2.2	Physical properties and classification of the Atterberg Limits	8
2.3	Effect of salinity on S_t , c_{ur} and Atterberg limits	9
2.4	Comparison of soil grain sizes	10
2.5	Fall-cone test used to determine c_{ur}	11
2.6	Relationships between I_L and c_{ur} for Norwegian landslides	12
2.7	Typical quickness test slump profiles	14
2.8	Proposed range of c_{ur} and Q for assessing flow slide potential	15
2.9	Flow curves for different fluid types	16
2.10	Bingham approximation of yield stress	17
2.11	Schematic of viscometer apparatus	19
2.12	Velocity gradients in coaxial cylinder viscometers	20
2.13	Non-linear velocity gradient in a coaxial cylinder viscometer	20
2.14	Quickness test data on Norwegian sensitive clays	22
2.15	Quickness test slump observed for remoulded Byneset clay	22
2.16	Flow curves for viscometer results on Canadian clays	23
2.17	Relationships between I_L , $\tau_{y,B}$ and c_{ur} for Canadian clays	24
2.18	Effect of salinity on flow curves	24
2.19	Effect of salinity on viscosity	25
2.20	Yield stress for Canadian and Norwegian sensitive clays	27
3.1	Tiller block sample showing effect of storage time	31
3.2	Quickness test procedure	34
3.3	Quickness test laboratory set-up	35
3.4	Quickness slump progression with time	35
3.5	Bohlin Visco 88 BV viscometer instrument	37
3.6	Bohlin Visco 88 BV viscometer components	38
5.1	Relationships between w and c_{ur}	47
5.2	Relationships between w/w_L and c_{ur}	47

5.3	Relationships between S and c_{ur}	48
5.4	Grain size distributions for the fine-grained soils	49
5.5	Relationship between Q and c_{ur}	51
5.6	Relationship between Q and $c_{ur}^{-0.7}$	52
5.7	Relationships between Q , w and I_L	53
5.8	Relationship between Q and w/w_L	53
5.9	Relationship between Q , w/w_L and c_{ur}	54
5.10	Relationship between Q and S	55
5.11	Effect of salinity on quickness	56
5.12	Comparison of viscometer flow curves	58
5.13	T - N Curve type 1	59
5.14	T - N Curve type 2	60
5.15	Observed slippage between spindle and clay	63
5.16	Observed slippage between spindle and clay	64
5.17	Sensitivity of K^* and n	65
5.18	Effect of liquidity index on Herschel-Bulkley flow curves	66
5.19	Effect of salinity on Herschel-Bulkley flow curves	68
5.20	Effect of Temperature on Herschel-Bulkley flow curves	69
5.21	T - N viscometric curves for Tiller clays	70
5.22	Tiller clays: τ_y versus I_L	71
5.23	Tiller clays: τ_y versus S	72
5.24	Tiller clays: K^* versus I_L	73
5.25	Tiller clays: K^* versus S	73
5.26	Tiller clays: n versus I_L	74
5.27	Tiller clays: n versus S	75
5.28	T - N viscometric curves for Perniö Clay	76
5.29	Perniö Clay: τ_y versus I_L	77
5.30	Perniö Clay: τ_y versus S	77
5.31	Perniö Clay: K^* versus I_L	78
5.32	Perniö Clay: K^* versus S	79
5.33	Perniö Clay: n versus I_L	79
5.34	Perniö Clay: n versus S	80
5.35	T - N viscometric curves for Clayey Silt	81
5.36	Clayey Silt: τ_y versus I_L	82
5.37	Clayey Silt: τ_y versus S	82
5.38	Clayey Silt: K^* versus I_L	83
5.39	Clayey Silt: K^* versus S	84
5.40	Clayey Silt: n versus I_L	84
5.41	Clayey Silt: n versus S	85

5.42	Herschel-Bulkley τ_y versus I_L (categorized by site)	86
5.43	Herschel-Bulkley K^* versus I_L (categorized by site)	87
5.44	Herschel-Bulkley n versus I_L (categorized by site)	88
5.45	Herschel-Bulkley K^* versus n (categorized by site)	89
5.46	Relationship between Q and τ_y	90
A.1	Quickness test results - Tiller Clay 1	102
A.2	Quickness test results - Tiller Clay 2	103
A.3	Quickness test results - Finland clay	104
A.4	Quickness test results - Clayey Silt	105
A.5	Quickness test results - Silt	106
B.1	Herschel-Bulkley flow curves from Grue results	108
B.2	Past results for τ_y with varying I_L	109
B.3	Past results for K^* with varying I_L	109
B.4	Past results for n with varying I_L	110
B.5	Past results for K^* against n	110
C.1	Viscometer Test Data: Tiller Clay 1 $c_{ur} < 0.1\text{kPa}$	112
C.2	Viscometer Test Data: Tiller Clay 1 $c_{ur} = 0.1\text{kPa}$	113
C.3	Viscometer Test Data: Tiller Clay 1 $c_{ur} = 0.2\text{kPa}$	114
C.4	Viscometer Test Data: Tiller Clay 1 $c_{ur} = 0.29\text{kPa}$	115
C.5	Viscometer Test Data: Tiller Clay 2 $c_{ur} < 0.1\text{kPa}$	116
C.6	Viscometer Test Data: Tiller Clay 2 $c_{ur} = 0.1\text{kPa}$	117
C.7	Viscometer Test Data: Tiller Clay 2 $c_{ur} = 0.2\text{kPa}$	118
C.8	Viscometer Test Data: Tiller Clay 2 $c_{ur} = 0.29\text{kPa}$	119
C.9	Viscometer Test Data: Perniö Clay $c_{ur} < 0.1\text{kPa}$ 1	120
C.10	Viscometer Test Data: Perniö Clay $c_{ur} < 0.1\text{kPa}$ 2	121
C.11	Viscometer Test Data: Perniö Clay $c_{ur} = 0.1\text{kPa}$	122
C.12	Viscometer Test Data: Perniö Clay $c_{ur} = 0.2\text{kPa}$	123
C.13	Viscometer Test Data: Perniö Clay $c_{ur} = 0.29\text{kPa}$	124
C.14	Viscometer Test Data: Perniö Clay $c_{ur} = 0.39\text{kPa}$	125
C.15	Viscometer Test Data: Perniö Clay $c_{ur} = 0.5\text{kPa}$	126
C.16	Viscometer Test Data: Perniö Clay $c_{ur} = 0.7\text{kPa}$	127
C.17	Viscometer Test Data: Clayey Silt $c_{ur} < 0.1\text{kPa}$	128
C.18	Viscometer Test Data: Clayey Silt $c_{ur} = 0.1\text{kPa}$	129
C.19	Viscometer Test Data: Clayey Silt $c_{ur} = 0.2\text{kPa}$	130
C.20	Viscometer Test Data: Clayey Silt $c_{ur} = 0.29\text{kPa}$	131
D.1	Viscometer Test Results: Tiller Clay 1 $c_{ur} < 0.1\text{kPa}$	134

D.2	Viscometer Test Results: Tiller Clay 1 $c_{ur} = 0.1\text{kPa}$	134
D.3	Viscometer Test Results: Tiller Clay 1 $c_{ur} = 0.2\text{kPa}$	135
D.4	Viscometer Test Results: Tiller Clay 1 $c_{ur} = 0.29\text{kPa}$	135
D.5	Viscometer Test Results: Tiller Clay 2 $c_{ur} < 0.1\text{kPa}$	136
D.6	Viscometer Test Results: Tiller Clay 2 $c_{ur} = 0.1\text{kPa}$	136
D.7	Viscometer Test Results: Tiller Clay 2 $c_{ur} = 0.2\text{kPa}$	137
D.8	Viscometer Test Results: Tiller Clay 2 $c_{ur} = 0.29\text{kPa}$	137
D.9	Viscometer Test Results: Perniö Clay $c_{ur} < 0.1\text{kPa}$ 1	138
D.10	Viscometer Test Results: Perniö Clay $c_{ur} < 0.1\text{kPa}$ 2	138
D.11	Viscometer Test Results: Perniö Clay $c_{ur} = 0.1\text{kPa}$	139
D.12	Viscometer Test Results: Perniö Clay $c_{ur} = 0.2\text{kPa}$	139
D.13	Viscometer Test Results: Perniö Clay $c_{ur} = 0.29\text{kPa}$	140
D.14	Viscometer Test Results: Perniö Clay $c_{ur} = 0.39\text{kPa}$	140
D.15	Viscometer Test Results: Perniö Clay $c_{ur} = 0.5\text{kPa}$	141
D.16	Viscometer Test Results: Perniö Clay $c_{ur} = 0.7\text{kPa}$	141
D.17	Viscometer Test Results: Clayey Silt $c_{ur} < 0.1\text{kPa}$	142
D.18	Viscometer Test Results: Clayey Silt $c_{ur} = 0.1\text{kPa}$	142
D.19	Viscometer Test Results: Clayey Silt $c_{ur} = 0.2\text{kPa}$	143
D.20	Viscometer Test Results: Clayey Silt $c_{ur} = 0.29\text{kPa}$	143

Acronyms

Latin symbols

A_c	Activity of clay (-)
CF	Clay fraction (%)
c_u	Undrained shear strength (kPa)
c_{ur}	Remoulded shear strength (kPa)
D_f	Base dimension of quickness test (mm)
G_{HB}	Flow resistance (mNm)
h	Height of inner cylinder radius (mm)
H_{HB}	Viscosity factor (mNm s ^J)
H_f	Final height of quickness test (mm)
H_o	Initial height of quickness test (mm)
I_L	Liquidity index (%)
I_P	Plasticity index (-)
J	Flow index factor for Herschel-Bulkley fluid (-)
K	Consistency coefficient (Pa s ⁿ)
K^*	Normalized consistency coefficient (Pa)
L	Retrogression distance (m)
m_c	Mass of clay grains < 2 μ m (g)
m_w	Mass of water (g)
m_s	Total mass of dry soil grains (g)
N	Rotation speed (rps)
n	Herschel-Bulkley exponent
r	Radial cylindrical coordinate (mm)
Q	Quickness value (%)
R^2	Coefficient of determination (-)
R_i	Inner cylindrical radius (mm)
R_o	Outer cylindrical radius (mm)
S	Salinity (g/L)
S_t	Sensitivity (-)

T	Torque (mNm)
w	Water content (%)
w_L	Liquid limit (%)
w_P	Plastic limit (%)

Greek symbols

$\dot{\gamma}$	Shear rate (s^{-1})
$\dot{\gamma}_{ref}$	Reference shear rate (1 s^{-1})
τ	Shear stress (Pa)
τ_y	Herschel-Bulkley yield stress (Pa)
$\tau_{y,B}$	Bingham yield stress (Pa)
ω	Angular velocity at radius r (rad/s)
Ω_i	Angular velocity of the inner cylinder (rad/s) [=2 π N]

Chapter 1

Introduction

1.1 Background

Landslides in sensitive and quick clay deposits can result in large-scale devastation with significant social and economical impacts. Due to the semi-liquid state of these clays when subject to remoulding, small landslides can initiate flow slides which propagate large retrogression distances. These quick clay slides have the potential to involve massive soil movements as illustrated in Figure 1.1 (Thakur and Degago, 2014).

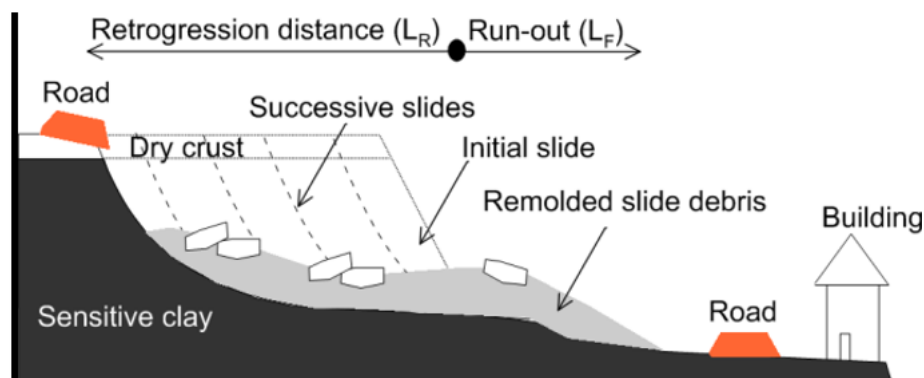


Figure 1.1: Retrogression flow slides in sensitive clays. From Thakur and Degago (2014)

Flow behaviour and assessment of quick clay flow slides are characterized and directly related to their remoulded shear strength (Thakur and Degago, 2014). There are four main slide types observed in Scandinavia and Canada (L'Heureux, 2013). These are:

- rotational slides;
- retrogression slides or flows;
- translational progressive slides; and
- spreads.

For flow slides to occur after an initial slide, there are two main criteria (Lebuis and Rissmann, 1979; Tavenas et al., 1983; Karlsrud et al., 1985; Trak and Lacasse, 1996; Leroueil, 2001; Vaunat and Leroueil, 2002; Thakur and Degago, 2012):

- the slide debris should be sufficiently remoulded; and
- the slide debris should be able to flow out of the slide area if remoulded.

Retrogression flows can occur if there is sufficient potential energy in the slope to remould the clay, as well as being liquid enough to flow out of the crater (L'Heureux, 2013). There are many contributing factors to the occurrence of these slides such as; site specific geotechnical properties, local topography and thickness of clay deposits; however if the two criteria stated above are not met, vast landslides are unlikely to occur.

A study of 14 large Norwegian landslides in sensitive clays by Thakur and Degago (2012) with retrogression distances greater than 100 m found that all slides have occurred in clays with $c_{ur} < 1.0$ kPa. This is illustrated in Figure 1.2 which presents the relationship between remoulded shear strength (c_{ur}), sensitivity (S_t) and retrogression distance (L).

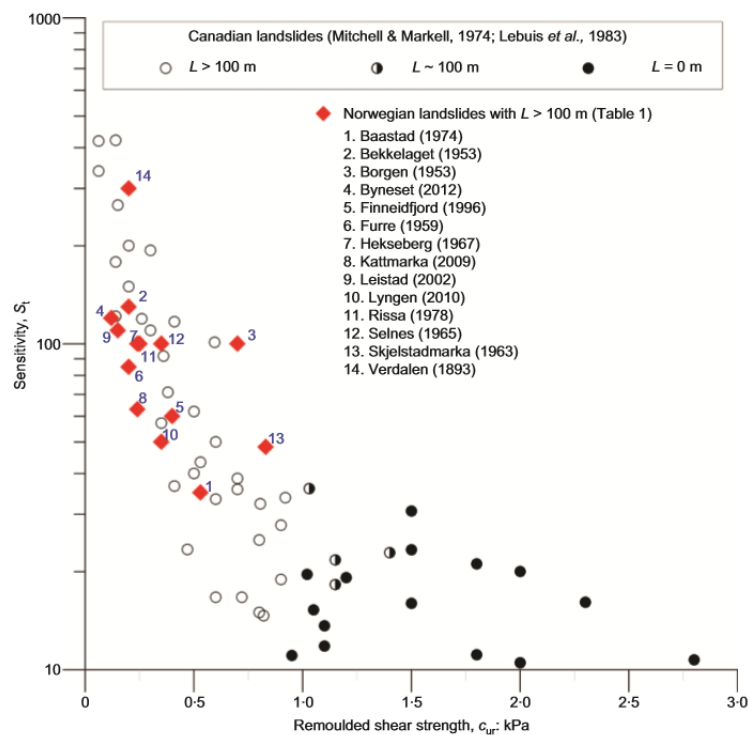


Figure 1.2: Relationship between retrogression length, remoulded shear strength and sensitivity. From Thakur and Degago (2014)

The study of Norwegian landslides is also supported by Canadian landslide data (Mitchell and Markell, 1974; Lebuis et al., 1983). Figure 1.2 shows there is a direct correlation between sensitivity and remoulded shear strength and how they may be used to predict potential retrogression distance.

Landslides can also occur in the form of debris flows. Debris flows develop in typically steep terrains and are triggered in connection with heavy rainfall or rapid snowmelt (NGU, 2015). Debris flows are characterized as containing at least 50% sand particles (> 0.06 mm) with abundant supply of loose debris. The differentiating factor from quick clay slides is that the loose particles in debris flows move independently as opposed to a coherent block of material that 'slides' over a failure surface (Morton and Hauser, 2001).

1.2 Objective

The objectives of this master thesis are as follows:

- Investigate the flow behavior of fine-grained soils (sensitive clays, clayey silts and silts) through laboratory tests including viscometer experiments and quickness approach by varying the remolded shear strength and liquidity index;
- Verify the uniqueness of the quickness test;
- Fit the Herschel-Bulkley rheological model to the viscometric test data;
- Determine the input parameters for the tested materials and validate the correlation between observed behavior and rheology; and
- Establish correlations between viscosity, quickness, remolded shear strength, and liquidity index for fine-grained soils.

1.3 Limitations and Approach

Laboratory experiments were performed in the Geotechnical laboratory during the Spring semester at NTNU. The viscometer used was a Bohlin Visco 88 BV provided by the Department of Geology and Mineral Resources Engineering at NTNU. The viscometric experiments and objectives have been continued and expanded on from the research undertaken by Grue (2015) with viscometric data presented in flow curves using the method described by Heirman et al. (2008).

Quick clay samples from Tiller, Norway and Perniö, Finland were used for the experiments, with the water content and remoulded shear stress varied to produce geotechnical parameter relationships.

The quickness experiments were performed according to the test methodology as described by Thakur and Degago (2012) using a standard proctor cylinder. Time limitations meant that only 35 quickness tests and 24 viscometric experiments were performed on the fine-grain soil samples.

1.4 Structure of the Thesis

Chapter 2 - literature review on sensitive clay and fine-grained soil flow behaviour, key geotechnical parameters, quickness and viscometer tests and their application in geotechnical engineering, overview of previous experimental results and the current practise of describing quick clay rheology.

Chapter 3 - descriptions of the materials tested as part of this study and overview of the laboratory program and tests performed.

Chapter 4 - presents the procedures for processing the quickness and viscometric test data.

Chapter 5 - presents laboratory test results and critical discussion.

Chapter 6 - conclusion of the study and suggestions for future work.

Chapter 2

Literature Study on the Characteristics and Flow Behaviour of Fine-Grained Soils

2.1 Fine-Grained Soils

2.1.1 Sensitive Clays

Sensitive clay materials are found in the northern regions of the world which include; Scandinavia, Canada, Alaska and Russia (L'Heureux, 2013; Issler et al., 2013). They occur in saline marine environments where clay deposits were formed by the transportation and deposition of fine grained sediments at river and glacier mouths, during the last ice age (NGU, 2016). Post-glacial uplift resulted in these deposits being elevated to near or above sea level, hence exposing these marine clays to groundwater flow and infiltration from precipitation. Over time, leaching of the electrically charged salt particles from the pore water occurs, which leads to instability within the grain structure (Helle, 2013). As the attractive forces between grains become weaker due to the loss of chemical bonds, disturbance causes the particles to flow in the pore water instead of re-flocculate (Dahl et al., 1997).

Figure 2.1 shows the change in structure of a marine clay due to fresh-water leaching. The initial deposition of clay particles after flocculation in seawater is shown in (A) with attractive forces between particles. (B) illustrates the marine clay structure after fresh-water leaching. The attractive bond forces are now weaker as a result of lower salt concentration and the clay becomes 'quick'. If the structure becomes disturbed and remoulded, the clay particles will not re-flocculate but instead flow in the pore water (C). Over time the grains will form a denser structure (D) however do not re-establish initial strength before leaching.

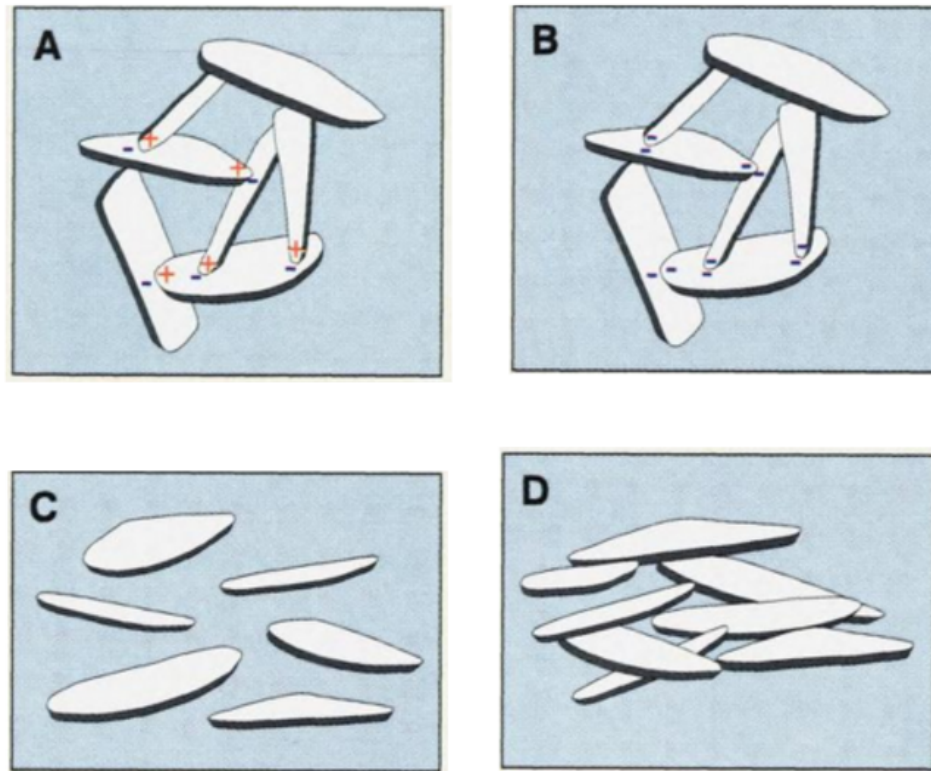


Figure 2.1: Change in the structure of marine clays due to leaching by fresh water. A) initial structure with attraction forces between grains. B) structure after leaching with decrease in salinity and bond strength. C) disturbance causes grains to flow in pore water. D) denser structure formed over time. From [Dahl et al. \(1997\)](#)

Sensitive clays have significantly reduced shear strength relative to their initial strength when subjected to high disturbances. Sensitive clays are categorized by their degree of sensitivity (S_t), defined as the ratio of undrained undisturbed shear strength (c_u) (in-situ strength) to undrained remoulded shear strength (c_{ur}). During the remoulding process, there should be no change in water content ([Terzaghi, 1944](#); [Skempton and Northey, 1952](#); [Rosenqvist, 1953](#); [Bjerrum, 1954, 1967](#); [Crawford, 1968](#); [L'Heureux et al., 2014](#)).

$$S_t = \frac{c_u}{c_{ur}} \quad (2.1)$$

The permeability of clay is very low and leaching occurs over a very long time. This process however, may be faster in areas of increased ground water flow, caused by topographical, geological or geographical conditions ([L'Heureux, 2013](#)).

2.1.2 Quick Clays

Quick clay develops in deposits of sensitive marine clay which has been subject to large groundwater flows. As a result, quick clays lose their shear strength and start to behave like a viscous fluid when heavily loaded or disturbed ([Gregersen, 2014](#)).

In Norway, there are four key criteria which must be met when classifying a clay as quick according to the Norwegian Geotechnical Society (NGF, 1982). These are:

- A remoulded shear strength (c_{ur}) less than 0.5 kPa;
- A sensitivity (S_t) greater than 30 (NGF, 1982);
- A natural water content greater than the liquid limit ($w > w_L$); and
- A salinity (S) less than 5 g/L.

2.2 Geotechnical Parameters

2.2.1 Water Content and Atterberg Limits

Fine-grained soils may occur as one of four states depending on its present water content; hard/dry, firm/crumbling, plastic or liquid. The water content, w (%), is defined as the ratio of water to solid in a material.

$$w = \frac{m_w}{m_s} = \frac{(m - m_s)}{m_s} \quad (\%) \quad (2.2)$$

where m_w is the mass of water, m_s is the mass of dry solids and m is the mass of the wet sample.

The Atterberg Limits (or consistency limits) define a relationship between the water content of a clay and its consistency. They represent the water contents at which a sample transitions from one state to another. The plastic limit, w_p (%), is the lowest water content at which a clay behaves as a plastic material in its remoulded state. The liquid limit, w_L (%), is the water content at which a remoulded clay changes consistency from plastic to liquid (refer to Figure 2.2).

The difference in water content between the plastic limit and the liquid limit is called the plasticity index, I_p (%). It represents the range of water content at which a remoulded clay behaves as a plastic.

$$I_p = w_l - w_p \quad (\%) \quad (2.3)$$

In Norway, clays are classified as having low plasticity with a plasticity index less than 10, while medium plastic clays range from 10–20. Typically, sensitive and quick Scandinavian clays occur within these plasticity ranges.

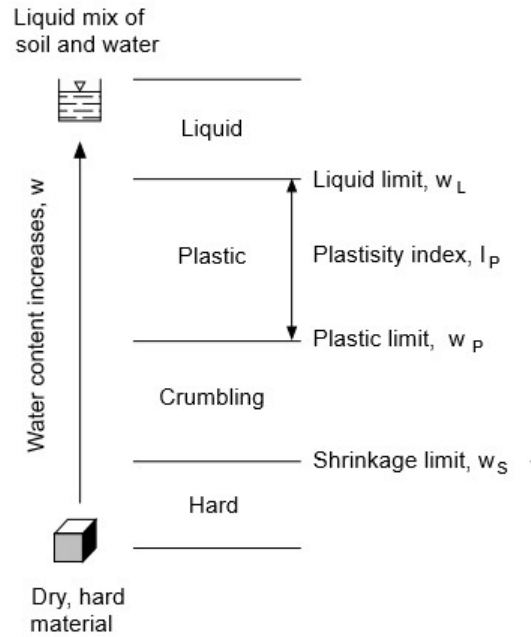


Figure 2.2: Physical properties and classification of the Atterberg Limits. From [NTNU \(2015\)](#)

The liquidity index, I_L (-), relates to how close the natural water content is to the liquid limit. For quick clays the natural water content is greater than the liquid limit resulting in a liquidity index greater than one.

$$I_L = \frac{(w - w_p)}{(w_L - w_p)} = \frac{(w - w_p)}{I_P} \quad (2.4)$$

2.2.2 Salinity

Due to leaching of marine clays, the reduction in salt content of the pore water is accompanied by a decrease in Atterberg limits, which in turn results in increased sensitivity ([Bjerrum, 1954](#)). Seawater has an average salinity of 35 g/L while the salinity of fjords in Norway range between 25-28 g/L. It has been shown by [Bjerrum \(1954\)](#) that marine clays commonly have a salt content of 3% (30 g/L) or greater while highly sensitive (quick) clays have salt contents lower than 0.5% (5 g/L).

Figure 2.3 shows the effect that salt concentration has on different geotechnical properties. The quick clay threshold is represented at 0.5% while observable changes to a clays properties and behaviour begins below 3%. Below the quick clay salinity limit, the sensitivity increases exponentially (Figure 2.3a). The reduction of salt concentration also reduces a marine clays undrained shear strength (Figure 2.3b) due to the loss of chemical bond strength on a molecular level (as discussed in Section 2.1.1).

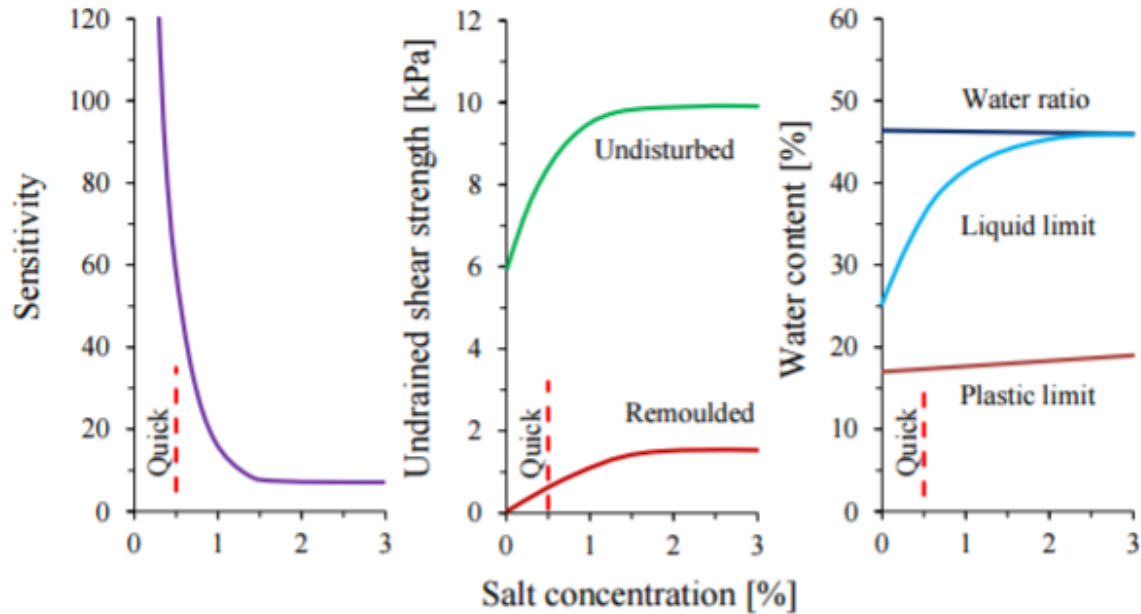


Figure 2.3: Effect of salinity on; a) sensitivity, b) shear strength and c) Atterberg limits. From [Mataić et al. \(2016\)](#)

During the leaching of ions from pore water, the salinity and liquid limit reduces while the water content remains relatively unchanged (Figure 2.3c). A slight reduction in plastic limit also occurs. When the water content becomes higher than the liquid limit, remoulded clay will flow.

For low-activity, non-swelling clays the liquid limit increases slightly with increasing salinity ([Bjerrum, 1954](#)).

2.2.3 Grain Size Distribution (or Molecular/Grain Structure)

The mineral grains found in marine clays are formed through deterioration and weathering; both physical and chemical; of rocks and rock fragments. The transportation of rock fragments beneath glaciers leads to sharp, angular grains as typically found in Norwegian clays.

The grain size distribution and mineralogy has a large influence on the behaviour and the mechanical properties of a soil. Clay particles have a grain size smaller than $2\mu\text{m}$ (0.002mm). A soil with clay content, CF (%) greater than 30% is classified as a 'clay' where the clay content of a soil is determined by the relative grain weight of the clay fraction.

$$CF = \frac{m_c}{m_s} \quad (\%) \quad (2.5)$$

where m_c is the mass of clay grains ($< 2\mu\text{m}$), and m_s is the total mass of soil grains in grams.

The silt fraction ranges from 0.002 mm and 0.06 mm in grain size with sub-size denotations. Silt classifications; fine silt: 0.002–0.006 mm, medium silt: 0.006–0.02 mm, coarse silt: 0.02–0.06 mm. A soil with greater than 45% of the grains less than 60 μ m is classified as a silt. If the clay content ranges between 5 and 15% the soil is classified as ‘clayey’ in adjective form. Less than 5% clay content is no associated with the material classification. Figure 2.4 shows the relative grain sizes between clay, silt and sand particles.

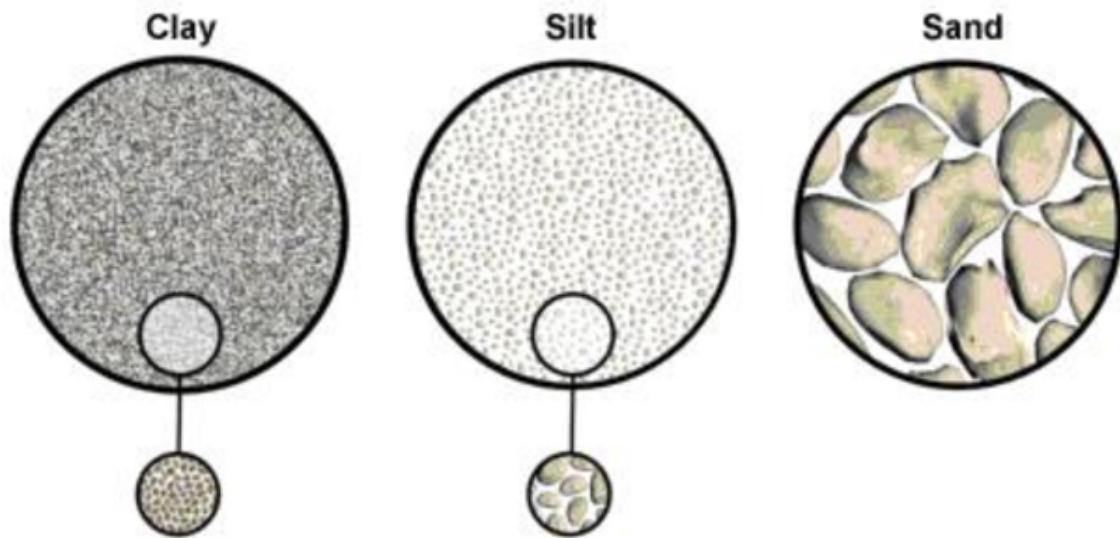


Figure 2.4: Comparison of soil grain sizes. Clay grain size less than 0.002 mm, silt grain size fraction between 0.002 mm - 0.06 mm, and sand fraction 0.06 mm - 6 mm. Adapted from [Csaba and Csaba \(2011\)](#)

2.2.4 Clay Activity

The activity of a clay describes its ability to bind water molecules to the grain structure. Activity varies with different types of clay minerals. Sensitive clays found in Norway are predominantly Illite-rich, which is a stable mineral, and produces inactive materials when subject to leaching ([Bjerrum, 1954](#); [Terzaghi et al., 1996](#)). A clay is considered as low-active if the activity is less than 0.75. Activity, A_c (-), is defined as the ratio of plasticity index to clay fraction.

$$A_c = \frac{I_P}{CF} \quad (2.6)$$

2.3 Flow Behaviour of Fine-grained Soils

The flow behaviour of fine-grained soils can be investigated through a number of methods. Remoulded shear strength is one of the key geotechnical characterization parameters of a soil. It provides an indication of a soils resistance to deformation and measured using the

fall-cone test. The quickness test, developed by [Thakur and Degago \(2012\)](#), defines a process to determine the flow behaviour of sensitive clays. Lastly, viscometer tests have been used to show the rheological properties of sensitive Norwegian and Canadian clays, initially by [Locat and Demers \(1988\)](#) as well as [Jeong et al. \(2012\)](#) and [Grue \(2015\)](#). These three methods of determining a soils flow behaviour have been discussed in depth in the following sections.

2.4 Remoulded Shear Strength

Remoulded shear strength has often be used in the assessment of flow slides in sensitive clays. The fall-cone test is used to measure a soils undrained remoulded shear strength through a point-specific calibration method (shown in Figure 2.5). There have been a number of relationships proposed between undrained remoulded shear strength and water content in the form of liquidity index ([O'Kelly, 2013](#)). These relationships have been presented in Table 2.1.



Figure 2.5: Fall-cone test used to determine the remoulded shear strength of clays. Measured penetration used along with calibrated tables to provide point-specific shear strength.

These discrepancies in derived formulas illustrate that there is no definitive correlation that can be applied for a generic application. The equations proposed by [Lebuis et al. \(1983\)](#) and [Locat and Demers \(1988\)](#) however are considered the most applicable to sensitive clays and Norwegian applications.

Table 2.1: Proposed relationships between liquidity index and remoulded shear strength. Adapted from O'Kelly (2013)

Reference	Equation (c_{ur} in kPa)
Wroth and Wood (1978)	$c_{ur} = 170\exp(-4.6I_L)$
Leroueil et al. (1983)	$c_{ur} = (I_L - 0.21)^{-2}$
Locat and Demers (1988)	$c_{ur} = 1.46(I_L)^{-2.44}; I_L > 1.0$
Hirata et al. (1990)	$c_{ur} = \exp(-3.361I_L + 0.376)$
Terzaghi et al. (1996)	$c_{ur} = 2(I_L)^{-2.8}$
Yilmaz (2000)	$c_{ur} = \exp(0.026 - 1.21I_L)$
Koumoto and Houlby (2001)	$c_{ur} = \exp[(1.070 - I_L)/0.217]$
NGI (2002a)	$c_{ur} = 4.2(I_L)^{-1.6}$
NGI (2002b)	$c_{ur} = 3.9(I_L)^{-2}$
Yang et al. (2006)	$c_{ur} = 159.6\exp(-3.97I_L)$

Furthermore, based on the data from 14 of the largest landslides in Norway extracted from Thakur and Degago (2012), there is no accurate relationship between remoulded shear strength and liquidity index as demonstrated in Figure 2.6. The c_{ur} value along the slip surface is plotted against I_L for each landslide (blue dots).

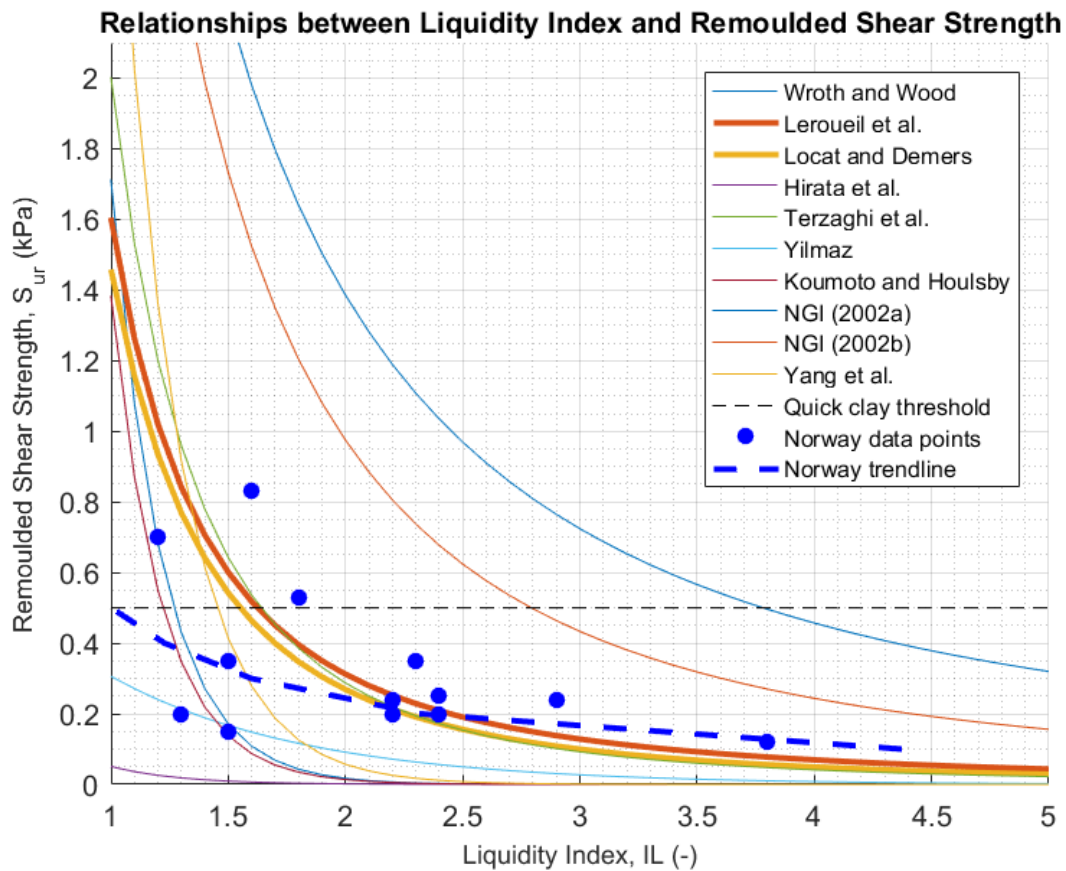


Figure 2.6: Relationships between liquidity index and remoulded shear strength. Data from 14 significant Norwegian landslides plotted for comparison to proposed relationships.

It can be seen that the trendline does not fit any of the proposed relationships in Table 2.1, with an R^2 value of 0.276. This suggests that there is no definitive relationship and that other various geotechnical parameters such as salinity, sensitivity and clay fraction can influence a soils remoulded shear strength and not just the liquidity index alone. It must be noted that for sensitive Norwegian clays, the minimum liquidity index value is 1.2.

2.5 Quickness

Norwegian landslides in sensitive clays with $c_{ur} < 1$ kPa are subject to large retrogression distances ($L > 100$ m) (Thakur and Degago, 2012), with their direct relationship illustrated in Figure 1.2. The extent of the flow slide decreases with increasing remoulded shear strength for both Norwegian and Canadian sensitive clays (Mitchell and Markell, 1974). Lebuis et al. (1983) have also proposed that $c_{ur} < 1$ kPa defines the threshold limit for the occurrence of flow slides.

Sensitive clays encompass a wide range of clays depicting significant variations in engineering behaviour, including remoulded shear strength. Fluidity of sensitive clays is difficult to interpret by small numerical changes of c_{ur} alone, as small variations result in significant alterations in soil behaviour. To investigate the potential of flow slides to occur in sensitive clays and the significance that remoulded shear strength plays, the quickness test has been developed.

The quickness test follows the similar concept to the slump test used for concrete, which measures the consistency of freshly mixed concrete. It is performed by filling an open-ended cylinder with a thoroughly remoulded material. The cylinder is then lifted upwards allowing the material to flow out. The final deformation height, H_f (mm), and lateral spread, D_f (mm), are measured. The quickness value, Q (%), of a remoulded clay is then calculated as the ratio between initial height, H_0 (mm), and deformation height and expressed as:

$$Q = \left(1 - \frac{H_f}{H_0}\right) \cdot 100 \quad (2.7)$$

where Q is calculated as a percentage and H_0 and H_f measured in mm. A Q value of 100% represents complete collapse while 0% represents no visual deformation.

Quickness tests performed by Thakur and Degago (2012) found that sensitive clays with a $c_{ur} < 0.2$ kPa behaved more like a soup, as predicted by Mitchell et al. (2005). Semi-solid behaviour was observed for clays with $0.5 < c_{ur} < 1.0$ kPa. Deformation was negligible for $c_{ur} > 1.0$ kPa which reinforces the slide threshold limit proposed earlier. Typical slump shapes and quickness values for corresponding remoulded shear strengths can be seen in Figure 2.7.

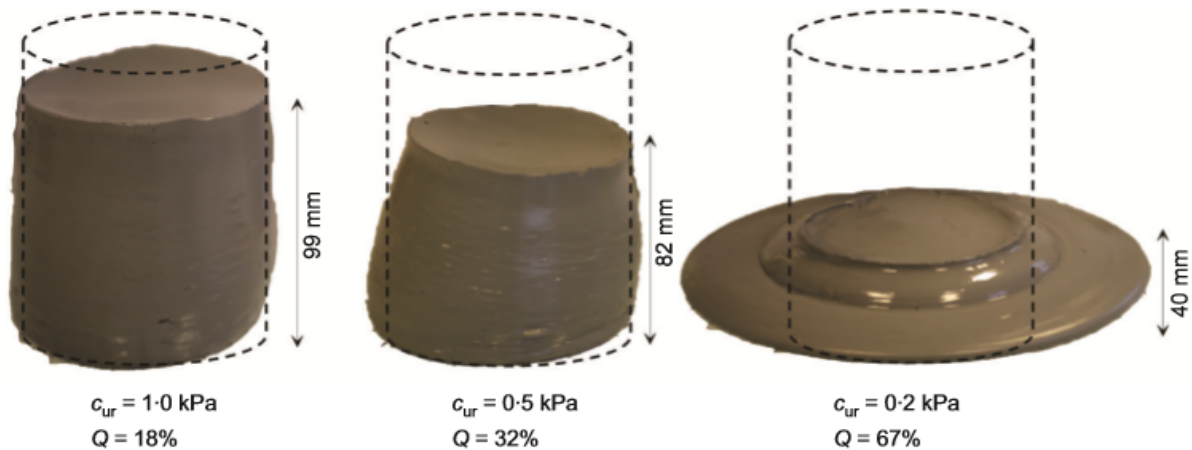


Figure 2.7: Slump of the remoulded sensitive clays (Heimdal clay, Norway) observed from the quickness test. From [Thakur and Degago \(2012\)](#)

Studies comparing various cylinder sizes used for quickness tests reveal the largest cylinder yields the most accurate results ([Thakur and Degago, 2012](#)). The largest cylinder used was a Standard Proctor test mould (100 mm x 120 mm) which is readily available in most geotechnical laboratories.

Principally, both c_{ur} and Q explain the same soil characteristic however the quickness test gives a value that is representative of the volume of soil tested as opposed to a point measurement as determined by the fall-cone test. Furthermore, the quickness test gives the possibility of amplifying the small range of c_{ur} to a scale that varies from 0 to 100%. The result is therefore a better visualization of the flow behaviour of sensitive clays, which improves the understanding of flow slides ([Thakur and Degago, 2012](#)).

Prior to the introduction of the quickness test, liquidity index was used when evaluating retrogression potential. It has been suggested that $I_L > 1.2$ defines the occurrence of flow slides ([Lebuis and Rissmann, 1979](#); [Lebuis et al., 1983](#); [Leroueil et al., 1983](#); [Karlsrud et al., 1985](#); [Locat and Demers, 1988](#); [Trak and Lacasse, 1996](#)). Numerous relationships have been proposed between c_{ur} and I_L (as discussed in Section 2.4), however no definitive outcome has been reached. Furthermore, determination of I_L requires calculating w , w_L and w_P which involves significant drawbacks. Quickness is independent of I_L and therefore arguably a more convenient parameter when evaluating slide potential.

Laboratory testing as well as back-calculation on 14 significant Norwegian quick clay slides showed that for $c_{ur} = 1$ kPa, $Q = 15\%$ ([Thakur and Degago, 2012](#)). It was therefore proposed that flow slides were not possible when $Q < 15\%$. Figure 2.8 shows the proposed range of

remoulded shear strength and quickness for assessing the potential for the occurrence of flow slides, after an initial slide, in sensitive clays.

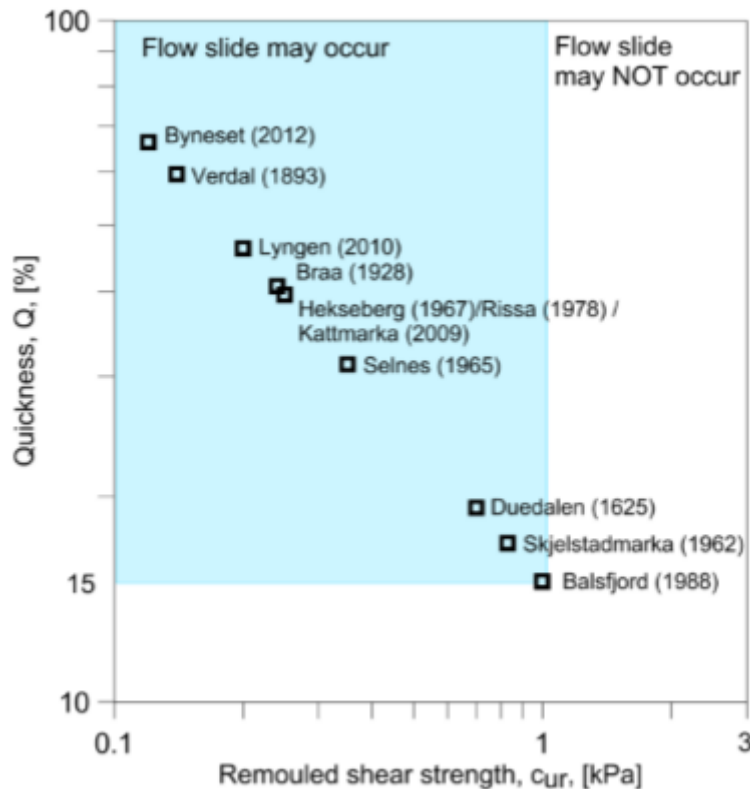


Figure 2.8: Proposed range of c_{ur} and Q for assessing flow slide potential. No flow slides if $Q < 15\%$ or $c_{ur} > 1.0$ kPa. From [Thakur and Degago \(2014\)](#)

2.6 Rheology

Rheology is the theory of deformation and flow of matter ([Irgens, 2014](#)). Rheological theory describes relationships and equations between applied stress and deformation of a body. Ideal solids deform elastically, which is completely reversible. Ideal fluids deform by flowing, which is irreversible deformation ([Schramm, 1994](#)). Fine-grained soils exhibit a rheological behaviour like that of viscoplastic fluid and therefore lies between the idyllic liquid and solid states.

2.6.1 Viscosity

The viscosity of a fluid is its resistance against deformation. For steady state flow the viscosity is defined as the ratio between the shear stress and shear rate, and can be expressed as:

$$\tau = \eta(\dot{\gamma}) \cdot \dot{\gamma} \quad (2.8)$$

where τ is the shear stress in Pa, $\eta(\dot{\gamma})$ is the viscosity function in Pa.s, and $\dot{\gamma}$ is the rate of shear strain (or shear rate) in s^{-1} . As well as shear rate, viscosity can also change with temperature.

Fine-grained soils are classified as non-Newtonian fluids in which their viscosity varies with shear rate. Shear thinning behaviour is observed as the viscosity decreases with increasing shear rate. The viscosity function for non-Newtonian fluids is called the apparent viscosity (Irgens, 2014) and can be expressed as:

$$\eta(\dot{\gamma}) = K|\dot{\gamma}|^{n-1} \quad (2.9)$$

where K is the consistency parameter in $Pa.s^n$ and n is the power law index which is dimensionless. For shear thinning fluids $n < 1$.

Flow curves are produced by plotting applied shear rate against resultant shear stress. Figure 2.9 shows the stress-strain relationships for different types of fluids. A Newtonian fluid (curve 1) experiences a constant increase in shear stress with shear rate. A shear thinning fluid however has a decreasing rate of shear stress. The flow curve for a typical shear thinning fluid is illustrated by curve 3, while a shear thickening fluid is represented by curve 2.

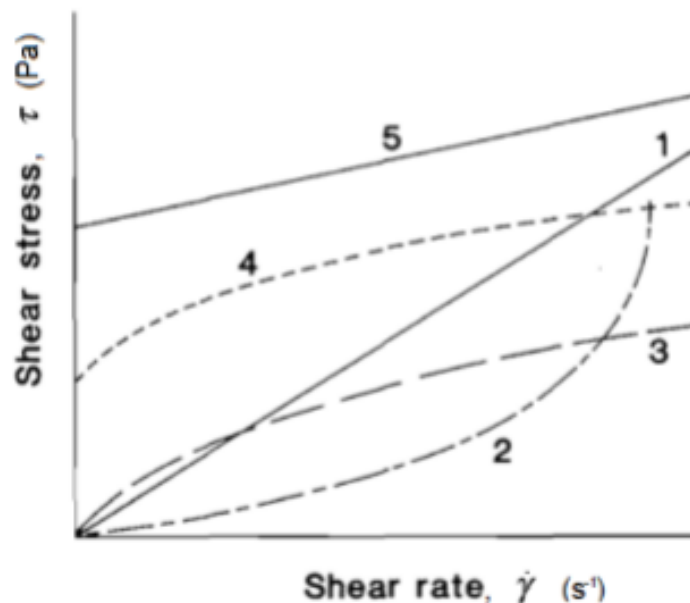


Figure 2.9: Flow curves for different fluid types (shear stress vs. shear rate). 1: Newtonian. 2: Shear thickening. 3: Shear thinning. 4: Herschel-Bulkley. 5: Bingham. From L'Heureux (2013)

To predict quick clay slides and debris flow characteristics it is necessary to determine the rheological properties of these fine-grained soils. For viscoplastic fluids at rest, the dispersion can build up a network of inter-molecular binding forces. Externally applied

stress needs to be higher than the internal binding forces to make a fluid flow. This applied stress required to make the fluid flow is called the yield stress, at which the internal network of bindings collapse (Schramm, 1994). Elastic deformation (recoverable) is experienced below the yield stress threshold.

Rheological models for fine-grained soils are required to describe both the yield stress and viscous flow components. Initially the Bingham model (represented by curve 5 in Figure 2.9) has been used to describe the viscoplastic behaviour of quick clays. For shear stresses below the yield stress in the Bingham model, the material will not flow. Once the yield stress is reached, deformation and shear stress increases linearly with constant viscosity. The Bingham model is given by the equation:

$$\tau = \tau_{y,B} + \eta\dot{\gamma} \quad \text{if } |\tau| > \tau_y, \text{ and } 0 \text{ otherwise} \quad (2.10)$$

where $\tau_{y,B}$ is the Bingham yield strength (Pa) and η the plastic viscosity (Pa s).

Furthermore, the Bingham model describes the rheological behaviour well for strain rates $> 20 \text{ s}^{-1}$, however overestimates the shear stress at lower strain rates (Jeong et al., 2012). Figure 2.10 shows the Bingham yield stress approximation with test results based on linear extrapolation.

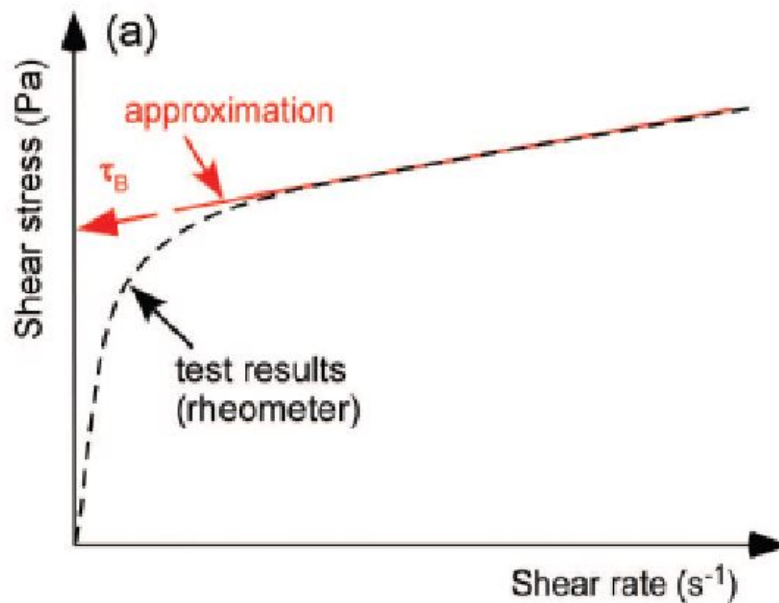


Figure 2.10: Bingham approximation of yield stress based on rheometer test results and flow curve. From Jeong et al. (2012)

Due to the shear thinning behaviour of clays however, the Herschel-Bulkley model has since been adopted as the preferable rheological model for fine-grained soils (represented by curve 4 in Figure 2.9).

2.6.2 Herschel-Bulkley Model

Jeong et al. (2012) concluded that the flow curves from viscometric tests on clay are fitted better by the Herschel-Bulkley model. Coussot and Piau (1994) proposed to fit this model to the experimental data over the whole experimental shear rate range. Similar to quick clays, the behaviour of debris flows has been found to be mainly viscoplastic, with the main body of a flow considered a mass of a single viscous material. The Bingham model, initially proposed for debris flows by Johnson (1970) has since been superseded with the use of the Herschel-Bulkley model which takes into account the shear thinning behaviour of the water-clay-grain mixtures (Coussot et al., 1998).

The Herschel-Bulkley model is given by the equation:

$$\tau = \tau_y + K\dot{\gamma}^n \quad \text{if } |\tau| > \tau_y, \text{ and } 0 \text{ otherwise} \quad (2.11)$$

where τ_y is the yield stress (Pa), K is the consistency parameter ($\text{Pa}\cdot\text{s}^n$), and n is the Herschel-Bulkley exponent (-).

A challenge with the Herschel-Bulkley model is that the set of parameters found from fitting the experimental data is not unique with possibilities for large discrepancies. If the fitted τ_y changes slightly, the K - and n -values will change Coussot and Piau (1994). The final value of τ_y will be a good approximation of the yield stress however the values of K and n can vary more (Grue, 2015).

2.6.3 Use of Viscometers For Geotechnical Applications

Even though fine-grained soils with high water contents behave like a fluid, determining the yield stress can prove difficult with conventional soil mechanics apparatus. Viscometer tests have been used to show the yield stress of clayey soils with high water contents (Locat and Demers, 1988).

The coaxial cylinder viscometer is a constant speed motor with a torque detection system. The instrument (shown in Figure 2.11) has a stationary outer cylinder with radius, R_o (mm), and an internal cylinder with radius, R_i (mm), and height, h (mm). The test sample is placed in the annular gap. The internal cylinder, or spindle, rotates causing the fluid in the gap to flow.

The instrument uses a controlled shear rate. The resistance from the fluid against the spindle; keeping the rotational speed, N (rps), constant; is the resultant shear stress, or torque, T (mNm). Both the torque and rotational speed are measured.

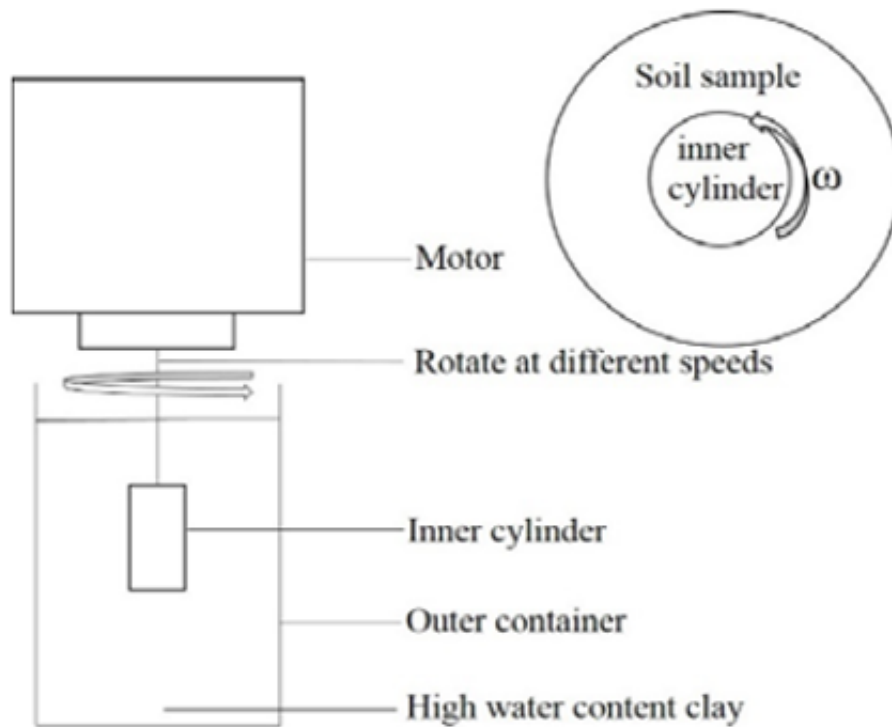


Figure 2.11: Schematic of viscometer apparatus. Rotational speeds can be varied as well as the inner cylinder dimensions and outer container diameter. From [Weerakoon \(2015\)](#)

Flow of a material in a concentric cylinder viscometer is considered approximately a simple shear flow if the gap is narrow. The gap classification is determined by the ratio of outer radius to inner radius. For a narrow gap system, the radii ratio is $1 \leq R_o/R_i \leq 1.1$ ([Schramm, 1994](#)). For simple shear flow, the shear stress and shear rate can be calculated with formulas that assume a linear speed drop over the gap. This approximation of a linear speed drop can be applied for both narrow and wide gap systems, however, a large error is observed for wide gap systems.

Figure 2.12 illustrates the speed drop error observed in coaxial cylinder viscometers. The assumed linear velocity gradient is indicated by curve (1) while the real non-linear velocity gradient across the gap is indicated by curve (2). The maximum tangential velocity, v_{max} , occurs at the inner cylinder. The area in between the assumed linear and real non-linear gradients indicates the error when calculating the shear rate (*black shaded region*). The ratio of radii contributes to the error with the gradient becoming even more non-linear when non-Newtonian liquids are tested. To reduce the linear speed drop assumption error, alternative formulas should be used.

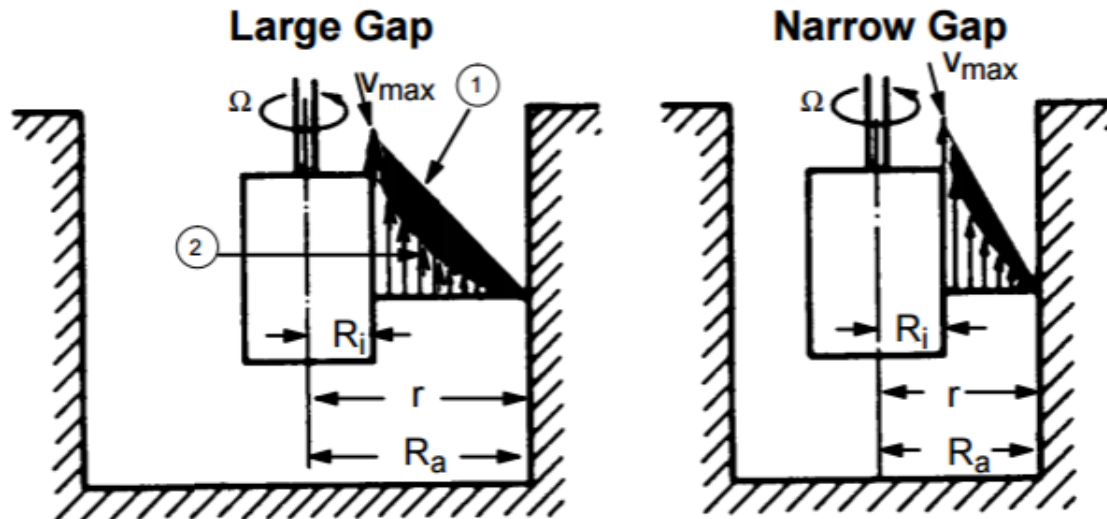


Figure 2.12: Velocity gradients over wide and narrow gap coaxial cylinder viscometer systems (elevation view). Assumed linear speed drop vs. real non-linear speed drop. Adapted from Schramm (1994)

Figure 2.13 shows the non-linear velocity profile of a coaxial cylinder viscometer, in plan view. The maximum velocity occurs at the inner cylinder with zero velocity at the outer cylinder (boundary conditions).

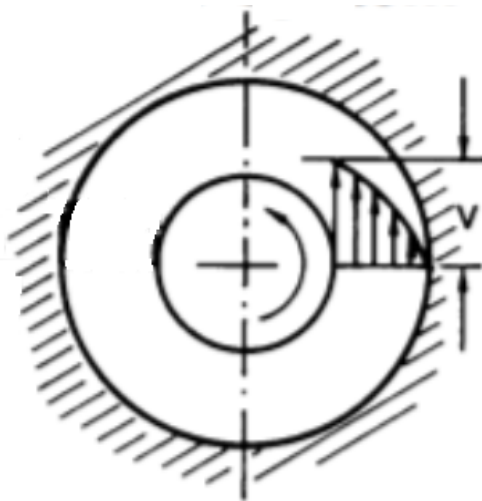


Figure 2.13: Non-linear velocity gradient in a coaxial cylinder viscometer (plan view). Adapted from Schramm (1994)

The *Couette Inverse Problem* is used to calculate the shear stress and shear rate from torque and rotational speed measurements. The solution to this problem for a Herschel-Bulkley fluid in a wide gap is described by Heirman et al. (2008). The method was used for a coaxial cylinder system with radius ratio $R_o/R_i = 1.45$, which is a wide gap system ($R_o/R_i > 1.1$). The radius ratio for tests performed in this thesis is 1.96 and it is assumed that the equations presented by Heirman et al. (2008) are valid. Section 4.2 outlines the basic equations used to calculate viscometer parameters for wide gap systems.

2.7 Previous Studies

2.7.1 Quickness Tests

Quickness tests were performed on sensitive clay samples taken from three landslide sites in central Norway, by [Thakur and Degago \(2014\)](#). The sites; Lersbakken, Olsøy and Byneset; have been studied extensively in connection to landslide hazards. The raw test data has been interpreted and reproduced from plots published in *Quickness Test Approach for Assessment of Flow Slide Potentials* ([Thakur and Degago, 2014](#)).

Material Properties

Characterization of each site and test material was done to provide background information for further geotechnical evaluation with respect to their quickness values. Table 2.2 shows the soil characteristics for these three sensitive clays.

Table 2.2: Soil characteristics for Norwegian sensitive clays used in quickness testing

Site	Depth (m)	c_{ur} (kPa)	S_t (-)	w (%)	I_p (%)	I_L (-)	CF (%)
Lersbakken	6-10	0-2.0	16-29	22-34	5-7	0.7-2.0	30
Byneset	4-12	0-3.0	4-400	27-48	3-15	0.9-5.4	30-55
Olsøy	4-15	0-2.1	30-100	28-38	3-10	0.6-3.0	50-65

Quickness Results

The results come from quickness tests performed using a large cylinder size (100 mm x 120 mm) at varying remoulded shear strengths, determined using the fall-cone method. The tests were carried out according to the procedure reported by [Thakur and Degago \(2014\)](#) and discussed in Section 3.5.1. Based on the test results, upper and lower limits for quickness values have been proposed as functions of remoulded shear strength.

The proposed quickness limits are expressed as:

$$Q_{Upper} = 25(c_{ur})^{-0.7} \quad (2.12)$$

$$Q_{Lower} = 15(c_{ur})^{-0.7} \quad (2.13)$$

where Q is measured as a percentage and c_{ur} in kPa.

Figure 2.14 shows a combined plot of the quickness test data for the three landslide locations.

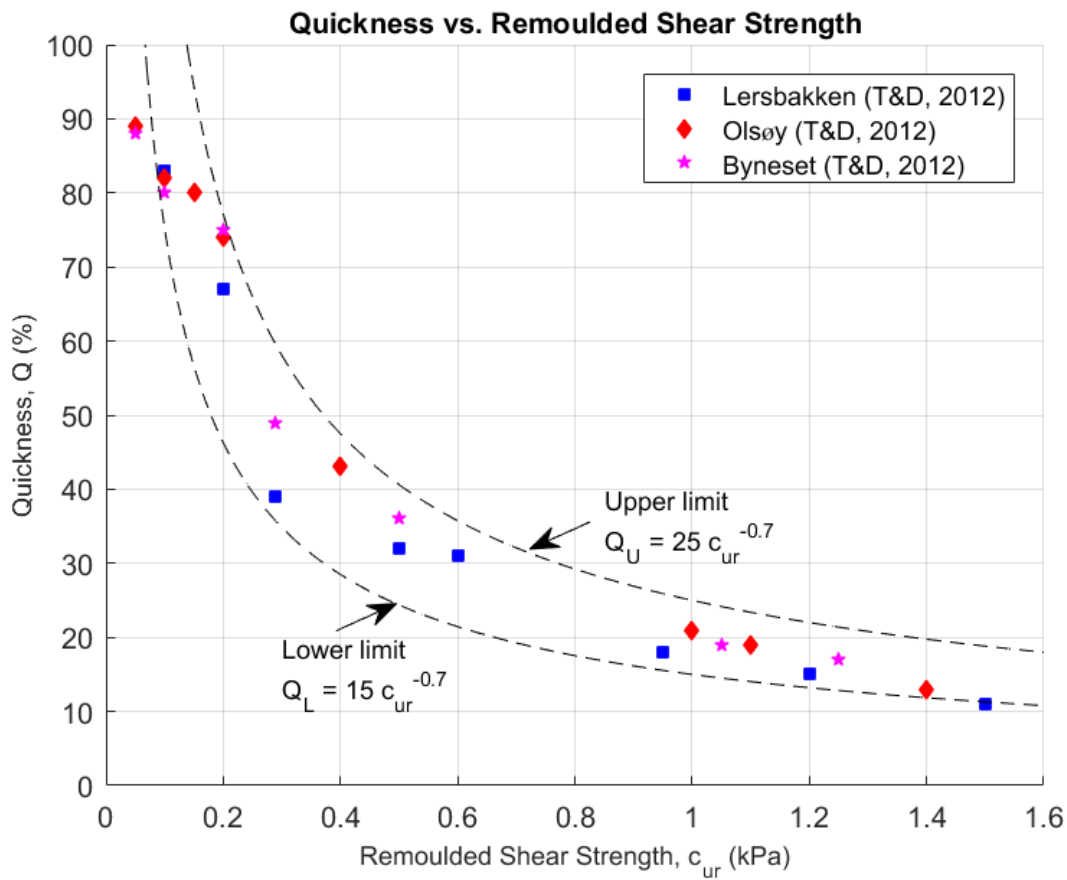


Figure 2.14: Quickness test data on Norwegian sensitive clays. Tests performed by [Thakur and Degago \(2012\)](#)

Figure 2.15 shows a variation in flow behaviour observed for quickness tests performed on remoulded Byneset clay ranging from 0.1 kPa to 2.0 kPa.



Figure 2.15: Slump and spread observed for remoulded Byneset clay, Norway. Quickness tests performed at $c_{ur} = 0.1$ kPa, 0.2 kPa, 0.5 kPa, 1.1 kPa and 2.0 kPa. From [Thakur and Degago \(2014\)](#)

2.7.2 Viscometer Tests on Canadian Clays

Viscosity of sensitive clays was first related to remoulded shear strength by [Eden and Kubota \(1961\)](#), who used a rotating coaxial viscometer to measure their remoulded shear strength. [Torrance \(1987\)](#) and [Locat and Demers \(1988\)](#) were the pioneers at routinely using viscometers on sensitive clays to develop positive relationships between geotechnical parameters and rheological behaviour.

Six different Canadian sensitive clay samples were used and over 70 viscometer tests run by [Locat and Demers \(1988\)](#). The results were fitted to the Bingham model to compute viscosity and yield stress, however flow curves suggested a shear thinning nature. This is illustrated in Figure 2.16 where changes to shear stress are observed as the shear rate increases.

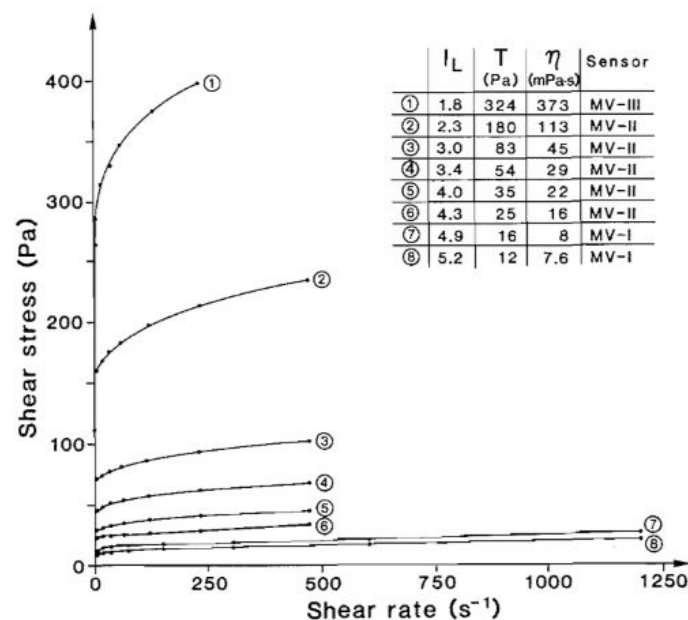


Figure 2.16: Flow curves for St. Alban, Canada soil. Samples have varying liquidity index from 1.8 to 5.2 and constant salinity of 0.2 g/L. T indicates the Bingham yield stress (Pa). From [Locat and Demers \(1988\)](#)

Although the Bingham model was used initially, some strong relationships between liquidity index, yield stress and remoulded shear strength were still observed and some key conclusions could be drawn. As shown in Figure 2.17, the yield stress increases as the liquidity index decreases. Furthermore, soils with a very high liquidity index demonstrated behaviour closer to a Bingham material while lowering the liquidity index changed the behaviour to more a Hershel-Bulkley material. This is also indicated in Figure 2.16 by the shape of the flow curves. It was also found that increasing the pore water salinity not only effected the remoulded shear strength but also the viscosity and yield stress ([Locat, 1997](#)). This confirms that at a given liquidity index, leaching would reduce the yield stress.

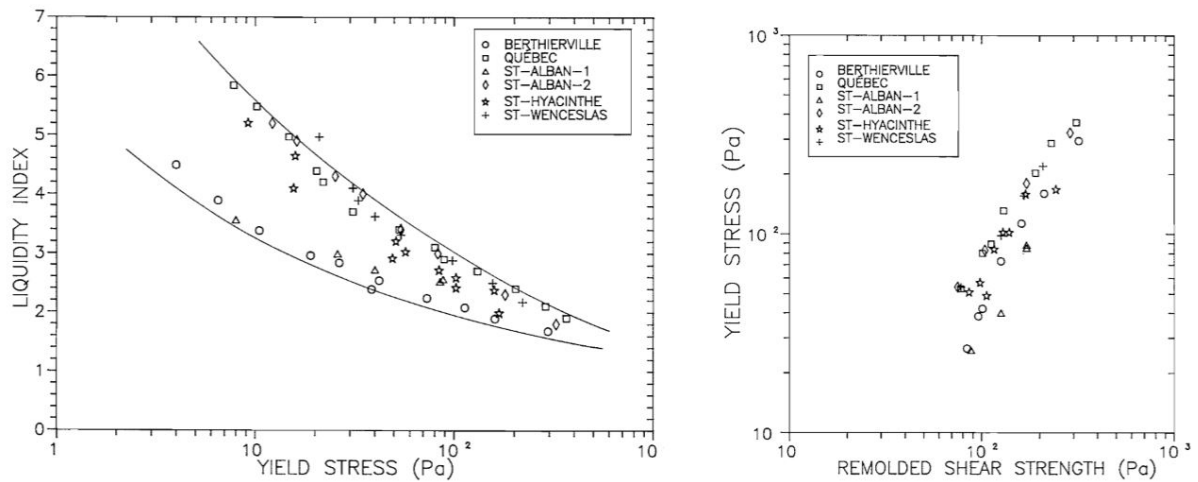


Figure 2.17: Relationships between liquidity index, Bingham yield stress and remoulded shear strength for Canadian clays. From [Locat and Demers \(1988\)](#)

[Jeong et al. \(2012\)](#) performed rheology tests on a naturally soft, low-activity illite-rich clay from Jonquiere, Quebec, Canada. The rheology analysis was performed using a Rotovisco RV-12 coaxial cylinder viscometer.

It was found that when keeping the I_L constant, the shear stress increases with the increase in salinity. Figure 2.18 illustrates the effect of salinity on the Herschel-Bulkley flow curves.

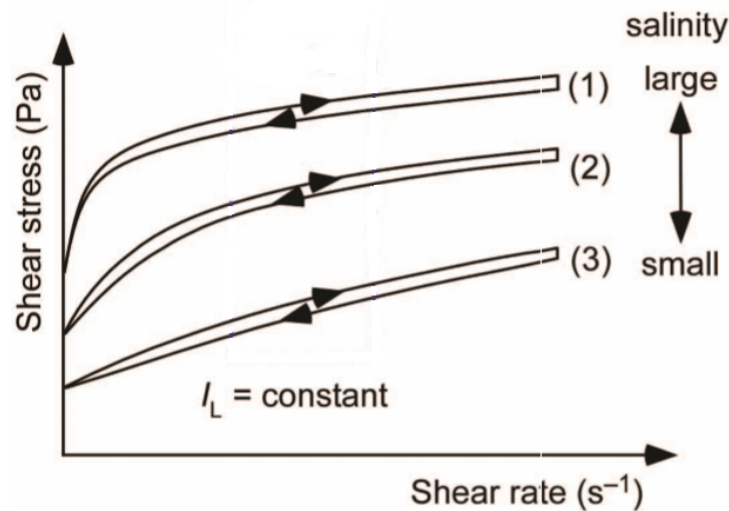


Figure 2.18: Effect of salinity on flow curves. Adapted from [Jeong et al. \(2012\)](#)

The Jonquiere clay exhibited characteristics of a pseudoplastic (shear thinning) fluid with a flow behaviour index (n) that ranged from 0.1 to 0.4 for salinities ranging from 0.1 to 30 g/L and a liquidity index of 3.0. Table 2.3 presents the rheological properties of the Jonquiere clay. The rheological behaviour of Jonquiere clays at low salinity (0.1 g/L) shows Bingham-like behaviour, however, it exhibits shear thinning behaviour for increased salinities (30 g/L). This is consistent with [Locat and Demers'](#) earlier work.

Table 2.3: Rheological properties of Jonquiere clay. Adapted from Jeong et al. (2012)

I_L	S	τ_y	K	n	R^2
3.0	0.1	15.0	4.8	0.165	0.791
3.0	0.3	37.7	1.9	0.393	0.976
3.0	0.7	44.1	4.2	0.306	0.997
3.0	1.0	44.7	3.3	0.360	0.997
3.0	10	42.1	3.8	0.349	0.975
3.0	30	44.0	8.5	0.228	0.985

It can be seen that the shear stress (τ_y) increases with salinity however there are no distinct correlations with the consistency parameter (K) or the Herschel-Bulkley exponent (n). Furthermore, a linear relationship between viscosity and shear rate is observed (on a log-log scale) with increased salinity resulting in higher viscosities (Figure 2.19).

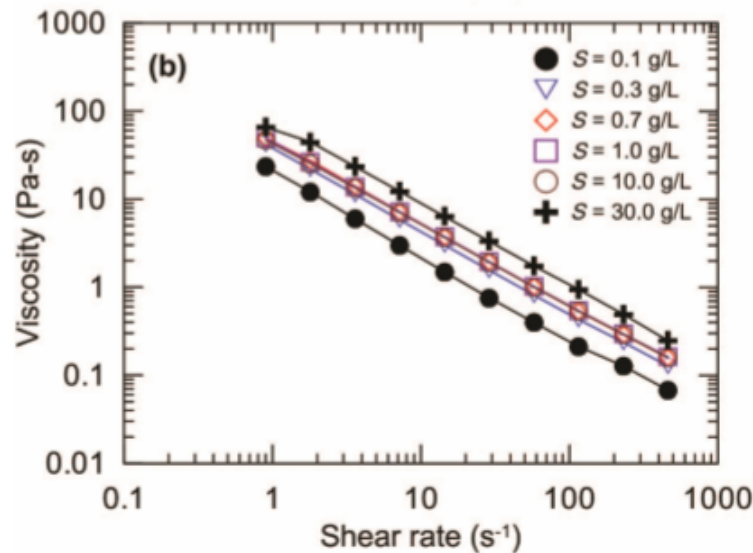


Figure 2.19: Effect of salinity on viscosity. From Jeong et al. (2012)

The results revealed that the clay exhibit time-dependant, non-Newtonian behaviour. The flow curves were better fitted by the Herschel-Bulkley model than by the perfect plastic Bingham model.

Studies into rheological properties of debris flows have shown the behaviour of water-debris mixtures for a given solids concentration changes mostly with their clay fraction. For very low clay fractions, granular interactions prevail, resulting in granular debris flows in the field. For higher clay fractions these mixtures behave as a viscoplastic fluid and the Herschel-Bulkley model is an accurate predictor of flow behaviour. Furthermore, the Herschel-Bulkley model has been successfully applied to natural debris flow materials having a fine fraction ($< 40 \mu\text{m}$) higher than 10% (Cousot and Piau, 1995). These mixtures result in mudflows or muddy debris flows.

It has been found from testing on various natural concentrated suspensions that the Herschel-Bulkley model can be fitted to rheological data keeping the exponent constant ($n = 0.33$) (Laigle and Coussot, 1997). The yield stress, τ_y and K increase roughly proportionally for increasing solid concentration values (Coussot et al., 1998).

Studies and investigations into the rheological properties of sensitive clays and fine-grained soils using viscometers had previously only been applied to Canadian clays. Grue (2015) expanded upon the previous work by Locat and Demers (1988), Jeong et al. (2012), etc. and performed viscometer tests on Norwegian clays.

2.7.3 Viscometer Tests on Norwegian Clays

Viscometer tests were performed on Norwegian quick clay samples from Tiller and Esp by Grue (2015). Data from previous viscometer tests on clay samples from Canada and the Mediterranean by Locat and Demers was also used as part of the research into the rheological behaviour of Norwegian sensitive clays (Grue, 2015). The raw data was received as Excel files by Grue, which had been interpreted for the Bingham model and bi-linear model, however, not for the Herschel-Bulkley model. Grue (2015) therefore fitted the data to the Herschel-Bulkley model with the results contained in Appendix B.

Material Properties and Data

The raw data sets were obtained from different sites. Two data sets were from Saint Alban (Quebec, Canada), three were from Saguenay Fjord (Quebec, Canada), one was from Jonquiere (Quebec, Canada) and one data set was from the Mediterranean Sea (Gulf of Lyon). Table 2.4 shows the soil characteristics for these clays as well as the Norwegian clays tested.

Table 2.4: Soil characteristics for Norwegian and Canadian clays used in viscometer testing

Site	c_{ur} (kPa)	S_t (-)	w (%)	w_L (%)	I_p (%)	CF (%)	S (g/L)	A_c (-)
Tiller	0.1	-	38	25	7.2	30	0.5	0.24
Esp	0.59	42	35	29	6.4	35-50	1.1	0.17
Saint Alban 1	0.97	70	46.5	36.1	17.4	46	0.3	0.38
Saint Alban 2	0.38	40	45	33.1	16.9	38	0.85	0.45
Saguenay Fjord 1	-	-	-	35.9	15.6	35	21.5	0.45
Saguenay Fjord 2	0.29	-	95.6	69.4	27.1	-	30	-
Saguenay Fjord 3	1.3	9	64	59	33	-	27.5	-
Saguenay Fjord 3	1.2	7	78	70	41	-	23.4	-
Jonquiere	-	-	-	51.3	29.2	58-61	0.1	0.49
Mediterranean	0.63	-	67.5	62.8	38.4	52	29	0.74

These clays are considered low- to medium-active clays (Jeong, 2013; Grue, 2015). The sensitive clays tested as part of this thesis are low-active clays, and it is assumed that they are comparable to past Norwegian and Canadian clays. The test clays soil characteristics are shown in Table 3.1.

The data sets are results from dynamic response tests using coaxial viscometers. The tests were carried out according to the procedure reported by Locat and Demers (1988) and outlined by Grue (2015). Locat and Demers used a Haake Rotovisco 12 viscometer with narrow gap cylinder systems while Grue used a Bohlin Visco 88 BV viscometer with wide gap cylinder systems. The data provided by Grue (2015) as part of this thesis had already been converted to shear stress and shear rate (refer to Appendix B).

Viscometer Results

It was found that the Norwegian and Canadian clays data fit well together however the Canadian clays have a generally higher salinity (Grue, 2015).

Clear trends can be observed between yield stress and liquidity index when both the Canadian and Norwegian clay results are plotted (as shown in Figure 2.20). There were no such relationships observed for the consistency parameter or Herschel-Bulkley exponent (as shown in Appendix B).

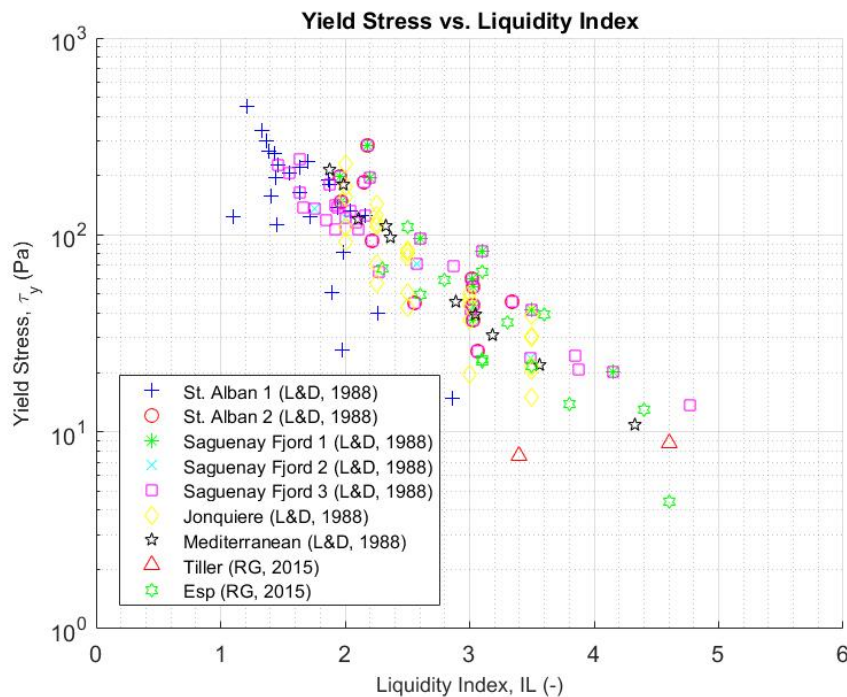


Figure 2.20: Results of calculated yield stress from viscometer tests on Canadian and Norwegian sensitive clays. Adapted from Grue (2015)

Grue (2015) was the first to propose relationships between Herschel-Bulkley parameters (τ_y , K^* and n) and liquidity index, albeit only specific to Esp clay. The following equations are as follows:

$$\tau_y = \left(\frac{7.86}{I_L} \right)^{3.75} \quad (\text{Pa}) \quad (R^2 = 0.823) \quad (2.14)$$

$$K^* = \left(\frac{3.49}{I_L} \right)^{4.80} \quad (\text{Pa}) \quad (R^2 = 0.819) \quad (2.15)$$

$$n = 0.092 \cdot I_L + 0.339 \quad (-) \quad (R^2 = 0.308) \quad (2.16)$$

where the liquidity index ranges between 2.4 and 4.6 for the Esp clay with salinity 1.0-2.0 g/L.

2.8 Expected Findings

The expected findings from this study on the rheological properties and flow behaviour of fine-grained soils are as follows:

Remoulded Shear Strength

- Increasing salinity also increases remoulded shear strength for a given liquidity index.

Quickness tests

- Quickness test results verify proposed quickness limits for remoulded shear strength.

Viscometer tests

- Viscometer results and fine-grained soils behaviour described by Herschel-Bulkley model;
- Herschel-Bulkley exponent (n) decreases as liquidity index increases. ie. Flow curve becomes more linear at higher liquidity indexes; and
- Increasing the salinity also increases yield stress.

Chapter 3

Laboratory Experiments

This chapter outlines and describes the laboratory experiments undertaken as part of this research topic. The geotechnical properties of the tested materials is provided at the beginning of this chapter, followed by a list of the performed tests for each sample . A description of the index tests, quickness test and viscometric experiment procedure is also documented.

3.1 Materials

Two different quick clays were used for the experiments, a clay from Trondheim, Norway and Perniö, Finland. The clay from Tiller, Trondheim was extracted from the field on the 23rd of August, 2013, and stored as a block sample for approximately 3.5 years in cold storage at 4°C before testing. The Perniö clay was extracted in October, 2016 and stored as a block sample for 4 months. To prevent pore water evaporation during storage both samples were wrapped in plastic wrap. Table 3.1 shows the characteristic values for the two clays tested. The clay properties for Tiller and Perniö were obtained from [Gylland et al. \(2013\)](#) and [D'Ignazio et al. \(2016\)](#) respectively.

Table 3.1: Soil characteristics for tested clays

Site	Depth (m)	c_{ur} (kPa)	S_t (-)	w (%)	I_p (%)	I_L (-)	CF (%)	S (g/L)	A_c (-)
Tiller	10	0.1	200	30-45	4-7	3-6	35-45	1.0	0.15
Perniö	6	0.1	31-57	75-84	14-27	1.9-2.8	52-77	-	0.18-0.5

3.1.1 Material Description

Five fine-grained soil materials were used for testing, ranging from quick clays to silts. For each material the soil was first tested at the natural conditions before being altered by varying the liquidity index and salinity with the addition of de-ionized water or a brine solution. Table 3.2 provides an overview and description of each test material.

Table 3.2: Material and sample descriptions

#	Material Description	Soil Type	Water Added	Salt Added	Desired Sample Remoulded Shear Strengths (kPa)
1	Tiller Clay 1	Quick Clay	X	-	0.1, 0.2, 0.29, 0.39, 0.49, 1.0
2	Tiller Clay 2	Quick Clay	X	X	0.1, 0.2, 0.29, 0.39, 0.49, 1.0
3	Perniö Clay	Quick Clay	X	-	0.1, 0.2, 0.29, 0.39, 0.49, 1.0
4	Vassfjellet Silt with Tiller Clay	Clayey Silt	X	-	0.1, 0.2, 0.29, 0.39, 0.49, 1.0
5	Vassfjellet Silt	Silt	X	-	0.1, 0.2, 0.29, 0.39, 0.49, 1.0

3.2 Test Program

Quickness and viscometer tests were used to determine the flow behaviour of various fine-grained soils materials. To determine correlations between rheology parameters and geotechnical properties other index tests were also required. The number of tests performed is indicated in parentheses.

For each material the following tests were carried out:

- Grain size distribution (5 tests);
- Atterberg limits (24 measurements);
- Natural water content (3 measurements); and
- Natural salinity (3 measurements).

For each sample the following tests were carried out:

- Quickness test (35 tests);
- Fall-cone test (84 tests);
- Water content (250+ measurements);
- Viscometric test (24 tests); and
- Salinity (35 measurements).

The water content was also determined for each sample both before and after viscometric testing in order to detect evaporation (Locat and Demers, 1988; Grue, 2015). All tests were performed at room temperature in accordance with the Norwegian Standards apart from the viscometric tests which were done in a climate controlled room.

3.3 Preparation of Samples

Material 1 – Tiller Clay 1 (Quick clay)

Due to the considerable storage time (3.5 years), the Tiller sample had become stiff as a result of moisture loss. This made it very difficult to remould, and hence, small slices of the block sample were cut and remoulded separately before being added to a bucket. To reduce the remoulded shear strength, de-ionized water was added and gradually the clay transitioned from a stiff plastic clay to a quick clay slurry. Once each of the desired remoulded shear strengths (outlined in Table 3.2) were obtained, approximately 400 mL of the clay slurry was sealed in plastic containers and stored in the fridge until further testing.

Material 2 – Tiller Clay 2 (Quick clay with constant salinity)

The remainder of the Tiller clay block sample was used, with the salinity kept constant. The salinity of the clay was determined to be 2.3 g/L. It is important to note that the natural salinity of Tiller clay is typically 1.8 g/L, however, due to the long storage time and water evaporation the salinity measure has increased. Figure 3.1 shows the effect that storage and time contributes to water content. A brine solution of de-ionized water and salt was made with a ratio of 2.3 g of salt per litre. Brine was continuously added to the remoulded clay, maintaining a constant salinity with increasing water content. Samples of the slurry, at the required remoulded shear strength, were taken and stored in the fridge until further testing.

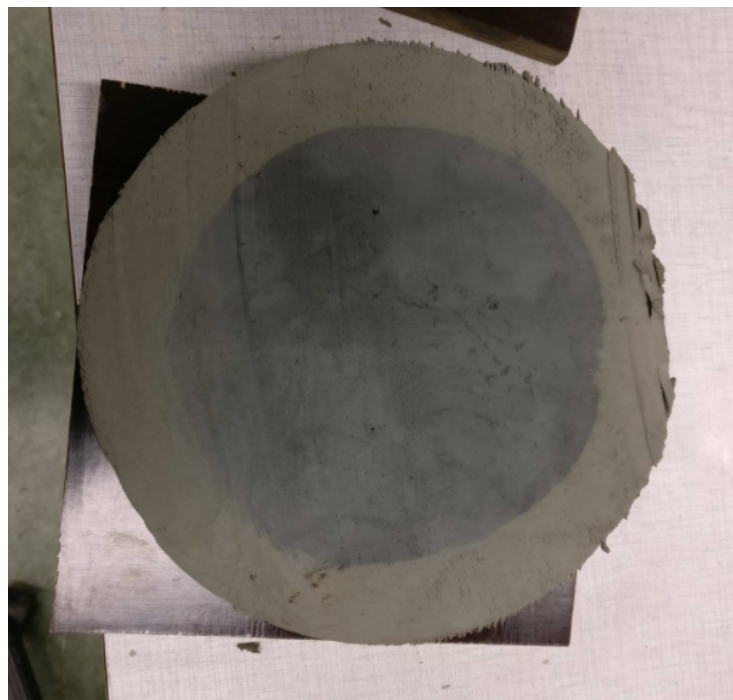


Figure 3.1: Cross-section of Tiller block sample showing the effect of storage time on the natural water content. Block sample stored at 4°C for 3.5 years. Dark grey inner portion shows closer to natural clay while outer light grey represents clay with water loss due to exposure.

Material 3 – Perniö Clay (Quick clay)

Due to the high water content and short storage time (4 months) in comparison with the Tiller clay, remoulding was relatively straight forward. Care was, however taken to ensure all small clumps were fully broken down. The initial remoulded shear strength was 0.1 kPa so drying of the sample was required. This was achieved by moisture evaporation at room temperature as well as using a hair dryer to speed up the process. Once each of the desired remoulded shear strengths were obtained and quickness test performed, approximately 200-400 mL of the clay slurry was sealed in plastic containers and stored in the fridge until further testing.

Material 4 – Clayey Silt

An artificial clayey silt was produced. As stated in Section 2.2.3, the clay content of a 'clayey' soil must be between 5-15%. Vassfjellet soil was used which composed of 94% silt particles (smaller than 75 μm) and 2.5% clay particles (smaller than 2 μm). The soil was sieved extracting out 2500 g of material less than 75 μm . No grains larger than 75 μm were used as the natural clay soils (Materials 1-3) contained no sand particles. To increase the clay content to a desired amount of approximately 15%, a measured quantity of Tiller clay 2 (*CF* 55%) was reused and added. To thoroughly mix the Vassfjellet silt and Tiller clay, de-ionized water was used and hence the initial shear strength was less than 0.1 kPa. Drying was required and achieved using a hair dryer. Once each of the desired remoulded shear strengths were obtained, approximately 200-400 mL of the clay slurry was sealed in plastic containers and stored in the fridge until further testing.

Material 5 – Silt

Similar to Material 4, an artificial silt was produced. Vassfjellet soil was sieved extracting out 2000 g of silt particles less than 75 μm . This contained approximately 2.7% of clay particles. To increase the clay content of the silt to approximately 5%, 120 g of dry, ground Tiller clay particles from Material 1 (*CF* 40%) were added and thoroughly mixed. The same process of increasing the remoulded shear strength by drying was followed and samples taken and stored for further testing.

3.4 Index Tests

3.4.1 Water Content

The water content was measured by first weighing the wet sample, before being left to oven dry at a temperature of 110°C for a minimum of 24 hours. The weight of the dry sample was then measured and the water content calculated using equation (2.2). The procedure was in accordance with NS8013 (1982).

3.4.2 Salinity

Pore water was pressed out of the sample using air pressure and the electric conductivity was measured in NaCl-equivalents. A calibration chart was used to convert the conductance to salt content (g/L).

3.4.3 Atterberg Limits

Determination of the plastic limit was done by rolling the remoulded material into threads by using a flat hand against a glass surface. The threads were folded and re-rolled until they started to crumble at a diameter of 3 mm. The pieces were stored in a small glass vial with a lid to prevent evaporation. Once 20 g of crumbled material was collected, the water content was determined (by the procedure described in 3.4.1). This water content corresponds to the material's plastic limit, w_p . The procedure was in accordance with NS8003 (1982).

The liquid limit was determined using the Casagrande method as described in NS8001 (1982). Remoulded material was placed into the Casagrande cup and divided down the centre by a grooving tool, 2mm in width. The liquid limit was found when it took 25 drops of the cup to close the 2 mm wide gap over a length of 12.5 mm. The water content, corresponding to the liquid limit, w_L , was then determined (by the procedure described in 3.4.1). With the Atterberg limits determined, the plasticity index, I_p , and the liquidity index, I_L were calculated using equations (2.3) and (2.4).

3.4.4 Remoulded Shear Strength

The remoulded shear strength was determined using the fall-cone apparatus. The cone types used were the 60 g, 60° and 10 g, 60° cones. The procedure was in accordance with NS8015 (1982). The indentation was recorded and converted to shear strength using the calibration tables. As the materials strength reduced and the indentations became greater than 15.0 mm using the 60 g cone, the 10 g was used.

3.5 Quickness Tests

3.5.1 Test Setup and Procedure

The material's quickness was determined with a similar procedure to the slump test used for concrete. A Standard Proctor mould (height: 123 mm, diameter: 100 mm, volume: 966 cm³) was coated with a thin layer of silicon oil internally to provide a non-stick surface. Oil was also applied to the test surface to reduce frictional forces during testing.

The mould was filled with remoulded material with the top surface levelled off. Material with a remoulded shear strength greater than 0.5 kPa required additional stirring within the mould to ensure no air voids remained which would compromise the test and produce erroneous results.

The mould was manually lifted vertically, in a smooth fluid motion allowing the material to flow out unsupported. The quickness test procedure is illustrated in Figure 3.2.

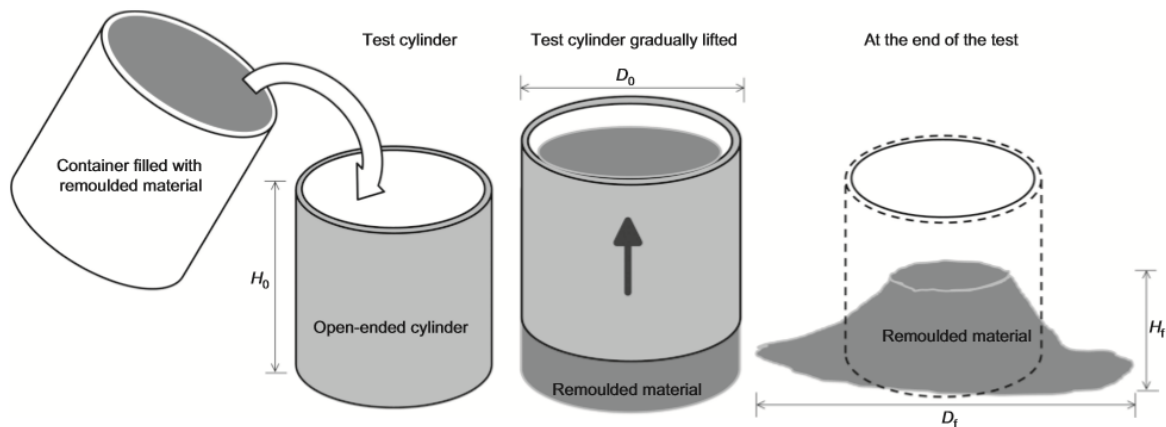


Figure 3.2: Quickness test procedure. From (Thakur and Degago, 2012)

The quickness tests were performed in the laboratory at room temperature on a sheet of clear plastic. A high-definition camera was used to film and document the tests, with grid paper (10mm x 10mm squares) placed on both the horizontal and vertical planes to offer an indication of scale (Figure 3.3).

After testing, final height measurements were taken by inserting a clean blade into the middle of the sample, then withdrawing it to measure the extent that the slurry reached using a 30 cm ruler. Base measurements were taken using a 1 m ruler. The quickness value, Q (%), was then calculated using equation (2.7). Figure 3.4(a-f) shows the slump progression for a typical quickness test.

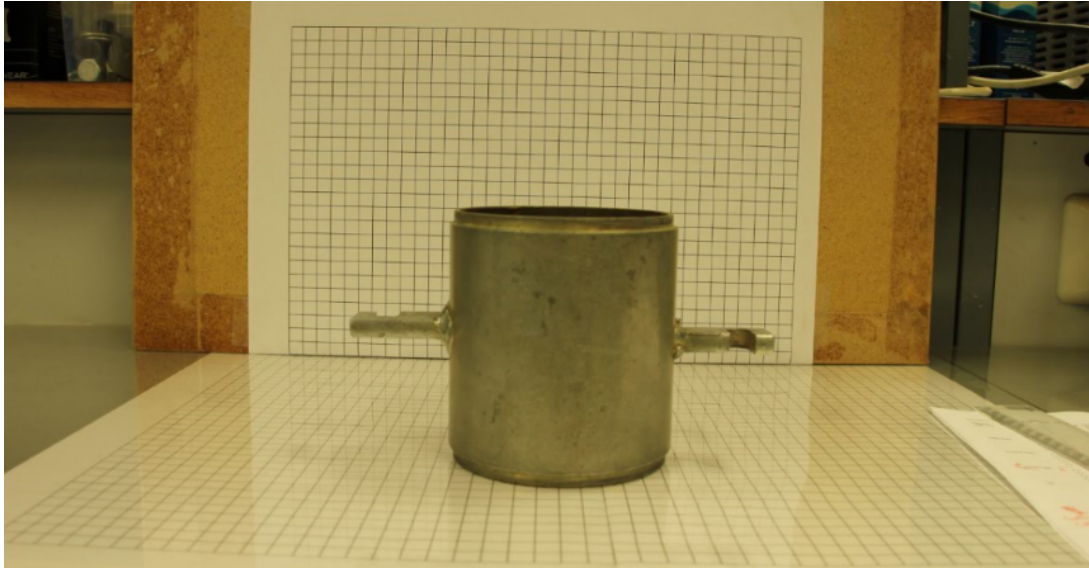


Figure 3.3: Quickness test laboratory set-up

The water content was determined (by the procedure described in Section 3.4.1) with 200-400mL of the slurry taken and stored for later viscometer testing (as discussed in Section 3.3).

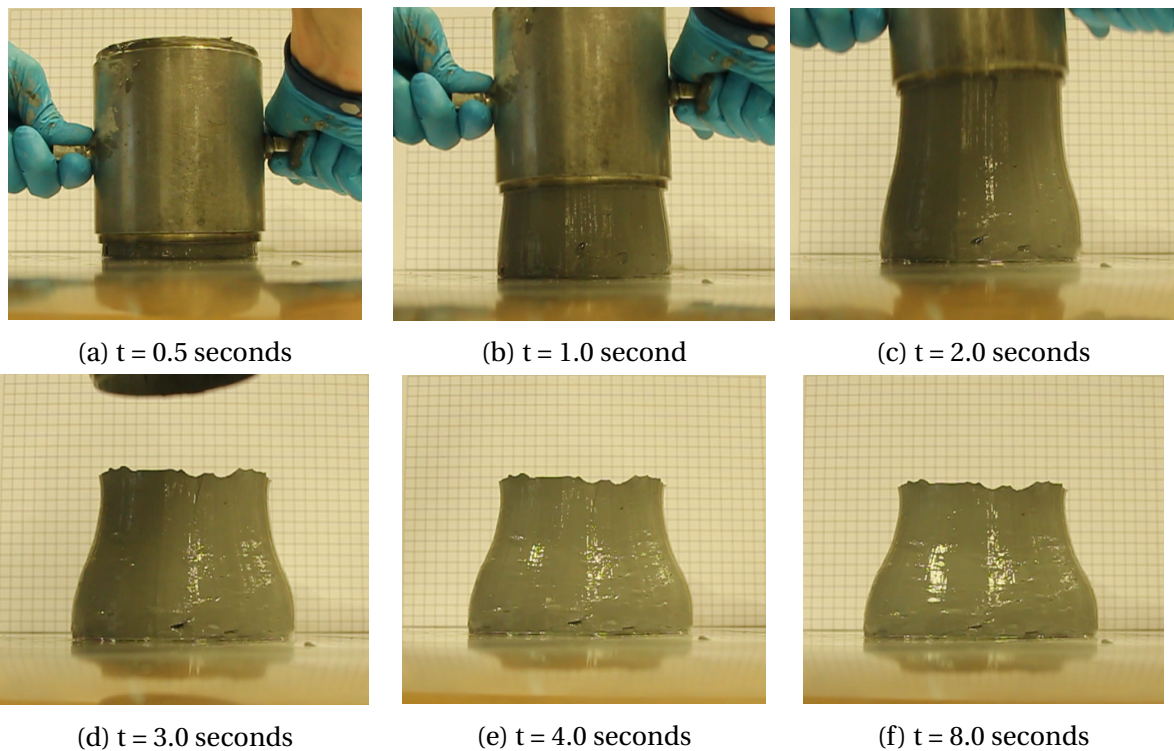


Figure 3.4: Slump and spread progression with time for a quickness test performed on Tiller Clay 1, $c_{ur} = 0.39$ kPa. Final deformation shape reached after 8 seconds.

3.5.2 Sample Preparation

As stated in Section 3.3, de-ionized water (or brine) was intermittently added to the material slurries, increasing the water content and reducing the shear strength. After the addition of water, fall-cone tests were performed and the remoulded shear strength calculated. Once the material had been deemed to reach the required strength (refer to Table 3.2), based on multiple fall-cone tests (more than 5 measurements) on a representative sample of the slurry, the quickness test was performed. After the quickness test measurements were taken, and the water content and viscometer testing samples obtained, the remainder of the material was placed back into the mixing bowl for re-use and the procedure repeated.

3.5.3 Basic Assumptions

Once the mould had been filled and the sample mixed thoroughly to remove air voids, the cylinder was lifted as shortly as possible afterwards. This negates the effect of soil segregation, which is particularly prevalent in soils with high silt contents.

The cylinder is gradually lifted vertically upwards, in a constant motion to ensure uniformity between tests which allows for accurate comparison of results. It also limits the effect of any possible friction between the soil and mould. Furthermore, it is assumed there is no friction between the soil and the test surface which could effect the degree of material slump and spread.

The deformation of the sample begins as soon as the mould is lifted. The final deformation shape is reached shortly after the mould has been removed (approximately 8 seconds). The final slump and spread measurements are taken approximately 30 seconds after testing.

Due to the large quantity of tests required and time constraints, the fall-cone tests and quickness tests were performed as soon as possible after the addition of water to the remoulded soils. As a result, any effects that time plays on the shear strength from a molecular structure have been neglected, and the remoulded shear strength calculated from the fall-cone test accepted as the characteristic strength of the soil sample.

3.6 Viscometer Tests

A coaxial cylinder sensor viscometer was used to determine the rheological behaviour of fine-grained soils and measure the viscometrical properties in the laboratory as part of this thesis.

3.6.1 Instrument

A Bohlin Visco 88 BV viscometer was used in these experiments (seen in Figure 3.5). The apparatus uses coaxial cylinder geometry and features eight speed settings in geometric progression ranging from 20 to 1000 rpm. The inner cylinder spins at the desired speed within the stationary outer cylinder. The shear rate is directly proportional to the rotational speed, N , where angular velocity, ω (rad/s) is calculated by:

$$\omega = 2\pi N \quad (3.1)$$



Figure 3.5: Bohlin Visco 88 BV viscometer instrument

The instrument measures torque (mNm), frequency (Hz) and temperature ($^{\circ}\text{C}$). It also calculates and displays; viscosity (Pa.s), shear rate (1/s) and shear stress (Pa); however these values are calculated based on formulas for Newtonian liquids (Bohlin, 2006) and should therefore not be used when testing fine-grained soils which exhibit non-Newtonian liquid behaviour. By using the rotational speed and torque readings, the shear rate and shear stress for a Hershel Bulkeley fluid can be calculated.

Table 3.3: Rotation speed options for the Bohlin Visco 88 BV. From Bohlin (2006)

Speed Switch Position	Rotational Speed, N (Hz/rps)	Angular Velocity, ω (rad s ⁻¹)
1	0.33	2.09
2	0.58	3.67
3	1.02	6.39
4	1.78	11.21
5	3.12	19.58
6	5.45	34.24
7	9.53	59.90
8	16.67	104.72

A wide-gap system was used for testing, with only one combination of cylinders used for simplicity and to utilize the smallest gap ratio with the available equipment. The viscometer cylinder properties can be seen in Table 3.4 and components shown in Figure 3.6.

Table 3.4: Viscometer Cylinder Properties

Inner cylinder radius, R_i (mm)	Height, h (mm)	Outer cylinder radius, R_o (mm)	R_o/R_i (-)
7.0	21.1	13.75	1.96



(a) Viscometer



(b) Inner Cylinder (Spindle)



(c) Outer Cylinder

Figure 3.6: Bohlin Visco 88 BV viscometer components

3.6.2 Sample Preparation and Steady State Conditions

Once the samples were prepared in the laboratory by varying the water content and the desired remoulded shear strength was obtained, they were then stored in the testing room. The room temperature varied between 4-7°C, with the aim was to test the samples at 7°C which represents the approximate ground temperature.

Before testing, the samples were thoroughly mixed to ensure a homogeneous material, before being placed into the outer cylinder of the viscometer. The apparatus was lowered until the inner cylinder was submerged in the sample, and the outer cylinder locked into place. The instrument was then started and the sample sheared until an equilibrium torque was obtained. Equilibrium torque was achieved by applying different rotational speeds for 2 minutes each, every time with the highest speed (Speed 8) for 2 minutes in between. This procedure could take from 30 minutes to over 2 hours. Equilibrium torque was chosen as the lowest recorded value that was attained every time the speed was changed from a lower speed to speed 8. The value was chosen as the start value to ensure the same start conditions for every new rotational speed during the dynamic test.

Remoulding the sample prior to testing resulted in a temperature increase due to internal friction effects. Once the instrument was started the sample was sheared at the maximum speed (Speed 8) until the temperature reduced and stabilized, before the equilibrium torque procedure could begin.

3.6.3 Dynamic Response Test

After the steady state torque conditions were reached, the viscometric test was started. The velocity of the inner cylinder was decreased stepwise from speed 8 to lower speeds, until the final step was from speed 8 to speed 1 (ie. the sequence was speed 8, speed 7, 8, 6, 8, 5, ... 8, 2, 8, 1). The rotational speeds corresponding to each speed setting is presented in Table 3.3. The torque (T) required to maintain a constant rotation speed at 15 seconds was recorded as well as the rotation speed (N). The recorded torque values at 15 seconds were plotted against the rotation speeds. One test consisted of 8 speeds, which resulted in a torque-rotation speed ($T-N$) curve consisting of 8 points. This test sequence used was based on precedent (Locat and Demers, 1988; Grue, 2015). After 2 minutes at one speed, the rotation speed was increased to speed 8, and held at this speed until the equilibrium torque was reattained. The speed was then reduced to the next value in the sequence.

In addition to recording the torque at 15 seconds, measurements were also taken at 0 s, 5 s, 10 s, 20 s, 30 s, 40 s, 60 s and 120 s after the rotation speed had been decreased. This was done to

investigate how the torque varied with time at constant rotational speeds. The temperature and rotational speed were recorded after 60 seconds.

Recordings were taken manually and achieved by reading the instrument display (shown in Figure 3.6a) at each time interval. A stopwatch taped to the viscometer next to the display was used to record time. The stopwatch was only started each time the speed was reduced from speed 8 when an initial torque value was registered. In some instances, particularly at lower speeds, there would be a delay of a few seconds between changing the speed setting and the display registering a torque measurement.

3.6.4 Basic Assumptions

The basic assumptions for measuring viscosity with a coaxial cylinder viscometer as proposed by Schramm (1994) are:

- Laminar flow;
- Steady state flow;
- No slippage; and
- Samples must be homogeneous.

The applied shear must lead only to laminar flow with any turbulence results excluded from the flow curves. The torque required to maintain a turbulent flow is much higher than to maintain laminar flow and hence the torque measured is not proportional to the true viscosity of the fluid (Schramm, 1994). Grue (2015) showed that turbulent flow can be detected when the initial equilibrium torque value is much higher than the torque at lower speeds, and doesn't fit the trend curve created by the torque values for speeds 1 to 7.

The applied shear stress is correlated to the shear rate. The torque should not be recorded during acceleration or deceleration of the flow as the change in flow might require more energy than to continue a steady state flow. For this reason the torque measurement after 15 seconds is used as the rotation speed is assumed to have attained a constant value.

An important assumption is that the tested material is uniformly sheared without slip between the sample and outside cylinder wall. At the moving boundary the velocity and torque is recorded, however, there should be no slippage between the test material and the stationary boundary ie. zero flow velocity.

Chapter 4

Data Processing

This chapter outlines and describes the processing of quickness test and viscometric test raw data. Determining the quickness value of a sample is straight forward. Processing the viscometer data however is more complicated, with the calculation procedure of shear stress and shear rate from the measured torque and rotation speed presented.

4.1 Quickness Test Data

The quickness test is performed in accordance with the procedure outlined in Section 3.5.1. The initial height, H_o , of the sample is measured. Ideally the mould is completely full and the starting height of each test consistent. After testing, the final height, H_f , and lateral spread, D_f , are measured and the quickness value is calculated by the following expression:

$$Q = \left(\frac{H_o - H_f}{H_o} \right) \cdot 100 \quad (\%) \quad (4.1)$$

4.2 Viscometer Test Data

The basic equations for how the shear rate and shear stress varies over a wide gap concentric cylinder viscometer are described. The shear rate in a rotational flow is defined as:

$$\dot{\gamma}(r) = r \frac{\partial \omega(r)}{\partial r} \quad (4.2)$$

with r the radial cylindrical coordinate (m) and $\omega(r)$ the angular velocity at radius r (rad/s) (Heirman et al., 2008). This equation can be applied for both narrow or wide gap systems.

The shear stress of a fluid in a concentric rheometer depends only on the rheometer geometry and not the nature of the fluid (Heirman et al., 2008). The shear stress applied to the inner cylinder by the test material can be expressed by:

$$\tau(r) = \frac{T}{2\pi r^2 h} \quad (4.3)$$

where T is the measured torque (Nm) and h the height of the inner cylinder (m).

Using the Herschel-Bulkley model to fit the rheological model of the fine-grained soils tested, the derived equations for shear rate (equation 4.2) and shear stress (equation 4.3) are substituted into equation 2.11. The resultant Herschel-Bulkley model formula becomes:

$$\frac{T}{2\pi r^2 h} = \tau_y + K \left(r \frac{\partial \omega(r)}{\partial r} \right)^n \quad (4.4)$$

Assuming idealistic no slip boundaries conditions, zero flow velocity at the stationary outer cylinder $\omega(R_o) = 0$, and the maximum angular velocity at the inner cylinder $\omega(R_i) = \Omega_i$, where Ω_i is the angular velocity of inner cylinder (rad/s). Using equation 3.1, angular velocity may be expressed as:

$$\Omega_i = 2\pi N \quad (4.5)$$

where N is the rotation speed (rps).

Expressing equation 4.4 as an integral in terms of the variable r :

$$\int_{R_o}^{R_i} \left(\left(\frac{T}{2\pi r^2 h} - \frac{\tau_y}{K} \right)^{1/n} \frac{1}{r} \right) dr = \int_0^{\Omega_i} d\omega(r) \quad (4.6)$$

Since the Herschel-Bulkley model assumes shear thinning behaviour, the exponent n can range between 0 and 1. This integral can not be solved analytically into a general form when $n \neq 1$, however Heirman et al. (2008) developed an expression used to transform the solution into a general form. It involves dividing the flow behaviour of a material into a flow resistance constant, G_{HB} , which is independent of flow rate, and a flow dependant component, $H_{HB}H^J$, where H_{HB} is the viscosity factor and J is the flow index factor. Therefore, a relationship between torque and rotational speed is reached and expressed as:

$$T = G_{HB} + H_{HB}N^J \quad (4.7)$$

where G_{HB} is calculated in mNm, H_{HB} in $mNms^J$ and J dimensionless.

To determine the general solution terms based on the dynamic response test results, the function $T = G_{HB} + H_{HB}N^J$ was fitted to the data $T(N)$ in Matlab[®] R2016b by using the non-linear least square method, represented by a 'power2' fit. For each test, 7 fits were

performed based on precedent ([Grue, 2015](#)).

These data fits were to:

- Fit 1: All eight points;
- Fit 2: The seven last points (data point, T , at the lowest rotation speed, N , excluded);
- Fit 3: The seven first points (point at highest speed excluded);
- Fit 4: The six first points (points at the two highest speeds excluded);
- Fit 5: The five first points (points at the three highest speeds excluded);
- Fit 6: The five middle points (points at the lowest speed and two highest speeds excluded); and
- Fit 7: The six middle points (points at the lowest speed and highest speeds excluded).

After selecting the best fit, the Herschel-Bulkley parameters τ_y , n and K were calculated with the following equations:

$$\tau_y = \frac{G_{HB}}{4\pi h} \left(\frac{1}{R_i^2} - \frac{1}{R_o^2} \right) \frac{1}{\ln(R_o/R_i)} \quad (4.8)$$

$$n = J \quad (4.9)$$

$$K = \frac{H_{HB}}{2^{2n+1}\pi^{n+1}h} n^n \left(\frac{1}{R_i^{2/n}} - \frac{1}{R_o^{2/n}} \right)^n \quad (4.10)$$

Refer to [Heirman et al. \(2008\)](#) for the derivation of formulas.

Chapter 5

Results and Discussion

In this chapter, laboratory test results are presented for the five fine-grained soils studied. The quickness test results are contained in Appendix A. Fitted Herschel-Bulkley parameters are presented including past data with the results analysed and correlations drawn. The viscometer data and results can be found in Appendix C and D. All past viscometer results outlined in Chapter 2.7.3 can be found in Appendix B. The soil characteristics for the fine-grained soils can be found in Table 5.1.

5.1 Index Tests

Results from index testing for all tests are presented in Table 5.1. The initial water content for each sample was determined after the remoulded shear strength was measured using the fall-cone test, and the quickness test performed. In excess of 250 water content measurements were taken, providing accurate characterization for each soil. Figure 5.1 shows the results of the remoulded shear strength plotted against water content. Figure 5.2 shows the remoulded shear strength plotted against normalized water content (w/w_L), which is a more accurate tool for comparison than using the liquidity index. The results show that the water content before (w_{before}) and after (w_{after}) viscometric testing are approximately the same for all tests (within 1.3%).

Due to the addition of salt as well as de-ionized water to clay, the Atterberg Limits vary with water content (observed for the Tiller Clay 2). De-ionized water alone does not change the liquid and plastic limits of a soil, hence the Atterberg Limits of the other soils remain constant with varying water content. The liquidity indices (I_L) for the samples vary from 1.16 to 5.31, and the salinity (S) is in the range of 1.01 to 2.30 g/L.

Table 5.1: Results from index testing on fine-grained soils

Material	c_{ur} (kPa)	S (g/L)	w (%)	w_{before} (%)	w_{after} (%)	w_L (%)	w_P (%)	I_P (%)	I_L (-)
Tiller Clay 1 (Tiller clay + water)	< 0.10	1.74	63.45	63.80	63.54	33.80	21.37	12.43	3.39
	0.10	1.84	55.82	55.26	55.12	33.80	21.37	12.43	2.77
	0.20	1.88	50.83	51.14	50.49	33.80	21.37	12.43	2.37
	0.29	1.90	47.53	47.40	47.53	33.80	21.37	12.43	2.10
	0.39	1.91	45.83	-	-	33.80	21.37	12.43	1.97
	0.49	1.92	45.75	-	-	33.80	21.37	12.43	1.96
	0.65	1.94	44.42	-	-	33.80	21.37	12.43	1.85
	0.80	1.95	43.11	-	-	33.80	21.37	12.43	1.75
	0.95	1.96	42.49	-	-	33.80	21.37	12.43	1.70
Tiller Clay 2 (Tiller clay + brine)	< 0.10	2.30	92.81	92.48	91.75	36.00	23.00	13.00	5.31
	0.10	2.30	66.32	66.67	66.64	37.91	24.45	13.46	3.11
	0.20	2.30	57.56	57.91	57.93	37.99	24.94	13.05	2.50
	0.29	2.30	52.00	51.46	51.32	38.05	24.26	13.79	2.01
	0.39	2.30	48.65	-	-	38.22	24.39	13.83	1.76
	0.49	2.30	47.64	-	-	38.34	24.56	13.78	1.67
	0.59	2.30	45.38	-	-	39.58	24.53	15.05	1.39
	0.78	2.30	43.63	-	-	39.71	24.61	15.10	1.26
	0.95	2.30	42.78	-	-	40.39	24.87	15.52	1.16
Perniö Clay (Perniö clay + water)	< 0.10	1.01	95.22	95.77	94.66	56.98	25.76	31.22	2.23
	< 0.10	1.02	90.68	92.18	91.71	56.98	25.76	31.22	2.08
	0.10	1.04	83.08	85.37	84.37	56.98	25.76	31.22	1.84
	0.20	1.26	81.05	80.65	81.99	56.98	25.76	31.22	1.70
	0.29	1.40	74.28	74.19	74.80	56.98	25.76	31.22	1.56
	0.39	1.51	70.79	71.44	72.64	56.98	25.76	31.22	1.45
	0.50	1.61	69.08	70.35	70.63	56.98	25.76	31.22	1.39
	0.70	1.78	68.40	68.82	68.81	56.98	25.76	31.22	1.28
	0.98	1.95	61.14	-	-	56.98	25.76	31.22	1.19
Clayey Silt (Vassfjellet silt + Tiller clay + water)	< 0.10	1.56	58.49	58.00	58.05	32.68	22.53	10.15	3.54
	0.10	1.66	52.18	51.74	52.00	32.68	22.53	10.15	2.92
	0.20	1.71	50.47	50.91	51.02	32.68	22.53	10.15	2.75
	0.29	1.74	47.66	47.97	48.00	32.68	22.53	10.15	2.48
	0.39	1.76	44.74	-	-	32.68	22.53	10.15	2.19
	0.49	1.78	43.23	-	-	32.68	22.53	10.15	2.04
	0.69	1.81	41.85	-	-	32.68	22.53	10.15	1.90
	0.98	1.84	40.16	-	-	32.68	22.53	10.15	1.74
	Silt (Vassfjellet silt + water)	< 0.10	0.41	42.98	41.70	55.68	25.22	0.00	25.22
0.10		0.44	38.98	39.93	44.91	25.22	0.00	25.22	1.55
0.20		0.45	37.52	37.30	45.37	25.22	0.00	25.22	1.49
0.29		0.46	36.31	36.06	44.42	25.22	0.00	25.22	1.44
0.39		0.47	35.33	-	-	25.22	0.00	25.22	1.40
0.59		0.48	34.50	-	-	25.22	0.00	25.22	1.37
1.00		0.52	34.04	-	-	25.22	0.00	25.22	1.35

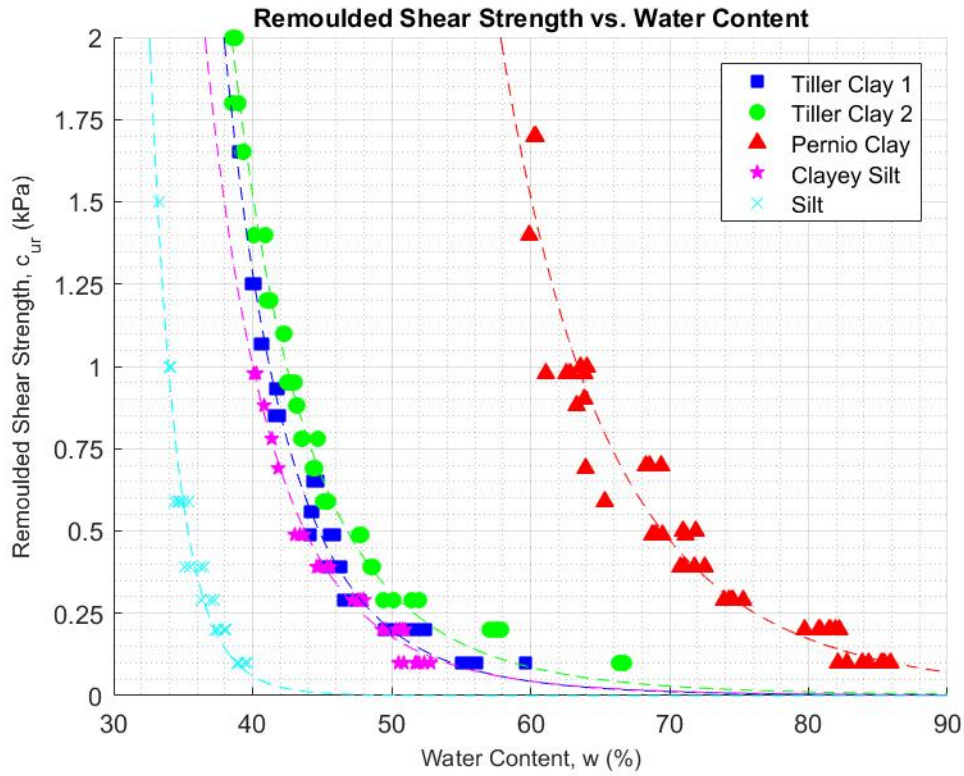


Figure 5.1: Relationships between water content and remoulded shear strength

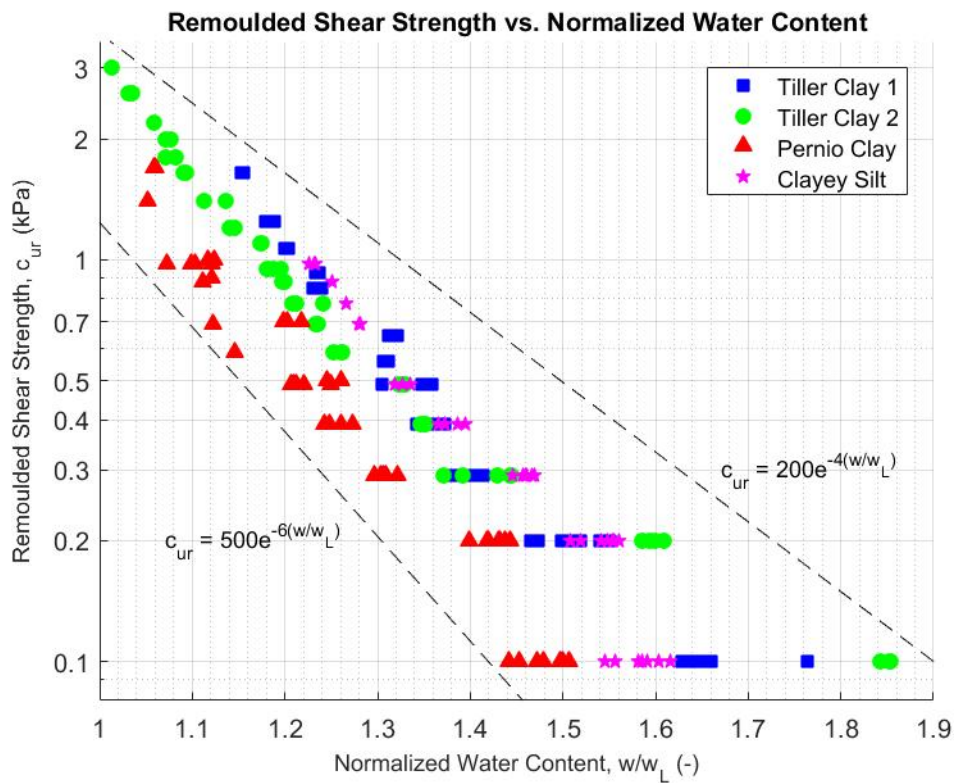


Figure 5.2: Relationships between normalized water content and remoulded shear strength

The salinity for each sample was measured and plotted (Figure 5.3). Some irregularities were noted, particularly for the Perniö clay material, in that some samples with higher water content measured a higher salinity when the presence of more water should lower the salinity levels. This may be due to the small samples used to determine the salinity, which may not have been representative of the parent sample, as well as possible evaporation during testing at room temperature. To rectify these sources of error, exponential trend lines have been fitted to the raw data results to determine the reducing salinity with reducing shear strength. The Tiller Clay 2 soil has a linear relationship given the salinity was kept constant.

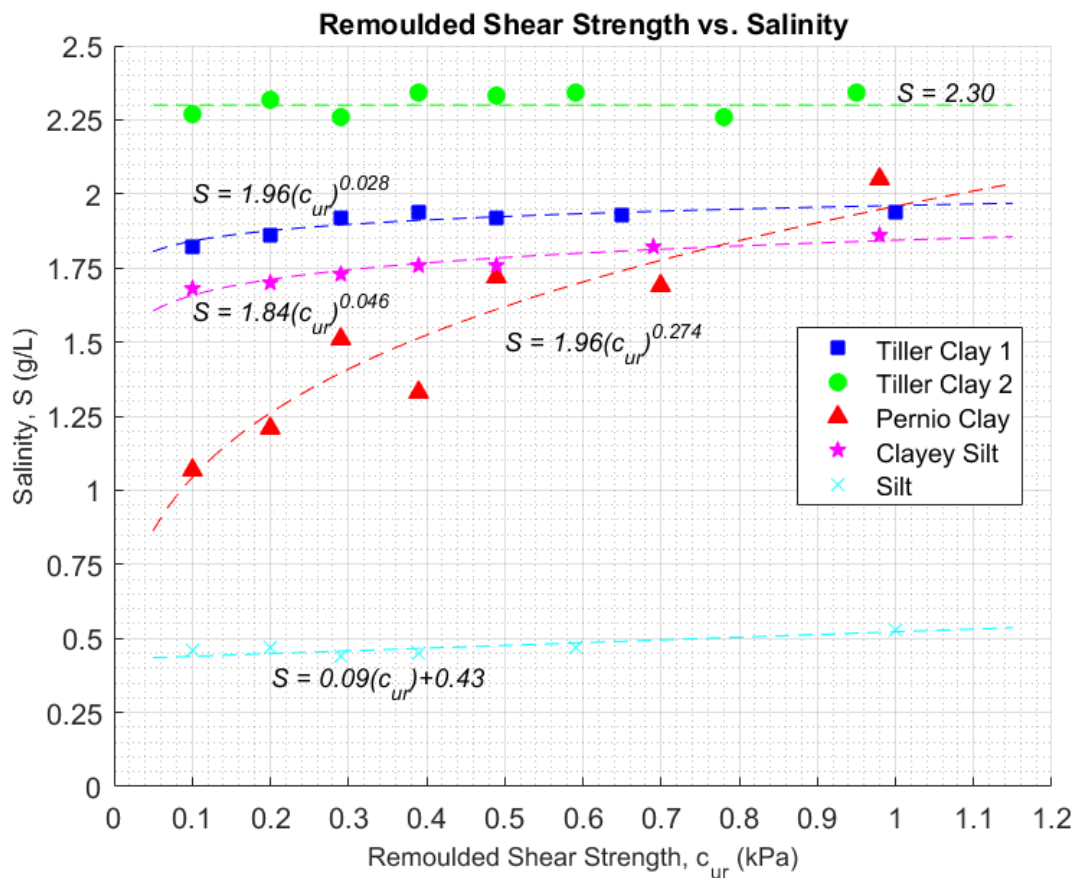


Figure 5.3: Relationships between salinity and remoulded shear strength

Hydrometer analysis revealed the clay content of the Tiller Clay 1 sample tested to be 37% (Figure 5.4). Hence confirming the material designation of clay (CF higher than 30%). The clay content of the Tiller Clay 2 material was 51%. Both values are within the expected values range for the Tiller site at a depth of 10m, found in Table 3.1 (Gylland et al., 2013). It must be noted that the analysis done on the Tiller Clay 1 was a natural sample taken from the block sample. The analysis for the Tiller Clay 2 material came from a sample taken after quickness testing was completed, at a remoulded shear strength of 0.1kPa. The higher concentration of fines may be attributed to the repeated use of the material and high water content. The clay

content of the Perniö clay was measured to be approximately 64% which is in fitting with the expected values as published by Mataić et al. (2016) (found in Table 3.1). The clay content for the reconstituted Clayey Silt and the Silt are 31% and 3% respectively, and hence confirming their material designation (refer to Section 2.2.3).

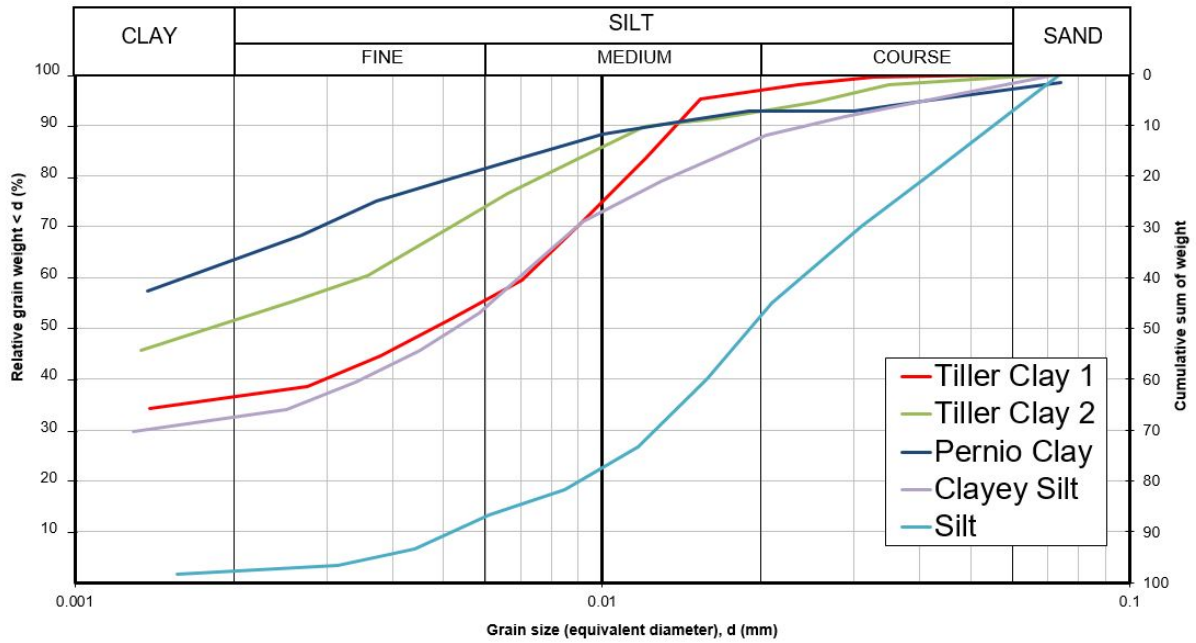


Figure 5.4: Grain size distributions for the fine-grained soils

5.2 Quickness Tests

In total 35 quickness tests were performed on the five fine-grained soils. The water content (and remoulded shear strength) was varied for each test in order to explore potential relationships with quickness. Test results and photos can be found in Appendix A. Table 5.2 outlines the key results.

Table 5.2: Results of quickness tests

Material	Remoulded Strength, c_{ur} (kPa)	Water Content, w (%)	Liquidity Index, I_L (-)	Normalized w.c., w/w_L (-)	Quickness, Q (%)
Tiller Clay 1	0.10	55.8	2.77	1.65	81.30
	0.20	50.8	2.37	1.50	66.67
	0.29	47.5	2.10	1.41	47.15
	0.39	45.8	1.97	1.36	40.65
	0.49	45.7	1.96	1.35	37.40
	0.65	44.4	1.85	1.31	31.71
	0.80	43.1	1.75	1.28	27.64
	0.95	42.5	1.70	1.26	25.20
Tiller Clay 2	0.10	66.3	3.11	1.75	80.49
	0.20	57.6	2.50	1.52	65.04
	0.29	52.0	2.01	1.37	46.34
	0.39	48.7	1.76	1.27	39.02
	0.49	47.6	1.67	1.24	34.15
	0.59	45.4	1.39	1.15	25.20
	0.78	43.6	1.26	1.10	24.39
	0.95	42.8	1.16	1.06	22.76
Perniö Clay	0.10	83.1	1.84	1.46	81.30
	0.20	81.1	1.70	1.42	60.16
	0.29	74.3	1.56	1.30	44.44
	0.39	70.8	1.45	1.24	37.84
	0.50	69.1	1.39	1.21	28.81
	0.98	62.6	1.19	1.07	13.33
Clayey Silt	0.10	52.2	2.92	1.60	70.73
	0.20	50.5	2.75	1.54	65.85
	0.29	47.7	2.48	1.46	55.28
	0.39	44.7	2.19	1.37	40.37
	0.49	43.2	2.04	1.32	33.65
	0.69	41.9	1.90	1.28	25.53
	0.98	40.2	1.74	1.23	17.95
Silt	0.10	39.0	1.55	1.55	57.73
	0.20	37.5	1.49	1.49	44.72
	0.29	36.3	1.44	1.44	40.95
	0.39	35.3	1.40	1.40	39.02
	0.59	34.5	1.37	1.37	26.39
	1.00	34.0	1.35	1.35	6.67

5.2.1 Effect of Remoulded Shear Strength on Quickness

Figure 5.5 shows the relationship between quickness and remoulded shear strength. The current test results have been plotted (*in colour*) as well as the past test results as discussed in Section 2.7.1 (*in black*). It can be seen that the clay materials as well as the clayey silt fit well with the proposed upper and lower quickness limits. The Silt material however did not behave the same due to high levels of segregation. This was clearly evident when the material was allowed to sit for a short period of time. The silt grains would settle and consolidate on the bottom while the water would rise to the top. It is for this reason of segregation that the results from quickness tests on the Silt have been excluded from any further analysis.

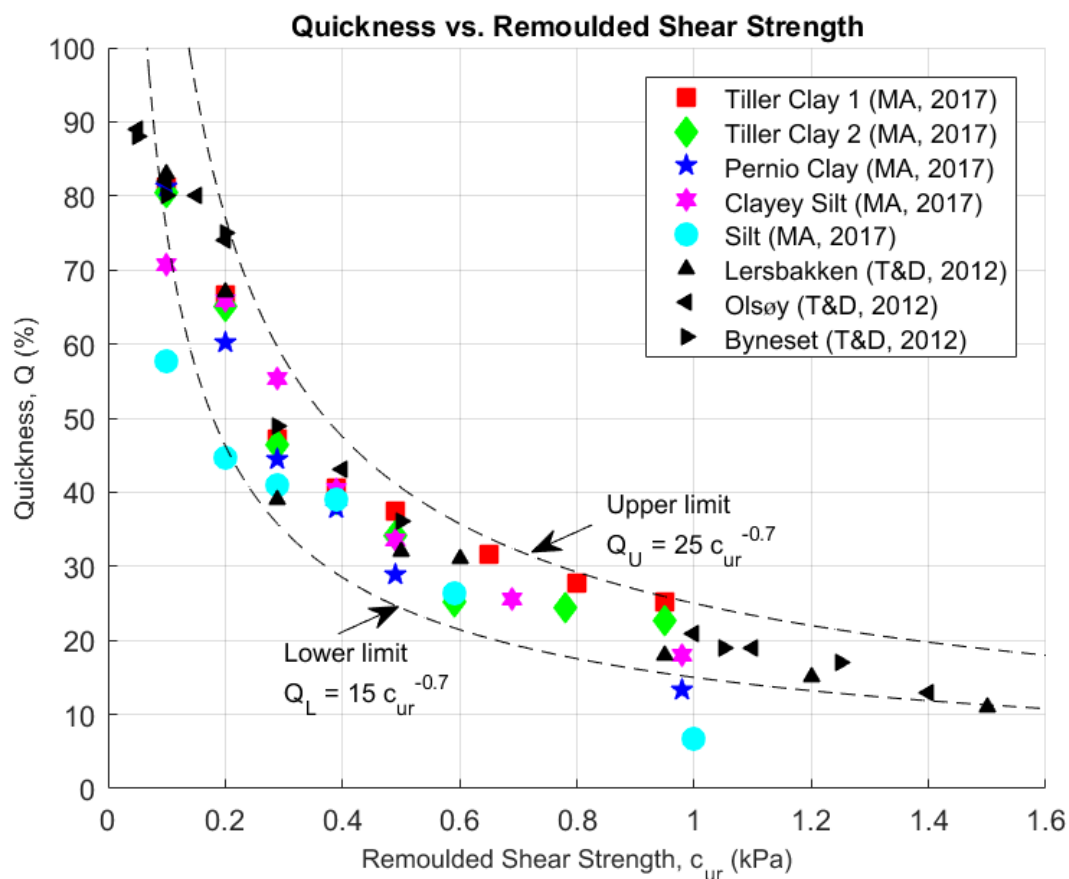


Figure 5.5: Relationship between quickness and remoulded shear strength

The relationships between remoulded shear strength and quickness can be expressed as:

Table 5.3: Relationship between c_{ur} and Q

Material	Relationship	R^2
Tiller Clay 1	$Q = 24.90(c_{ur})^{-0.54}$	0.984
Tiller Clay 2	$Q = 21.19(c_{ur})^{-0.62}$	0.966
Perniö Clay	$Q = 15.64(c_{ur})^{-0.79}$	0.954
Clayey Silt	$Q = 20.88(c_{ur})^{-0.63}$	0.909

The quickness relationships can also be expressed by adjusting the power coefficient of remoulded shear strength to -0.7, keeping it constant with the proposed quickness limits. Therefore, the best fit relationships with the lowest degree of variation become:

Table 5.4: Relationship between c_{ur} and Q with constant power coefficient of -0.7

Material	Relationship
Tiller Clay 1	$Q = 19.0(c_{ur})^{-0.7}$
Tiller Clay 2	$Q = 18.2(c_{ur})^{-0.7}$
Perniö Clay	$Q = 17.4(c_{ur})^{-0.7}$
Clayey Silt	$Q = 17.7(c_{ur})^{-0.7}$

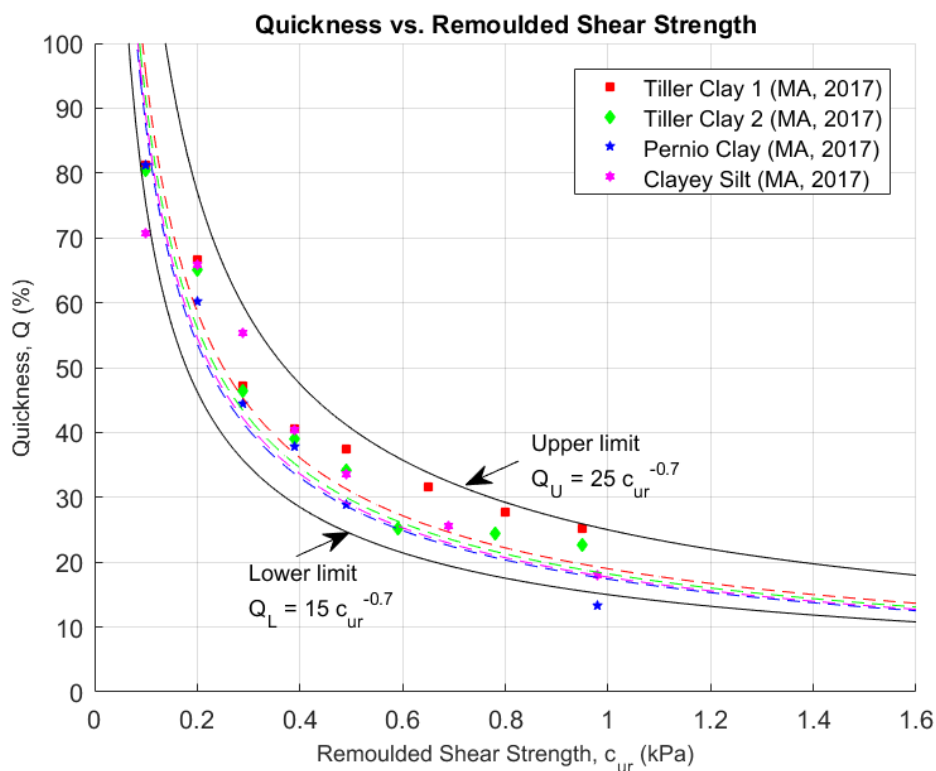


Figure 5.6: Relationship between quickness and remoulded shear strength with constant power coefficient of -0.7

5.2.2 Effect of Water Content on Quickness

Figure 5.7 shows the relationships between quickness and both the water content and liquidity index. There are no observable key trends when comparing the water content results between the different soils other than a decrease in quickness in observed with decreasing water content, as expected. Similarly, it is hard to draw concise conclusions from the liquidity index plot given the materials vary in clay content, plasticity and salinity which effect the flow properties as stated in Chapter 2.

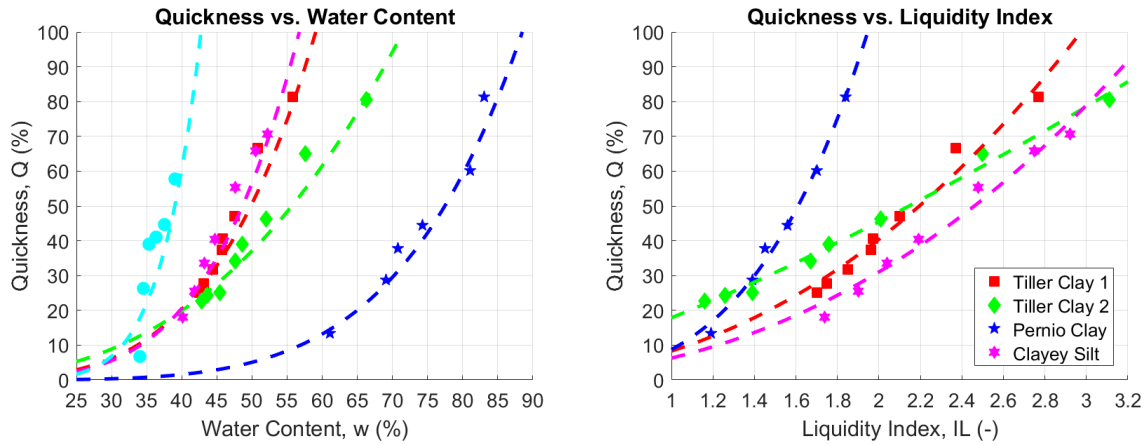


Figure 5.7: Relationships between quickness, water content and liquidity index

Figure 5.8 shows the relationships between quickness and the normalized water content calculated as a ratio of water content to liquid limit (w/w_L). An overall linear trend can be observed. The Tiller Clay 1, Pernio Clay and Clayey Silt have a similar gradient, while the Tiller Clay 2 has a gentler line gradient as a result of the addition of salt and the changing liquid limit.

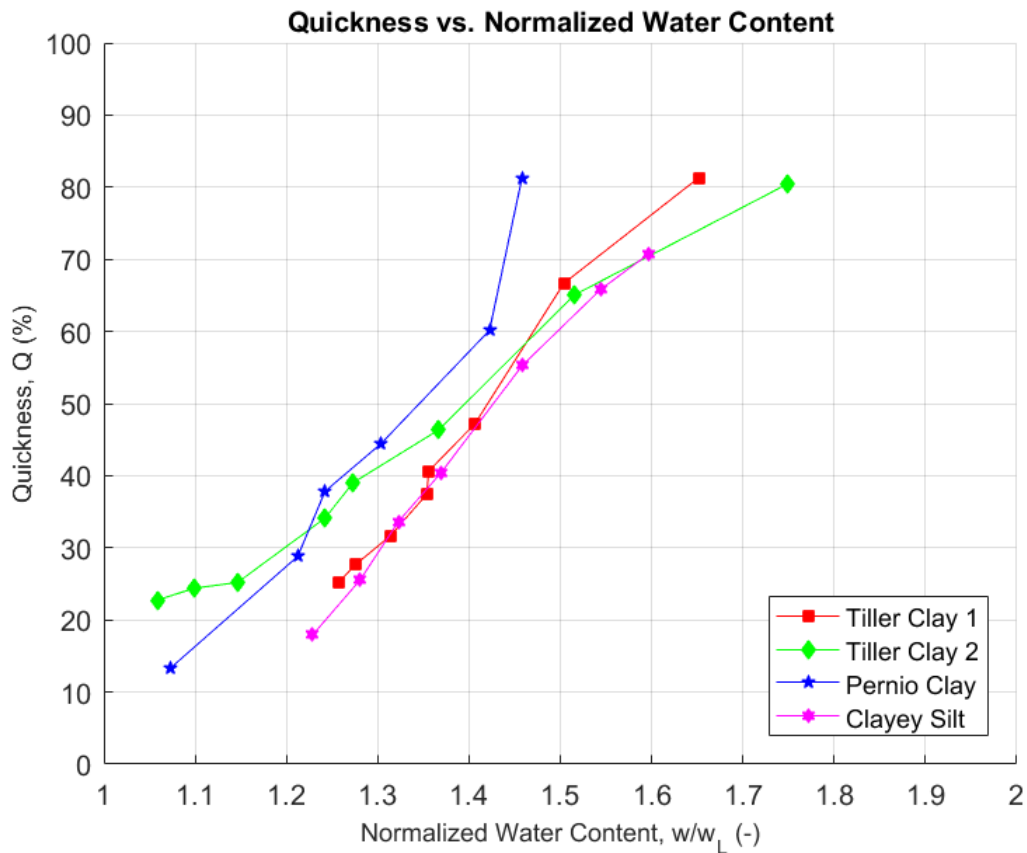


Figure 5.8: Relationship between quickness and normalized water content

It is also interesting to note that the Perniö Clay, with a much higher clay fraction is on the upper side of the trend as opposed to the Tiller Clay 1 and Clayey Silt with lower clay fractions on the lower side. It could also be proposed that as the Tiller Clay 2 has a clay fraction in between Perniö and Tiller 1 clays, the Q to w/w_L trend would also lie between the two (without the effect of altering the salinity). The relationships between normalized water content and quickness can be expressed as:

Table 5.5: Relationship between w/w_L and Q

Material	Relationship	R^2
Tiller Clay 1	$Q = 150(\frac{w}{w_L}) - 163$	0.986
Tiller Clay 2	$Q = 89(\frac{w}{w_L}) - 75$	0.987
Perniö Clay	$Q = 163(\frac{w}{w_L}) - 166$	0.946
Clayey Silt	$Q = 147(\frac{w}{w_L}) - 161$	0.994

The figure relating quickness and normalized water content (Figure 5.8) can be expanded upon, separating the data points not by material but by remoulded shear strength. In doing so, bands or areas can be established which represent certain c_{ur} values. This is illustrated in Figure 5.9.

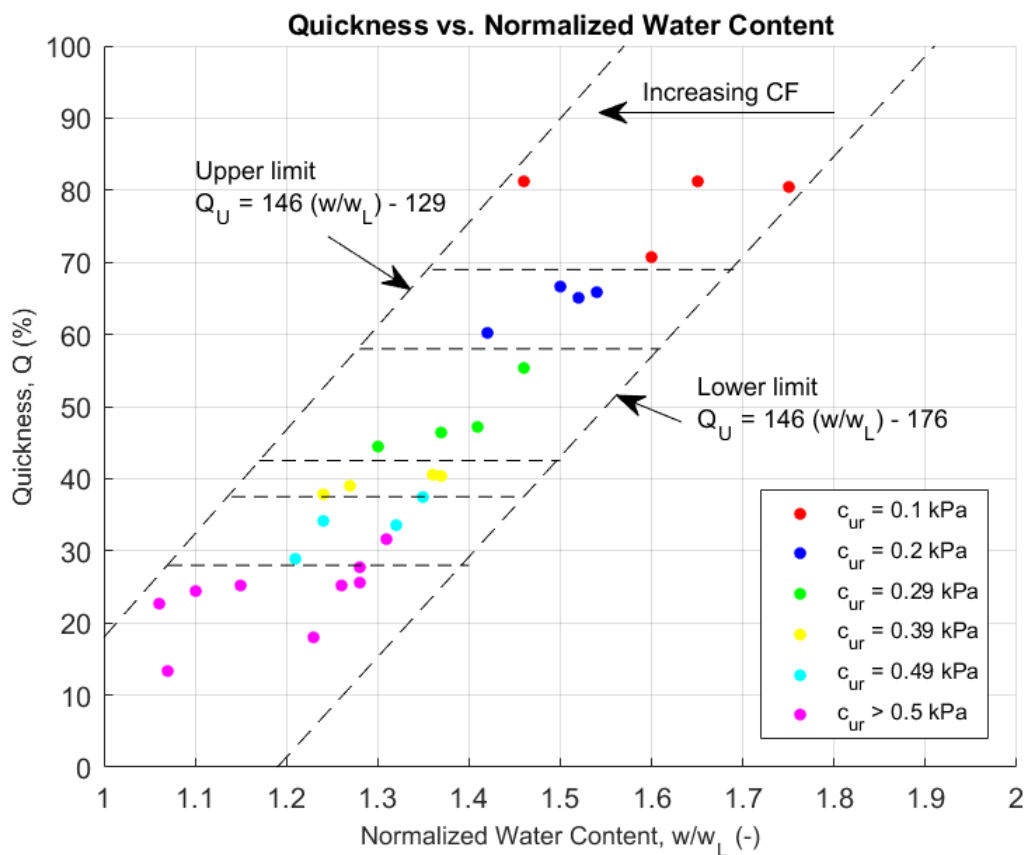


Figure 5.9: Relationship between quickness, normalized water content and remoulded shear strength

The upper and lower quickness limits are expressed as:

$$Q_U = 146 \left(\frac{w}{w_L} \right) - 129 \quad (5.1)$$

$$Q_L = 146 \left(\frac{w}{w_L} \right) - 176 \quad (5.2)$$

5.2.3 Effect of Salinity on Quickness

Figure 5.10 shows the relationships between quickness and salinity. There are no correlations between quickness and salinity, however it is known that reducing the water content of a soil increases the salinity and remoulded shear strength while decreasing the quickness.

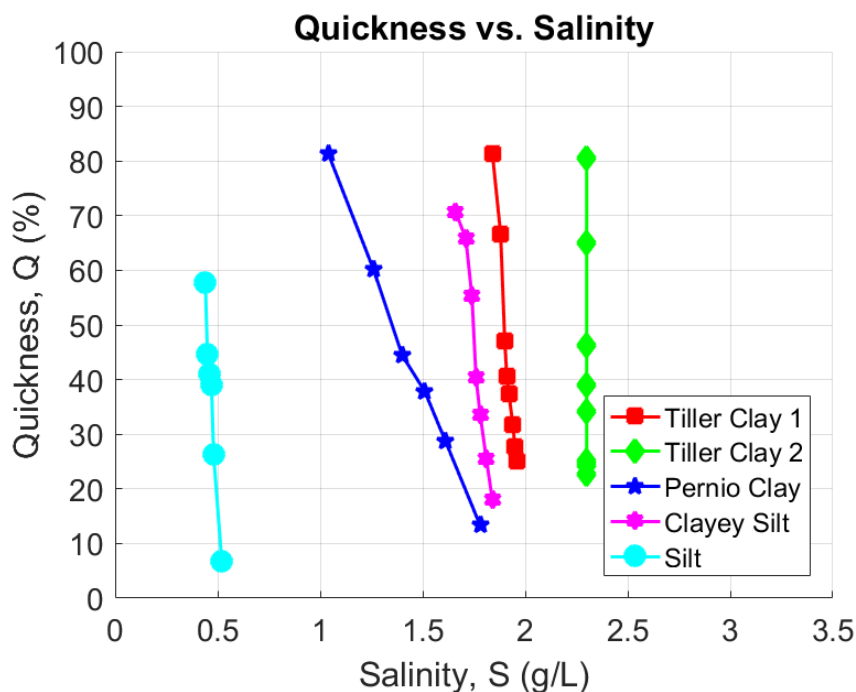


Figure 5.10: Relationship between quickness and salinity

The effect of increasing the salinity of a soil can be shown when comparing the quickness against water content plots for the two Tiller clays tested (Figure 5.11). It can be seen that for the same water content, the quickness value is lower for the clay with a higher salt content. This is due to the molecular binding on the internal grain structure, increasing the strength and conversely reducing the quickness. Therefore, more water is required to achieve the same remoulded shear strength and ultimately the same quickness.

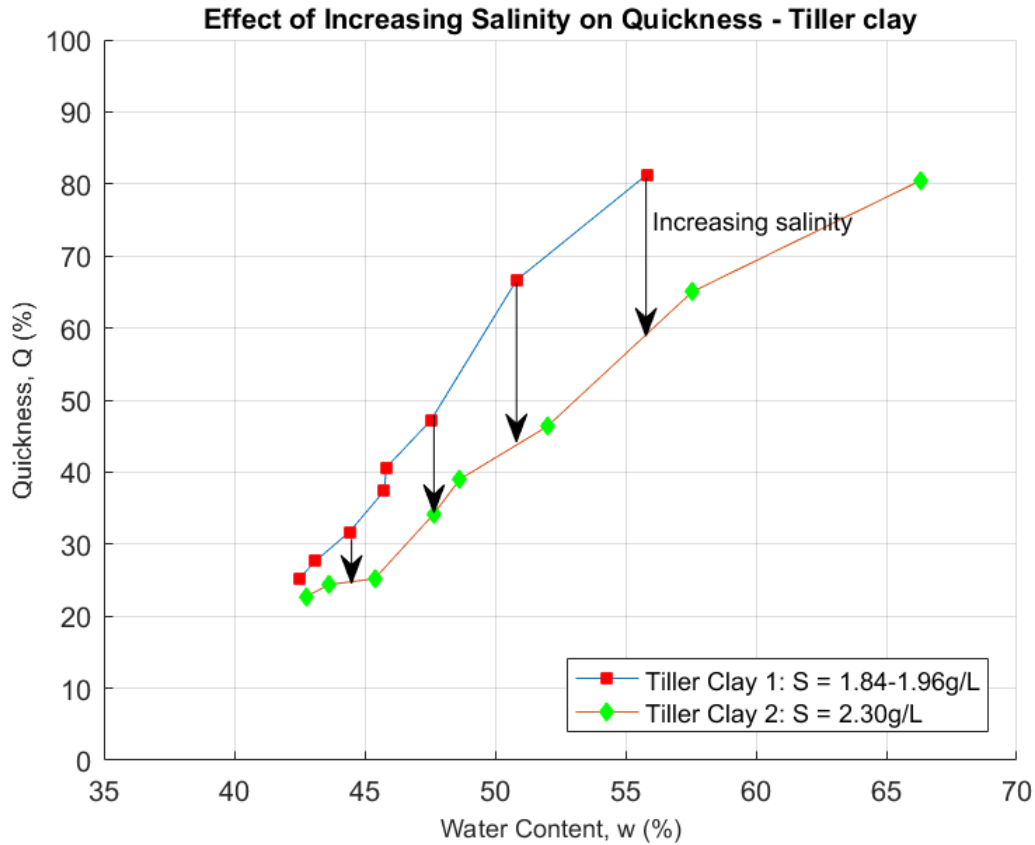


Figure 5.11: Effect of salinity on quickness

It must be noted that the clay fraction varied by approximately 15% and the material was taken from different sections of the Tiller block sample so this must be considered in the comparison also.

5.2.4 Limitations and Experimental Problems

Determination of c_{ur}

Fall-cone testing measures the remoulded shear strength of a small volume of material, whereas a much larger quantity is required for quickness testing. Although the homogeneous material is thoroughly stirred in a large bowl, there is a potential for the measured c_{ur} with the fall-cone test to differ from that of the parent material. To reduce the chance of discrepancy, a minimum of 3 fall-cone tests were performed on samples for each material.

Experimental Procedure

Silicon oil was applied to act as a lubricant between the cylindrical mould and the slurry material. The additional mixing within the cylinder to remove air voids for stiffer materials

was such that the friction-less layer became compromised. This meant that side friction was present as the cylinder was lifted which may effect results. For 'quick' materials with very low shear strengths (less than 0.5 kPa), this was not an issue.

The test was conducted at room temperature, hence time and exposure to air can influence the water content of the material. After the mould was removed and quickness measurements obtained, the water content samples are taken from the centre of the slurry slump (internally), limiting the atmospheric effects that the external surface of the slurry is subject to.

As the material is re-used there may be some effect of the silicon oil; that is applied to the cylinder and test surface; as it interacts with the slurry mix during testing then scooped back into the bowl. Visual inspection of the slurry slump revealed a shiny, watery surface as a result of the oil coating, however, the usage of oil is minimal and any effects have been considered negligible.

Limiting Quickness Value

To investigate the effect of surface friction, tests were conducted using just water. Small droplets of water molecules pooled together with a height of 5 mm (independent of the volume of water used). Therefore, the maximum actual quickness value obtainable is 95.6% (idealized conditions, $c_{ur} = 0$ kPa effectively). For fine-grained materials, the threshold would be less than 95.6% and hence the reason why the quickness plots appear to be reaching a limiting quickness value, and not 100%, even as the liquidity index is increased.

5.3 Viscometric Tests

In total 24 viscometric tests were performed, of which 19 tests had a similar flow curve. There were 5 tests however, that displayed a different curve shape due to a much lower recorded torque at the lowest speed setting. This will be discussed in Section 5.3.1. The salinity, water content and remoulded shear strength was varied for each viscometer test to explore the rheological behaviour of the fine-grained soils with differing salinity and liquidity index. Viscometric raw data and results can be found in Appendix C and D respectively.

5.3.1 Dynamic Response Test

The dynamic response test was performed as described in Section 3.6.3. The torque (T) measured at 15 seconds was plotted against rotational speed (N). A total of 19 tests showed a torque-rotational speed (T - N) curve with a similar shape as 'Curve type 1', and 5 tests with a similar shape as 'Curve type 2' as observed in Figure 5.12. The difference between the two curves regards the torque measurement at the lowest speed setting as mentioned in Section 2.6.1.

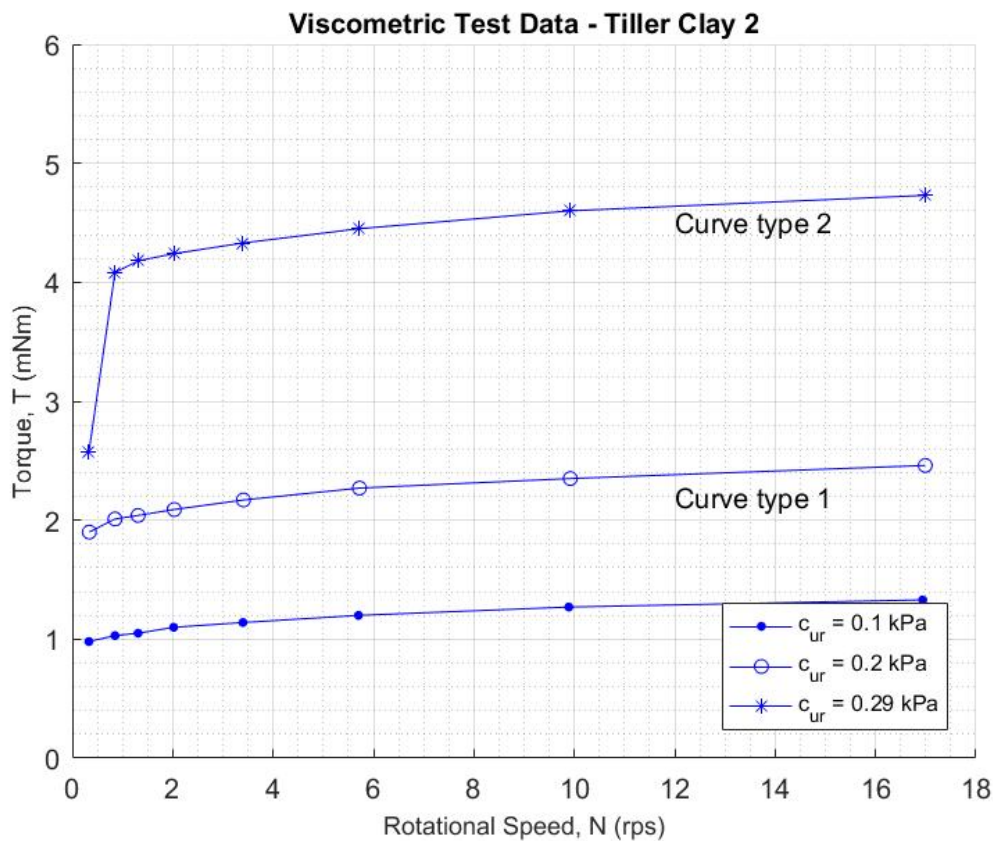


Figure 5.12: Comparison of viscometer flow curves

For all tests, the torque at the lowest rotational speed is greater than zero which indicates the materials have a yield stress. Also, the inclination of the curve tangent at lower rotational speeds is steeper than at higher speeds suggesting the materials have shear thinning behaviour. This agrees with Herschel-Bulkley flow curve and the assumption that fine-grained materials fit the Herschel-Bulkley model.

5.3.2 Data Processing

The viscometric test data was processed from torque and rotation speed measurements to a flow curve as described in Section 4.2. Examples of the fitted curves are shown in Figure 5.13 and 5.14 for the test data discussed in Section 5.3.3.

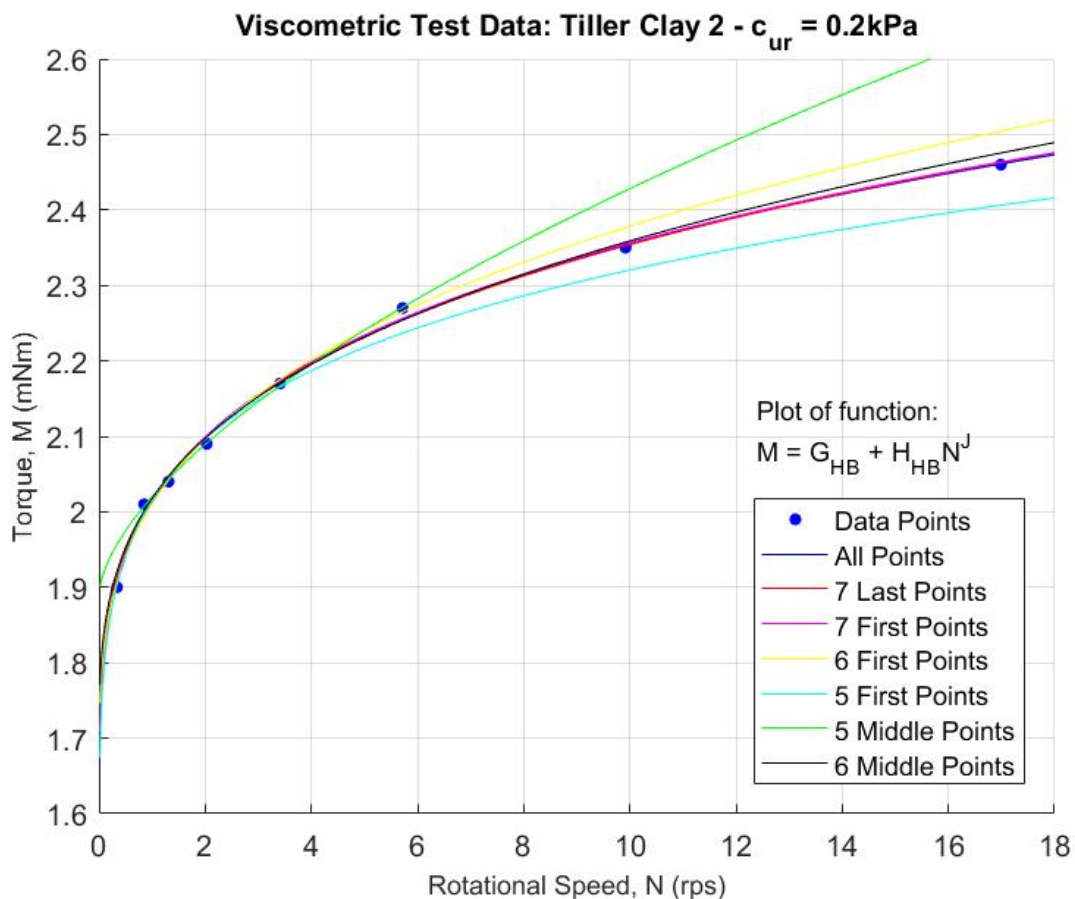


Figure 5.13: T - N Curve type 1 (from Tiller Clay 2 $c_{ur} = 0.2\text{kPa}$)

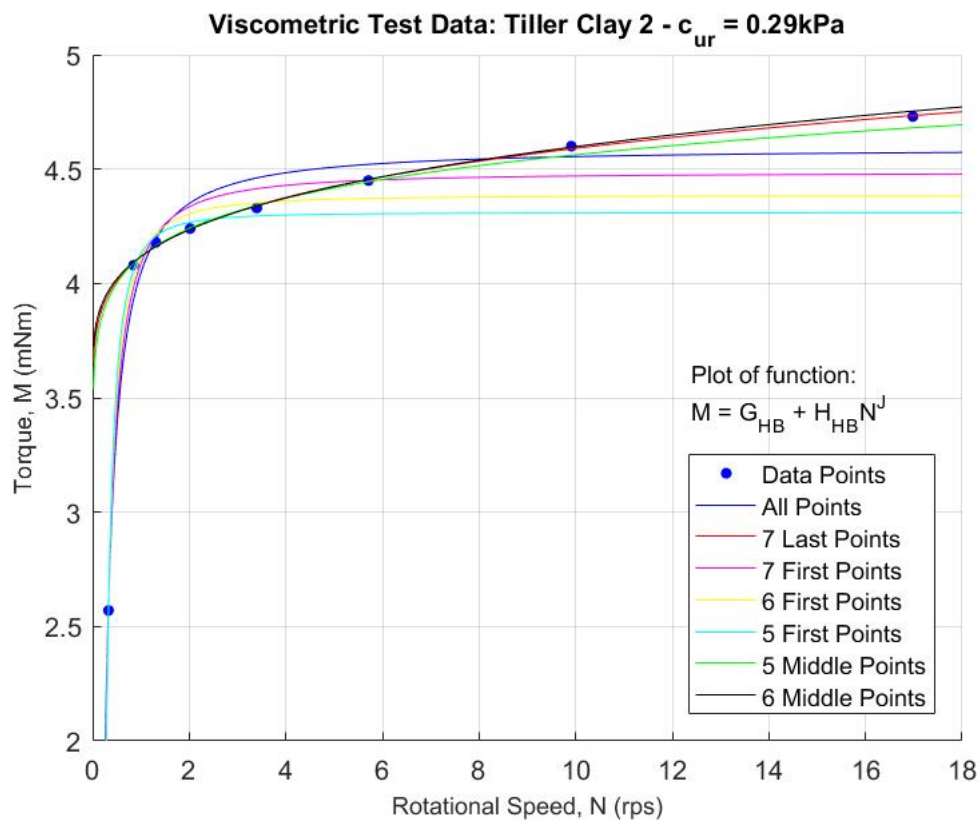
All the fitted curves in Figure 5.13 have very high R^2 values suggesting very good fits with the recorded data based on regression analysis. The fitted curves using the 5 first points and 5 middle points however are not as accurate based on their visual representation (*light blue and green lines*). Table 5.6 shows the fit parameters for the seven curves which was used to investigate the sensitivity of the fit. The most accurate and representative best fit occurs when all the data points are used (*blue line*).

Table 5.6: Results for curve fitting for Tiller Clay 2 - $c_{ur} = 0.2\text{kPa}$

Curve fitted to	G_{HB} (mNm)	H_{HB} (mNm s ^J)	J (-)	R^2 (-)	τ_y (Pa)	K (Pa s ⁿ)	n (-)
All points	1.483	0.5306	0.2159	0.9975	125.25	33.95	0.22
7 last points	1.574	0.4431	0.2457	0.9967	132.92	25.92	0.25
7 first points	1.500	0.5131	0.2224	0.9958	126.70	32.19	0.22
6 first points	1.630	0.3802	0.2940	0.9942	137.68	19.34	0.29
5 first points	1.241	0.7742	0.1444	0.9923	104.80	62.54	0.14
5 middle points	1.891	0.1294	0.6186	0.9993	159.67	2.87	0.62
6 middle points	1.660	0.3576	0.2910	0.9942	140.21	18.35	0.29

NB: Data in bold represents best fit Herschel-Bulkley parameters

For the materials that exhibit relatively low torque readings on the lowest speed setting, curve fitting using all the data points is not the most applicable. This can be seen in Figure 5.14 where the first data point significantly effects the fit curves.

Figure 5.14: $T-N$ Curve type 2 (from Tiller Clay 2 $c_{ur} = 0.29\text{kPa}$)

The fit using 7 points, excluding the first point, is considered the best fit. The parameters are shown in Table 5.7. These parameters are used to investigate the sensitivity of the fit. Negative values for H_{HB} and J result in imaginary numbers for the Herschel-Bulkley exponent and consistency parameter, hence the need to fit a number to curves to the data to find the most accurate analysis.

Table 5.7: Results for curve fitting for Tiller Clay 2 - $c_{ur} = 0.29\text{kPa}$

Curve fitted to	G_{HB} (mNm)	H_{HB} (mNm s ^J)	J (-)	R^2 (-)	τ_y (Pa)	K (Pa s ⁿ)	n (-)
<i>All points</i>	4.591	-0.5451	-1.1710	0.9733	[387.78]	[259.11]	[-1.17]
7 last points	3.289	0.8272	0.1969	0.9977	277.78	56.17	0.20
<i>7 first points</i>	4.485	-0.3984	-1.4110	0.9842	[378.81]	[583.98]	[-1.41]
<i>6 first points</i>	4.385	-0.2681	-1.7230	0.9940	[370.35]	[157.46]	[-1.72]
<i>5 first points</i>	4.309	-0.1786	-2.0530	0.9986	[363.97]	[1242.66]	[-2.05]
5 middle points	2.352	1.765	0.0979	0.9938	198.61	168.87	0.10
6 middle points	3.496	0.6213	0.2488	0.9963	295.31	36.00	0.25

NB: Data in bold represents best fit Herschel-Bulkley parameters. Data in italics represent trendlines not fitting the Herschel-Bulkley model

The best fit for each test was also selected based on the calculated Herschel-Bulkley yield stress, ensuring that the yield stress increases as the remoulded shear strength of the sample increases.

5.3.3 Best Fit Herschel-Bulkley Parameters for all Tests

The test procedure was performed for all materials of varying strength. The best fit Herschel-Bulkley parameters are show in Table 5.8. The Herschel-Bulkley model equation is:

$$\tau = \tau_y + K^* \left(\frac{\dot{\gamma}}{\dot{\gamma}_{ref}} \right)^n \quad (5.3)$$

Where $K^* = K(\dot{\gamma})^n$ and $\dot{\gamma}_{ref} = 1 \text{ s}^{-1}$ is a reference value to normalize the K parameter.

The results from the viscometer tests and analysis on the Silt have been excluded from further interpretation due to the segregation between grains and water, as observed in viscometer tests and discussed in Section 5.2.1 also.

Table 5.8 shows a yield stress, τ_y range from 39.80 Pa to 361.95 Pa. The normalized consistency parameter, K^* ranges from 1.35 Pa up to 79.47 Pa while the Herschel-Bulkley exponent, n lies between 0.17 and 0.46.

There are observable trends in the Herschel-Bulkley parameter results. The yield stress increases with increasing remoulded shear strength (best fit parameters selected so this was the case). The normalized consistency parameter also increases while the Herschel-Bulkley exponent decreases with increasing remoulded shear strength.

Table 5.8: Best fit Herschel-Bulkley parameters for all samples

Material	Remoulded Shear Strength, c_{ur} (kPa)	Points excluded from fit (-)	Liquidity Index, I_L (-)	Salinity, S (g/L)	Yield Stress, τ_y (Pa)	Normalized Consistency Index, K^* (Pa)	Herschel-Bulkley exponent, n (-)
Tiller Clay 1	< 0.10	None	3.39	1.74	90.39	20.54	0.27
	0.10	None	2.77	1.84	142.41	21.23	0.31
	0.20	First	2.37	1.88	276.23	23.80	0.29
	0.29	First 2	2.10	1.90	361.95	9.66	0.46
Tiller Clay 2	< 0.10	Last 2	5.31	2.30	14.31	8.55	0.28
	0.10	None	3.11	2.30	65.94	14.37	0.27
	0.20	None	2.50	2.30	125.25	33.95	0.22
	0.29	First	2.01	2.30	277.80	56.17	0.20
Perniö Clay	< 0.10	Last	2.23	1.01	43.42*	2.36	0.42
	< 0.10	Last	2.08	1.02	51.19*	1.86	0.41
	0.10	None	1.84	1.04	14.21	2.66	0.45
	0.20	None	1.70	1.26	28.11	4.78	0.40
	0.29	None	1.56	1.40	47.60	5.17	0.41
	0.39	First	1.45	1.51	64.81	6.62	0.40
	0.50	None	1.39	1.61	82.88	27.07	0.35
	0.70	None	1.28	1.78	166.27	75.90	0.30
Clayey Silt	< 0.10	None	3.54	1.56	59.06	15.90	0.28
	0.10	First	2.92	1.66	79.23	21.74	0.28
	0.20	First2/last	2.75	1.71	116.13	22.26	0.28
	0.29	First2/last	2.48	1.74	152.84	48.49	0.22
Silt*	< 0.10	None	1.70	0.41	6.55	0.98	0.73
	0.10	None	1.55	0.44	4.15	1.82	0.66
	0.20	None	1.49	0.45	4.61	1.89	0.69
	0.29	None	1.44	0.46	1.40	2.47	0.61

5.3.4 Observed Errors in Tests and Experimental Problems

There were a number of sources of error, particularly for samples with higher shear strengths. Temperature, remoulded shear strength, liquidity index and instrument limitations also contributed to the effectiveness of the testing procedure.

Instability at Higher Remoulded Shear Strength and Liquidity Index

As alluded to in Section 5.3.1, some low torque readings were measured at low speeds. This may be due to an initial yield stress required to be overcome. One of the key assumptions when using viscometers is that the velocity gradient over the gap decreases from maximum velocity at the rotating spindle, to zero at the stationary outer cylinder (as shown in Figure 2.12 and Figure 2.13). The significantly lower torque values at low rotational speeds may be a result of a shear band being formed within the wide gap system, and therefore the velocity profile terminating before the boundary. This proposed phenomenon can be seen in Figure 5.15. This would result in lower shear as only a portion of the material is flowing.

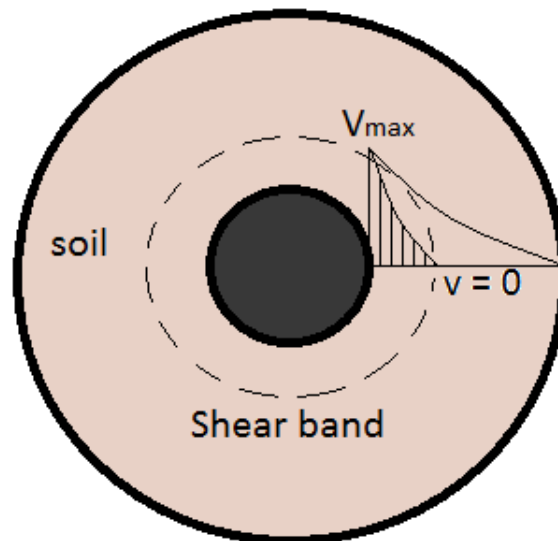


Figure 5.15: Observed slippage between spindle and clay. Hole remains in clay after the spindle has been removed.

This behaviour was observed in materials with higher remoulded shear strengths and low liquidity indices.

Establishing Equilibrium Torque

Since the process to determine the equilibrium torque required cycling through the speeds from low to high then back, the sample would undergo periods of temperature increase. This would ultimately cause the viscosity to drop and torque readings would reduce. There were a number of tests carried out initially where the equilibrium torque could not be re-established during testing as the material had cooled, resulting in higher torque values. To overcome this issue of temperature, extended amounts of time (greater than 2 hours) were required to establish an accurate equilibrium torque measurement. Also in some cases, the equilibrium torque process would have to be repeated mid-test to bring back the sample to the temperature and state that it started the testing at.

Slippage

Another error that occurred during some tests was slippage between the sample and inner spindle cylinder. At low shear strengths, this was not critical as the material acted more like a fluid and flowed during testing. At higher strengths however, the material did not flow and hence the torque measured was between the rotating spindle and the material at the interface. This was evident as it would result in much lower than expected data as well as a hole remaining within the sample when the spindle was removed (Figure 5.16). These tests were hence excluded from the analysis.



Figure 5.16: Observed slippage between spindle and clay with high remoulded shear strength. Hole remains in clay after the spindle has been removed.

Temperature

Another source of error was the temperature control. Even though the tests were performed in an isolated cold room, the temperature of the room varied by a few degrees due to the cooling process of the fans. Also opening the door caused slight temperature changes as well as pressure differentials. The viscometer speed setting also effected the temperature of the sample. The faster speeds caused temperature increase while low speeds caused temperature decrease. This was a result of the friction between grains on the micro level. This phenomenon added to the difficulty in some samples to determine the initial equilibrium torque, particularly those with higher shear strength and liquidity index. An isolation fitting for the viscometer could have made temperature control achievable and negated any detrimental temperature effects.

Instrument Limitations

The maximum torque range for the viscometer was 10 mNm. This meant that only low strength clays were capable of being tested. At shear strengths greater than 0.29 kPa, the torque readings were unstable with the measurements fluctuating wildly with constant rotation. Perniö clays with higher strengths were able to be tested due to their large liquidity index. Based on the flow curves calculated for 0.5 kPa and 0.7 kPa along with the Herschel-Bulkley parameters produced, it can be recommended that viscometer tests be applied to fine-grained soils with $c_{ur} < 0.5$ kPa.

Narrow gap tests were initially trialled however for both consistency with previous work and complications due to grain size, wide gap viscometer tests were undertaken. Due to the outer cylinder size availability, the smallest wide gap ratio possible was 1.96.

Sensitivity of K^* and n Values

The Herschel-Bulkley parameters K^* and n are highly sensitive to small variations in calculated τ_y . It can be seen in Figure 5.17 that although the flow curves demonstrate the same shear thinning behaviour and curvature, K^* and n greatly vary. The yield stress ranges from 62.69-74.37 Pa, while the consistency parameter lies between 0.92-8.30 Pa.sⁿ and the Herschel-Bulkley exponent 0.37-0.80. The various flow curves plotted show that the same curve can be produced with any number of K^* and n combinations.

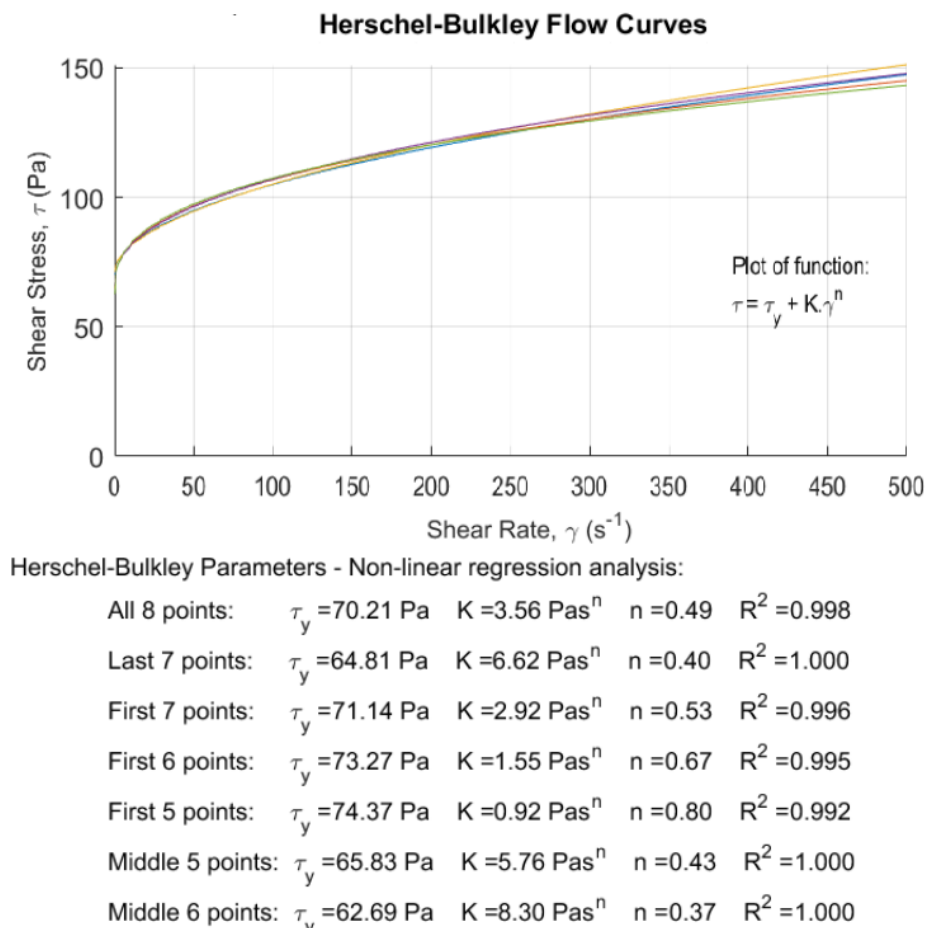


Figure 5.17: Sensitivity of K^* and n on Herschel-Bulkley flow curves. Parameters determined from viscometer tests and best fit analysis on Perniö Clay, $c_{ur} = 0.39$ kPa.

This makes selecting the best fit and Herschel-Bulkley parameter triplets very difficult. More effort is required to determine worthwhile relationships with liquidity index given their sensitive nature. K^* and n are considered curve fitting parameters, and possible correlations may exist for greater values of I_L than the range tested.

5.4 Influence of Liquidity Index, Salinity and Temperature on Flow Curves

The salinity and liquidity index as well as temperature of a sample play a large role in determining a materials viscometrical and rheological properties. It is simple to isolate and compare the contribution that temperature plays however salinity and liquidity index are inter-connected and hence less straightforward to compare.

5.4.1 Effect of Liquidity Index

To isolate the role that liquidity index plays on a fine-grained soils rheological properties, the salinity must be kept constant. Flow curves for Tiller clay with a constant salinity of 2.3g/L, for different liquidity indices are plotted in Figure 5.18. The flow curves have been calculated with the Herschel-Bulkley model (equation 5.3) with the best fit parameters shown in Table 5.8.

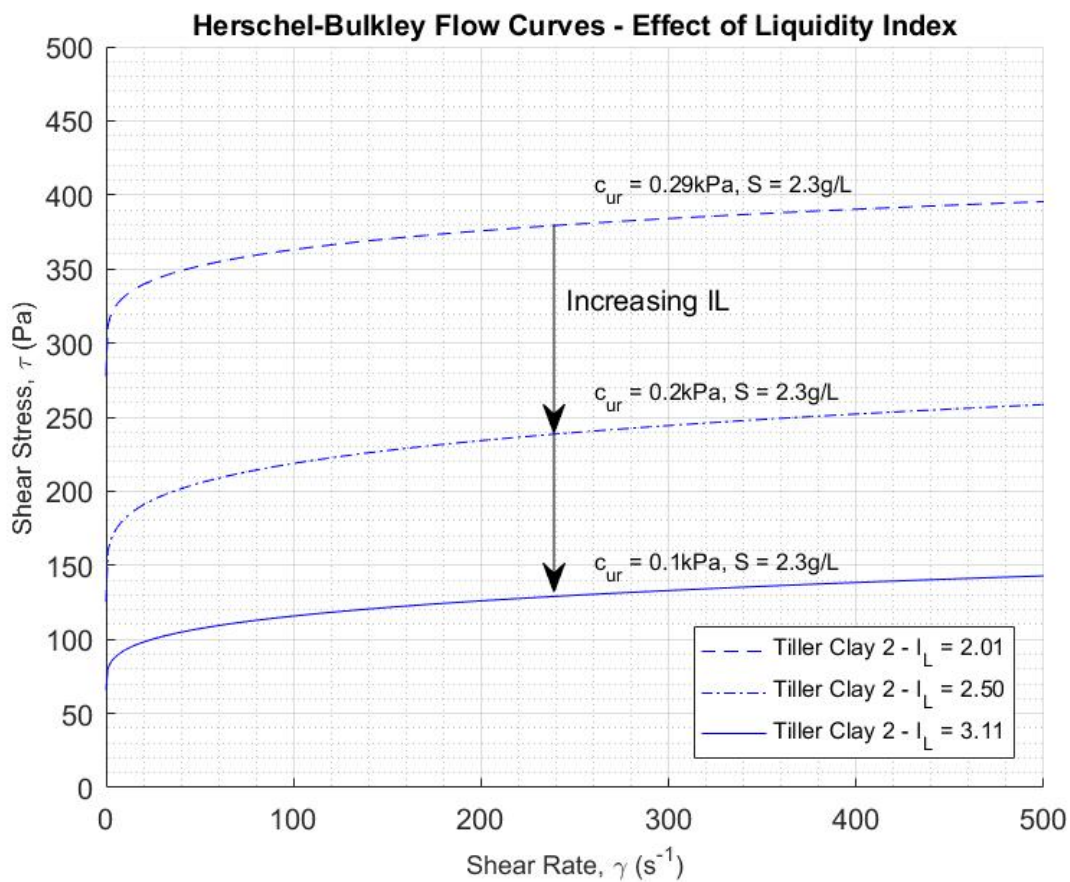


Figure 5.18: Effect of liquidity index on Herschel-Bulkley flow curves

The top flow curve has the lowest liquidity index, while the bottom curve has the highest liquidity index. The curves cross the y-axis at different values, which represents the yield stress at zero shear rate. This indicates that the yield stress decreases for increasing liquidity index for clays with the same salinity, and confirmed by Grue (2015). The shape of the curve remains approximately the same, which is governed by the combination of K^* and n parameters.

It can be expected that by increasing the water content of the sample and therefore the liquidity index, the viscosity of the sample reduces i.e. it flows easier. In doing so, the remoulded shear strength of the sample also reduces given the direct correlation between I_L and c_{ur} .

From this analysis, it can be concluded that there is a strong relationship between remoulded shear strength, salinity and liquidity index (which is site/material dependant).

5.4.2 Effect of Salinity

To study the effect of salinity, flow curves were calculated for Tiller clay samples with remoulded shear strengths of 0.1 kPa and 0.2 kPa at different salinities. The flow curves have been calculated with the Herschel-Bulkley model (equation 5.3) with the best fit parameters shown in Table 5.8.

As previously discussed, the addition of salt to a sensitive clay increases the inter-molecular bonds and as a result its strength. The viscosity would also increase as the materials propensity to flow is reduced.

Tiller clay samples were first tested with the natural salinity and varying shear strengths (*solid lines*) before secondary samples were produced with a constant salinity (*dashed lines*), Figure 5.19. Comparing each sample at the same shear strength, a reduction in viscosity can be seen when the salinity increases (for a constant c_{ur}). This is the opposite to what is expected which suggests that the clay content plays a significant role. The CF of the Tiller Clay 2 is 51% as opposed to 37% and hence the two different clays should not be compared to one another, even though they are taken from the same block sample.

It is important to note however, that increasing the salinity of a sensitive clay also changes the plasticity and liquidity indices. Therefore, the water content required to obtain the same shear strength is higher and the reason why the shear stress curves are lower. For the remoulded shear strength of 0.1 kPa, the water content increased from 55.8% ($I_L = 2.77$) to 66.3% ($I_L = 3.11$). Similarly, for the remoulded shear strength of 0.2 kPa, the water content increased from 50.8% ($I_L = 2.37$) to 57.6% ($I_L = 2.50$).

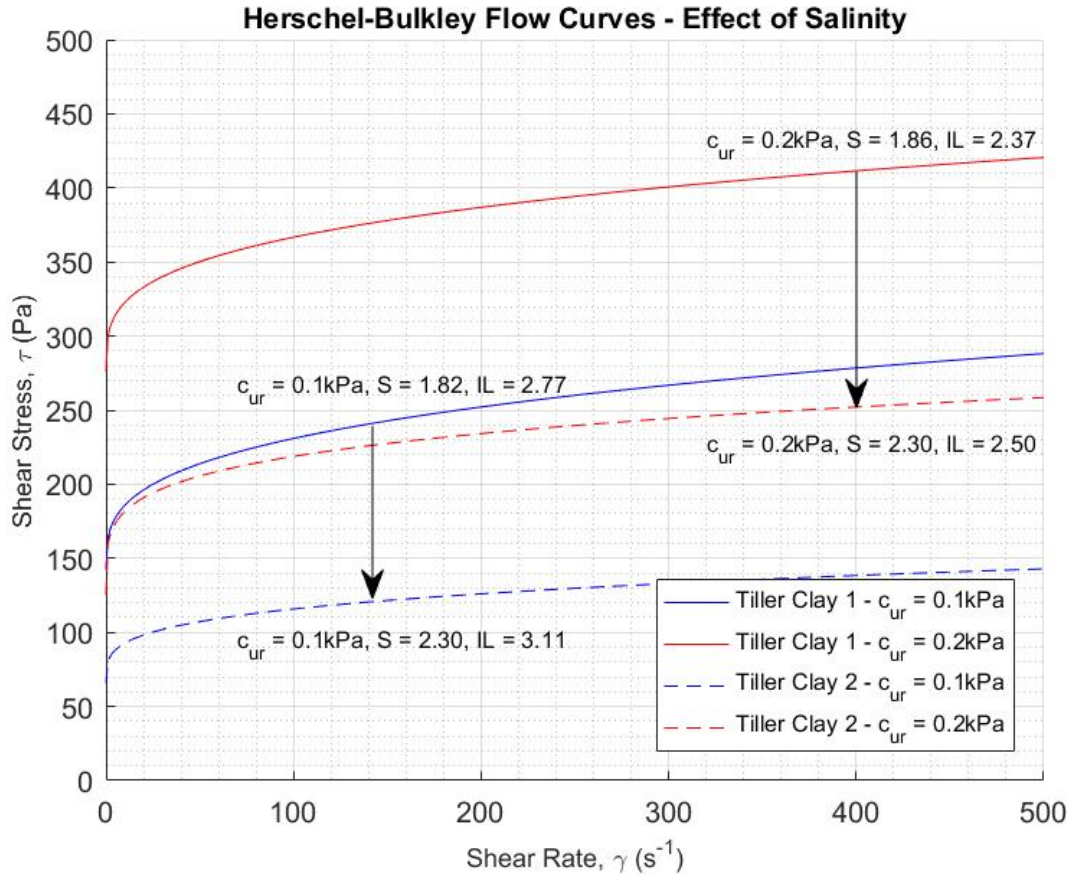


Figure 5.19: Effect of salinity on Herschel-Bulkley flow curves

To further illustrate the effect of salinity, the flow curve for Tiller Clay 1 with $I_L = 2.77$ and $S = 1.82$ g/L (*blue solid line*) has the same yield stress as Tiller Clay 2 with $I_L = 2.5$ and $S = 2.30$ g/L (*red dotted line*) with a similar flow curve profile. This reinforces the fact that increasing salinity reduces the liquidity index of a soil.

Since it has been shown there is an inverse relationship between I_L and τ_y , as well as an inverse relationship between S and I_L , it can be concluded that as salinity increases, so too does yield stress for a constant liquidity index.

5.4.3 Effect of temperature

To study the effect of temperature, the same soil material was tested in the cold room at 7° Celsius as well as at room temperature (approximately 24.5°C). Tiller Clay 1 with a remoulded shear strength of 0.2 kPa and liquidity index of 2.37 was used for the comparison. The flow curves are plotted in Figure 5.20.

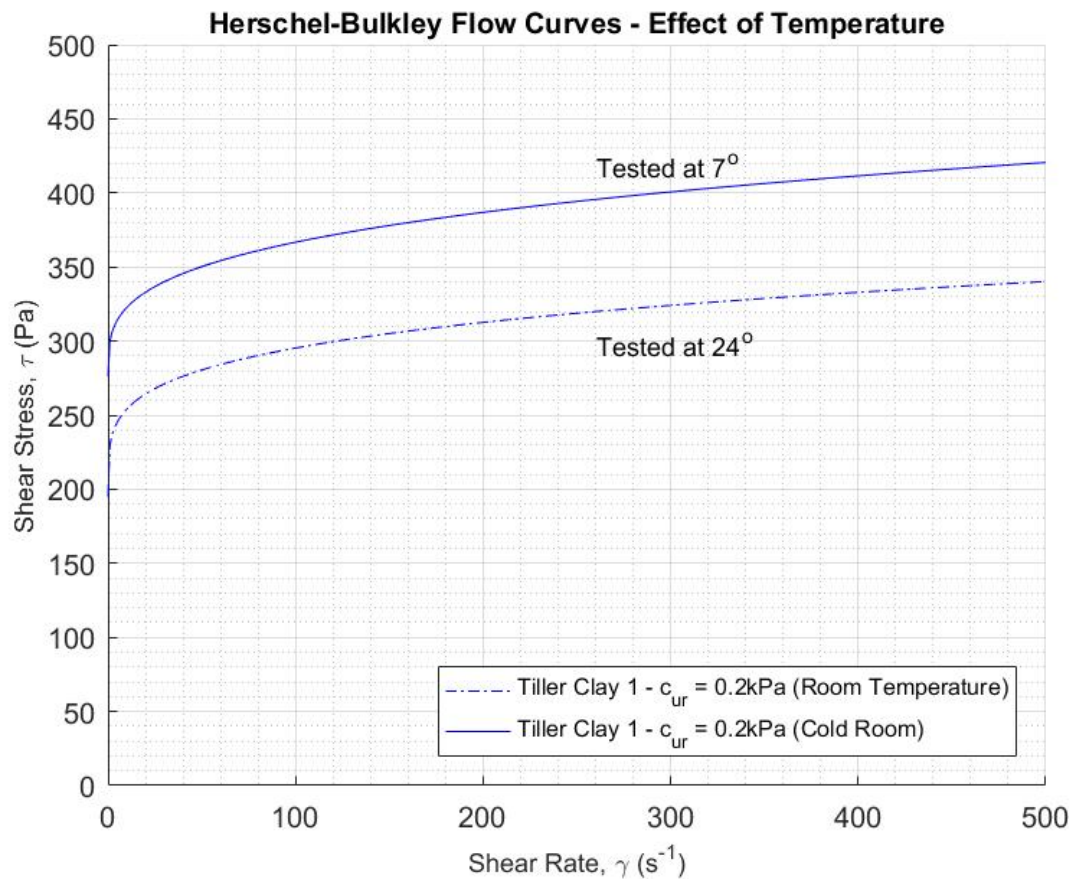


Figure 5.20: Effect of Temperature on Herschel-Bulkley flow curves

From this analysis, the effect of temperature changes the yield stress of the soil material, however, the shape of the flow-curve remains fairly constant. This is also observed as the torque readings are lower at warmer temperatures than at colder temperatures. This may be attributed to the effect the water molecules have on binding the soil grains together which increases as the water approaches its freezing point.

5.5 Herschel-Bulkley Parameters for Tiller Clay

In this section, the Herschel-Bulkley parameters for the Tiller clays are plotted with respect to liquidity index and salinity to determine how they vary with flow properties. The parameters are shown in Table 5.8. Figure 5.21 shows the $T-N$ curves for Tiller Clay 1 and Tiller Clay 2.

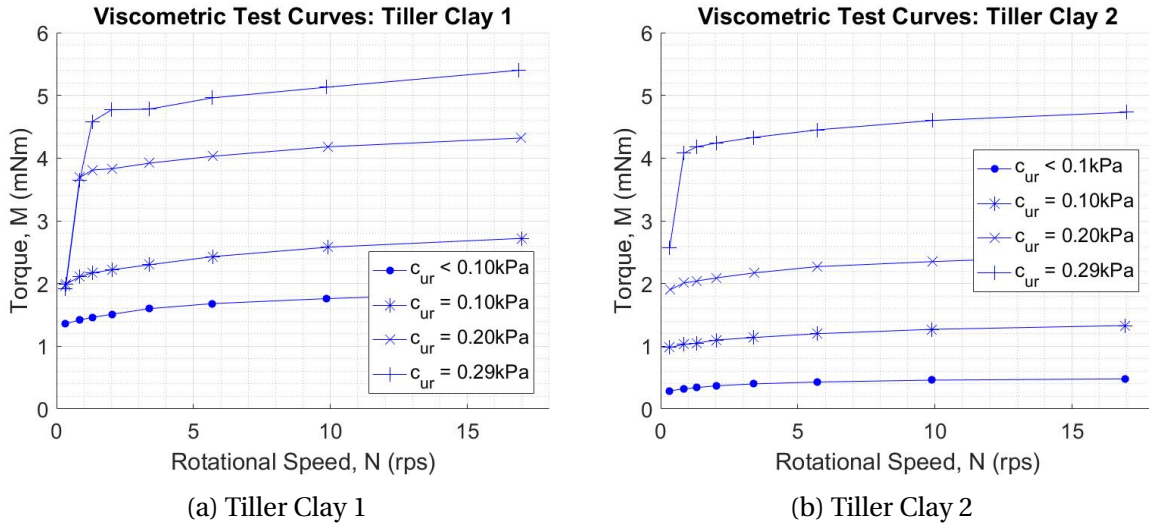


Figure 5.21: Torque-Speed viscometric curves for Tiller clays

For the Tiller Clay 1, the torque value at the lowest speed setting is the same for $c_{ur} = 0.1, 0.2,$ and 0.29 kPa. This may be related to the introduction of a shear band within the wide gap, as hypothesized in Section 5.3.4. The torque values are also the same at the second lowest speed for $c_{ur} = 0.2,$ and 0.29 kPa. This suggests that depending on the shear strength of the material, a certain rotational speed is required to fully activate the whole sample between the gap within the viscometer (refer to Figure 5.15).

5.5.1 Yield Stress

Figure 5.22 shows the relationship between the yield stress and liquidity index. The yield stress is increasing with increasing salinity and reducing liquidity index. This is also shown in Figure 5.23 where the yield stress increases with increasing salinity.

Given yield stress increases with increasing salinity for a constant liquidity index (Grue, 2015), Figure 5.22 can not be used to find a common trend based on the collective data of Tiller Clay 1 and Tiller Clay 2 as they are effectively different soils (albeit from the same site). This is evident as the yield stress for Tiller 1 (*red markers*) is larger than the yield stress for Tiller 2 (*blue markers*) when it has a lower salinity. One thing that can be drawn from Figure 5.22 is the relationship between τ_y and I_L which can be given by the expression:

$$\tau_y = \left(\frac{\text{constant}}{I_L} \right)^{3.0} \tag{5.4}$$

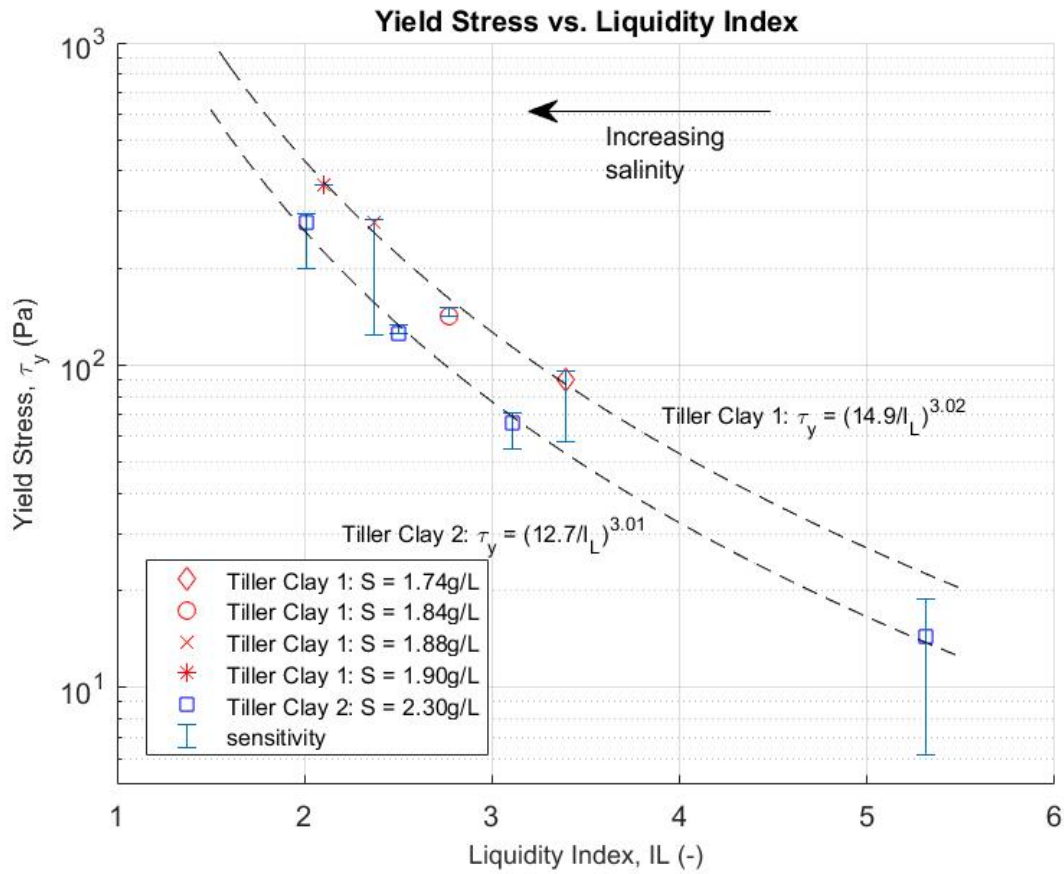


Figure 5.22: Yield stress versus liquidity index for Tiller clays

The black dashed lines in Figure 5.22 are the regression lines for salinities 1.74-1.90 g/L and 2.30 g/L. The relationships and coefficient of determination are shown in Table 5.9.

Table 5.9: Regression lines between τ_y and I_L for Tiller clays

Material	Salinity	Relationship	R^2
Tiller Clay 1	1.74-1.90 g/L	$\tau_y = (14.9/I_L)^{3.02}$	0.982
Tiller Clay 2	2.30 g/L	$\tau_y = (12.7/I_L)^{3.01}$	0.997

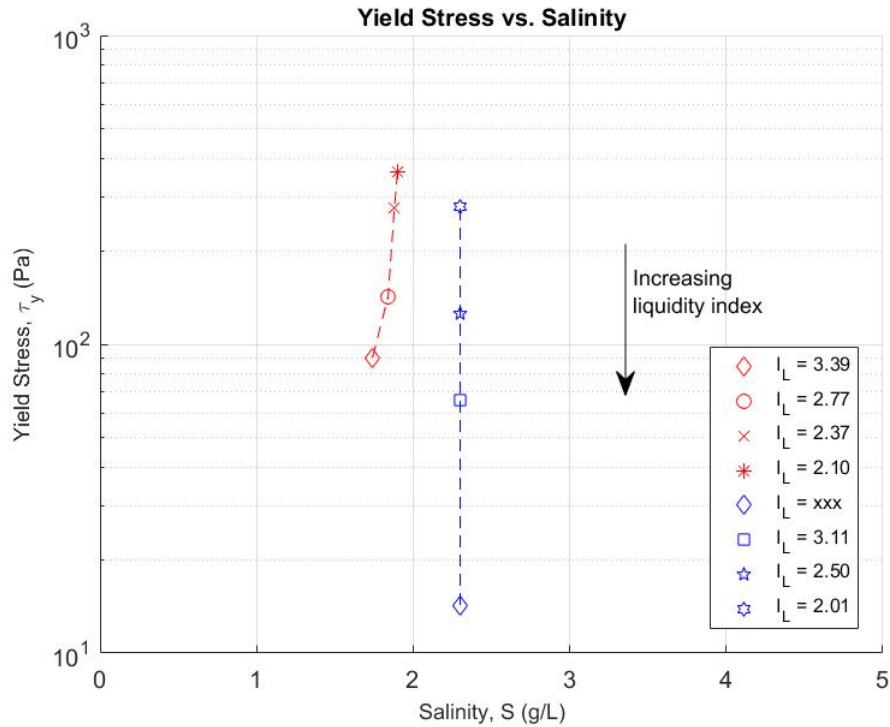


Figure 5.23: Yield stress versus salinity for Tiller clays

5.5.2 Consistency Parameter

Figure 5.24 shows the relationship between the consistency parameter and liquidity index. The K^* is decreasing with increasing liquidity index for Tiller Clay 2 however no trend is observed for Tiller Clay 1 due to the extreme outlier produced from fluctuating torque readings at high shear strength.

The black dashed line in Figure 5.24 is the regression line for the salinity of 2.30 g/L. The relationship and coefficient of determination are shown in Table 5.10.

Table 5.10: Regression lines between K^* and I_L for Tiller clays

Material	Salinity	Relationship	R^2
Tiller Clay 1	1.74-1.90 g/L	-	-
Tiller Clay 2	2.30 g/L	$K^* = (14.9/I_L)^{1.94}$	0.914

The sensitivity of the consistency parameter is clearly evident in Figure 5.24, with large errors bars plotted. This therefore makes it difficult to predict accurate correlations. Furthermore, no conclusion can be drawn between the consistency parameter and salinity, again due to the outlier, as presented in Figure 5.25.

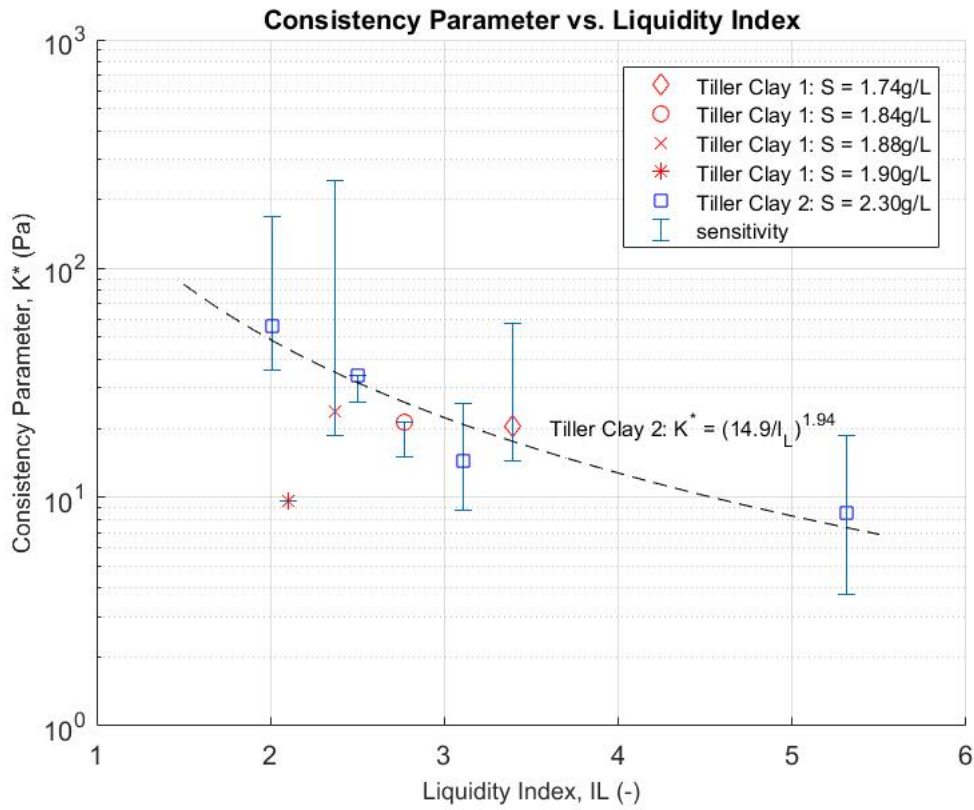


Figure 5.24: Consistency parameter versus liquidity index for Tiller clay

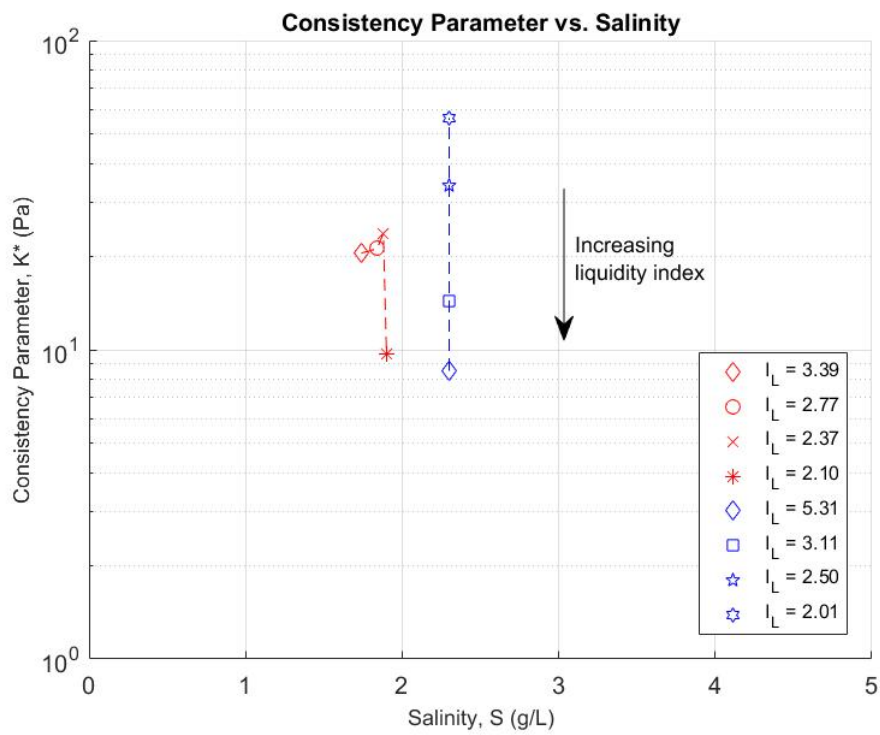


Figure 5.25: Consistency parameter versus salinity for Tiller clay

5.5.3 Herschel-Bulkley Exponent

The Herschel-Bulkley exponent is plotted against the liquidity index in Figure 5.26. The value of n is increasing with increasing liquidity index for Tiller Clay 2 while there is no trend observable for Tiller Clay 1. The black dashed line in Figure 5.26 are the regression line for the salinity of 2.30 g/L.

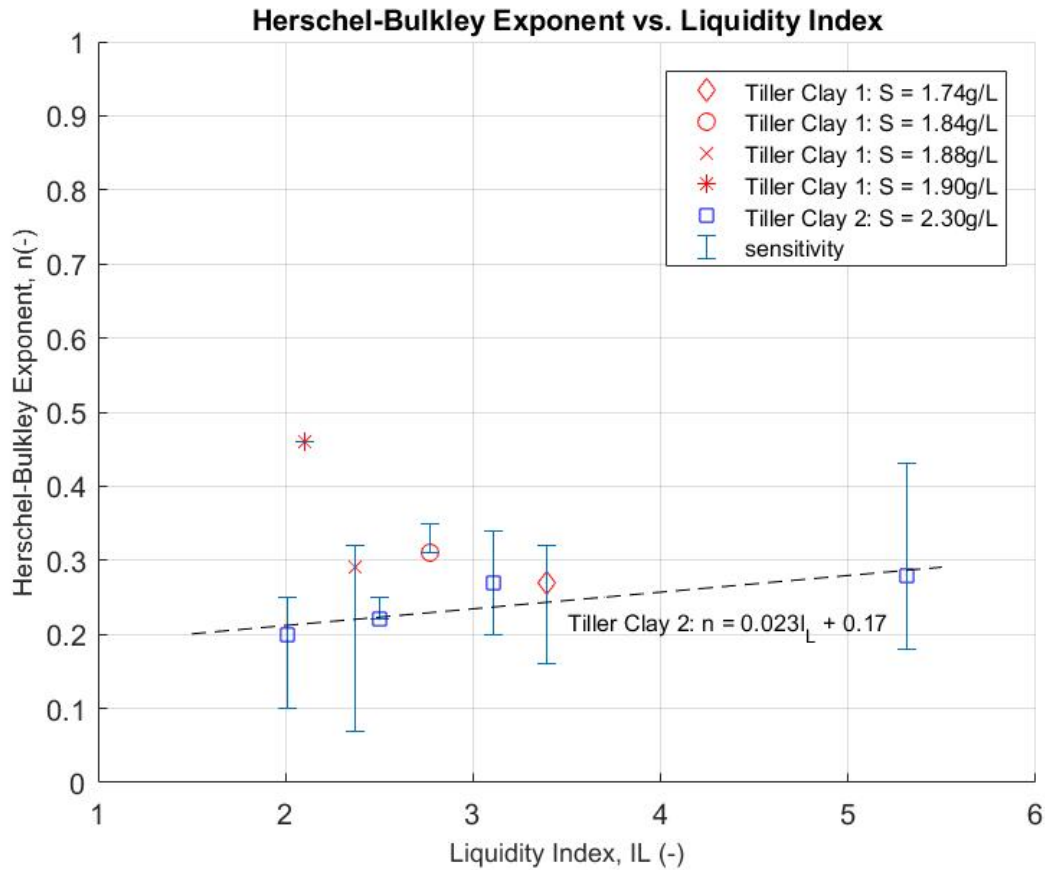


Figure 5.26: Herschel-Bulkley exponent versus liquidity index for Tiller clays

Table 5.11: Regression lines between n and I_L for Tiller clays

Material	Salinity	Relationship	R^2
Tiller Clay 1	1.84-1.90 g/L	-	-
Tiller Clay 2	2.30 g/L	$n = 0.023I_L + 0.17$	0.718

Large sensitivities in the Herschel-Bulkley exponent exist, similar to K^* , with no observable relationship with salinity as shown in Figure 5.27.

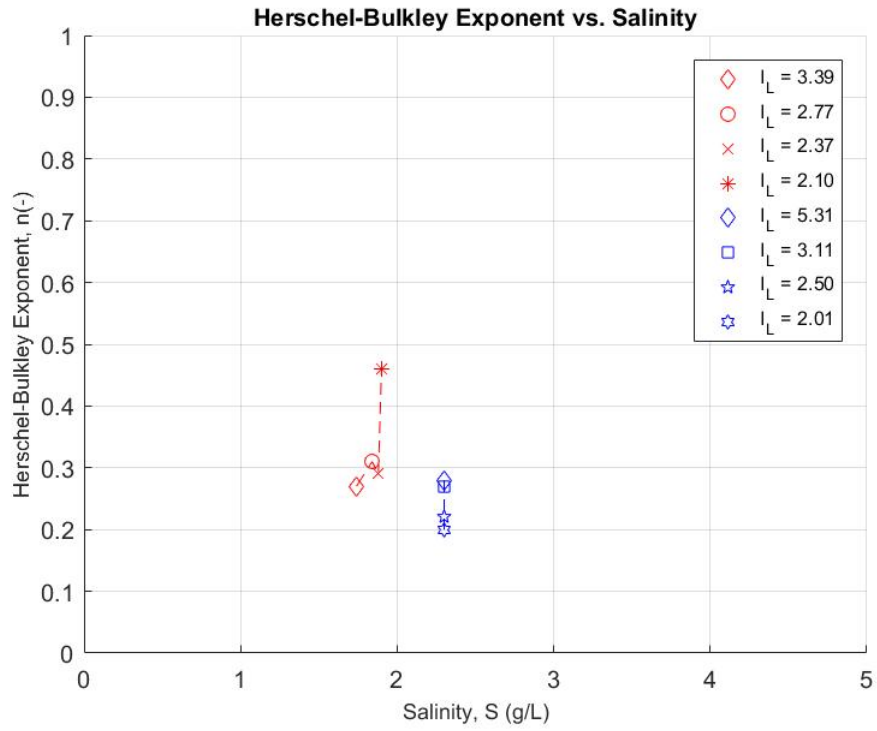


Figure 5.27: Herschel-Bulkley exponent versus salinity for Tiller clays

5.6 Herschel-Bulkley Parameters for Perniö Clay

In this section, the Herschel-Bulkley parameters for the Perniö Clay are plotted with respect to liquidity index and salinity. The parameters are shown in Table 5.8. Figure 5.28 shows the $T-N$ curves for the Perniö Clay.

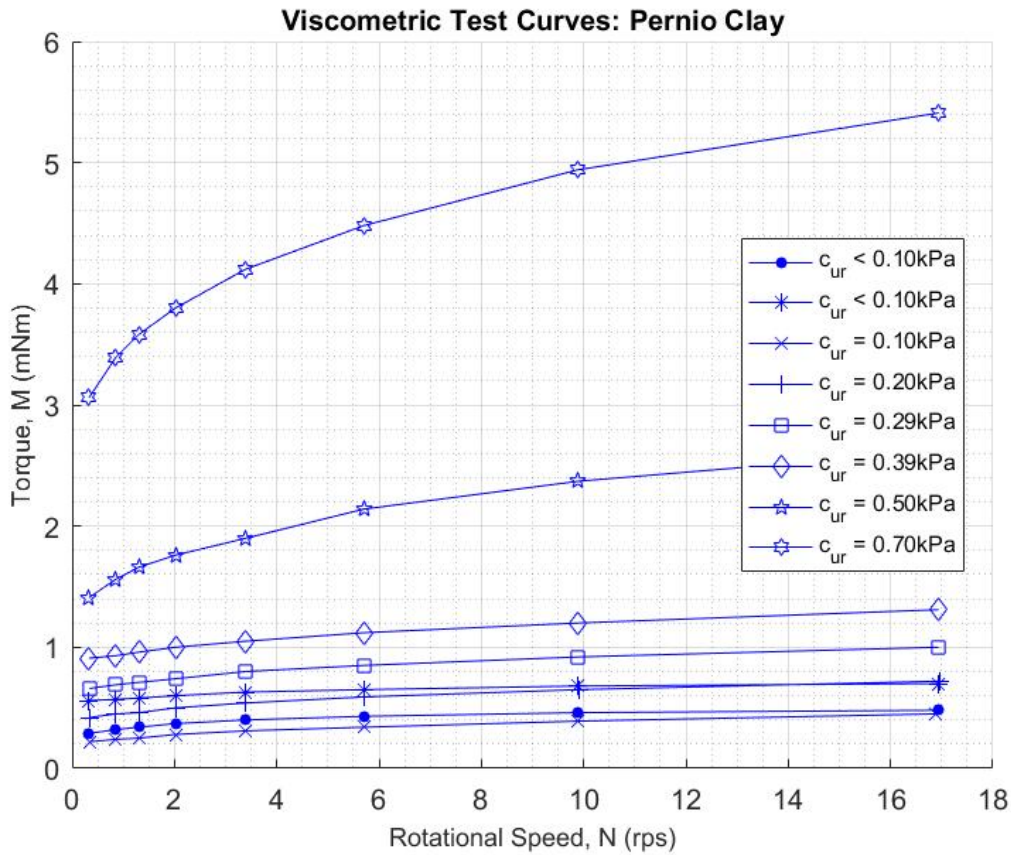


Figure 5.28: Torque-Speed viscometric curves for Perniö Clay

The flow behaviour of the fine-grained material changes when the remoulded shear strength reaches and exceeds 0.5 kPa as illustrated by the curve shapes in Figure 5.28. This is consistent with the Norwegian criteria for classifying a quick clay as discussed in Section 2.1.2.

5.6.1 Yield Stress

Figure 5.29 shows the relationship between the yield stress and liquidity index. The yield stress is decreasing with increasing liquidity index. Figure 5.30 shows the relationship between the yield stress and salinity. A regression line has been found for the results with salinity 1.04-1.78 g/L and liquidity index 1.28-1.84 (shown in Figure 5.29). The relationship is given by the expression:

$$\tau_y = \left(\frac{2.83}{I_L}\right)^{6.36} \tag{5.5}$$

where τ_y is in Pa and I_L is the liquidity index. The coefficient of determination, $R^2 = 0.979$.

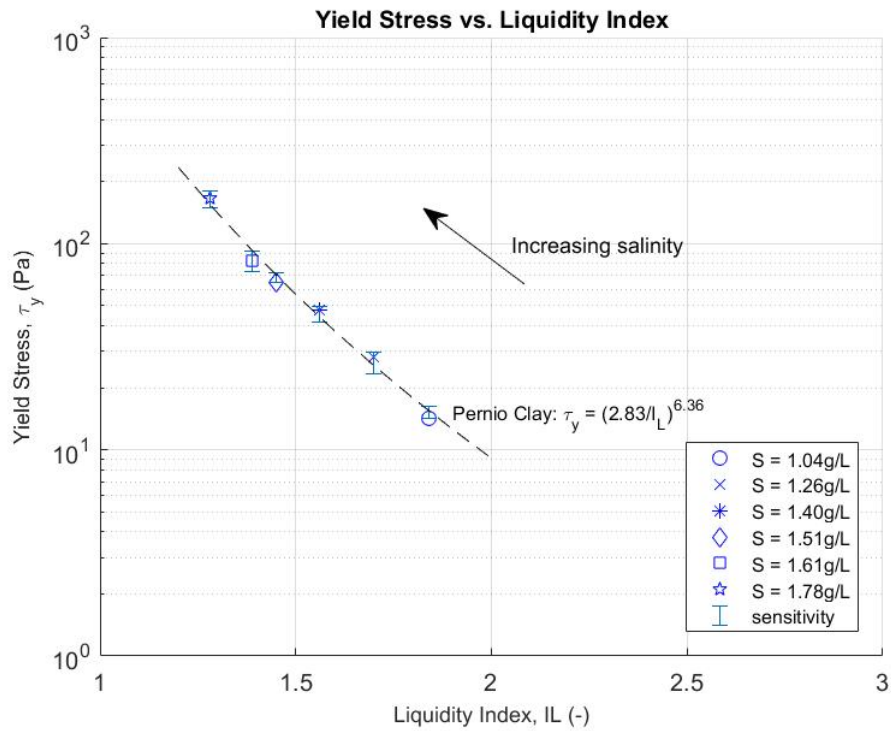


Figure 5.29: Yield stress versus liquidity index for Perniö Clay

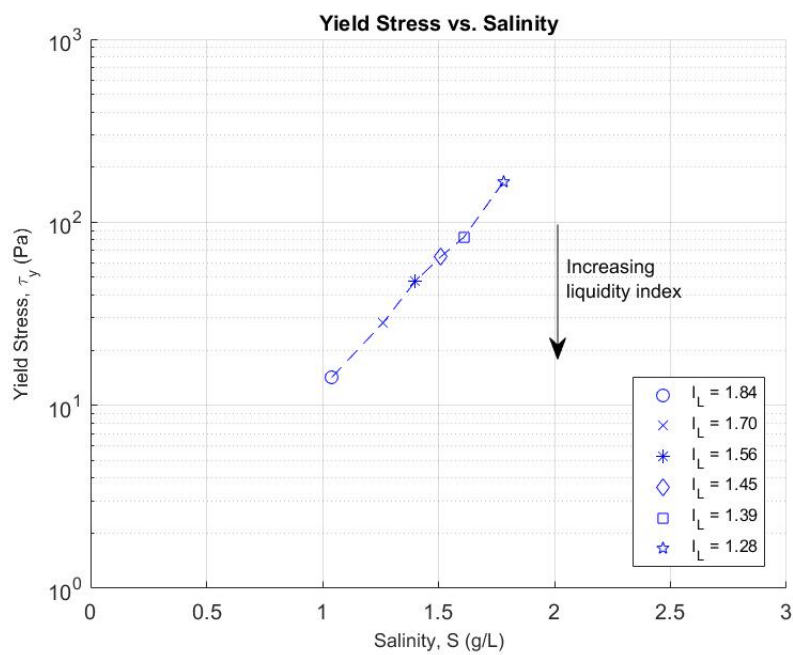


Figure 5.30: Yield stress versus salinity for Perniö Clay

5.6.2 Consistency Parameter

Figure 5.31 shows the relationship between the consistency parameter and liquidity index. The consistency parameter (K^*) is decreasing with increasing liquidity index. Conversely, as the salinity increases, so to does K^* . This is also shown in Figure 5.32.

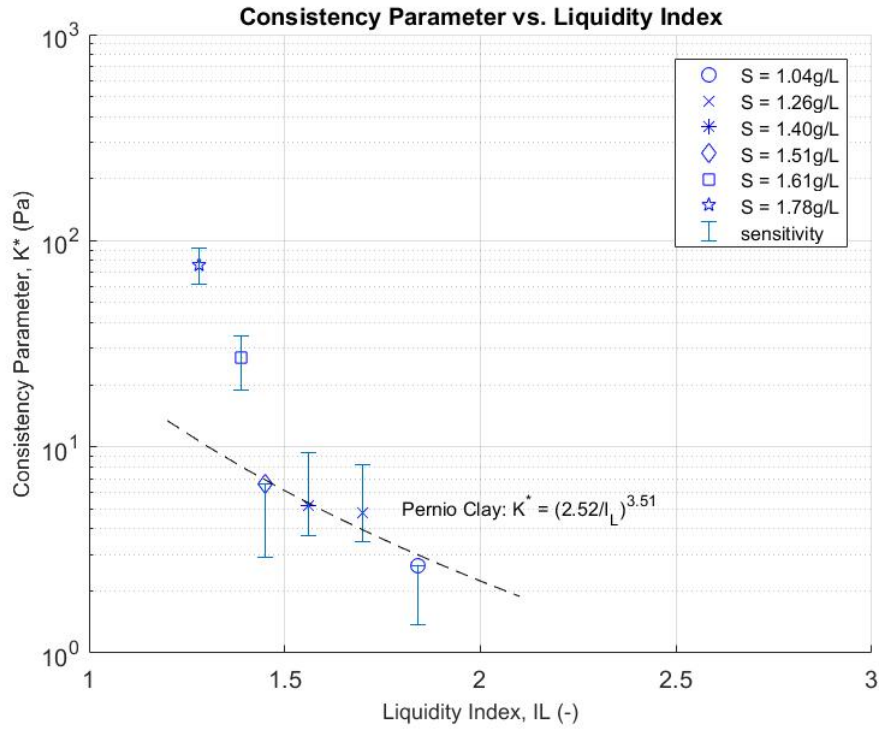


Figure 5.31: Consistency parameter versus liquidity index for Perniö clay

A regression line has been found for the results with salinity 1.04-1.51 g/L and liquidity index 1.45-1.84 (shown in Figure 5.31). Only the results for the clays with remoulded shear strength less than 0.5 kPa were considered. The relationship is given by the expression:

$$K^* = \left(\frac{2.52}{I_L} \right)^{3.51} \quad (5.6)$$

where K^* is in Pa and I_L is the liquidity index. The coefficient of determination, $R^2 = 0.882$.

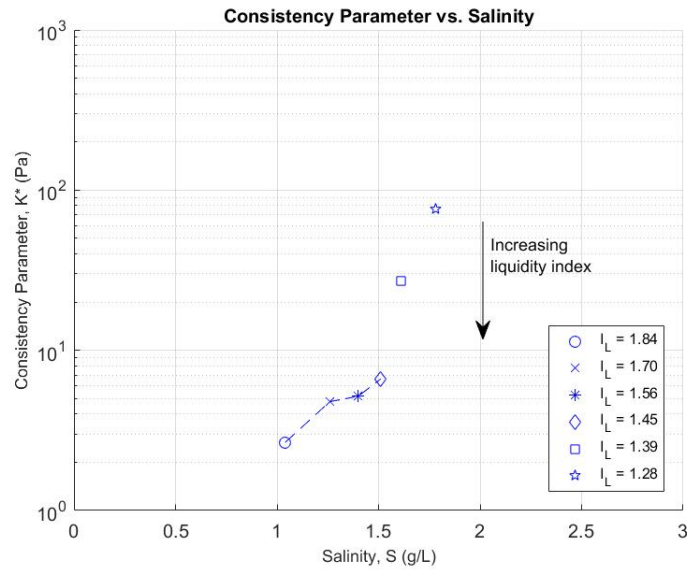


Figure 5.32: Consistency parameter versus salinity for Perniö clay

5.6.3 Herschel-Bulkley Exponent

The Herschel-Bulkley exponent is plotted against the liquidity index in Figure 5.33. Figure 5.34 shows how n varies with salinity for different value of I_L . The value of n is increasing with increasing liquidity index. Salinity also contributes to the Herschel-Bulkley exponent with a decrease in salinity resulting in a higher n value.

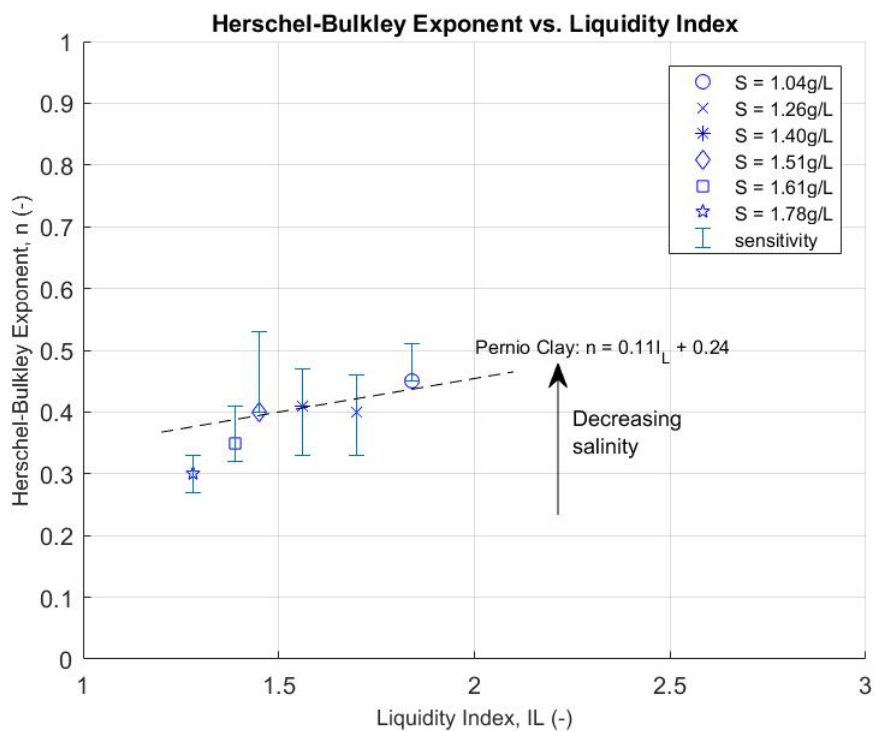


Figure 5.33: Herschel-Bulkley exponent versus liquidity index for Perniö clay

A relationship between n and I_L has been found for points with a salinity 1.04-1.51 g/L and I_L 1.45-1.84:

$$n = 0.11I_L + 0.24 \quad (5.7)$$

where n is dimensionless and I_L is the liquidity index. The coefficient of determination, $R^2 = 0.597$.

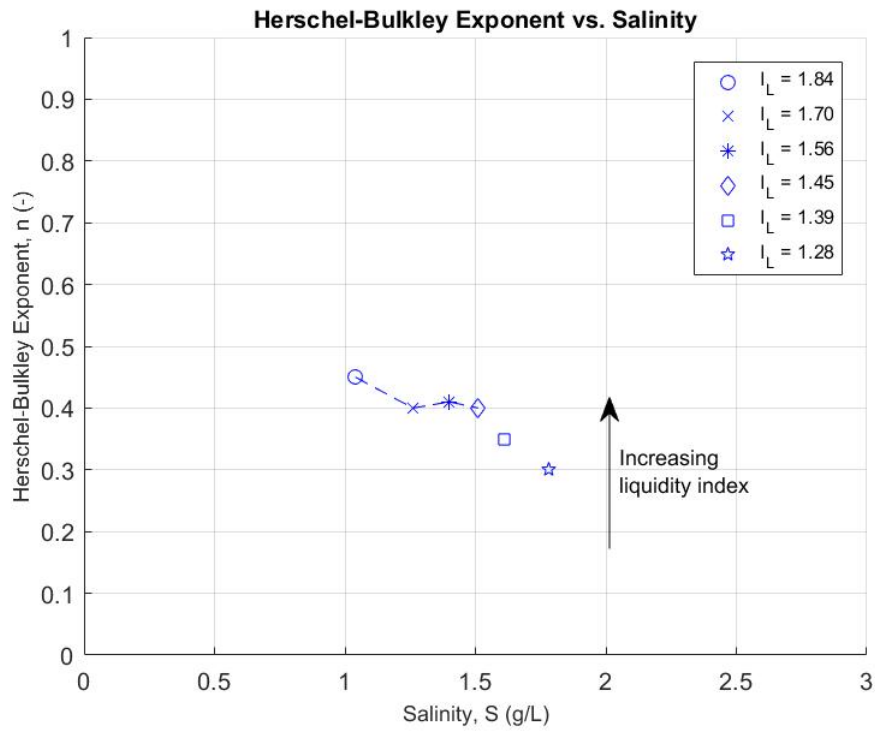


Figure 5.34: Herschel-Bulkley exponent versus salinity for Perniö clay

5.7 Herschel-Bulkley Parameters for Clayey Silt

In this section, the Herschel-Bulkley parameters for the Clayey Silt are plotted with respect to liquidity index and salinity. The parameters are shown in Table 5.8. Figure 5.35 shows the $T-N$ curves for the Clayey Silt.

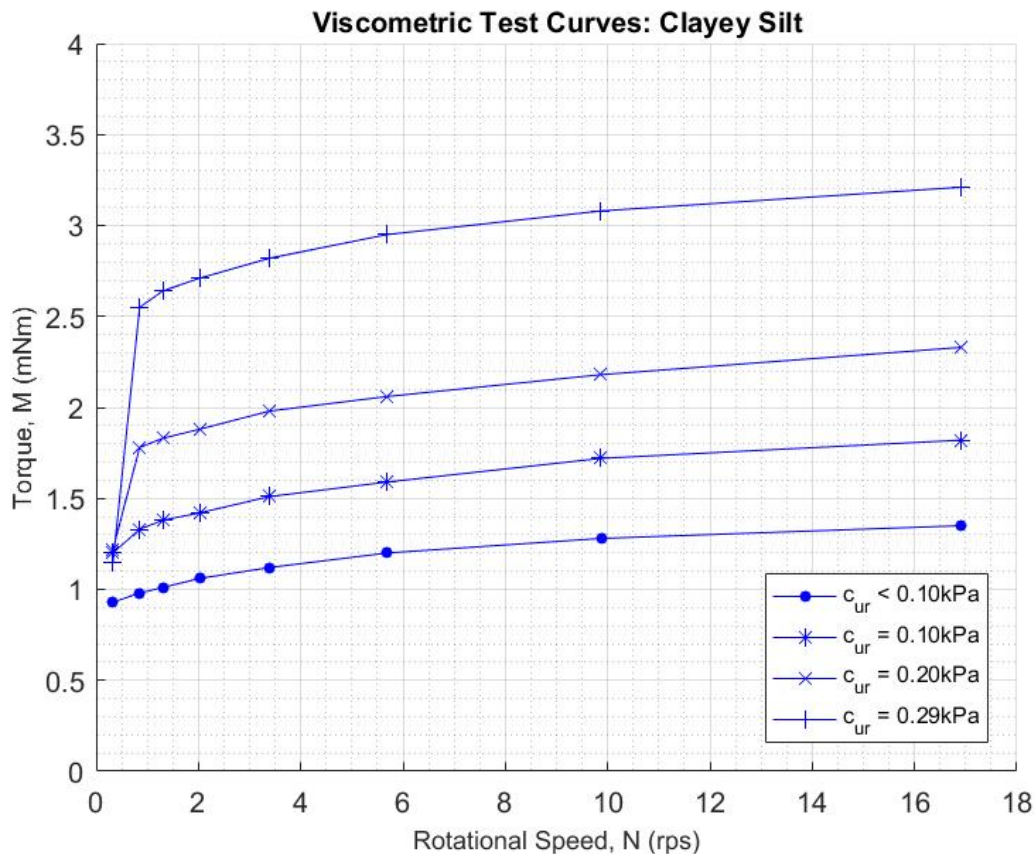


Figure 5.35: Torque-Speed viscometric curves for Clayey Silt

Similar to the Tiller clays, low torque values were measured at the lowest speed speeding for remoulded shear strength of 0.2 kPa and 0.29 kPa. The shape of the curves however, remains constant for speed settings 2 to 8.

5.7.1 Yield Stress

Figure 5.36 shows the relationship between the yield stress and liquidity index. The yield stress is decreasing with increasing liquidity index. Figure 5.37 shows the relationship between the yield stress and salinity.

A regression line has been found for the results with salinity 1.56-1.74 g/L and liquidity index 2.48-3.54 (shown in Figure 5.36). The relationship is given by the expression:

$$\tau_y = \left(\frac{15.7}{I_L} \right)^{2.7} \quad (5.8)$$

where τ_y is in Pa and I_L is the liquidity index. The coefficient of determination, $R^2 = 0.930$.

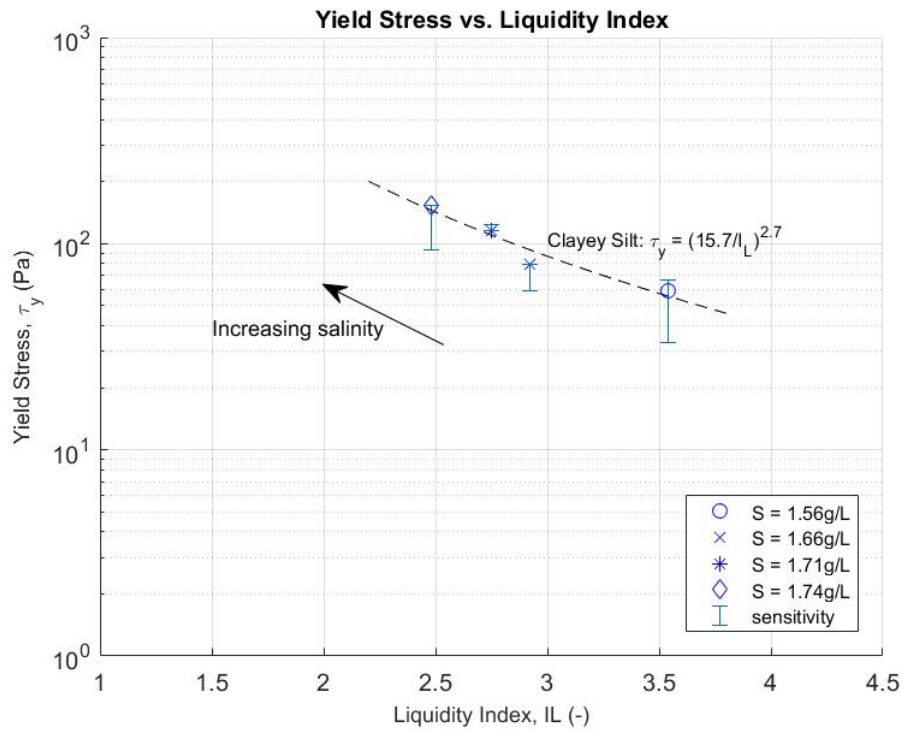


Figure 5.36: Yield stress versus liquidity index for Clayey Silt

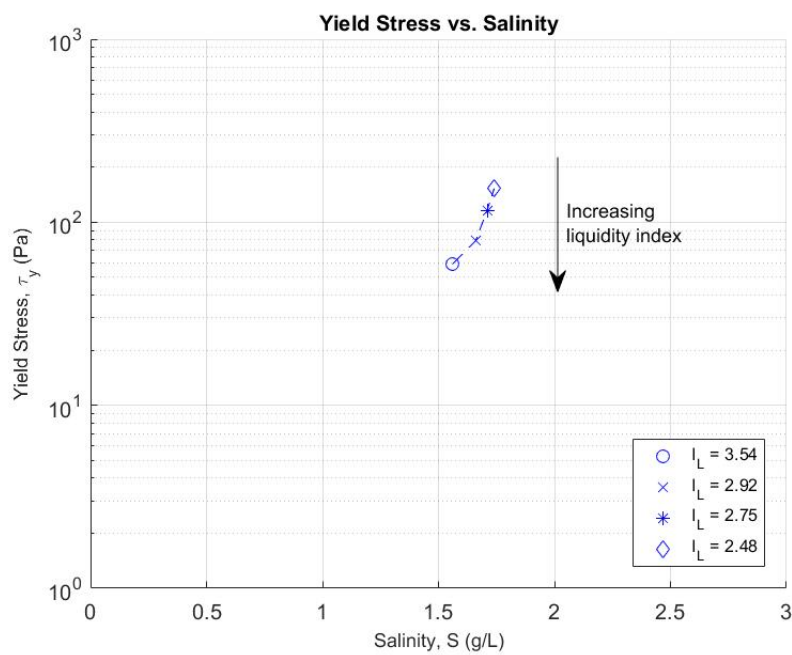


Figure 5.37: Yield stress versus salinity for Clayey Silt

5.7.2 Consistency Parameter

Figure 5.38 shows the relationship between the consistency parameter and liquidity index. The consistency parameter (K^*) is decreasing with increasing liquidity index. Conversely, as the salinity increases, so to does K^* . This is also shown in Figure 5.39.

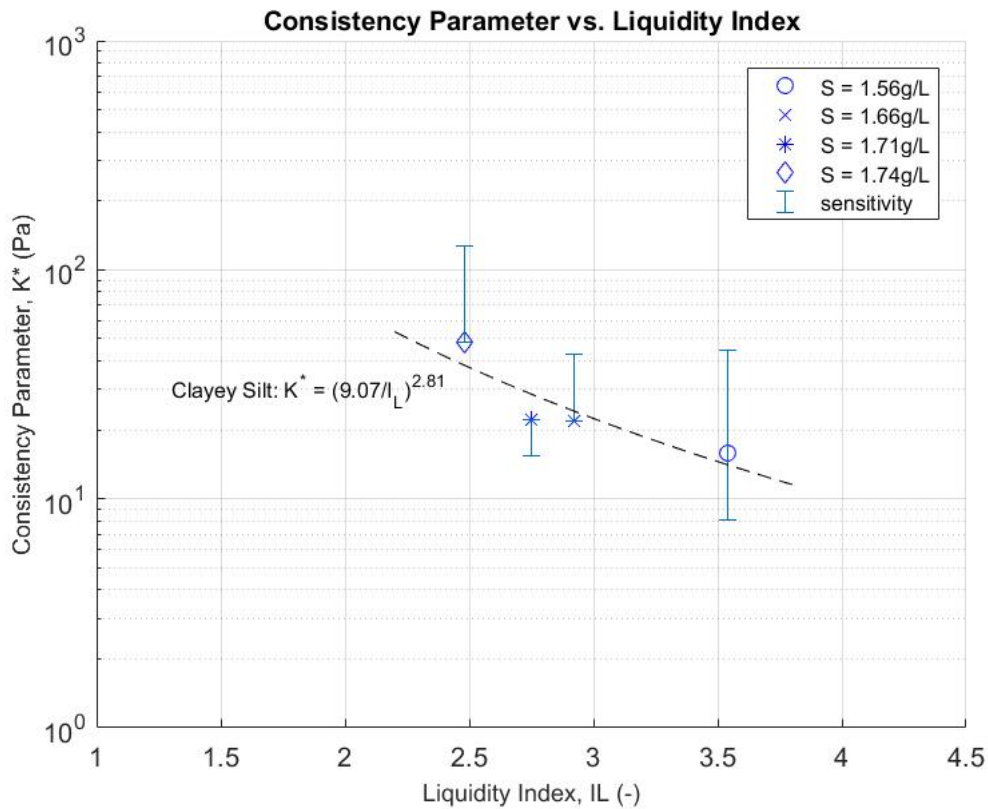


Figure 5.38: Consistency parameter versus liquidity index for Clayey Silt

A regression line has been found for the results with salinity 1.56-1.74 g/L and liquidity index 2.48-3.54 (shown in Figure 5.38). The relationship is given by the expression:

$$K^* = \left(\frac{9.07}{I_L} \right)^{2.81} \quad (5.9)$$

where K^* is in Pa and I_L is the liquidity index. The coefficient of determination, $R^2 = 0.785$.

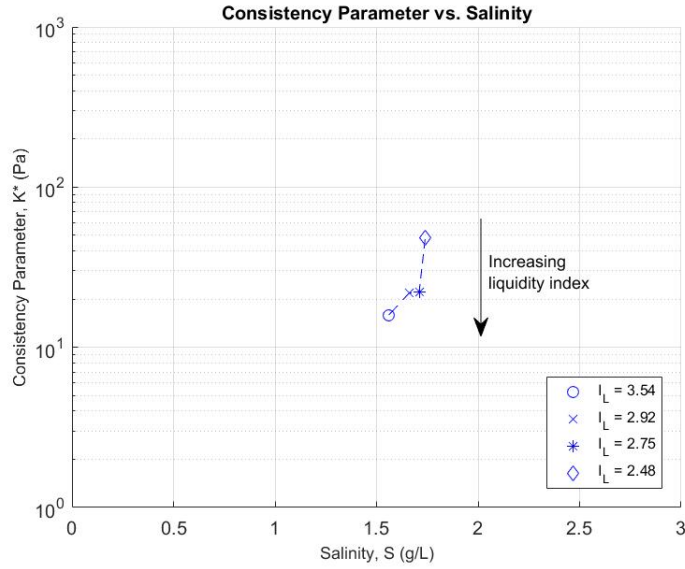


Figure 5.39: Consistency parameter versus salinity for Clayey Silt

5.7.3 Herschel-Bulkley Exponent

The Herschel-Bulkley exponent is plotted against the liquidity index in Figure 5.40. Figure 5.41 shows how n varies with salinity for different value of I_L . The value of n is increasing with increasing liquidity index. Salinity also contributes to the Herschel-Bulkley exponent with a decrease in salinity resulting in a higher n value.

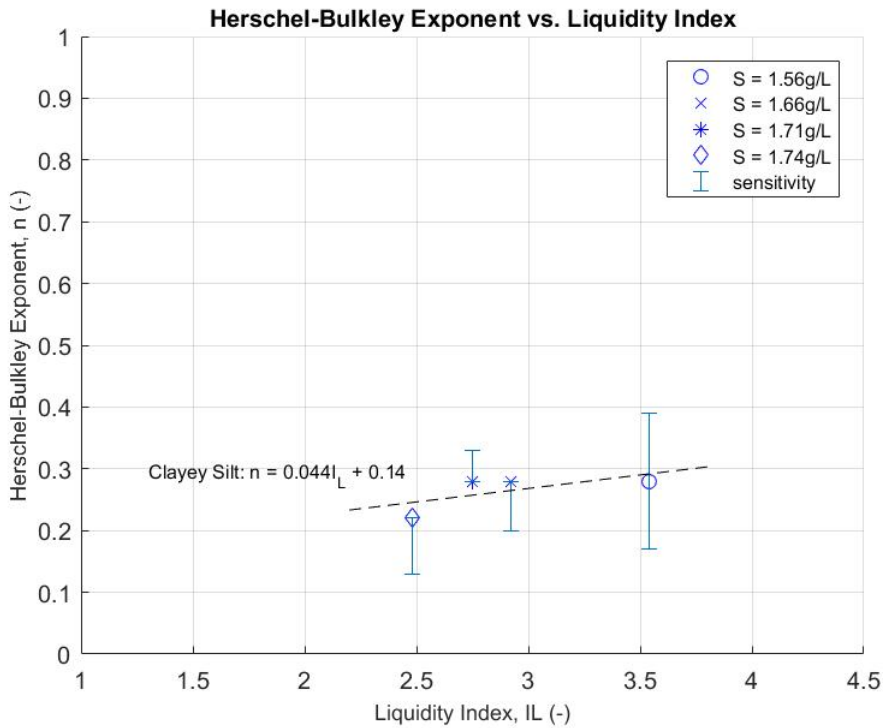


Figure 5.40: Herschel-Bulkley exponent versus liquidity index for Clayey Silt

A relationship between n and I_L has been found for points with a salinity 1.56-1.74 g/L and I_L 2.48-3.54:

$$n = 0.044I_L + 0.14 \quad (5.10)$$

where n is dimensionless and I_L is the liquidity index. The coefficient of determination, $R^2 = 0.430$.

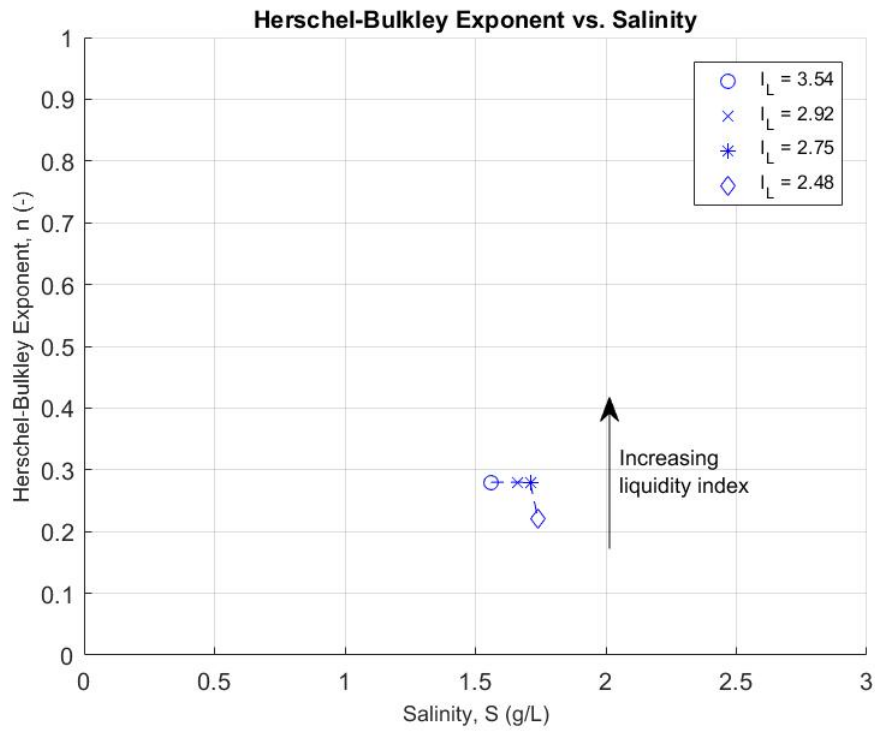


Figure 5.41: Herschel-Bulkley exponent versus salinity for Clayey Silt

5.8 Comparing All Results

This section shows the best fit Herschel-Bulkley parameters for all attainable past viscometric test results on Norwegian and Canadian fine-grained soils.

The Herschel-Bulkley model has been fitted to the Norwegian and Canadian test data (performed by [Locat and Demers](#); [Grue](#)) and the equivalent parameters were calculated by [Grue](#) as described in Chapter 2.7.3. A total of 15 Herschel-Bulkley resultant parameter sets were produced by [Grue \(2015\)](#) as well as another 112 sets calculated from [Locat et al.](#) data, with results plotted in Appendix B.

5.8.1 Yield Stress

The yield stress from fitting the Herschel-Bulkley model to viscometric results are plotted against the liquidity index for all fine-grained materials tested (*in red*). The past results have also been plotted (*in black*) and can be seen in Figure 5.42.

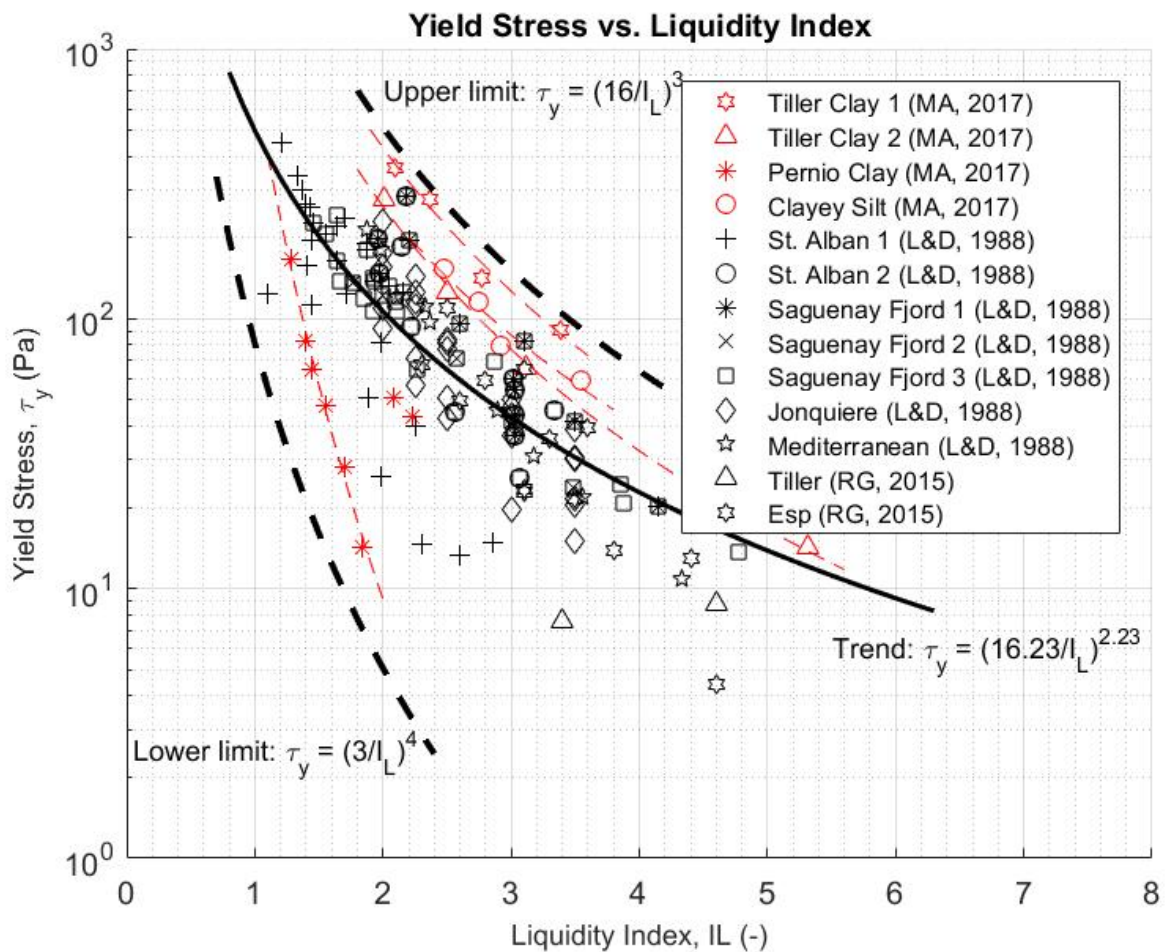


Figure 5.42: Herschel-Bulkley yield stress versus liquidity index (categorized by site)

Based on the results, the yield stress increases with decreasing liquidity index. Similarly, increasing the salinity also increases the yield stress of a fine-grained soil. A relationship between yield stress and liquidity index can be determined given the 127 data points, and expressed as:

$$\tau_y = \left(\frac{16.23}{I_L} \right)^{2.23} \quad (5.11)$$

where τ_y is in Pa and I_L is the liquidity index. The coefficient of determination, $R^2 = 0.570$.

Limits for the yield stress can be determined and expressed as:

$$\tau_{yUpper} = \left(\frac{16}{I_L} \right)^3 \quad (5.12)$$

$$\tau_{yLower} = \left(\frac{3}{I_L} \right)^4 \quad (5.13)$$

5.8.2 Consistency Parameter and Herschel-Bulkley Exponent

The consistency parameter and Herschel-Bulkley exponent for each viscometric sample tested have been plotted (*in red*) against the liquidity index in Figure 5.43 and Figure 5.44 respectively, along with past results (*in black*).

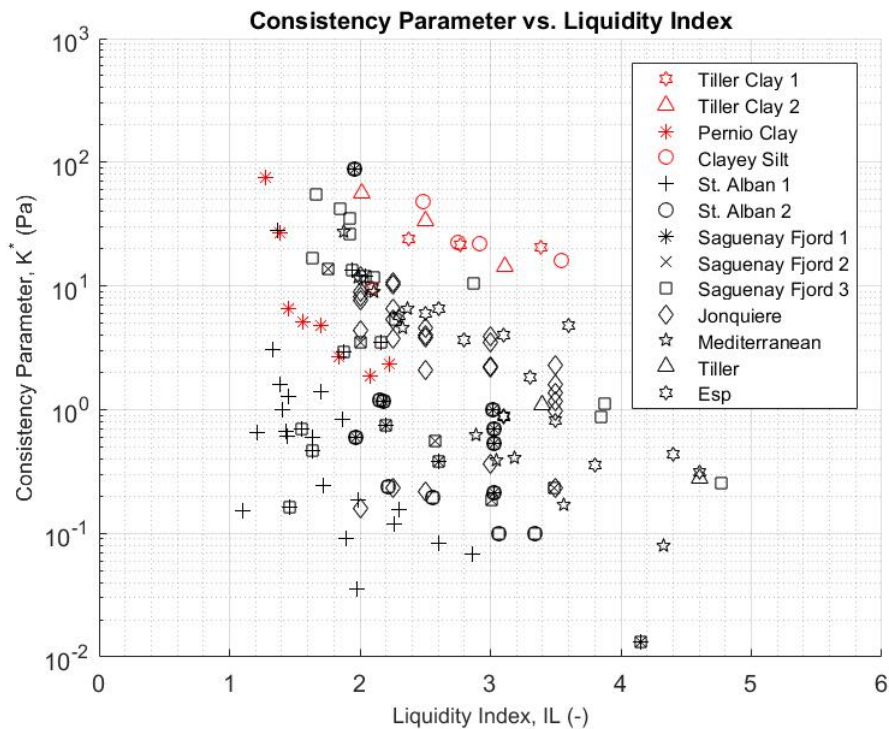


Figure 5.43: Herschel-Bulkley consistency parameter versus liquidity index (categorized by site)

There is no clear trend between liquidity index and the consistency parameter or Herschel-Bulkley exponent however the fine-grained soils tested produced a higher K^* value and lower n value than most Canadian clay results. This is demonstrated in Figure 5.45 where the consistency parameter is plotted against Herschel-Bulkley exponent. A

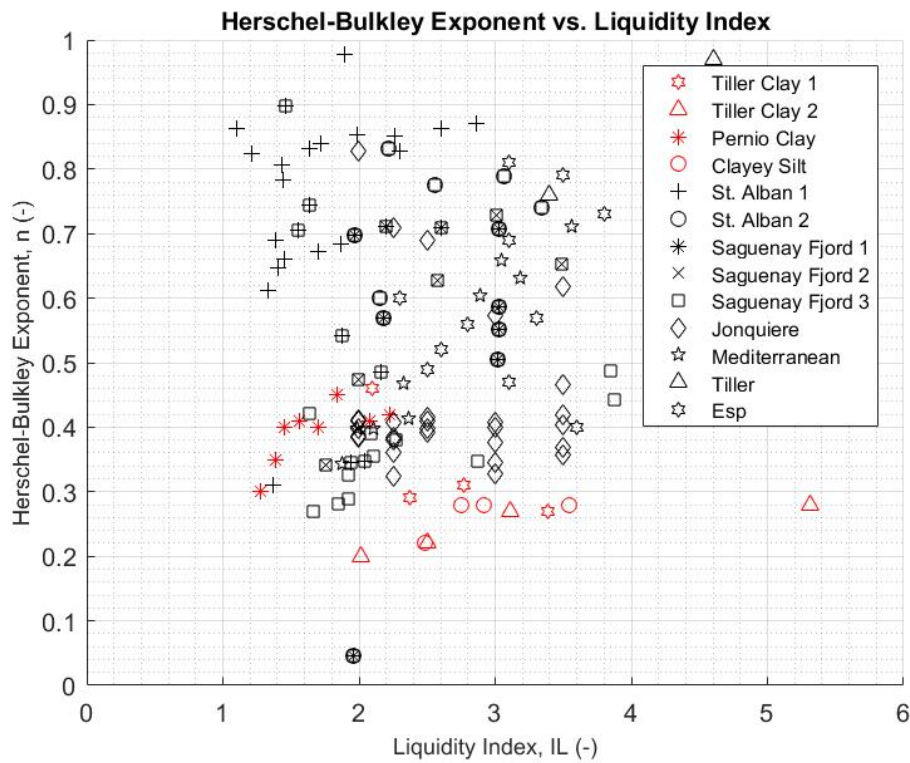


Figure 5.44: Herschel-Bulkley exponent versus liquidity index (categorized by site)

relationship between consistency parameter and Herschel-Bulkley exponent can be derived and expressed as:

$$K^* = 152e^{-8.2n} \quad (5.14)$$

$$n = 0.65 - 0.1 \ln(K^*) \quad (5.15)$$

where K^* is in Pa and n is dimensionless. The coefficient of determination, $R^2 = 0.852$ and the correlation coefficient is -0.583 which suggests a strong correlation between the two parameters.

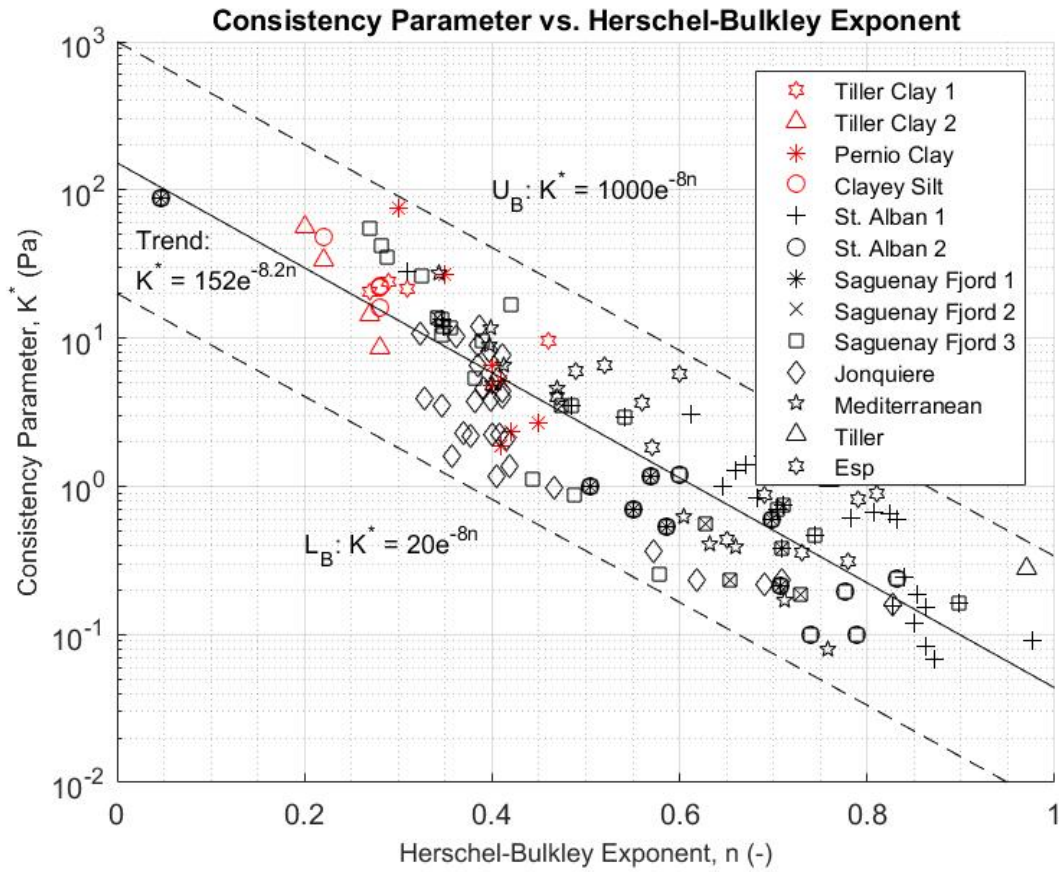


Figure 5.45: Herschel-Bulkley consistency parameter versus exponent (categorized by site)

Proposed consistency parameter limits can be expressed as:

$$K^*_{Upper} = 1000e^{-8n} \tag{5.16}$$

$$K^*_{Lower} = 20e^{-8n} \tag{5.17}$$

where K^* is measured as in Pa and n dimensionless.

5.9 Relationship Between Quickness and Flow Behaviour

Figure 5.46 shows the relationship between measured quickness and yield stress of the fine-grained soils tested. The yield stress increases as the quickness reduces. This was also observed in Figure 5.5 which compares the quickness to remoulded shear strength. Although there is no equation that can be derived to express the relationship between the two, a clear observable trend exists in that yield stress decreases with increasing quickness.

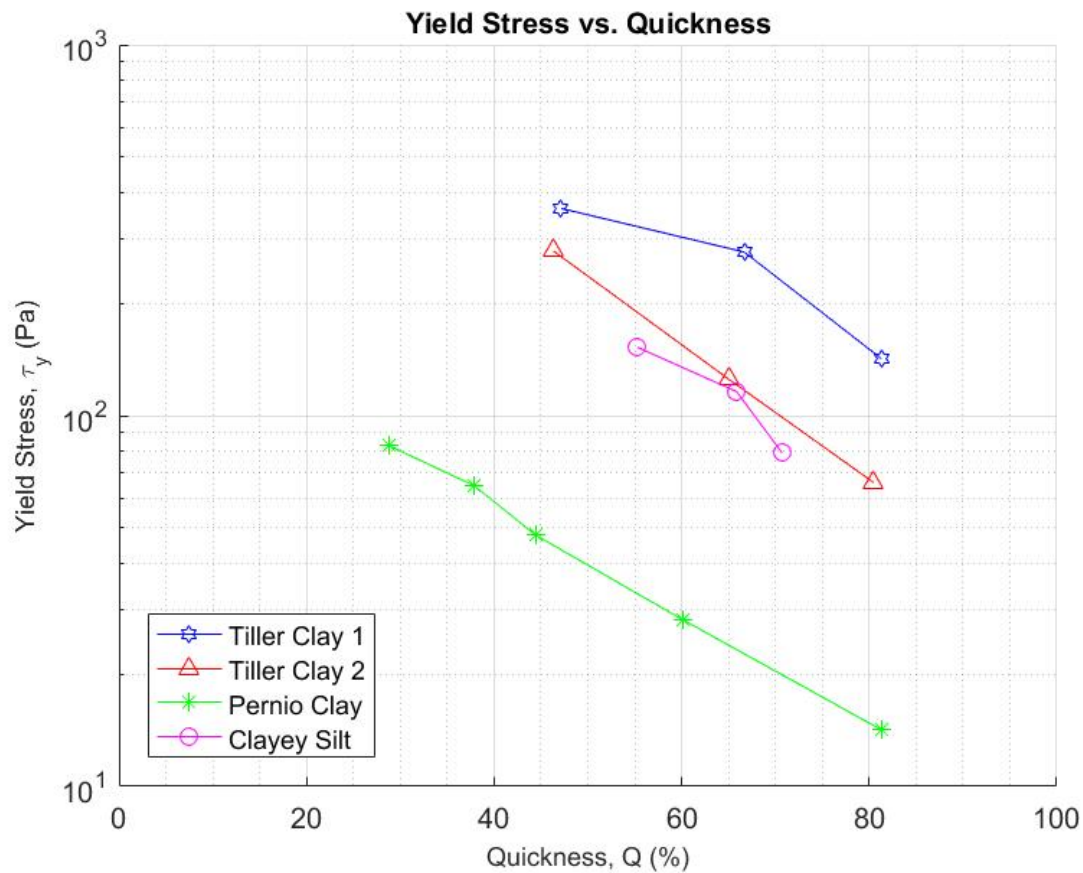


Figure 5.46: Relationship between quickness and yield stress

There are no definitive relationships between quickness and the consistency parameter or Herschel-Bulkley exponent due to their sensitivity and complex nature as discussed in Sections 2.7.2, 5.3.4 and 5.8.2. Trends, however, have been observed and can also be linked to quickness. As the yield stress increases, so too does the consistency parameter and inversely the Herschel-Bulkley exponent.

It is envisaged that in the future, quickness tests will be simulated numerically to generate calibrated rheology parameters which can be used for modelling and analysis.

5.10 Use of Data for Norwegian Applications

This thesis is a part of a new 'Slide run-out' module in the software GeoSuite Toolbox as a part of the GeoFuture II R&D project (www.geofuture.no). This R&D project aims at integrating geotechnical design calculations with the management of in-situ and laboratory geotechnical data, selection of input parameters for analysis, online assistance to the user and 3D visualisation. The 'Slide run-out' module will assist in the assessment of the retrogression and run-out distances with the above empirical relationships, and will illustrate the run-out over an area in three dimensions.

Chapter 6

Conclusions and Further Work

6.1 Conclusions

The flow behaviour of fine-grained soils, including quick clays, has been examined through quickness and viscometer testing. The Herschel-Bulkley model was used to describe the shear thinning nature of soils and to produce flow curves from the viscometric results.

A total of 35 quickness tests were performed on natural quick clays from Tiller, Norway and Perniö, Finland as well as an artificial clayey silt and silt. The quickness results verified the proposed quickness limits by [Thakur and Degago \(2012\)](#):

$$Q_{Upper} = 25(c_{ur})^{-0.7} \quad (6.1)$$

$$Q_{Lower} = 15(c_{ur})^{-0.7} \quad (6.2)$$

It was found that the normalized water content (w/w_L) is a more suitable measure of comparison between soils than using the liquid limit. The Finnish clay had a significantly higher water content and plasticity than Norwegian clays. Proposed quickness limits can be expressed as a function of normalized water content:

$$Q_{Upper} = 146\left(\frac{w}{w_L}\right) - 129 \quad (6.3)$$

$$Q_{Lower} = 146\left(\frac{w}{w_L}\right) - 176 \quad (6.4)$$

Regions of varying remoulded shear strength have also been detected when plotting Q results against w/w_L . This provides the potential to predict quickness values for a given

remoulded shear strength and water content calculated from samples extracted from the field.

For a constant water content, the quickness of a soil decreases when the salinity is increased. This is also indicated by an increase in remoulded shear strength which is logical as relationships can be determined between Q , c_{ur} , w and S .

Although the quickness test is very effective for clays and clayey silts, it can be concluded that the quickness test is not suitable for silt soils due to high levels of segregation.

In total, 24 viscometer tests were performed. The fine-grained soils show shear thinning behaviour when exposed to shear. The flow curves are well fitted with the Herschel-Bulkley model. The Herschel-Bulkley parameters τ_y , K^* and n show a dependency on salinity and liquidity index. τ_y also showed a dependency on temperature.

The Tiller clays showed an increase in yield stress, τ_y with increasing salinity, for a constant water content. Conversely τ_y decreases with increasing liquidity index, for a constant salinity.

The Herschel-Bulkley triplet, τ_y , K^* and n , for a flow curve is not unique. Large variations in K^* and n are observed when τ_y varies. Herschel-Bulkley yield stress, however, is a good approximation of the real yield stress.

When plotting past Herschel-Bulkley results from Norwegian and Canadian clays with the parameters calculated as part of this study, a significant relationship between yield stress and liquidity index was observed. The proposed relationship and yield stress limits are expressed as:

$$\tau_y = \left(\frac{16.23}{I_L} \right)^{2.23} \quad (R^2 = 0.570) \quad (6.5)$$

$$\tau_{yUpper} = \left(\frac{16}{I_L} \right)^3 \quad (6.6)$$

$$\tau_{yLower} = \left(\frac{3}{I_L} \right)^4 \quad (6.7)$$

No such trend exists between liquidity index and either K^* or n , however a strong correlation between K^* and n is noted. The regression equation for the trend as well as the proposed limits are:

$$K^* = 152e^{-8.2n} \quad (R^2 = 0.852) \quad (6.8)$$

$$K^*_{Upper} = 1000e^{-8n} \quad (6.9)$$

$$K^*_{Lower} = 20e^{-8n} \quad (6.10)$$

No relationship between quickness and the Herschel-Bulkley parameters can be determined however a logical trend of increasing yield stress with decreasing quickness was observed.

It can be recommended that although this study into the application of the Herschel-Bulkley model on the rheological behaviour of fine-grained soils has provided valuable insights, there is no substitution for accurate and relevant test data from samples collected in the field when proposing geotechnical input parameters into run-out and regression models for three dimensional analysis and design.

6.2 Further Work

Further quickness tests could be performed to investigate the effect of different clay contents. It would also be beneficial to conduct more tests at varied salinities and liquidity indices, for the same soil to further investigate their effect on quickness.

Further viscometer tests could be performed on Norwegian quick clays, typically on samples from at-risk locations. Norwegian clay from Esp and Tiller have so far only been used for viscometric analysis. As stated for quickness tests, additional tests varying the salinity and liquidity index on the same soil would provide further information into their effect on the Herschel-Bulkley parameters.

Limited data meant that no relationship between remoulded shear stress and yield stress could be established. This would be a valuable addition in the future when more tests are performed.

The relationships between the Herschel-Bulkley parameters and index properties found in this thesis should be tested in numerical simulations of slides.

In future quickness will be used to predict the viscosity of a soil based on the geotechnical index parameters. Quickness tests will be modelled numerically using Computational Fluid Dynamics (CFD) simulations and calibrated with this thesis results to generate rheology parameter outputs based on a reverse-engineering approach from test data.

Bibliography

- Bjerrum, L. (1954). Geotechnical properties of norwegian marine clays. *Geotechnique*, 4(2):49–69.
- Bjerrum, L. (1967). Engineering geology of norwegian normally-consolidated marine clays as related to settlements of buildings. *Geotechnique*, 17(2):83–118.
- Bohlin (2006). *Technical manual for the Bohlin Visco 88 BV*.
- Coussot, P., Laigle, D., Arattano, M., Deganutti, A., and Marchi, L. (1998). Direct determination of rheological characteristics of debris flow. *Journal of hydraulic engineering*, 124(8):865–868.
- Coussot, P. and Piau, J. M. (1994). On the behavior of fine mud suspensions. *Rheologica Acta*, 33(3):175–184.
- Coussot, P. and Piau, J.-M. (1995). A large-scale field coaxial cylinder rheometer for the study of the rheology of natural coarse suspensions. *Journal of Rheology*, 39(1):105–124.
- Crawford, C. B. (1968). Quick clays of eastern canada. *Engineering Geology*, 2(4):239–265.
- Csaba, P. and Csaba, J. (2011). Hydrology.
- Dahl, R., Sveian, H., and Thoresen, M. K. (1997). Nord-trøndelag og fosen: geologi og landskap. *Norges geologiske undersøkelse, Trondheim. Utgitt i forbindelse med Samordnet geologiskundersøkelsesprogramforNord-TrøndelagogFosen*.
- D’Ignazio, M., Phoon, K.-K., Tan, S. A., and Länsivaara, T. T. (2016). Correlations for undrained shear strength of finnish soft clays. *Canadian Geotechnical Journal*, 53(10):1628–1645.
- Eden, W. J. and Kubota, J. K. (1961). Some observations on the measurement of sensitivity of clays. *Proceedings, American Society for Testing and Materials*, 61:1239–1249.
- Gregersen, O. (2014). *Skreddynamikk. In Skred: skredfare og sikringstiltak : praktiske erfaringerogteoretiskeprinsipper*. NGI.

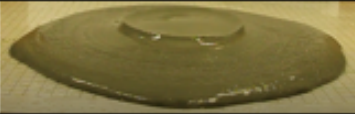
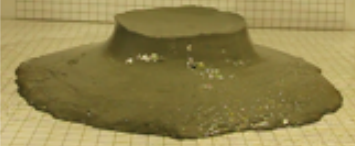
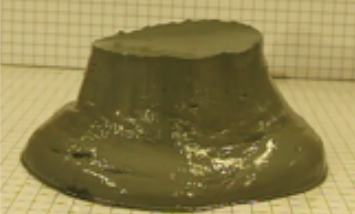
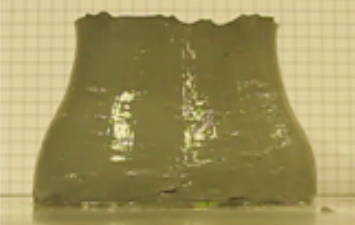
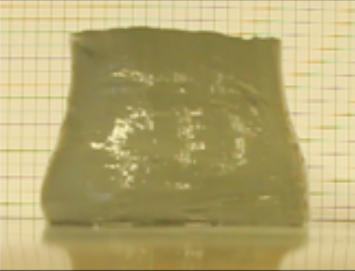
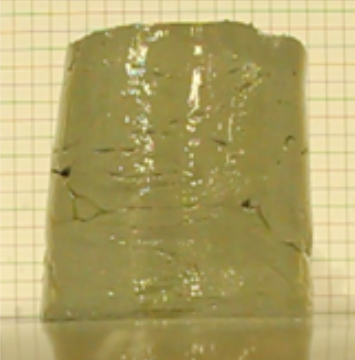
- Grue, R. H. (2015). Rheological parameters of norwegian sensitive clays, focusing on the herschel-bulkley model. Master's thesis, NTNU.
- Gylland, A., Long, M., Emdal, A., and Sandven, R. (2013). Characterisation and engineering properties of tiller clay. *Engineering Geology*, 164:86–100.
- Heirman, G., Vandewalle, L., Van Gemert, D., and Wallevik, O. (2008). Integration approach of the couette inverse problem of powder type self-compacting concrete in a wide-gap concentric cylinder rheometer. *Journal of non-Newtonian fluid mechanics*, 150(2):93–103.
- Helle, T. E. (2013). *Saltdiffusjon som grunnforsterking i kvikkleire : naturfareprosjektet : delprosjekt 6 kvikkleire*. Oslo : Norges vassdrags- og energidirektorat, 2013.
- Irgens, F. (2014). *Rheology and non-Newtonian fluids*. Springer.
- Issler, D., Cepeda, J. M., Luna, B. Q., and Venditti, V. (2013). Back-analyses of run-out for norwegian quick-clay landslides.
- Jeong, S. W. (2013). Determining the viscosity and yield surface of marine sediments using modified bingham models. *Geosciences Journal*, 17(3):241–247.
- Jeong, S. W., Locat, J., and Leroueil, S. (2012). The effects of salinity and shear history on the rheological characteristics of illite-rich and na-montmorillonite-rich clays. *Clays and Clay Minerals*, 60(2):108–120.
- Johnson, A. (1970). *Physical Processes in Geology: A Method for Interpretation of Natural Phenomena; Intrusions in Igneous Rocks, Fractures, and Folds, Flow of Debris and Ice*. Freeman, Cooper & Company.
- Karlsrud, K., Aas, G., and Gregersen, O. (1985). *Can We Predict Landslide Hazards in Soft Sensitive Clays?: Summary of Norwegian Practice and Experiences*. Norges Geotekniske Institutt. Norges geotekniske institutt.
- Laigle, D. and Coussot, P. (1997). Numerical modeling of mudflows. *Journal of Hydraulic Engineering*, 123(7):617–623.
- Lebuis, J. and Rissmann, P. (1979). Les coulées argileuses dans le région de québec et de shawinigan. in "argiles sensibles, pentes instables, mesures correctives at coulées de régions de québec et shawingen". *Geo. Assoc. of Canada Guidebook*, pages 19–40.
- Lebuis, J., Robert, J. M., and Rissman, P. (1983). Regional mapping of landslide hazard in quebec. *Proc. Symp. Slopes on Soft Clays, Linköping*, pages 205–262.
- Leroueil, S. (2001). Natural slopes and cuts: movement and failure mechanisms. *Geotechnique*, 51(3):197–243.

- Leroueil, S., Samson, L., and Bozozuk, M. (1983). Laboratory and field determination of preconsolidation pressures at gloucester. *Canadian Geotechnical Journal*, 20(3):477–490.
- L'Heureux, J.-S. (2013). Nifs-report nr. 8/2013: Characterisation of historical quick clay landslides and input for q-bing. prepared by ngi. published by norwegian water resources and energy directorate in collaboration with norwegian public roads administration and norwegian national railways administration.
- Locat, J. (1997). *Normalized Rheological Behaviour of Fine Muds and Their Flow Properties in a Pseudoplastic Regime*. Debris-Flow Hazards Mitigation: Mechanics, Prediction, and Assessment.
- Locat, J. and Demers, D. (1988). Viscosity, yield stress, remolded strength, and liquidity index relationships for sensitive clays. *Canadian Geotechnical Journal*, 25(4):799–806.
- L'Heureux, J.-S., Locat, A., Leroueil, S., Demers, D., and Locat, J. (2014). Landslides in sensitive clays—from geosciences to risk management. In *Landslides in Sensitive Clays*, pages 1–12. Springer.
- Mataić, I. et al. (2016). On structure and rate dependence of perniö clay.
- Mitchell, J. K., Soga, K., et al. (2005). Fundamentals of soil behavior.
- Mitchell, R. J. and Markell, A. R. (1974). Flow slides in sensitive soils. *Canad. Geotech. J.*, 11(1):11–31.
- Morton, D. M. and Hauser, R. M. (2001). A debris avalanche at forest falls, san bernardino county, california. *July 11, 1999: U.S. Geological Survey Open-File Report 01-146*, page 67.
- NGF (1982). *Veiledning for symboler og definisjoner i geoteknikk : presentasjon av geotekniske undersøkelser*. [Oslo] : Norsk geoteknisk forening.
- NGU (2015). Debris slides and debris flows.
- NGU (2016). Quick clay and quick clay landslides.
- NS8001 (1982). Geoteknisk prøving, laboratoriemetoder, støtflytegrensen. *Standard Norge, Lysaker*.
- NS8003 (1982). Geoteknisk prøving, laboratoriemetoder, plastisitetsgrensen. *Standard Norge, Lysaker*.
- NS8013 (1982). Geoteknisk prøving, laboratoriemetoder, vannhold. *Standard Norge, Lysaker*.

- NS8015 (1982). Geoteknisk prøving, laboriemetoder, bestemmelse av udrenert sklaerstyrke ved konusprøving. *Standard Norge, Lysaker*.
- NTNU (2015). *Geotechnics Field and Laboratory Investigations*. Norwegian University of Science and Technology.
- O'Kelly, B. C. (2013). Atterberg limits and remolded shear strength—water content relationships.
- Rosenqvist, I. T. (1953). Considerations on the sensitivity of norwegian quick-clays. *Geotechnique*, 3(5):195–200.
- Schramm, G. (1994). *A practical approach to rheology and rheometry*. Haake Karlsruhe.
- Skempton, A. and Northey, R. (1952). The sensitivity of clays. *Geotechnique*, 3(1):30–53.
- Tavenas, F, Flon, P, Lerouil, S., and Lebuis, J. (1983). Remoulding energy and risk of slide retrogression in sensitive clays. *Proc. Symp. Slopes on Soft Clays, Linköping*, pages 423–454.
- Terzaghi, K. (1944). *Ends and Means in Soil Mechanics*. Publications from the Graduate School of Engineering, Harvard University, 1944-45. Harvard University.
- Terzaghi, K., Peck, R. B., and Mesri, G. (1996). *Soil mechanics in engineering practice*. John Wiley & Sons.
- Thakur, V. and Degago, S. (2012). Quickness of sensitive clays. *Géotechnique Letters*, 2(3):87–95.
- Thakur, V. and Degago, S. (2014). Quickness test approach for assessment of flow slide potentials. *Geotechnical Engineering Journal of the SEAGS and AGSSEA: Physical Modelling in Geotechnical Engineering, March*, 45:45–55.
- Torrance, J. K. (1987). Shear resistance of remoulded soils by viscometric and fall-cone methods: a comparison for the canadian sensitive marine clays. *Canadian Geotechnical Journal*, 24(2):318–322.
- Trak, B. and Lacasse, S. (1996). *Soils susceptible to flow slides and associated mechanisms*, volume 1.
- Vaunat, J. and Leroueil, S. (2002). Analysis of post-failure slope movements within the framework of hazard and risk analysis. *Natural Hazards*, 26(1):81–107.
- Weerakoon, W. (2015). *Rheological properties of clayey soils at high water content measured by viscometer and laboratory vane shear test*. PhD thesis, thesis for the Degree of Master of Engineering.

Appendix A


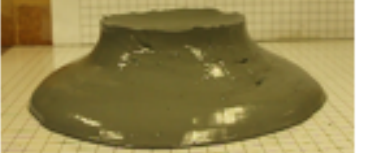
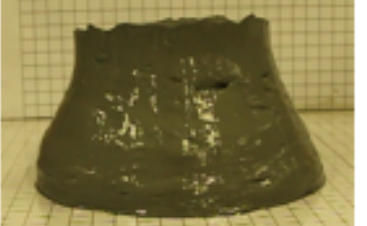
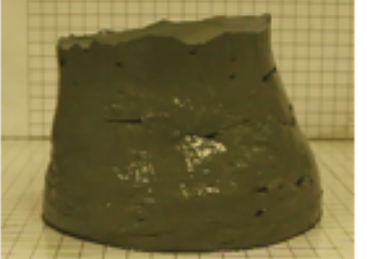
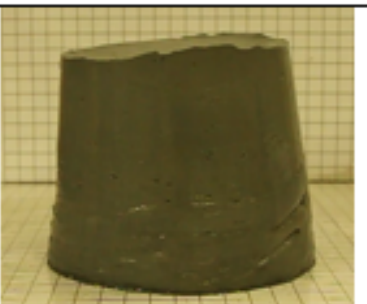

Quickness Test Results

Remoulded Shear Strength c_{ur} (kPa)	Initial Height H_0 (mm)	Final Height H_f (mm)	Base Dimensions D_f (mm)*	Quickness Q (%)	Laboratory Quickness Test**
0.10	123	23	307-317	81.30%	
0.20	123	41	262	66.67%	
0.29	123	65	182	47.15%	
0.39	123	73	143-148	40.65%	
0.49	123	77	143-150	37.40%	
0.65	123	84	-	31.71%	-
0.80	123	89	-	27.64%	-
0.95	123	92	120	25.20%	

*NB: Base diameter dimensions may vary due irregular slurry spread

**Not all test photos included, only typical slump shapes

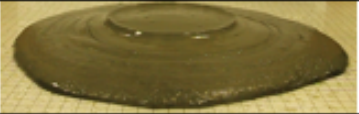


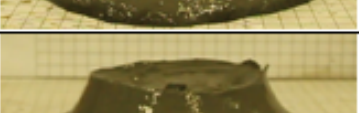


Figure A.1: Quickness test results - Tiller Clay 1

Remoulded Shear Strength c_u (kPa)	Initial Height H_0 (mm)	Final Height H_f (mm)	Base Dimensions D_f (mm)*	Quickness Q (%)	Laboratory Quickness Test**
0.10	123	24	306	80.49%	
0.20	123	43	215-220	65.04%	
0.29	123	66	156-160	46.34%	
0.39	123	75	142	39.02%	
0.49	123	81	133	34.15%	-
0.59	123	92	128	25.20%	
0.78	123	93	121	24.39%	
0.95	123	95	118	22.76%	-

*NB: Base diameter dimensions may vary due irregular slurry spread

**Not all test photos included, only typical slump shapes



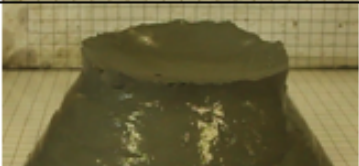



Figure A.2: Quickness test results - Tiller Clay 2

Remoulded Shear Strength c_{ur} (kPa)	Initial Height H_0 (mm)	Final Height H_f (mm)	Base Dimensions D_f (mm)*	Quickness Q (%)	Laboratory Quickness Test**
0.10	123	23	250-320	81.30%	
0.20	123	49	265-275	60.16%	
0.29	108	60	225-230	44.44%	
0.39	74	46	180	37.84%	
0.49	59	42	130	28.81%	
0.98	45	39	115	13.33%	

*NB: Base diameter dimensions may vary due irregular slurry spread

** Limited material for the latter tests meant that cylindrical moulds could not be filled



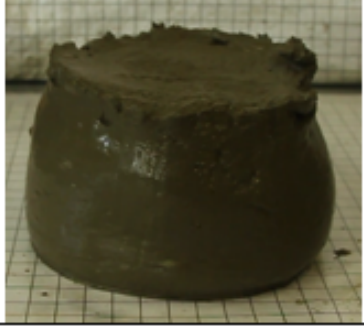
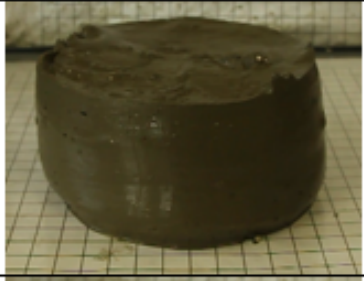
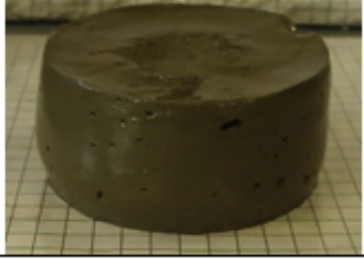
Figure A.3: Quickness test results - Finland clay

Remoulded Shear Strength c_{ur} (kPa)	Initial Height H_0 (mm)	Final Height H_f (mm)	Base Dimensions D_f (mm)*	Quickness Q (%)	Laboratory Quickness Test**
0.10	123	36	240	70.73%	
0.20	123	42	225	65.85%	
0.29	123	55	185	55.28%	
0.39	119	71	152	40.34%	
0.49	104	69	142	33.65%	-
0.69	94	70	119	25.53%	
0.98	78	64	112	17.95%	

*NB: Base diameter dimensions may vary due irregular slurry spread

** Limited material for the latter tests meant that cylindrical moulds could not be filled

Figure A.4: Quickness test results - Clayey Silt

Remoulded Shear Strength c_{ur} (kPa)	Initial Height H_0 (mm)	Final Height H_f (mm)	Base Dimensions D_f (mm)*	Quickness Q (%)	Laboratory Quickness Test**
0.10	123	52	174	57.72%	
0.20	123	68	150	44.72%	
0.29	105	62	134	40.95%	
0.39	82	50	121	39.02%	-
0.59	72	53	118	34.50%	
1.00	60	56	115	34.04%	

*NB: Base diameter dimensions may vary due irregular slurry spread

** Limited material for the latter tests meant that cylindrical moulds could not be filled

Figure A.5: Quickness test results - Silt

Appendix B

Previous Viscometer Test Results

The following data and results have been extracted from Table 6.4 and Appendix B of Grue’s thesis, ‘Rheological Parameters of Norwegian Sensitive Clays, Focusing on the Herschel-Bulkley Model’ (2015).

These Herschel-Bulkley parameters were found from viscometer tests performed on sensitive clay samples from Tiller and Esp, Trondheim, Norway as part of the research. Flow curves can be produced for each test material using the Herschel-Bulkley model which incorporates the three key parameters into the shear stress equation, $\tau = \tau_y + K\dot{\gamma}^n$.

Table B.1: Best fit Herschel-Bulkley parameters for all samples (Grue, 2015)

Material	Test #	Points excluded from fit	Remoulded Shear Strength, C_{ur} (kPa)	Salinity, S (g/L)	Liquidity Index, I_L (-)	Yield Stress, τ_y (Pa)	Normalized Consistency Index, K^* (Pa)	Herschel-Bulkley exponent, n (-)
Tiller	2-1	None	0.1	0.6	3.4	7.56	1.08	0.76
	2-2	Last	0.1	0.6	4.6	8.8	0.28	0.97
Esp	5-1	None	0.2	1.3	2.6	49.8	6.58	0.52
	5-2	None	0.1	1.3	2.8	59.0	3.67	0.56
	5-3	None	0.1	1.3	3.1	23.4	0.88	0.69
	5-4	Last	0.1	1.4	3.8	13.8	0.36	0.73
	7-2	None	0.1	4.6	3.6	39.3	4.80	0.40
	8-1	Last	0.1	2.2	4.4	13.0	0.44	0.65
	8-2	None	0.1	2.1	3.3	36.1	1.82	0.57
	8-3	None	0.2	1.7	2.5	109.2	5.98	0.49
	8-4	None	0.1	1.7	3.1	64.7	4.04	0.47
	9-1	None	0.1	1.3	3.5	21.6	0.81	0.79
	9-2	Last two	0.1	0.9	4.6	4.4	0.31	0.78
	9-3	None	0.2	1.2	2.3	67.3	5.75	0.60
	9-4	None	0.1	1.1	3.1	22.7	0.90	0.81

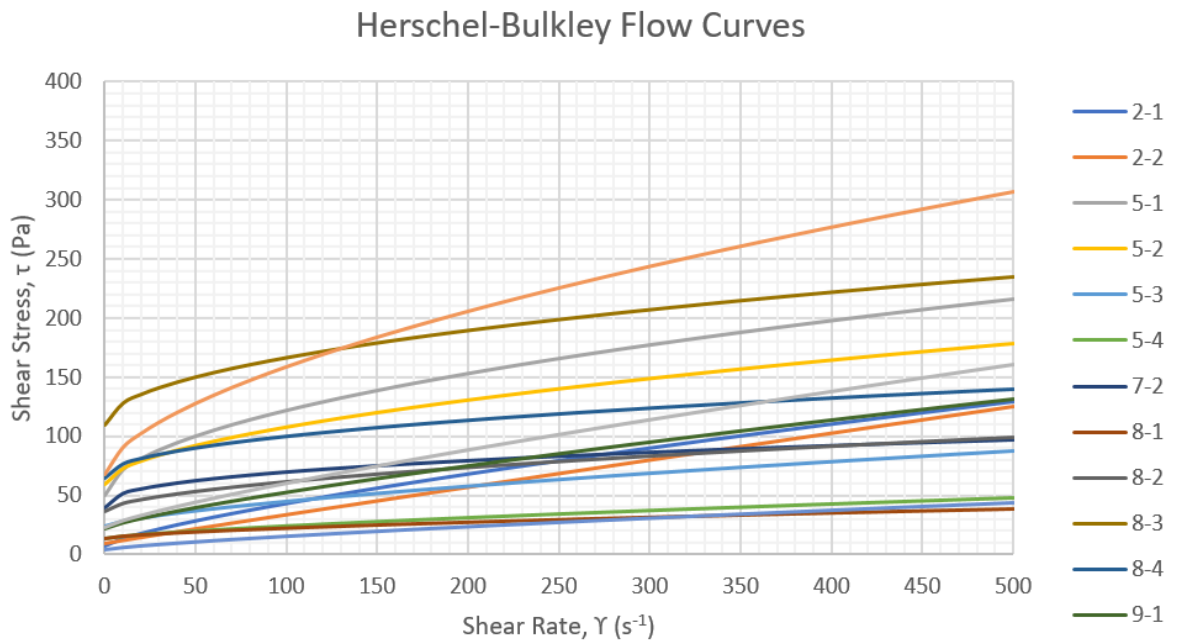


Figure B.1: Herschel-Bulkley flow curves from test results by Grue (2015)

The following results for the Herschel-Bulkley parameters were calculated by Grue (2015) from the viscometer tests performed by Locat and Demers (1988) and the data analyzed from L'Heureux (2013). The results were received in the form of an excel sheet by email correspondence with Grue (22/5/2017).

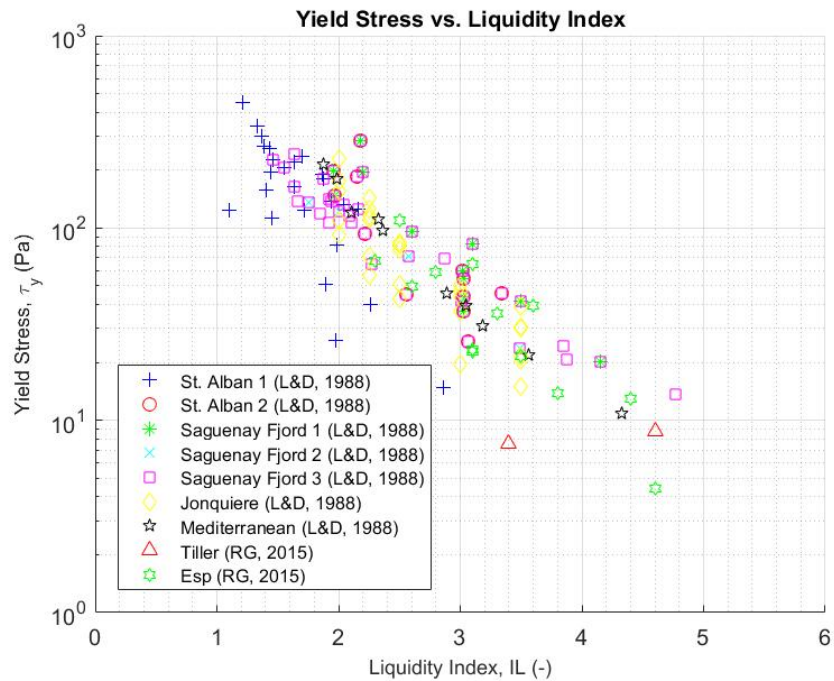


Figure B.2: Past results for yield stress with varying liquid limit

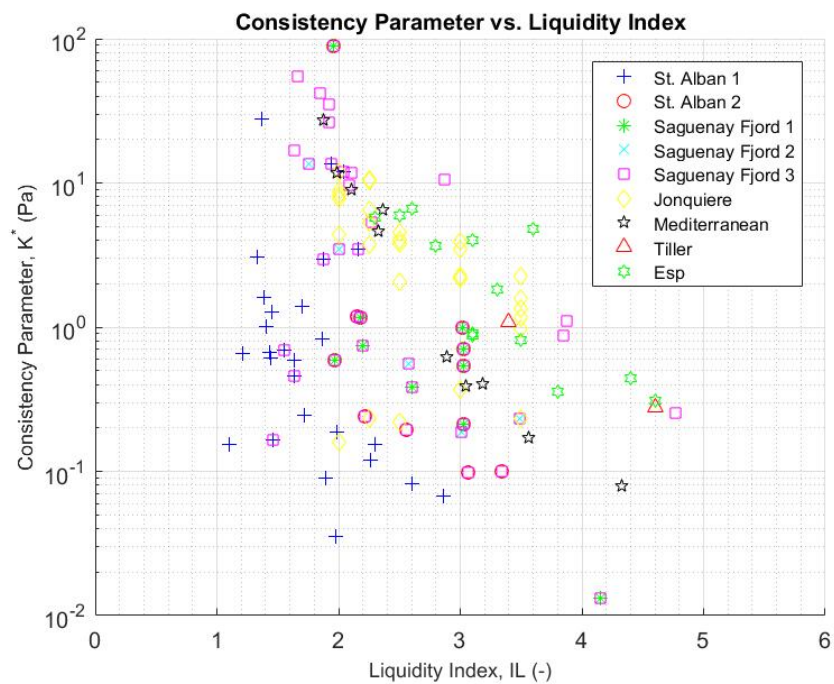


Figure B.3: Past results for consistency parameter with varying liquid limit

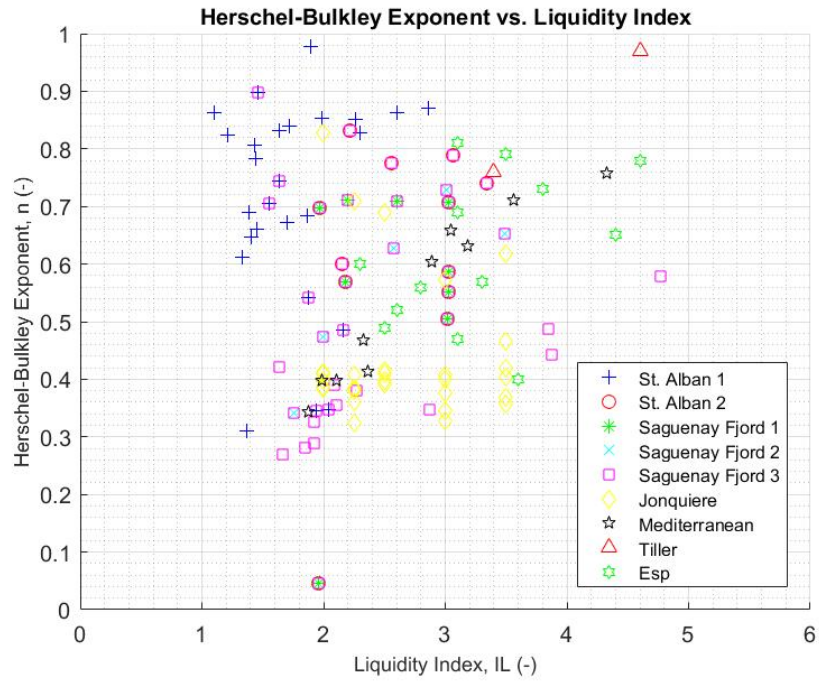


Figure B.4: Past results for Herschel-Bulkley exponent with varying liquid limit

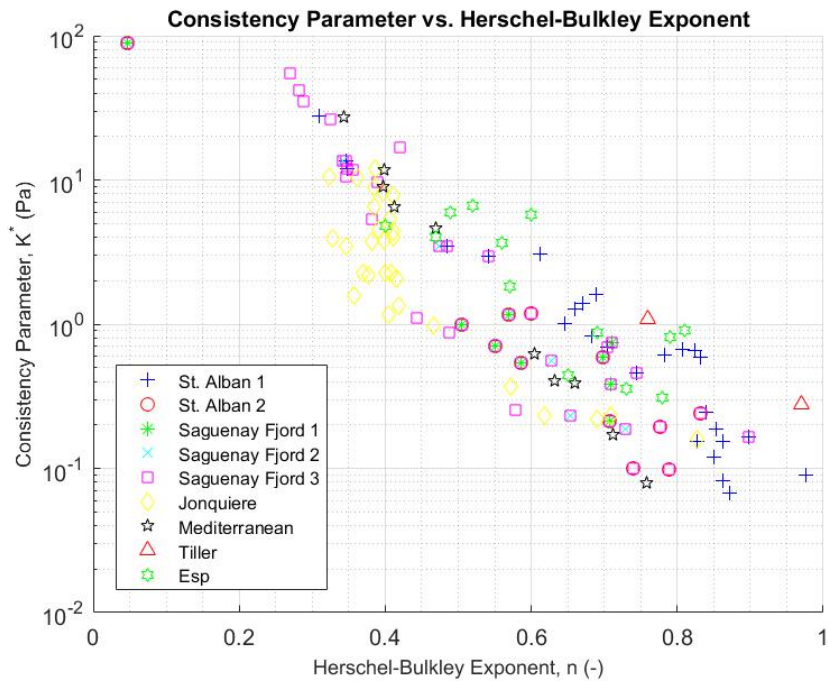


Figure B.5: Past results for consistency parameter against Herschel-Bulkley exponent

Appendix C

Viscometer Test Data

Material: Tiller Clay 1

Test date: 15/05/17

Remoulded Shear Strength	c_{ur}	<0.1	kPa
Water Content	w	63.5	%
Spindle Radius	R_i	7	mm
Cylinder Radius	R_o	13.75	mm
Ratio	R_o/R_i	1.96	-
Cylinder Height	h	21.1	mm
Equilibrium Torque	M	1.86	mNm
System Setting	Dial	7	-

Water content	Cup #	Cup (g)	Wet (g)	Dry (g)	w %
Before	66	22.69	29.93	27.11	63.80%
After	217	25.94	36.57	32.44	63.54%
wc reduction (-) =					0.996

Speed (-)	Start Torq (mNm)	Freq, N (Hz)	Torque reading, M (mNm) at time (seconds)									Temp. (°C)
			0	5	10	15	20	30	40	60	120	
8	-	16.91	-	-	-	1.86	-	-	-	-	-	-
7	1.86	9.87	1.75	1.76	1.76	1.76	1.76	1.76	1.76	1.76	1.77	7.1
6	1.86	5.69	1.66	1.68	1.68	1.68	1.68	1.68	1.68	1.68	1.67	6.8
5	1.86	3.39	1.59	1.60	1.60	1.60	1.60	1.61	1.60	1.60	1.58	6.4
4	1.86	2.02	1.50	1.51	1.52	1.51	1.51	1.51	1.51	1.50	1.48	6.5
3	1.86	1.30	1.46	1.46	1.47	1.46	1.46	1.46	1.45	1.44	1.42	6.7
2	1.86	0.85	1.42	1.42	1.42	1.42	1.41	1.41	1.40	1.38	1.36	6.9
1	1.86	0.33	1.37	1.37	1.37	1.36	1.35	1.34	1.33	1.30	1.26	6.9

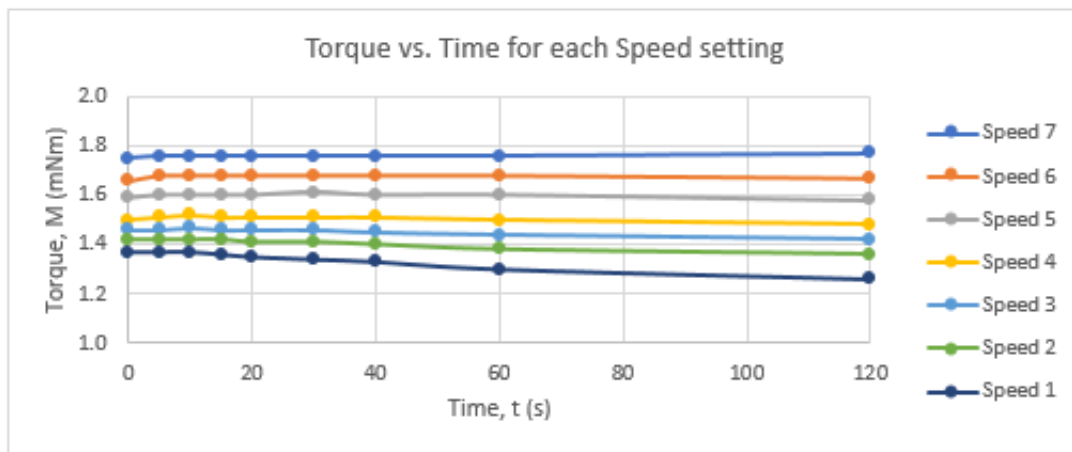
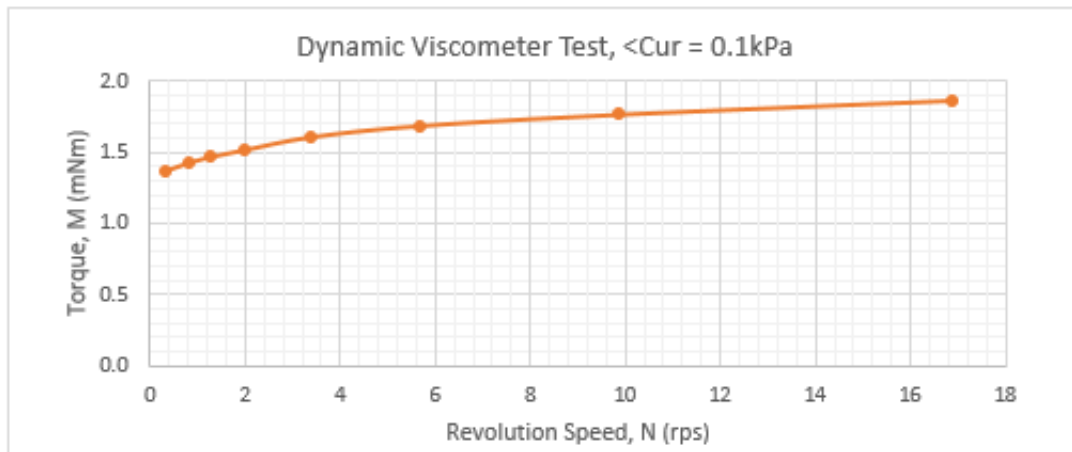


Figure C.1: Viscometer Test Data: Tiller Clay 1 $c_{ur} < 0.1\text{kPa}$

Material: Tiller Clay 1
 Test date: 16/03/17

Remoulded Shear Strength	C_{ur}	0.1	kPa
Water Content	w	55.8	%
Spindle Radius	R_i	7	mm
Cylinder Radius	R_o	13.75	mm
Ratio	R_o/R_i	1.96	-
Cylinder Height	h	21.1	mm
Equilibrium Torque	M	2.72	mNm
System Setting	Dial	7	-

Water content	Cup #	Cup (g)	Wet (g)	Dry (g)	w %
Before	232	25.18	32.12	29.65	55.26%
After	41	21.99	29.87	27.07	55.12%
wc reduction (-) =					0.9975

Speed (-)	Start Torq (mNm)	Freq, N (Hz)	Torque reading, M (mNm) at time (seconds)									Temp. (°C)	
			0	5	10	15	20	30	40	60	120		
8	-	16.98	-	-	-	2.72	-	-	-	-	-	-	-
7	2.72	9.91	2.57	2.57	2.57	2.58	2.58	2.58	2.57	2.57	2.56	8.1	
6	2.72	5.72	2.42	2.42	2.43	2.43	2.42	2.41	2.40	2.37	2.32	7.9	
5	2.72	3.40	2.32	2.32	2.31	2.30	2.29	2.28	2.28	2.26	2.21	7.7	
4	2.72	2.03	2.25	2.24	2.22	2.22	2.21	2.19	2.17	2.13	2.08	7.5	
3	2.72	1.31	2.20	2.20	2.18	2.17	2.15	2.13	2.12	2.09	2.02	7.2	
2	2.72	0.85	2.15	2.14	2.12	2.11	2.09	2.06	2.05	2.05	1.98	7.1	
1	2.72	0.34	1.99	1.98	1.99	1.99	1.99	1.98	1.97	1.92	1.85	7.0	

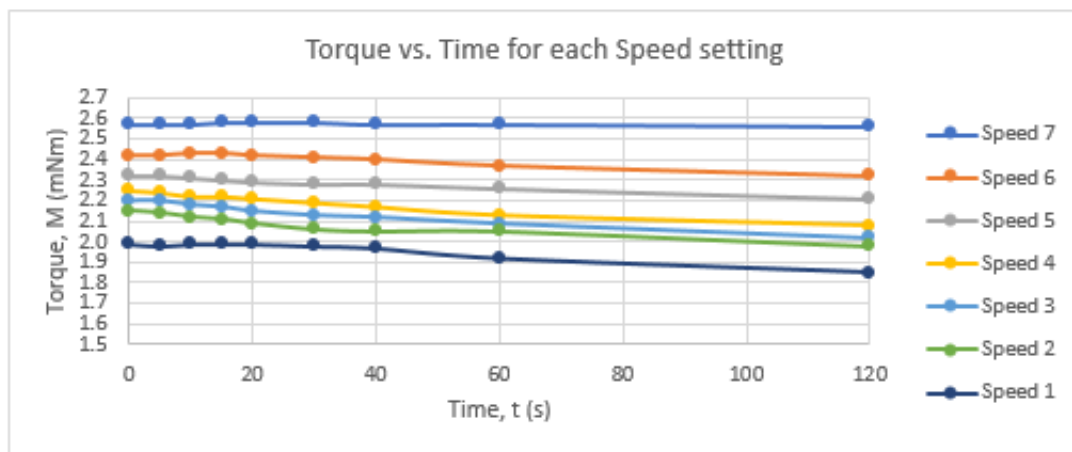
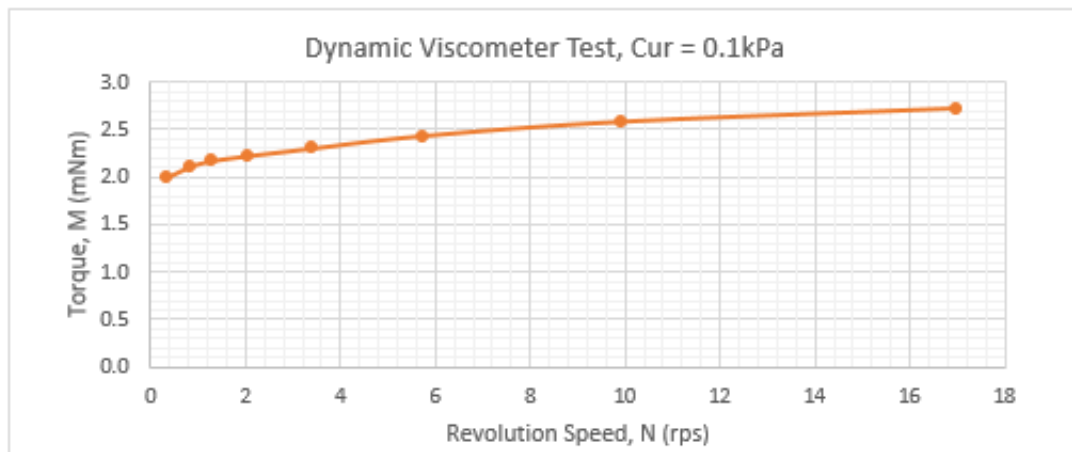


Figure C.2: Viscometer Test Data: Tiller Clay 1 $c_{ur} = 0.1\text{kPa}$

Material: Tiller Clay 1
 Test date: 17/03/17

Remoulded Shear Strength	C_{ur}	0.2	kPa
Water Content	w	50.8	%
Spindle Radius	R_i	7	mm
Cylinder Radius	R_o	13.75	mm
Ratio	R_o/R_i	1.96	-
Cylinder Height	h	21.1	mm
Equilibrium Torque	M	4.32	mNm
System Setting	Dial	7	-

Water content	Cup #	Cup (g)	Wet (g)	Dry (g)	w %
Before	225	27.09	31.75	30.17	51.30%
	50	19.56	28.15	25.25	50.97%
After	223	27.12	36.33	33.24	50.49%
wc reduction (-) =					0.9874

Speed (-)	Start Torq (mNm)	Freq, N (Hz)	Torque reading, M (mNm) at time (seconds)										Temp. (°C)
			0	5	10	15	20	30	40	60	120		
8	-	16.97	-	-	-	4.32	-	-	-	-	-	-	-
7	4.32	9.91	4.18	4.19	4.18	4.18	4.17	4.15	4.15	4.14	4.13	6.3	
6	4.32	5.71	4.13	4.08	4.05	4.03	4.01	3.99	3.97	3.95	3.90	6.5	
5	4.32	3.40	4.08	4.01	3.98	3.92	3.89	3.86	3.82	3.78	3.72	6.5	
4	4.32	2.02	4.05	3.94	3.88	3.83	3.79	3.74	3.71	3.66	3.57	6.5	
3	4.32	1.31	4.05	3.96	3.88	3.81	3.78	3.73	3.69	3.63	3.52	6.5	
2	4.32	0.85	4.06	3.91	3.79	3.69	3.64	3.57	3.52	3.42	3.27	6.4	
1	4.32	0.33	2.59	1.99	1.96	1.96	1.97	1.95	1.94	1.91	1.88	6.2	

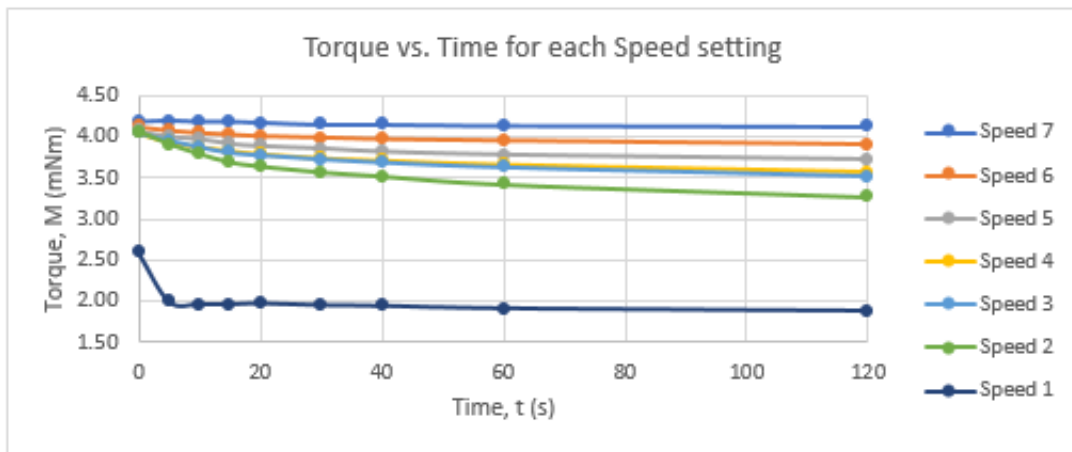
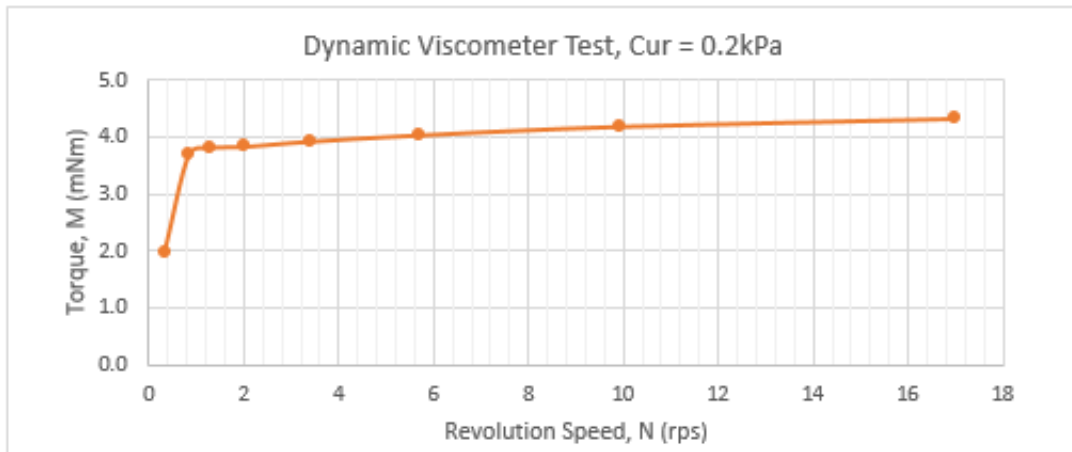


Figure C.3: Viscometer Test Data: Tiller Clay 1 $c_{ur} = 0.2\text{kPa}$

Material: Tiller Clay 1
 Test date: 15/05/17

Remoulded Shear Strength	c_{ur}	0.29	kPa
Water Content	w	47.5	%
Spindle Radius	R_i	7	mm
Cylinder Radius	R_o	13.75	mm
Ratio	R_o/R_i	1.96	-
Cylinder Height	h	21.1	mm
Equilibrium Torque	M	5.40	mNm
System Setting	Dial	7	-

Water content	Cup #	Cup (g)	Wet (g)	Dry (g)	w %
Before	231	27.06	41.49	36.85	47.40%
After	43	24.93	32.69	30.19	47.53%
wc reduction (-) =					1.003

Speed (-)	Start Torq (mNm)	Freq, N (Hz)	Torque reading, M (mNm) at time (seconds)									Temp. (°C)	
			0	5	10	15	20	30	40	60	120		
8	-	16.88	-	-	-	5.40	-	-	-	-	-	-	-
7	5.40	9.86	5.21	5.20	5.15	5.13	5.13	5.13	5.10	5.11	5.11	7.1	
6	5.40	5.68	5.05	5.07	5.02	4.96	4.95	4.90	4.86	4.78	4.66	7.3	
5	5.40	3.38	4.96	4.87	4.80	4.78	4.73	4.68	4.61	4.55	4.35	7.6	
4	5.40	2.01	4.98	4.85	4.82	4.77	4.72	4.65	4.56	4.36	4.10	7.7	
3	5.40	1.30	5.06	4.89	4.60	4.58	4.56	4.38	4.36	4.23	3.90	7.6	
2	5.40	0.85	4.02	3.88	3.75	3.65	3.62	3.80	3.69	3.63	3.64	8.0	
1	5.40	0.33	2.13	2.00	1.98	1.92	1.86	1.79	1.77	1.74	1.70	8.0	

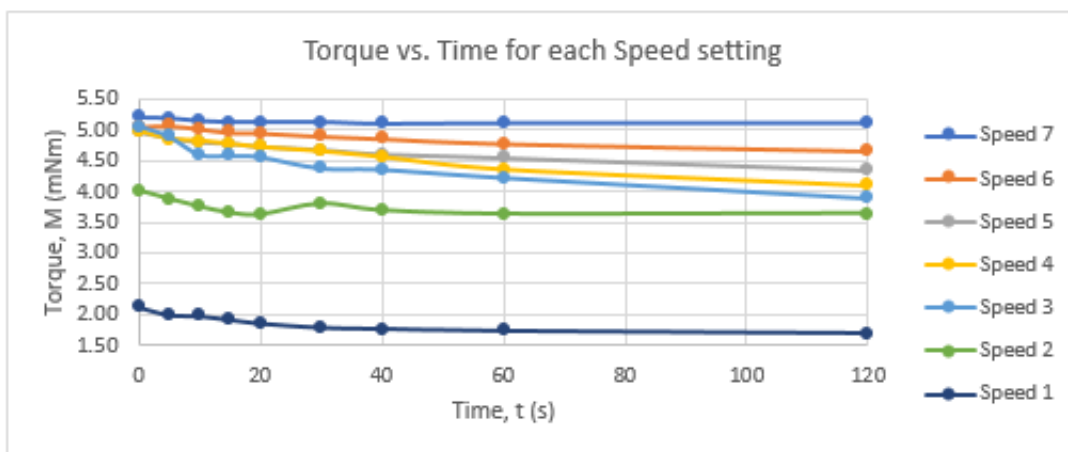
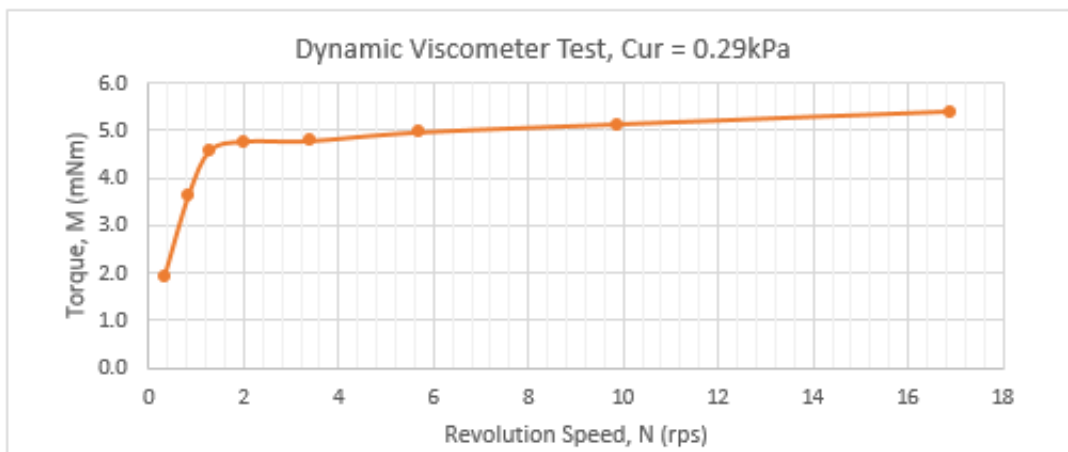


Figure C.4: Viscometer Test Data: Tiller Clay 1 $c_{ur} = 0.29\text{kPa}$

Material: Tiller Clay 2

Test date: 16/05/17

Remoulded Shear Strength	C_{ur}	<0.1	kPa
Water Content	w	92.8	%
Spindle Radius	R_i	7	mm
Cylinder Radius	R_o	13.75	mm
Ratio	R_o/R_i	1.96	-
Cylinder Height	h	21.1	mm
Equilibrium Torque	M	0.48	mNm
System Setting	Dial	7	-

Water content	Cup #	Cup (g)	Wet (g)	Dry (g)	w %
Before	159	19.97	29.19	24.76	92.48%
After	151	17.96	28.89	23.66	91.75%
wc reduction (-) =					0.992

Speed (-)	Start Torq (mNm)	Freq, N (Hz)	Torque reading, M (mNm) at time (seconds)										Temp. (°C)
			0	5	10	15	20	30	40	60	120		
8	-	16.93	-	-	-	0.48	-	-	-	-	-	-	-
7	0.48	9.88	0.46	0.46	0.46	0.46	0.46	0.46	0.46	0.46	0.46	0.46	6.6
6	0.48	5.70	0.43	0.43	0.43	0.43	0.44	0.44	0.44	0.44	0.44	0.44	6.3
5	0.48	3.39	0.39	0.40	0.40	0.40	0.40	0.40	0.40	0.40	0.41	0.40	6.4
4	0.48	2.02	0.37	0.37	0.37	0.37	0.37	0.37	0.37	0.37	0.37	0.37	6.5
3	0.48	1.30	0.34	0.34	0.34	0.34	0.35	0.35	0.35	0.35	0.35	0.35	6.7
2	0.48	0.85	0.33	0.32	0.32	0.32	0.31	0.32	0.32	0.32	0.32	0.32	6.6
1	0.48	0.33	0.28	0.31	0.30	0.29	0.29	0.30	0.30	0.30	0.30	0.30	6.3

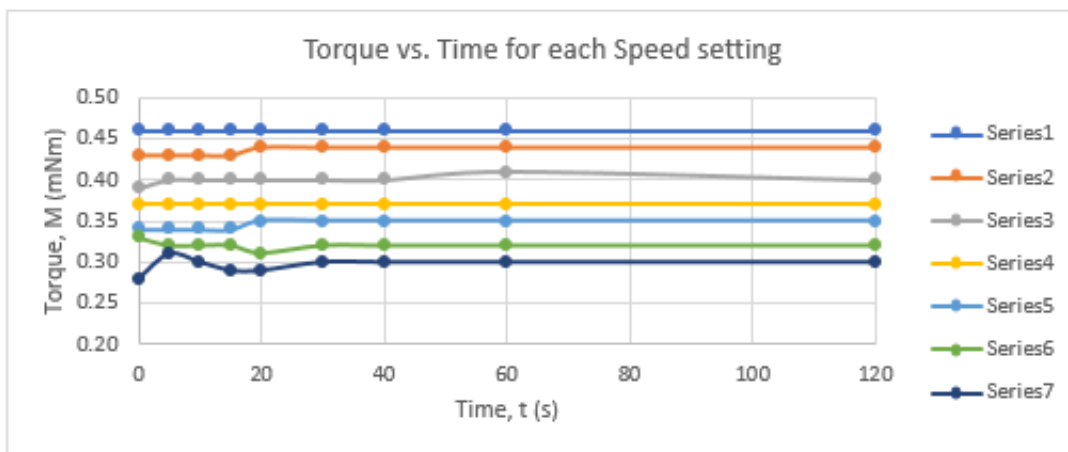
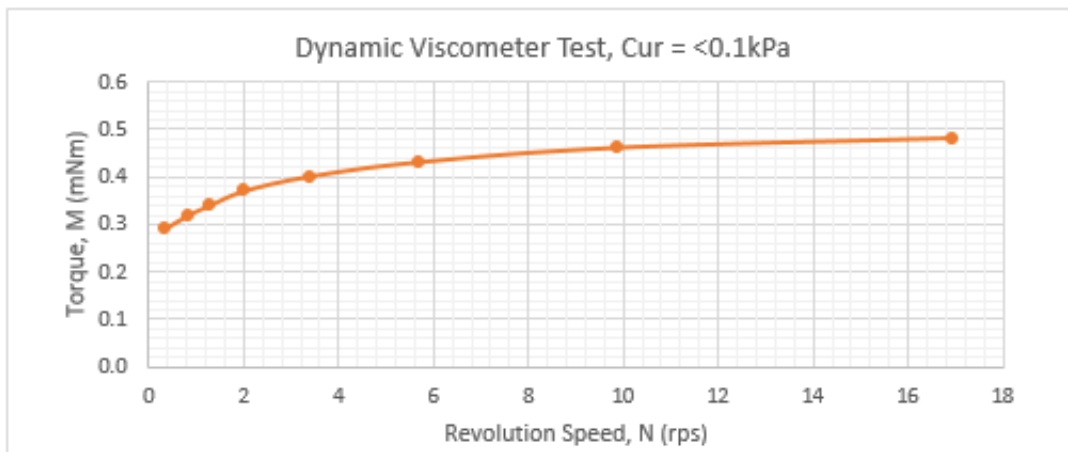


Figure C.5: Viscometer Test Data: Tiller Clay 2 $c_{ur} < 0.1\text{kPa}$

Material: Tiller Clay 2
 Test date: 15/03/17

Remoulded Shear Strength	C_{ur}	0.1	kPa
Water Content	w	66.3	%
Spindle Radius	R_i	7	mm
Cylinder Radius	R_o	13.75	mm
Ratio	R_o/R_i	1.96	-
Cylinder Height	h	21.1	mm
Equilibrium Torque	M	1.33	mNm
System Setting	Dial	7	-

Water content	Cup #	Cup (g)	Wet (g)	Dry (g)	w %
Before	160	19.35	34.20	28.26	66.67%
After	156	18.42	27.79	24.05	66.64%
wc reduction (-) =					0.9964

Speed (-)	Start Torq (mNm)	Freq, N (Hz)	Torque reading, M (mNm) at time (seconds)										Temp. (°C)
			0	5	10	15	20	30	40	60	120		
8	-	16.94	-	-	-	1.33	-	-	-	-	-	-	-
7	1.33	9.89	1.26	1.27	1.27	1.27	1.27	1.28	1.28	1.28	1.28	1.28	6.5
6	1.33	5.70	1.19	1.20	1.20	1.20	1.21	1.21	1.21	1.22	1.22	1.22	6.4
5	1.33	3.40	1.13	1.14	1.15	1.15	1.15	1.16	1.16	1.16	1.16	1.16	6.3
4	1.33	2.02	1.07	1.09	1.09	1.10	1.10	1.10	1.10	1.10	1.10	1.11	6.2
3	1.32	1.31	1.02	1.04	1.04	1.05	1.05	1.06	1.06	1.06	1.06	1.06	6.0
2	1.32	0.85	1.00	1.02	1.02	1.03	1.03	1.03	1.04	1.04	1.04	1.03	5.9
1	1.32	0.33	0.94	0.96	0.97	0.98	0.98	0.99	0.99	0.99	0.99	0.99	5.8

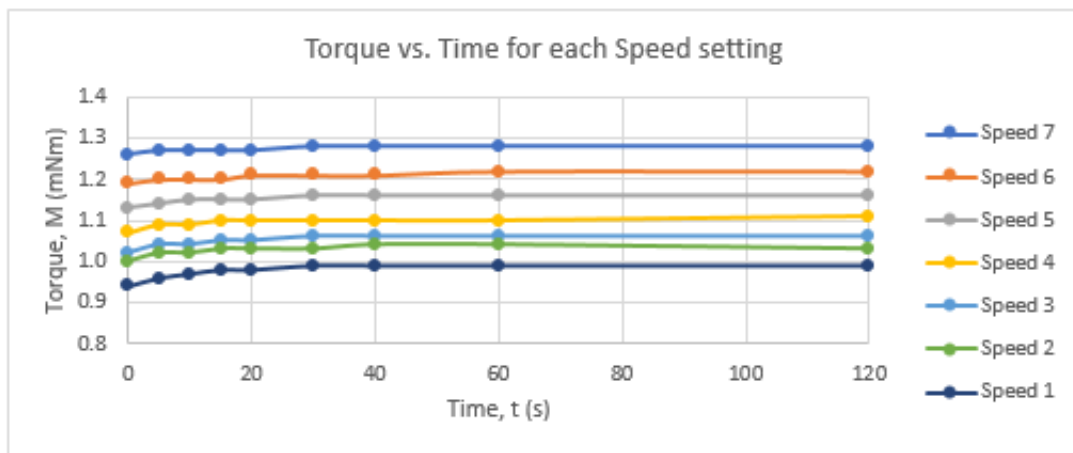
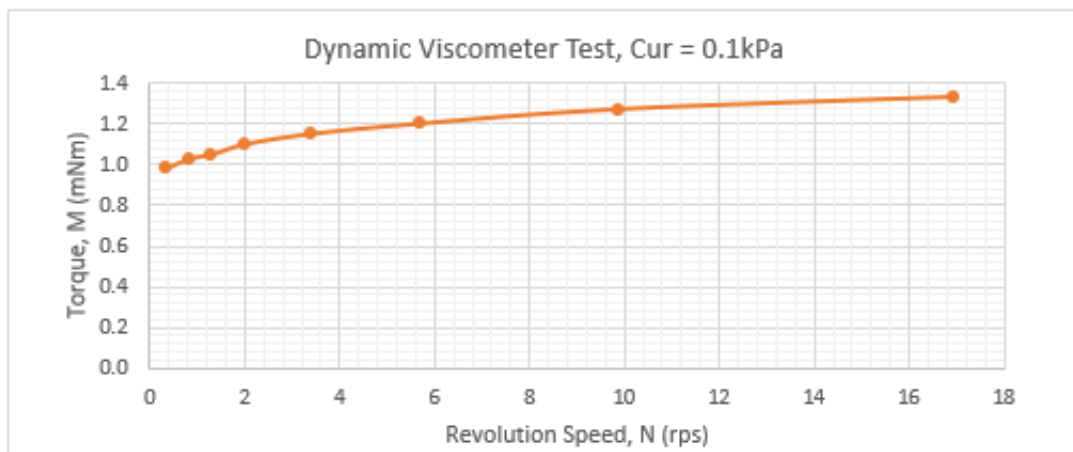


Figure C.6: Viscometer Test Data: Tiller Clay 2 $c_{ur} = 0.1\text{kPa}$

Material: Tiller Clay 2
 Test date: 15/03/17

Remoulded Shear Strength	C_{ur}	0.2	kPa
Water Content	w	57.6	%
Spindle Radius	R_i	7	mm
Cylinder Radius	R_o	13.75	mm
Ratio	R_o/R_i	1.96	-
Cylinder Height	h	21.1	mm
Equilibrium Torque	M	2.46	mNm
System Setting	Dial	7	-

Water content	Cup #	Cup (g)	Wet (g)	Dry (g)	w %
Before	60	21.98	33.76	29.44	57.91%
After	200	27.48	38.93	34.73	57.93%
wc reduction (-) =					1.0004

Speed (-)	Start Torq (mNm)	Freq, N (Hz)	Torque reading, M (mNm) at time (seconds)										Temp. (°C)
			0	5	10	15	20	30	40	60	120		
8	-	16.99	-	-	-	2.46	-	-	-	-	-	-	-
7	2.46	9.92	2.34	2.35	2.35	2.35	2.35	2.36	2.36	2.36	2.36	2.36	6.8
6	2.48	5.72	2.25	2.26	2.27	2.27	2.27	2.27	2.26	2.26	2.26	2.24	6.7
5	2.47	3.41	2.15	2.16	2.17	2.17	2.17	2.17	2.16	2.16	2.16	2.12	6.6
4	2.46	2.03	2.07	2.08	2.09	2.09	2.09	2.09	2.09	2.08	2.08	2.06	6.4
3	2.46	1.31	2.01	2.03	2.04	2.04	2.04	2.03	2.03	2.02	2.02	1.99	6.3
2	2.46	0.85	1.98	1.99	2.01	2.01	2.01	2.01	2.01	2.00	2.00	1.97	6.2
1	2.46	0.34	1.87	1.89	1.90	1.90	1.90	1.89	1.89	1.87	1.87	1.83	6.1

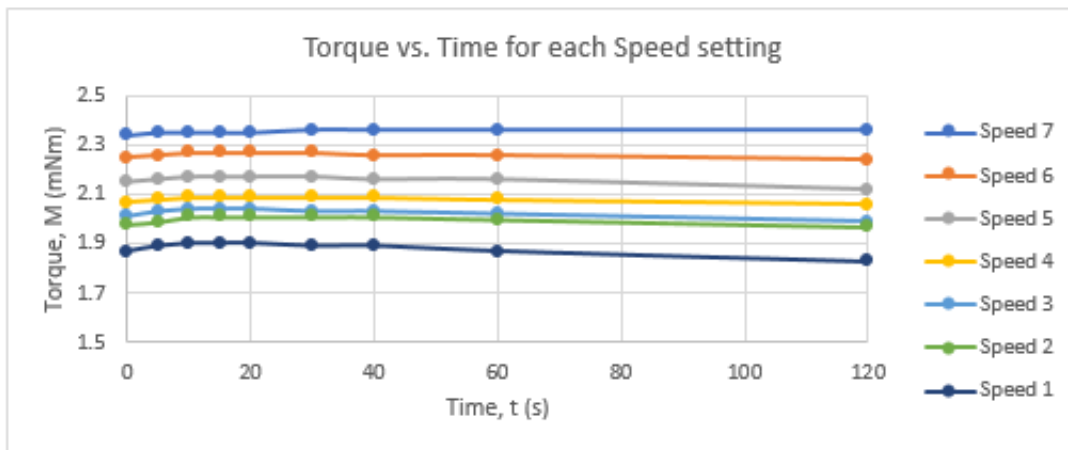
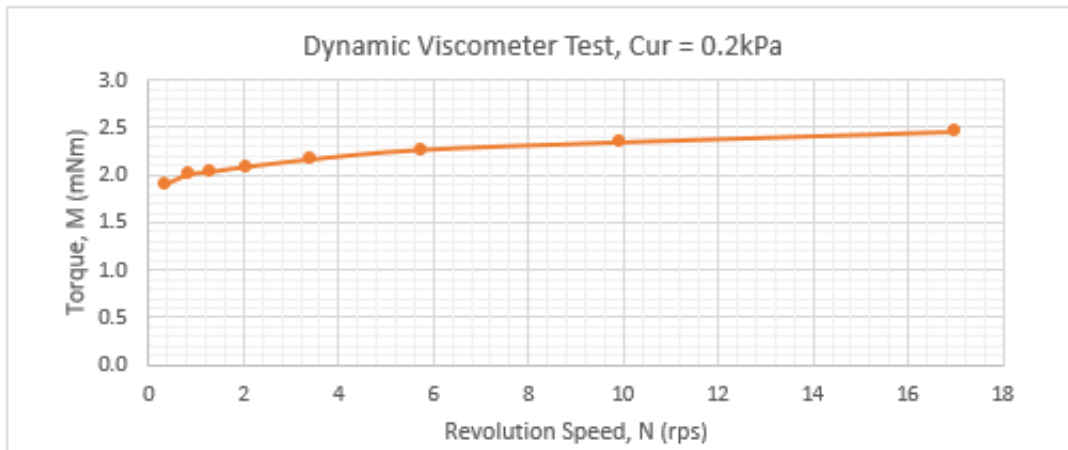


Figure C.7: Viscometer Test Data: Tiller Clay 2 $c_{ur} = 0.2\text{kPa}$

Material: Tiller Clay 2

Test date: 15/03/17

Remoulded Shear Strength	C_{ur}	0.29	kPa
Water Content	w	52.0	%
Spindle Radius	R_i	7	mm
Cylinder Radius	R_o	13.75	mm
Ratio	R_o/R_i	1.96	-
Cylinder Height	h	21.1	mm
Equilibrium Torque	M	2.46	mNm
System Setting	Dial	7	-

Water content	Cup #	Cup (g)	Wet (g)	Dry (g)	w %
Before	162	19.11	25.35	23.23	51.46%
After	169	18.9	26.95	24.22	51.32%
wc reduction (-) =					0.9973

Speed (-)	Start Torq (mNm)	Freq, N (Hz)	Torque reading, M (mNm) at time (seconds)									Temp. (°C)	
			0	5	10	15	20	30	40	60	120		
8	-	16.98	-	-	-	4.73	-	-	-	-	-	-	-
7	4.73	9.91	4.64	4.62	4.59	4.60	4.58	4.56	4.56	4.52	4.44	6.3	
6	4.73	5.71	4.51	4.50	4.48	4.45	4.44	4.39	4.36	4.30	4.21	6.3	
5	4.73	3.40	4.41	4.38	4.37	4.33	4.31	4.25	4.24	4.18	4.11	6.3	
4	4.69	2.02	4.33	4.30	4.22	4.20	4.17	4.12	4.08	4.05	3.95	6.2	
3	4.66	1.31	4.30	4.27	4.17	4.12	4.09	4.05	4.02	3.96	3.87	6.4	
2	4.52	0.85	4.21	4.17	4.11	4.08	4.04	3.97	3.90	3.84	3.74	6.5	
1	4.44	0.33	3.20	2.65	2.60	2.57	2.56	2.56	2.55	2.54	2.50	6.6	

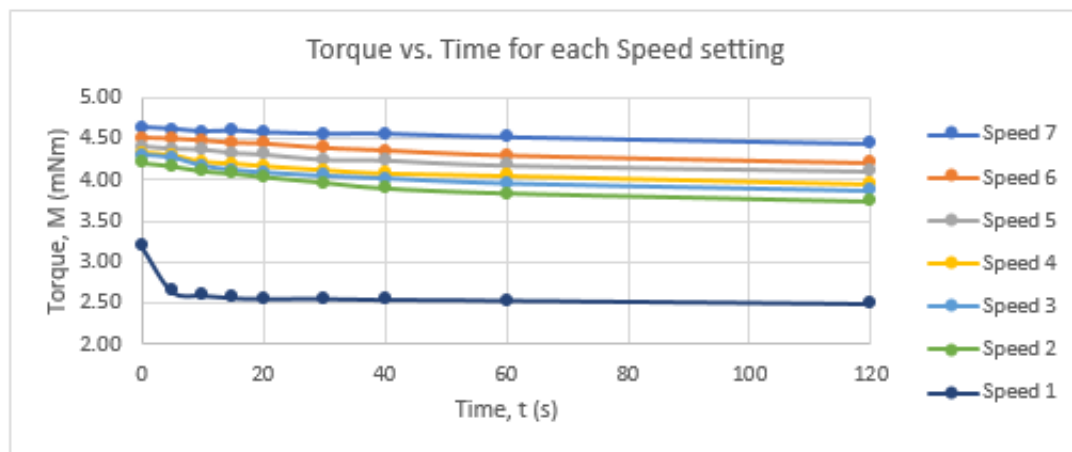
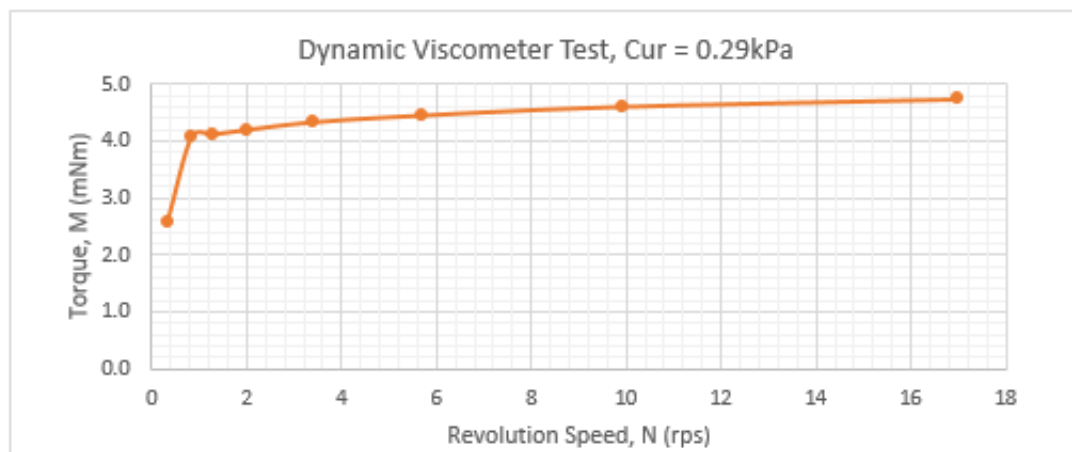


Figure C.8: Viscometer Test Data: Tiller Clay 2 $c_{ur} = 0.29\text{kPa}$

Material: Perniö Clay
 Test date: 12/05/17

Remoulded Shear Strength	c_{ur}	<0.1	kPa
Water Content	w	95.2	%
Spindle Radius	R_i	7	mm
Cylinder Radius	R_o	13.75	mm
Ratio	R_o/R_i	1.96	-
Cylinder Height	h	21.1	mm
Equilibrium Torque	M	0.70	mNm
System Setting	Dial	7	-

Water content	Cup #	Cup (g)	Wet (g)	Dry (g)	w %
Before	51	18.35	23.44	20.95	95.77%
After	214	26.86	33.42	30.23	94.66%
wc reduction (-) =					0.988

Speed (-)	Start Torq (mNm)	Freq, N (Hz)	Torque reading, M (mNm) at time (seconds)										Temp. (°C)
			0	5	10	15	20	30	40	60	120		
8	-	16.93	-	-	-	0.70	-	-	-	-	-	-	-
7	0.7	9.88	0.65	0.67	0.68	0.68	0.68	0.68	0.68	0.68	0.68	0.68	6.3
6	0.7	5.70	0.61	0.64	0.65	0.65	0.65	0.65	0.65	0.65	0.65	0.64	6.5
5	0.7	3.39	0.6	0.62	0.62	0.63	0.63	0.63	0.62	0.62	0.62	0.62	6.4
4	0.7	2.02	0.57	0.59	0.60	0.60	0.60	0.60	0.60	0.60	0.60	0.61	6.2
3	0.7	1.30	0.55	0.57	0.58	0.58	0.58	0.58	0.59	0.59	0.59	0.59	6.4
2	0.7	0.85	0.54	0.56	0.56	0.57	0.57	0.57	0.57	0.58	0.58	0.58	6.7
1	0.7	0.33	0.53	0.56	0.57	0.56	0.58	0.59	0.59	0.59	0.59	0.61	6.4

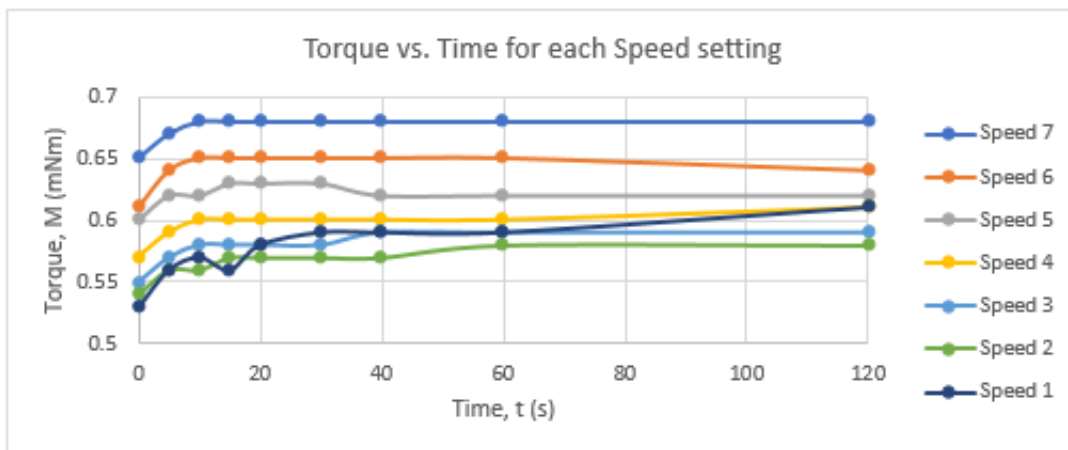
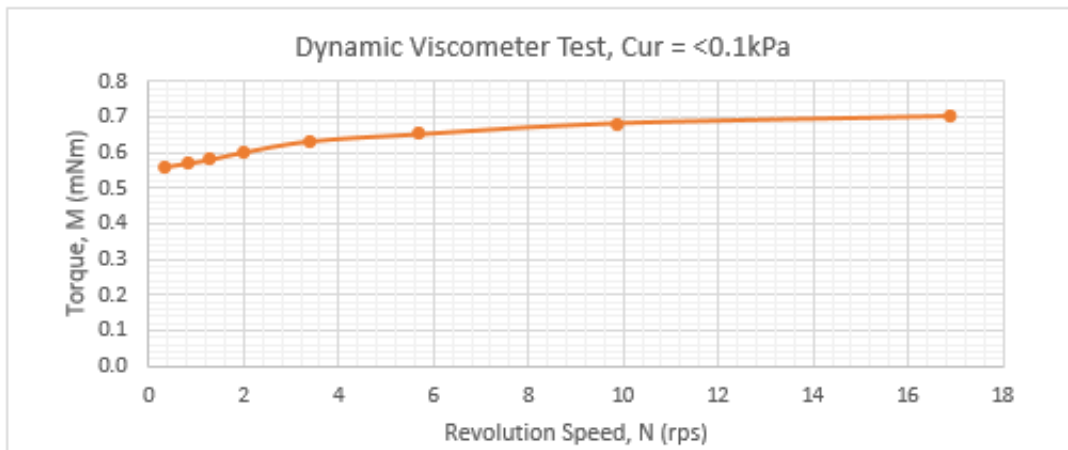


Figure C.9: Viscometer Test Data: Perniö Clay $c_{ur} < 0.1\text{kPa}$ 1

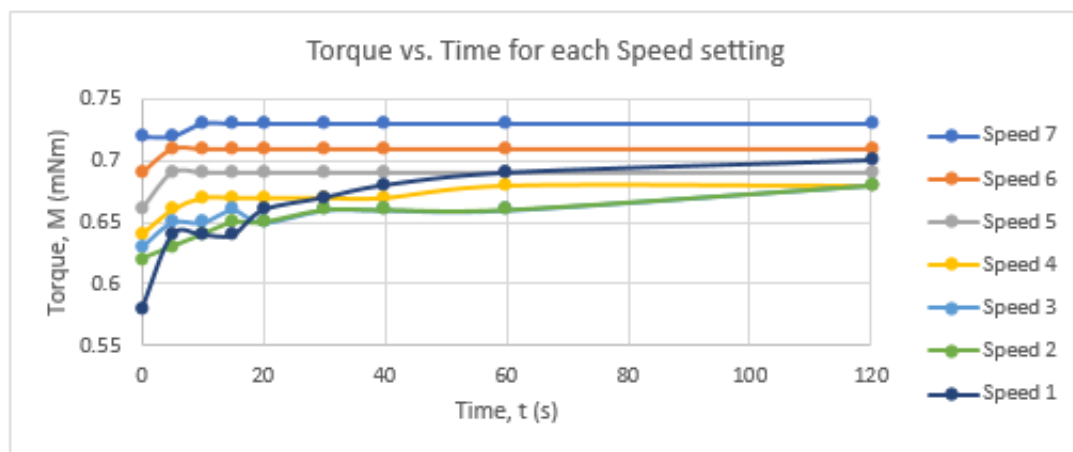
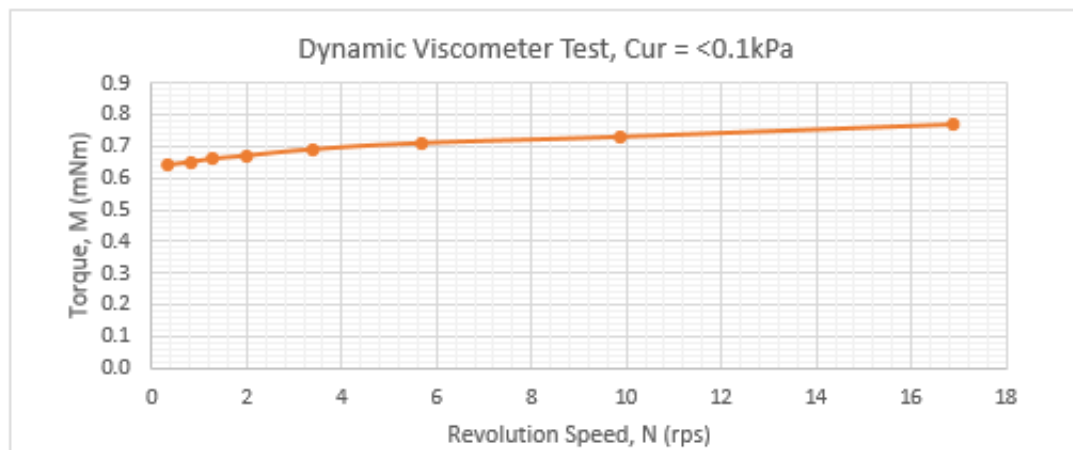
Material: Perniö Clay

Test date: 18/05/17

Remoulded Shear Strength	C_{ur}	<0.1	kPa
Water Content	w	90.7	%
Spindle Radius	R_i	7	mm
Cylinder Radius	R_o	13.75	mm
Ratio	R_o/R_i	1.96	-
Cylinder Height	h	21.1	mm
Equilibrium Torque	M	0.77	mNm
System Setting	Dial	7	-

Water content	Cup #	Cup (g)	Wet (g)	Dry (g)	w %
Before	153	18.9	24.8	21.97	92.18%
After	162	19.11	30.9	25.26	91.71%
wc reduction (-) =					0.995

Speed (-)	Start Torq (mNm)	Freq, N (Hz)	Torque reading, M (mNm) at time (seconds)									Temp. (°C)	
			0	5	10	15	20	30	40	60	120		
8	-	16.93	-	-	-	0.77	-	-	-	-	-	-	-
7	0.77	9.88	0.72	0.72	0.73	0.73	0.73	0.73	0.73	0.73	0.73	0.73	6.6
6	0.77	5.69	0.69	0.71	0.71	0.71	0.71	0.71	0.71	0.71	0.71	0.71	6.7
5	0.77	3.39	0.66	0.69	0.69	0.69	0.69	0.69	0.69	0.69	0.69	0.69	6.7
4	0.77	2.02	0.64	0.66	0.67	0.67	0.67	0.67	0.67	0.67	0.68	0.68	6.8
3	0.77	1.30	0.63	0.65	0.65	0.66	0.65	0.66	0.66	0.66	0.66	0.68	6.8
2	0.77	0.85	0.62	0.63	0.64	0.65	0.65	0.66	0.66	0.66	0.66	0.68	6.7
1	0.77	0.33	0.58	0.64	0.64	0.64	0.66	0.67	0.68	0.69	0.70	0.70	6.5

Figure C.10: Viscometer Test Data: Perniö Clay $c_{ur} < 0.1\text{kPa}$ 2

Material: Perniö Clay
 Test date: 8/03/17

Remoulded Shear Strength	C_{ur}	0.1	kPa
Water Content	w	83.1	%
Spindle Radius	R_i	7	mm
Cylinder Radius	R_o	13.75	mm
Ratio	R_o/R_i	1.96	-
Cylinder Height	h	21.1	mm
Equilibrium Torque	M	0.45	mNm
System Setting	Dial	7	-

Water content	Cup #	Cup (g)	Wet (g)	Dry (g)	w %
Before	229	26.02	29.17	27.72	85.29%
	240	26.16	28.07	27.19	85.44%
After	226	27.16	36.36	32.15	84.37%
wc reduction (-) =					0.98832

Speed (-)	Start Torq (mNm)	Freq, N (Hz)	Torque reading, M (mNm) at time (seconds)										Temp. (°C)
			0	5	10	15	20	30	40	60	120		
8	-	16.89	-	0.45	-	0.45	-	-	-	-	-	-	-
7	0.45	9.89	0.36	0.38	0.38	0.39	0.39	0.39	0.40	0.40	0.40	0.40	6.0
6	0.45	5.71	0.30	0.32	0.33	0.34	0.34	0.35	0.35	0.36	0.37	5.9	
5	0.45	3.40	0.24	0.28	0.30	0.31	0.31	0.32	0.33	0.33	0.35	5.8	
4	0.45	2.02	0.22	0.26	0.27	0.28	0.28	0.29	0.30	0.31	0.31	5.7	
3	0.45	1.31	0.17	0.23	0.25	0.25	0.26	0.27	0.28	0.28	0.29	5.6	
2	0.45	0.85	0.16	0.21	0.23	0.24	0.25	0.26	0.26	0.27	0.29	5.6	
1	0.45	0.34	0.13	0.19	0.20	0.22	0.23	0.23	0.24	0.25	0.26	5.5	

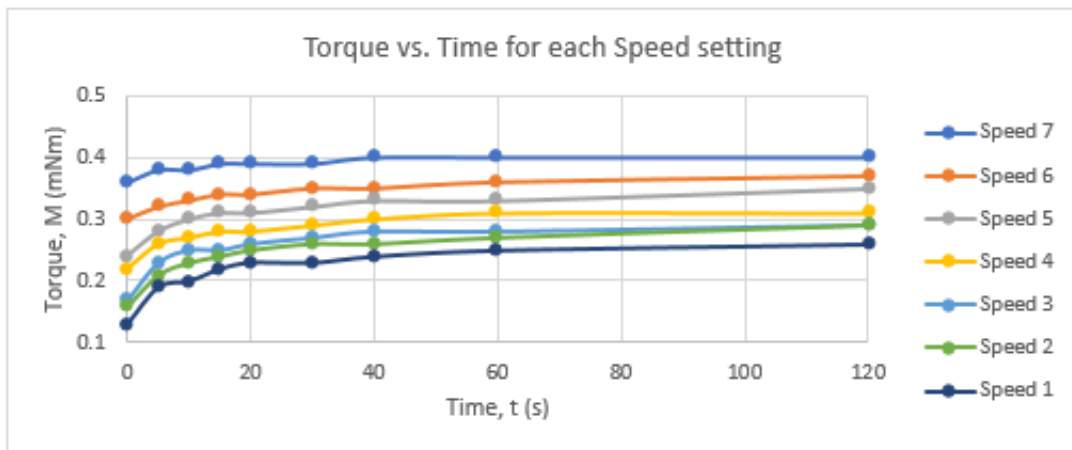
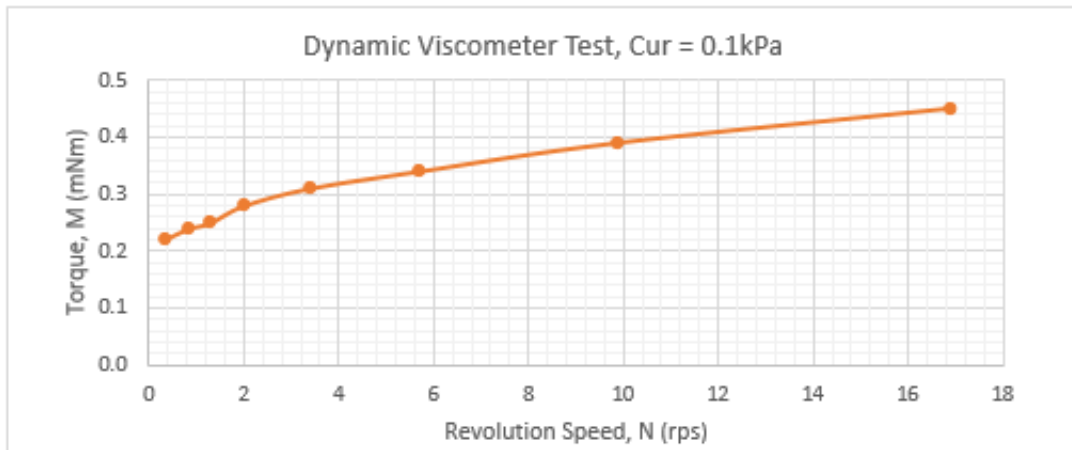


Figure C.11: Viscometer Test Data: Perniö Clay $c_{ur} = 0.1\text{kPa}$

Material: Perniö Clay
 Test date: 8/03/17

Remoulded Shear Strength	C_{ur}	0.2	kPa
Water Content	w	81.1	%
Spindle Radius	R_i	7	mm
Cylinder Radius	R_o	13.75	mm
Ratio	R_o/R_i	1.96	-
Cylinder Height	h	21.1	mm
Equilibrium Torque	M	0.72	mNm
System Setting	Dial	7	-

Water content	Cup #	Cup (g)	Wet (g)	Dry (g)	w %
Before	153	18.9	22.95	21.13	81.61%
	166	19.23	21.53	20.51	79.69%
After	150	19.67	24.2	22.16	81.93%
	156	18.42	25.32	22.21	82.06%
wc reduction (-) =					1.0166

Speed (-)	Start Torq (mNm)	Freq, N (Hz)	Torque reading, M (mNm) at time (seconds)										Temp. (°C)
			0	5	10	15	20	30	40	60	120		
8	0.72	16.95	-	-	-	0.72	-	-	-	-	-	-	-
7	0.72	9.90	0.61	0.63	0.64	0.65	0.65	0.65	0.66	0.66	0.66	0.66	5.2
6	0.72	5.71	0.53	0.57	0.58	0.59	0.59	0.60	0.60	0.60	0.60	0.60	5.1
5	0.72	3.40	0.48	0.52	0.54	0.54	0.54	0.55	0.55	0.56	0.56	0.57	5.1
4	0.72	2.02	0.44	0.48	0.49	0.50	0.50	0.51	0.51	0.51	0.51	0.51	5.3
3	0.71	1.31	0.35	0.44	0.46	0.46	0.47	0.47	0.48	0.48	0.48	0.48	5.5
2	0.70	0.85	0.38	0.42	0.44	0.45	0.45	0.45	0.46	0.46	0.46	0.47	5.7
1	0.70	0.34	0.30	0.40	0.41	0.42	0.42	0.43	0.43	0.44	0.44	0.45	5.9

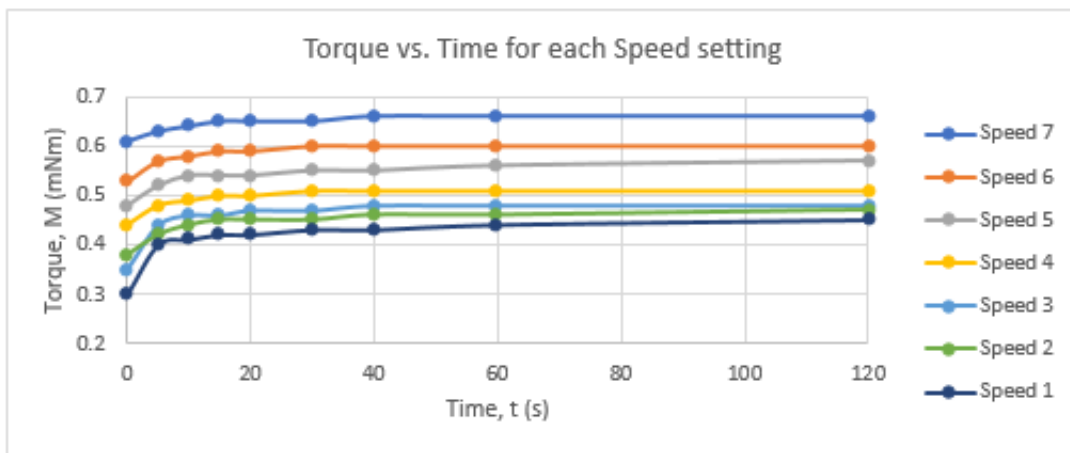
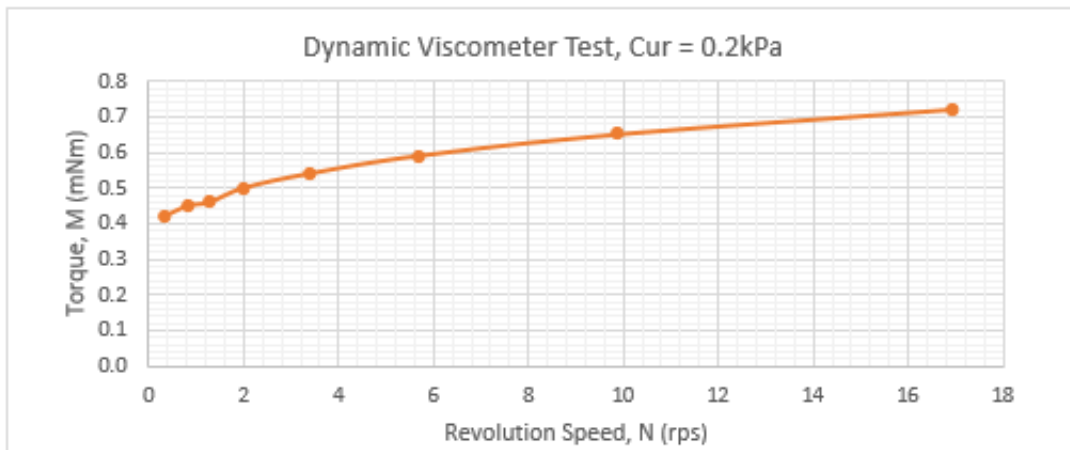


Figure C.12: Viscometer Test Data: Perniö Clay $c_{ur} = 0.2\text{kPa}$

Material: Perniö Clay
 Test date: 8/03/17

Remoulded Shear Strength	C_{ur}	0.29	kPa
Water Content	w	74.3	%
Spindle Radius	R_i	7	mm
Cylinder Radius	R_o	13.75	mm
Ratio	R_o/R_i	1.96	-
Cylinder Height	h	21.1	mm
Equilibrium Torque	M	1.00	mNm
System Setting	Dial	7	-

Water content	Cup #	Cup (g)	Wet (g)	Dry (g)	w %
Before	152	19.08	21.88	20.69	73.91%
	151	17.96	22.81	20.74	74.46%
After	161	18.43	23.77	21.48	75.08%
	154	18.51	23.92	21.61	74.52%
wc reduction (-) =					1.0083

Speed (-)	Start Torq (mNm)	Freq, N (Hz)	Torque reading, M (mNm) at time (seconds)										Temp. (°C)
			0	5	10	15	20	30	40	60	120		
8	-	16.94	-	-	-	1.00	-	-	-	-	-	-	-
7	1.00	9.89	0.86	0.90	0.91	0.92	0.92	0.92	0.93	0.93	0.93	0.93	7.2
6	1.00	5.70	0.78	0.83	0.85	0.85	0.86	0.86	0.87	0.87	0.86	0.86	7.1
5	1.01	3.40	0.74	0.78	0.79	0.8	0.79	0.80	0.80	0.80	0.80	0.80	6.8
4	1.00	2.02	0.67	0.72	0.73	0.74	0.74	0.74	0.74	0.75	0.75	0.75	6.7
3	1.00	1.30	0.62	0.68	0.70	0.71	0.71	0.71	0.71	0.72	0.72	0.72	6.6
2	1.00	0.85	0.61	0.66	0.68	0.69	0.69	0.69	0.70	0.70	0.70	0.70	6.4
1	1.00	0.34	0.57	0.64	0.65	0.66	0.66	0.67	0.68	0.68	0.70	0.70	6.3

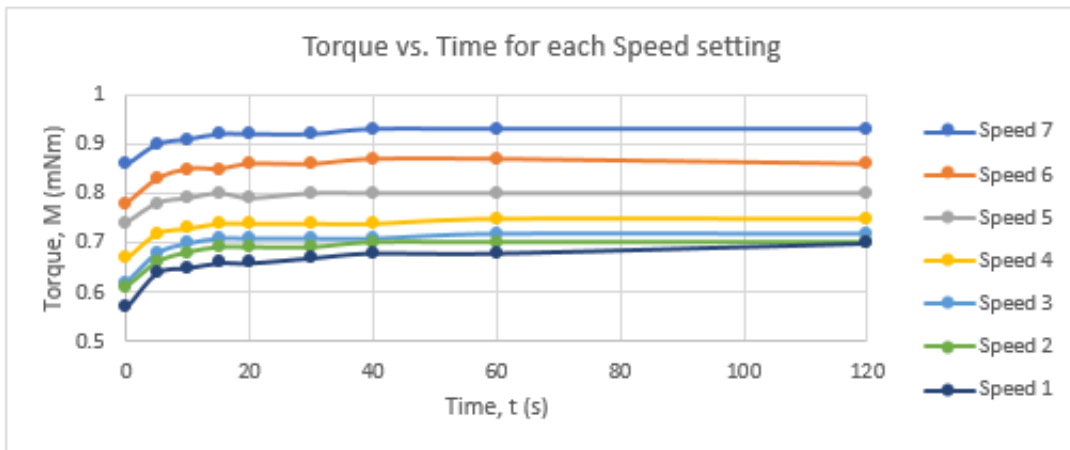
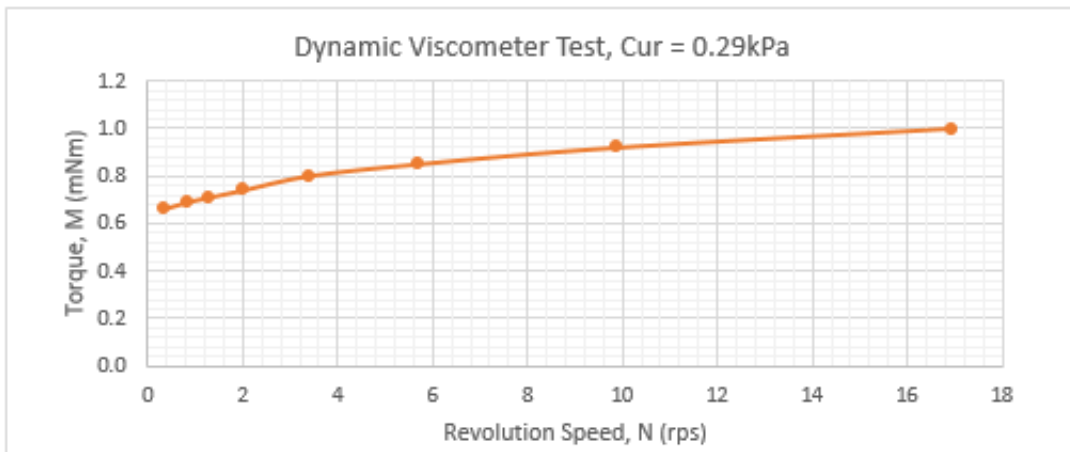


Figure C.13: Viscometer Test Data: Perniö Clay $c_{ur} = 0.29\text{kPa}$

Material: Perniö Clay
 Test date: 9/03/17

Remoulded Shear Strength	C_{ur}	0.39	kPa
Water Content	w	70.8	%
Spindle Radius	R_i	7	mm
Cylinder Radius	R_o	13.75	mm
Ratio	R_o/R_i	1.96	-
Cylinder Height	h	21.1	mm
Equilibrium Torque	M	1.31	mNm
System Setting	Dial	7	-

Water content	Cup #	Cup (g)	Wet (g)	Dry (g)	w %
Before	168	19.49	21.68	20.77	71.09%
After	104	22.02	26.83	24.82	71.79%
	53	22.93	28.04	25.89	72.64%
wc reduction (-) =					1.016

Speed (-)	Start Torq (mNm)	Freq, N (Hz)	Torque reading, M (mNm) at time (seconds)										Temp. (°C)
			0	5	10	15	20	30	40	60	120		
8	-	16.94	-	-	-	1.31	-	-	-	-	-	-	-
7	1.31	9.89	1.15	1.19	1.20	1.20	1.20	1.20	1.20	1.20	1.20	1.20	6.9
6	1.31	5.70	1.05	1.10	1.11	1.12	1.12	1.11	1.11	1.11	1.11	1.13	6.8
5	1.31	3.40	0.99	1.04	1.05	1.05	1.05	1.05	1.05	1.05	1.05	1.05	6.6
4	1.31	2.02	0.94	0.99	1.00	1.00	1.00	1.00	1.00	1.00	1.00	1.00	6.4
3	1.31	1.31	0.90	0.95	0.96	0.96	0.96	0.96	0.96	0.96	0.97	0.97	6.2
2	1.31	0.85	0.88	0.92	0.93	0.93	0.94	0.94	0.95	0.95	0.95	0.95	6.0
1	1.31	0.33	0.83	0.90	0.90	0.91	0.92	0.92	0.93	0.94	0.95	0.95	5.9

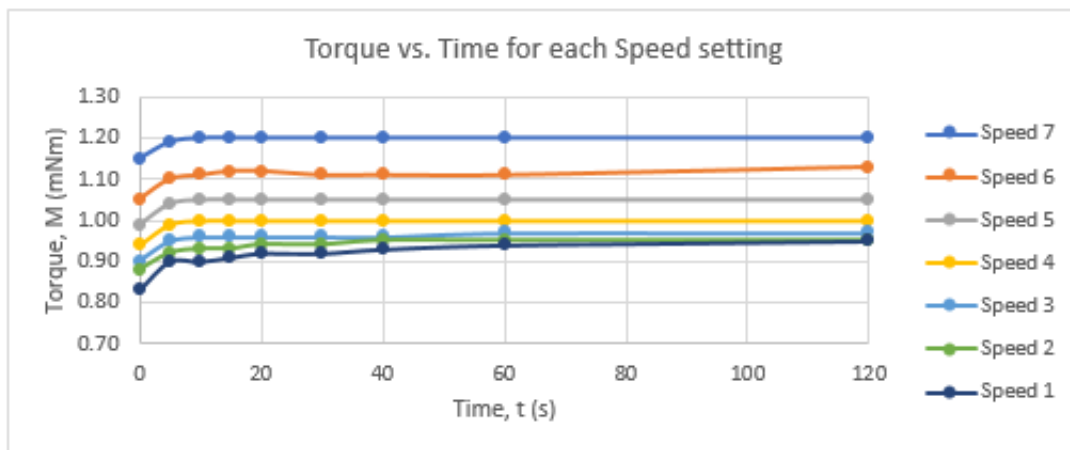
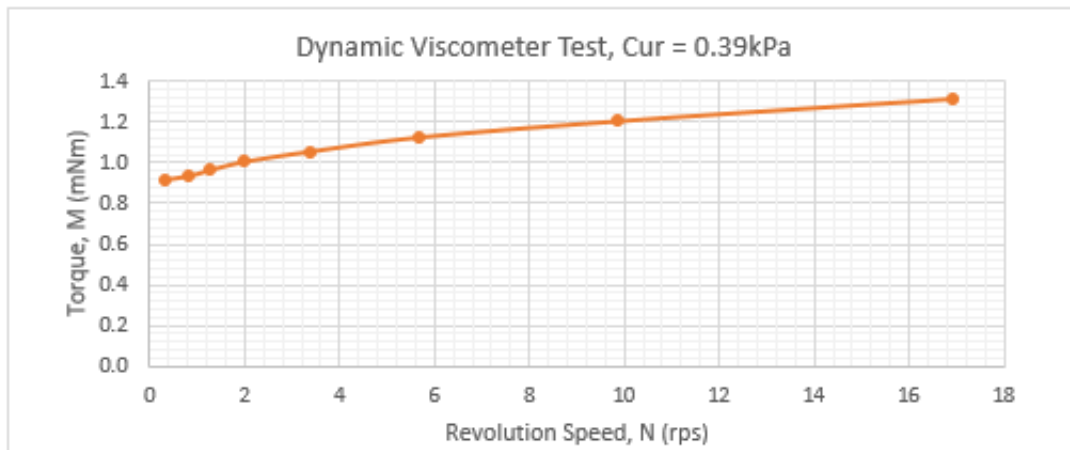


Figure C.14: Viscometer Test Data: Perniö Clay $c_{ur} = 0.39\text{kPa}$

Material: Perniö Clay
 Test date: 10/03/17

Remoulded Shear Strength	C_{ur}	0.5	kPa
Water Content	w	69.1	%
Spindle Radius	R_i	7.0	mm
Cylinder Radius	R_o	13.75	mm
Ratio	R_o/R_i	1.96	-
Cylinder Height	h	21.1	mm
Equilibrium Torque	M	2.62	mNm
System Setting	Dial	7	-

Water content	Cup #	Cup (g)	Wet (g)	Dry (g)	w %
Before	159	19.97	26.56	23.82	71.17%
	212	25.94	30.5	28.63	69.52%
After	44	25.71	32.45	29.66	70.63%
wc reduction (-) =					0.99247

Speed (-)	Start Torq (mNm)	Freq, N (Hz)	Torque reading, M (mNm) at time (seconds)										Temp (°C)
			0	5	10	15	20	30	40	60	120		
8	-	16.94	-	-	-	2.62	-	-	-	-	-	-	-
7	2.62	9.89	2.36	2.37	2.37	2.37	2.37	2.36	2.35	2.34	2.32	5.8	
6	2.62	5.70	2.11	2.12	2.13	2.14	2.14	2.15	2.15	2.16	2.19	5.7	
5	2.62	3.40	1.87	1.89	1.90	1.90	1.91	1.91	1.91	1.92	1.93	5.7	
4	2.62	2.02	1.74	1.75	1.76	1.76	1.77	1.78	1.78	1.79	1.81	6.0	
3	2.62	1.30	1.63	1.65	1.66	1.66	1.67	1.68	1.69	1.69	1.71	6.3	
2	2.62	0.85	1.54	1.55	1.56	1.56	1.57	1.57	1.57	1.59	1.60	6.6	
1	2.62	0.33	1.34	1.41	1.41	1.41	1.41	1.42	1.42	1.42	1.43	6.8	

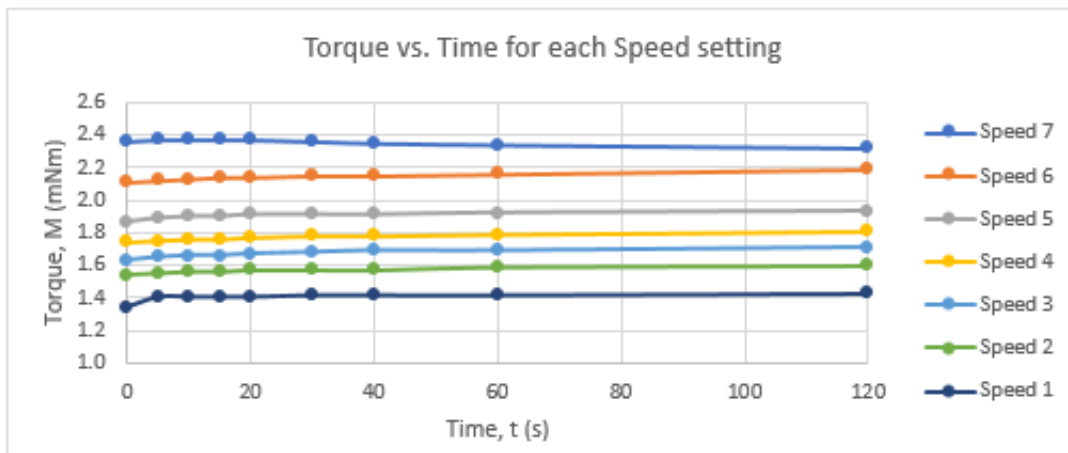
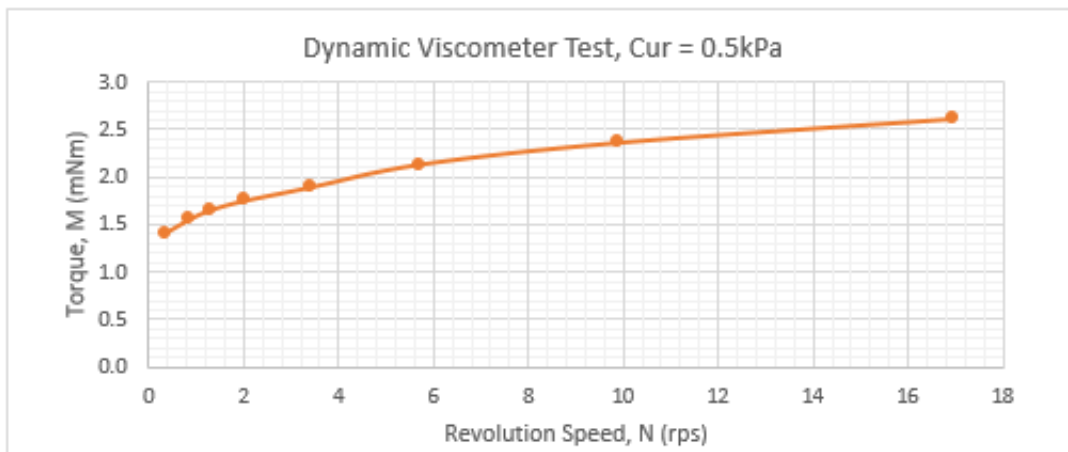


Figure C.15: Viscometer Test Data: Perniö Clay $c_{ur} = 0.5\text{kPa}$

Material: Perniö Clay

Test date: 10/03/17

Remoulded Shear Strength	C_{ur}	0.7	kPa
Water Content	w	68.4	%
Spindle Radius	R_i	7.0	mm
Cylinder Radius	R_o	13.75	mm
Ratio	R_o/R_i	1.96	-
Cylinder Height	h	21.1	mm
Equilibrium Torque	M	5.41	mNm
System Setting	Dial	7	-

Water content	Cup #	Cup (g)	Wet (g)	Dry (g)	w %
Before	108	21.89	24.7	23.56	68.26%
	227	26.83	32.47	30.16	69.37%
After	54	25.22	28.68	27.27	68.78%
	39	22.9	25.23	24.28	68.84%
wc reduction (-) =					0.9999

Speed (-)	Start Torq (mNm)	Freq, N (Hz)	Torque reading, M (mNm) at time (seconds)										Temp. (°C)
			0	5	10	15	20	30	40	60	120		
8	-	16.94	-	-	-	5.41	-	-	-	-	-	-	-
7	5.42	9.88	4.90	4.92	4.93	4.94	4.94	4.95	4.95	4.95	4.95	4.95	8.1
6	5.41	5.70	4.43	4.46	4.47	4.48	4.48	4.49	4.50	4.51	4.51	4.51	8.0
5	5.41	3.39	4.08	4.10	4.11	4.12	4.13	4.14	4.14	4.15	4.17	4.17	7.9
4	5.40	2.02	3.76	3.79	3.80	3.80	3.81	3.82	3.83	3.84	3.85	3.85	7.7
3	5.41	1.30	3.53	3.56	3.57	3.58	3.59	3.59	3.60	3.61	3.63	3.63	7.5
2	5.41	0.85	3.33	3.37	3.38	3.39	3.39	3.40	3.40	3.41	3.42	3.42	7.3
1	5.41	0.33	2.94	3.03	3.04	3.06	3.06	3.07	3.08	3.08	3.09	3.09	7.1

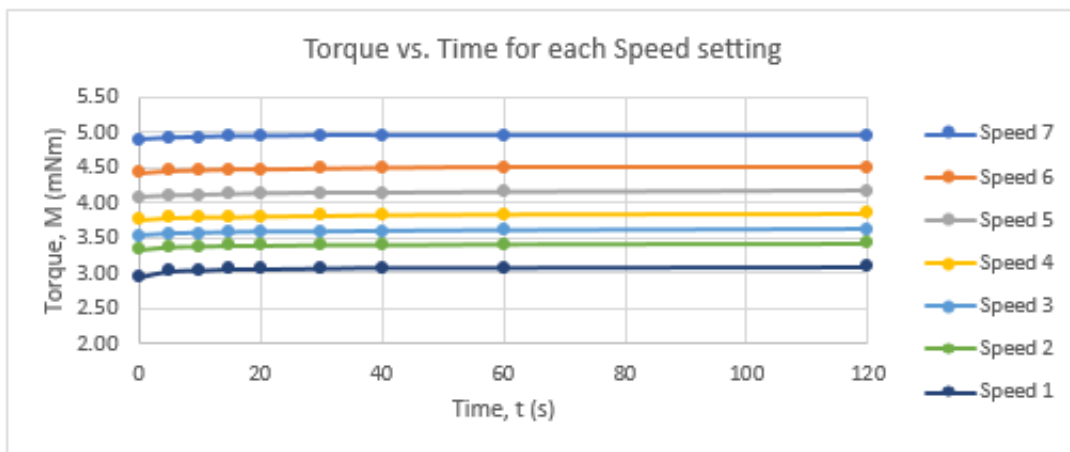
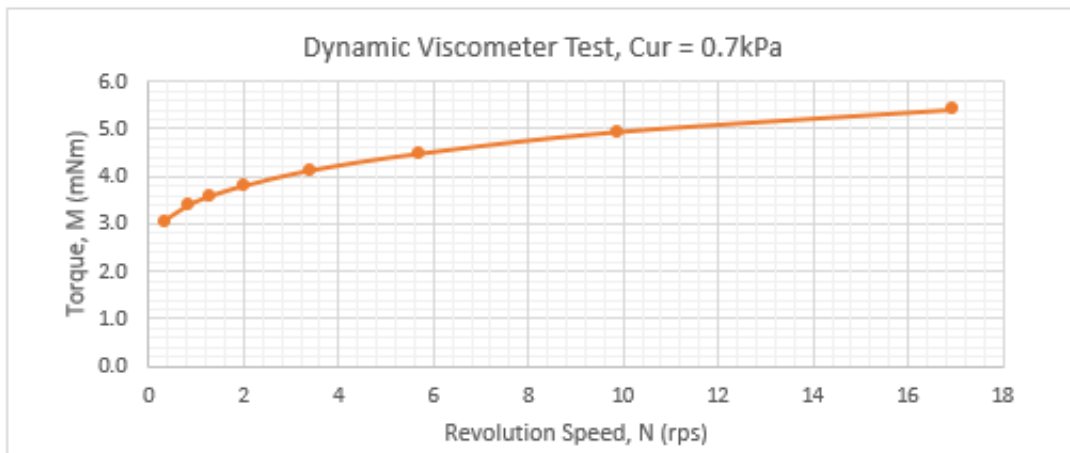


Figure C.16: Viscometer Test Data: Perniö Clay $c_{ur} = 0.7\text{kPa}$

Material: Clayey Silt
 Test date: 16/05/17

Remoulded Shear Strength	C_{ur}	<0.1	kPa
Water Content	w	58.5	%
Spindle Radius	R_i	7	mm
Cylinder Radius	R_o	13.75	mm
Ratio	R_o/R_i	1.96	-
Cylinder Height	h	21.1	mm
Equilibrium Torque	M	1.35	mNm
System Setting	Dial	7	-

Water content	Cup #	Cup (g)	Wet (g)	Dry (g)	w %
Before	152	19.08	25.7	23.27	58.00%
After	160	19.35	25.83	23.45	58.05%
wc reduction (-) =					1.001

Speed (-)	Start Torq (mNm)	Freq, N (Hz)	Torque reading, M (mNm) at time (seconds)										Temp. (°C)
			0	5	10	15	20	30	40	60	120		
8	-	16.92	-	-	-	1.35	-	-	-	-	-	-	-
7	1.35	9.88	1.26	1.27	1.28	1.28	1.28	1.28	1.28	1.27	1.26	7.1	
6	1.35	5.69	1.19	1.19	1.20	1.20	1.20	1.20	1.20	1.22	1.17	7.0	
5	1.35	3.39	1.11	1.11	1.11	1.12	1.11	1.11	1.11	1.10	1.09	7.1	
4	1.35	2.02	1.05	1.06	1.06	1.06	1.05	1.04	1.04	1.03	1.01	6.8	
3	1.35	1.30	1.02	1.02	1.02	1.01	1.01	1.00	0.99	0.98	0.96	7.1	
2	1.35	0.85	1.00	1.01	0.99	0.98	0.98	0.97	0.96	0.95	0.93	6.9	
1	1.35	0.33	0.97	0.95	0.96	0.93	0.92	0.91	0.89	0.89	0.84	6.7	

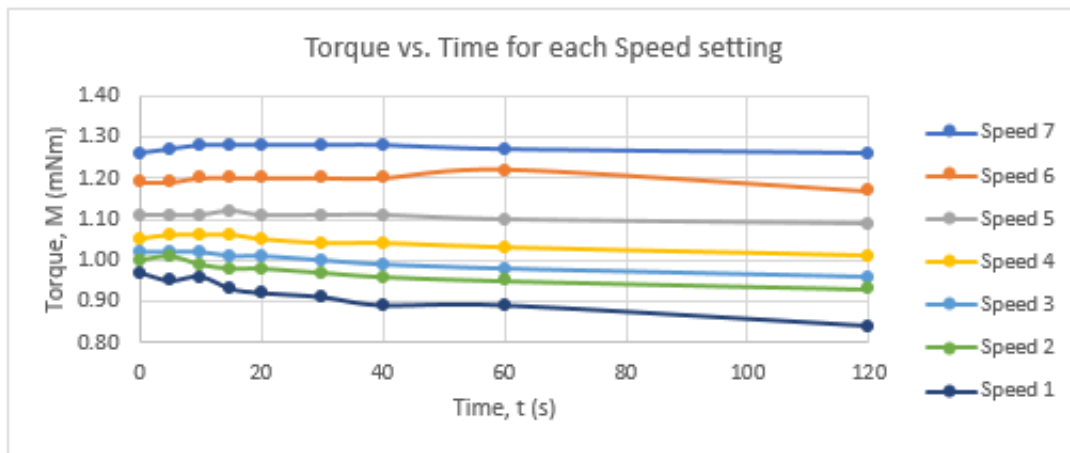
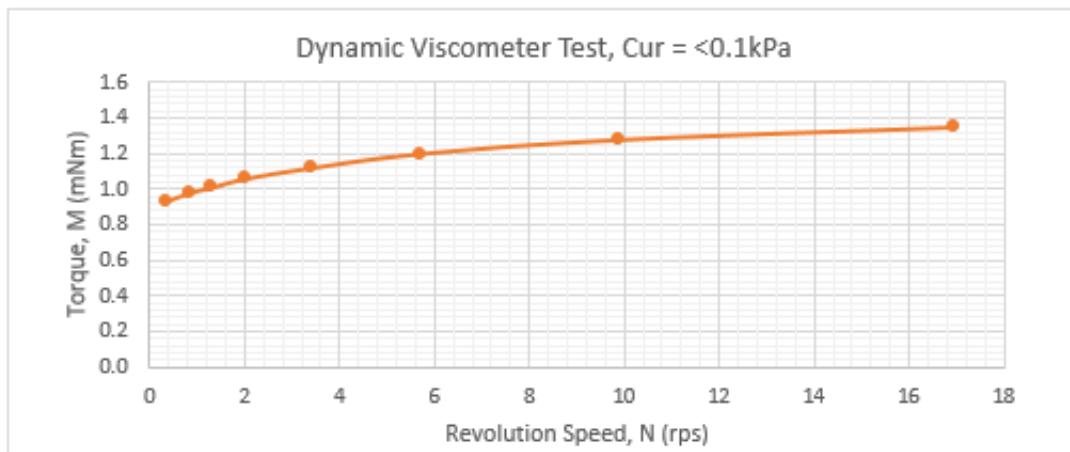


Figure C.17: Viscometer Test Data: Clayey Silt $c_{ur} < 0.1\text{kPa}$

Material: Clayey Silt
 Test date: 10/05/17

Remoulded Shear Strength	C_{ur}	0.1	kPa
Water Content	w	52.2	%
Spindle Radius	R_i	7	mm
Cylinder Radius	R_o	13.75	mm
Ratio	R_o/R_i	1.96	-
Cylinder Height	h	21.1	mm
Equilibrium Torque	M	1.82	mNm
System Setting	Dial	7	-

Water content	Cup #	Cup (g)	Wet (g)	Dry (g)	w %
Before	161	18.43	25.71	23.23	51.67%
	154	18.51	28.56	25.13	51.81%
After	166	19.23	29.5	25.69	52.41%
	156	18.42	31.46	27.21	53.26%
wc reduction (-) =					1.020

Speed (-)	Start Torq (mNm)	Freq, N (Hz)	Torque reading, M (mNm) at time (seconds)									Temp. (°C)	
			0	5	10	15	20	30	40	60	120		
8	-	16.91	-	-	-	1.82	-	-	-	-	-	-	-
7	1.82	9.87	1.71	1.71	1.71	1.72	1.72	1.71	1.72	1.72	1.71	1.71	6.2
6	1.82	5.69	1.60	1.60	1.60	1.59	1.59	1.58	1.57	1.55	1.52	1.52	6.1
5	1.82	3.39	1.53	1.53	1.52	1.51	1.50	1.49	1.48	1.46	1.44	1.44	6.3
4	1.82	2.02	1.43	1.42	1.41	1.42	1.38	1.37	1.35	1.34	1.32	1.32	6.2
3	1.82	1.30	1.45	1.43	1.40	1.38	1.36	1.33	1.32	1.29	1.24	1.24	6.6
2	1.82	0.85	1.42	1.39	1.37	1.33	1.32	1.30	1.28	1.25	1.19	1.19	6.8
1	1.82	0.33	1.26	1.22	1.21	1.20	1.20	1.19	1.17	1.16	1.14	1.14	6.7

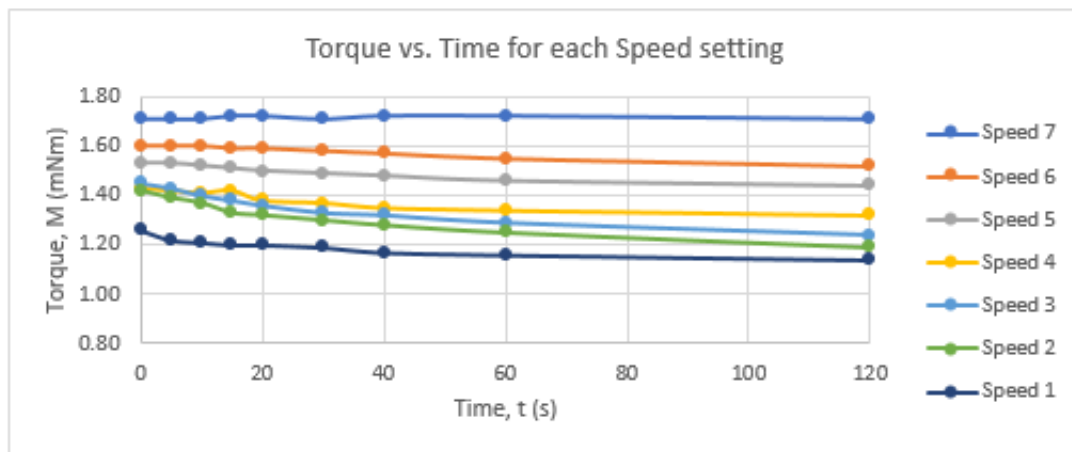
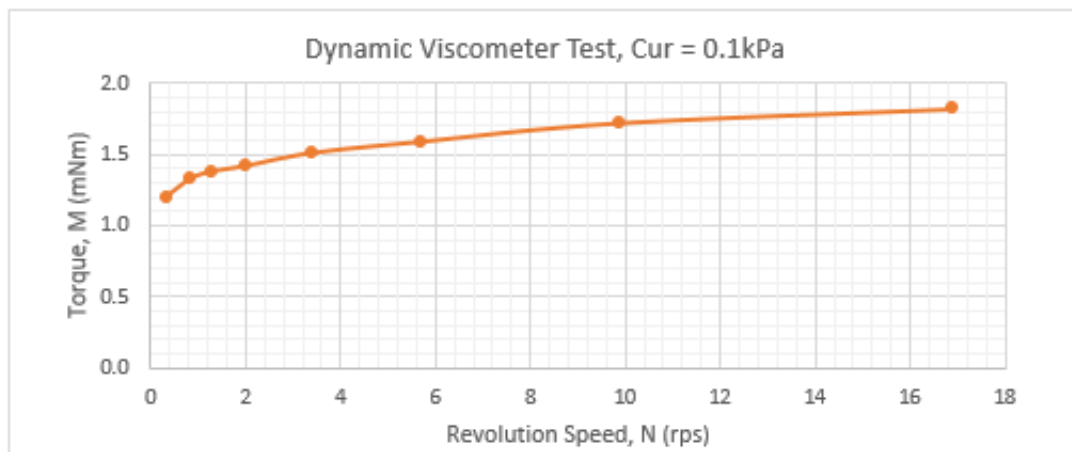


Figure C.18: Viscometer Test Data: Clayey Silt $c_{ur} = 0.1\text{kPa}$

Material: Clayey Silt
 Test date: 10/05/17

Remoulded Shear Strength	C_{ur}	0.2	kPa
Water Content	w	50.5	%
Spindle Radius	R_i	7	mm
Cylinder Radius	R_o	13.75	mm
Ratio	R_o/R_i	1.96	-
Cylinder Height	h	21.1	mm
Equilibrium Torque	M	2.33	mNm
System Setting	Dial	7	-

Water content	Cup #	Cup (g)	Wet (g)	Dry (g)	w %
Before	236	24.61	35.95	32.12	51.00%
	168	19.49	28.78	25.65	50.81%
After	158	20.02	31.42	27.57	50.99%
	159	19.97	30.68	27.06	51.06%
wc reduction (-) =					1.002

Speed (-)	Start Torq (mNm)	Freq, N (Hz)	Torque reading, M (mNm) at time (seconds)										Temp. (°C)
			0	5	10	15	20	30	40	60	120		
8	-	16.91	-	-	-	2.33	-	-	-	-	-	-	-
7	2.33	9.87	2.21	2.19	2.18	2.18	2.17	2.17	2.16	2.16	2.15	6.7	
6	2.33	5.69	2.11	2.10	2.08	2.06	2.05	2.03	2.03	2.01	2.00	6.6	
5	2.33	3.39	2.04	2.02	1.99	1.98	1.96	1.95	1.94	1.93	1.92	6.5	
4	2.33	2.02	1.97	1.94	1.90	1.88	1.86	1.85	1.84	1.82	1.80	6.8	
3	2.33	1.30	1.95	1.91	1.86	1.83	1.82	1.79	1.78	1.76	1.74	6.5	
2	2.33	0.85	1.92	1.88	1.84	1.81	1.80	1.77	1.76	1.73	1.68	6.8	
1	2.33	0.33	1.38	1.25	1.23	1.22	1.22	1.21	1.22	1.20	1.17	6.6	

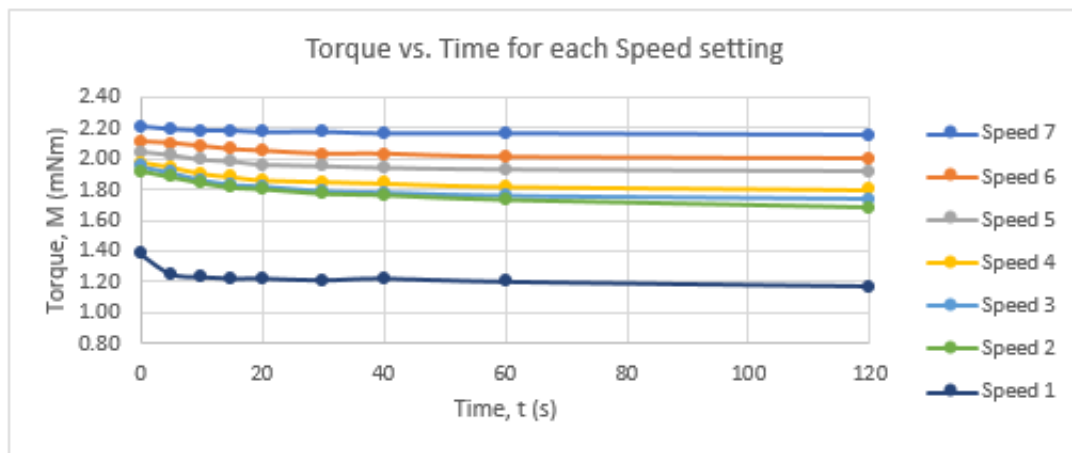
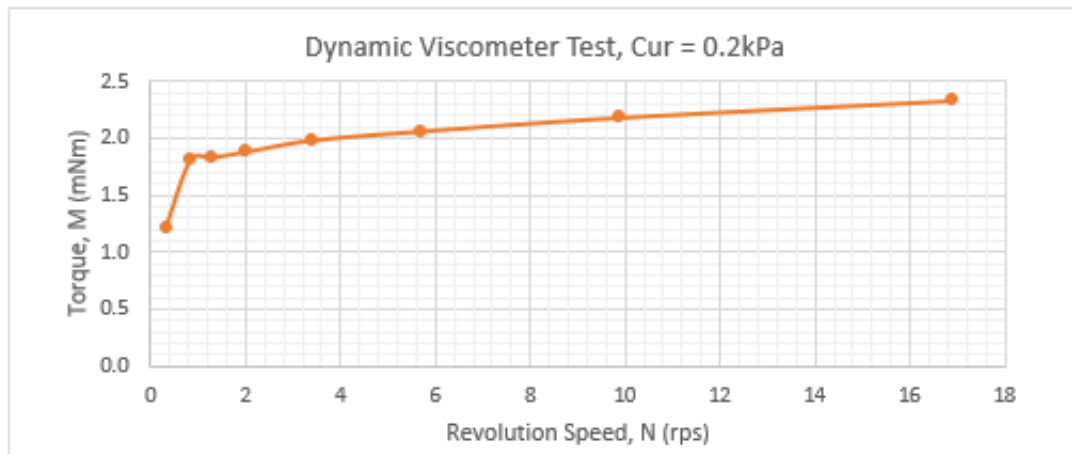


Figure C.19: Viscometer Test Data: Clayey Silt $c_{ur} = 0.2\text{kPa}$

Material: Clayey Silt
 Test date: 11/05/17

Remoulded Shear Strength	C_{ur}	0.29	kPa
Water Content	w	47.7	%
Spindle Radius	R_i	7	mm
Cylinder Radius	R_o	13.75	mm
Ratio	R_o/R_i	1.96	-
Cylinder Height	h	21.1	mm
Equilibrium Torque	M	3.21	mNm
System Setting	Dial	7	-

Water content	Cup #	Cup (g)	Wet (g)	Dry (g)	w %
Before	157	18.1	24.79	22.62	48.01%
	162	19.11	26.61	24.18	47.93%
After	151	17.96	28.8	25.27	48.29%
	153	18.9	30.23	26.57	47.72%
wc reduction (-) =					1.001

Speed (-)	Start Torq (mNm)	Freq, N (Hz)	Torque reading, M (mNm) at time (seconds)									Temp. (°C)	
			0	5	10	15	20	30	40	60	120		
8	-	16.90	-	-	-	3.21	-	-	-	-	-	-	-
7	3.21	9.87	3.12	3.07	3.10	3.08	3.07	3.04	3.02	2.98	2.96	6.8	
6	3.21	5.69	3.01	2.96	2.96	2.95	2.90	2.89	2.86	2.80	2.78	6.9	
5	3.21	3.39	2.95	2.88	2.87	2.82	2.80	2.76	2.74	2.71	2.67	6.9	
4	3.21	2.02	2.90	2.80	2.77	2.71	2.69	2.64	2.61	2.59	2.54	6.8	
3	3.21	1.30	2.88	2.78	2.68	2.64	2.61	2.56	2.54	2.50	2.44	6.8	
2	3.21	0.85	2.85	2.68	2.60	2.55	2.52	2.47	2.45	2.38	2.17	6.7	
1	3.21	0.33	1.40	1.19	1.16	1.15	1.15	1.15	1.13	1.11	1.06	7.1	

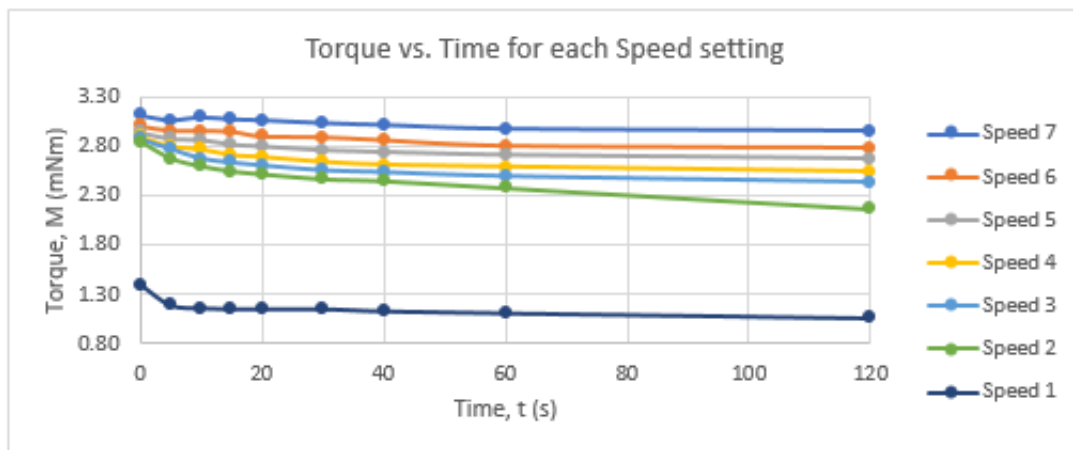
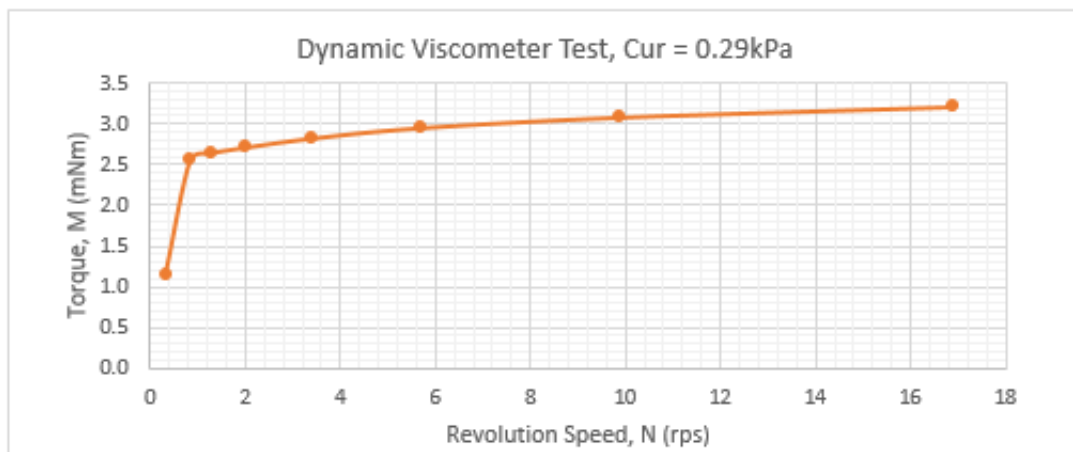
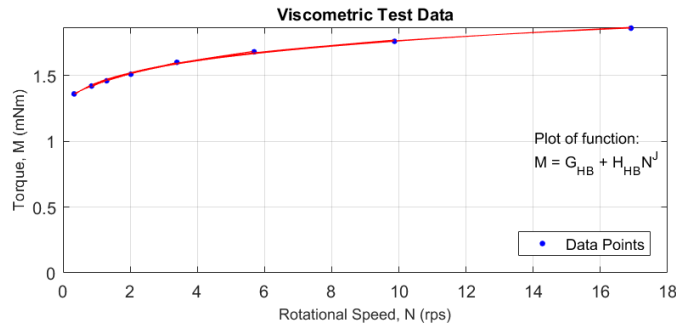


Figure C.20: Viscometer Test Data: Clayey Silt $c_{ur} = 0.29\text{kPa}$

Appendix D

Viscometer Test Results

Tiller Clay

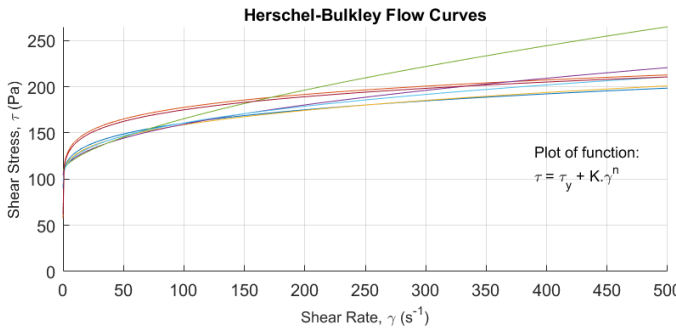


Tiller Clay 1 - Cur < 0.1kPa

Material: Tiller Clay 1
 Test date: 15/05/2017

Remoulded Shear Strength, $c_{ur} < 0.1$ kPa
 Water Content, $w = 63.5\%$
 Liquidity Index, $IL = 3.39$
 Salinity, $S = 1.74$ g/L

Viscometric System: Wide Gap
 Spindle Height, $h = 21.1$ mm
 Inner Cylinder Radius, $R_i = 7.0$ mm
 Outer Cylinder Radius, $R_o = 13.75$ mm

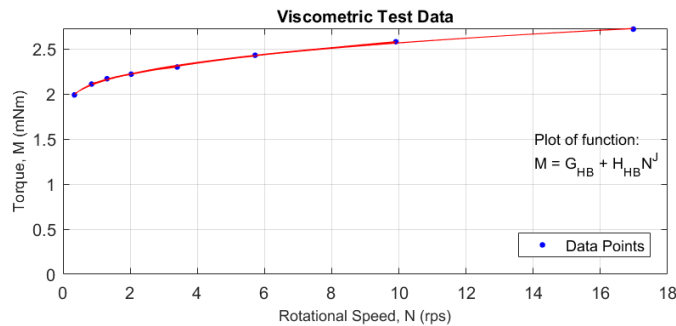


Herschel-Bulkley Parameters - Non-linear regression analysis:

All 8 points: $\tau_y = 90.39$ Pa $K = 20.54$ Pasⁿ $n = 0.27$ $R^2 = 0.996$
 Last 7 points: $\tau_y = 57.63$ Pa $K = 57.50$ Pasⁿ $n = 0.16$ $R^2 = 0.998$
 First 7 points: $\tau_y = 96.12$ Pa $K = 14.44$ Pasⁿ $n = 0.32$ $R^2 = 0.995$
 First 6 points: $\tau_y = 104.69$ Pa $K = 6.36$ Pasⁿ $n = 0.47$ $R^2 = 0.997$
 First 5 points: $\tau_y = 108.93$ Pa $K = 3.08$ Pasⁿ $n = 0.63$ $R^2 = 1.000$
 Middle 5 points: $\tau_y = 96.65$ Pa $K = 12.38$ Pasⁿ $n = 0.36$ $R^2 = 0.997$
 Middle 6 points: $\tau_y = 62.31$ Pa $K = 51.36$ Pasⁿ $n = 0.17$ $R^2 = 0.997$

NB: Only positive values plotted
 Experiment and analysis performed by: Matthew Adamson

Figure D.1: Viscometer Test Results: Tiller Clay 1 $c_{ur} < 0.1$ kPa

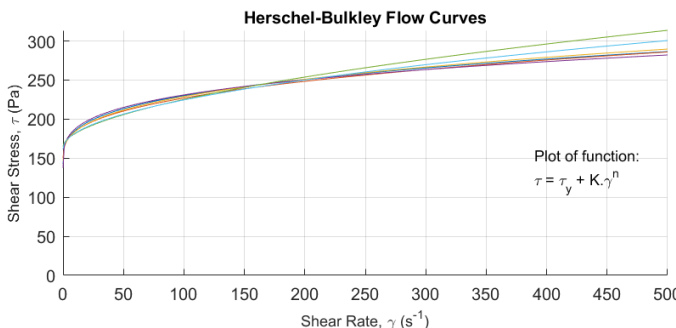


Tiller Clay 1 - Cur = 0.1kPa

Material: Tiller Clay 1
 Test date: 16/03/2017

Remoulded Shear Strength, $c_{ur} = 0.1$ kPa
 Water Content, $w = 55.8\%$
 Liquidity Index, $IL = 2.77$
 Salinity, $S = 1.84$ g/L

Viscometric System: Wide Gap
 Spindle Height, $h = 21.1$ mm
 Inner Cylinder Radius, $R_i = 7.0$ mm
 Outer Cylinder Radius, $R_o = 13.75$ mm



Herschel-Bulkley Parameters - Non-linear regression analysis:

All 8 points: $\tau_y = 142.41$ Pa $K = 21.23$ Pasⁿ $n = 0.31$ $R^2 = 0.998$
 Last 7 points: $\tau_y = 150.28$ Pa $K = 15.01$ Pasⁿ $n = 0.35$ $R^2 = 0.998$
 First 7 points: $\tau_y = 146.90$ Pa $K = 16.79$ Pasⁿ $n = 0.34$ $R^2 = 0.997$
 First 6 points: $\tau_y = 137.48$ Pa $K = 26.83$ Pasⁿ $n = 0.27$ $R^2 = 0.994$
 First 5 points: $\tau_y = -64.88$ Pa $K = 344.99$ Pasⁿ $n = 0.05$ $R^2 = 0.999$
 Middle 5 points: $\tau_y = 165.05$ Pa $K = 4.51$ Pasⁿ $n = 0.56$ $R^2 = 0.997$
 Middle 6 points: $\tau_y = 161.84$ Pa $K = 6.47$ Pasⁿ $n = 0.49$ $R^2 = 0.999$

NB: Only positive values plotted
 Experiment and analysis performed by: Matthew Adamson

Figure D.2: Viscometer Test Results: Tiller Clay 1 $c_{ur} = 0.1$ kPa

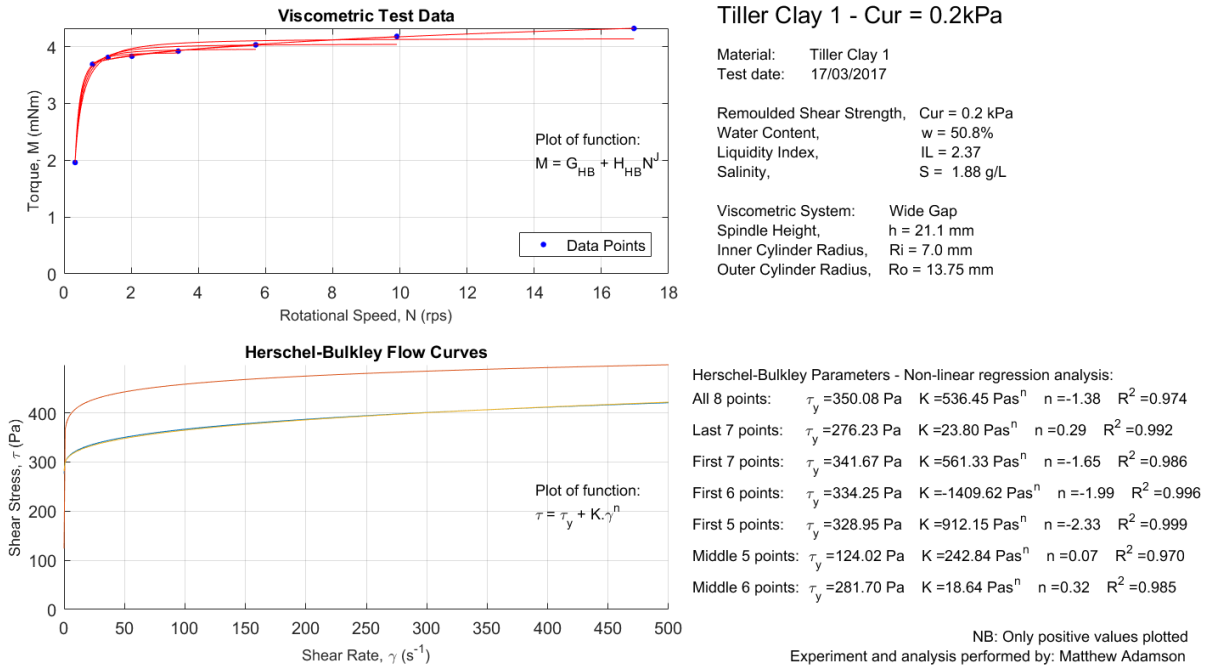


Figure D.3: Viscometer Test Results: Tiller Clay 1 $c_{ur} = 0.2\text{kPa}$

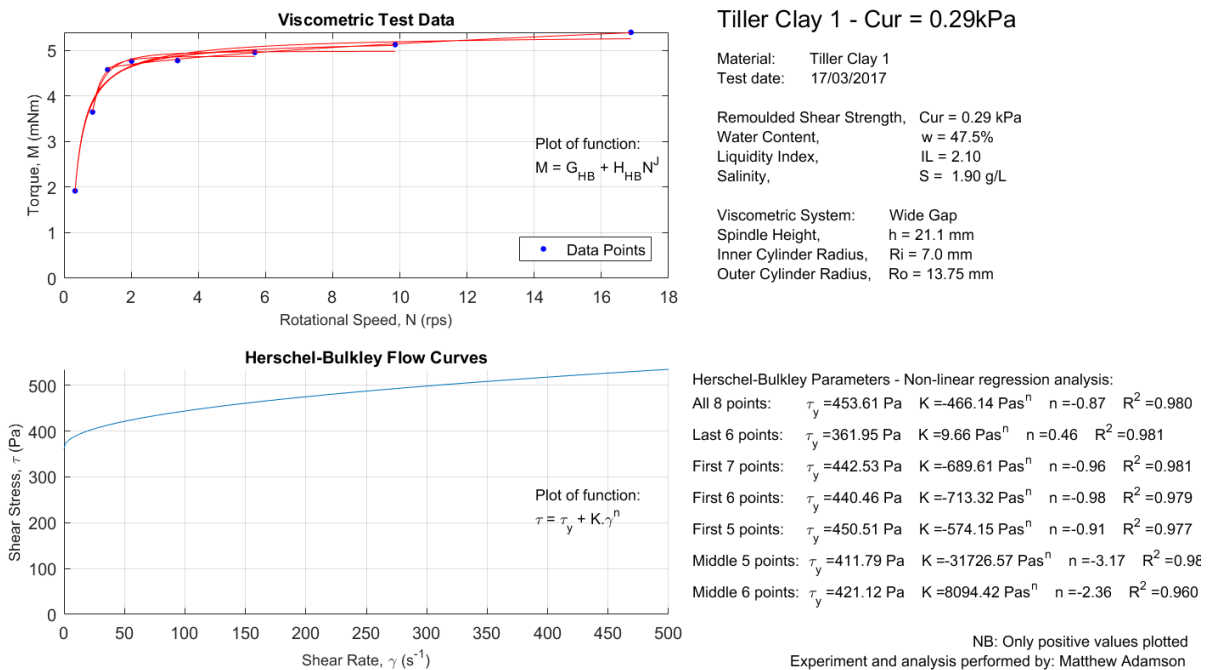
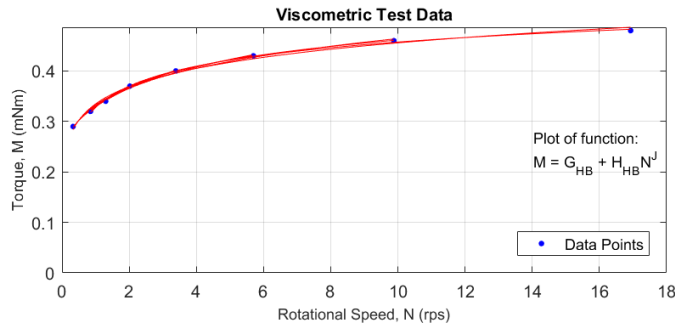


Figure D.4: Viscometer Test Results: Tiller Clay 1 $c_{ur} = 0.29\text{kPa}$

Tiller Clay 2

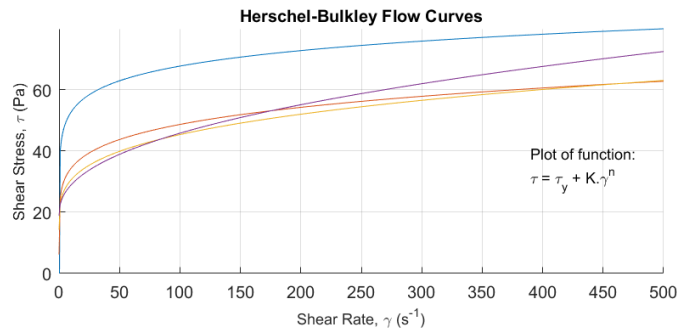


Tiller Clay 2 - Cur < 0.1kPa

Material: Tiller Clay 2
 Test date: 16/05/2017

Remoulded Shear Strength, Cur < 0.1 kPa
 Water Content, w = 92.8%
 Liquidity Index, IL = 5.31
 Salinity, S = 2.30 g/L

Viscometric System: Wide Gap
 Spindle Height, h = 21.1 mm
 Inner Cylinder Radius, Ri = 7.0 mm
 Outer Cylinder Radius, Ro = 13.75 mm

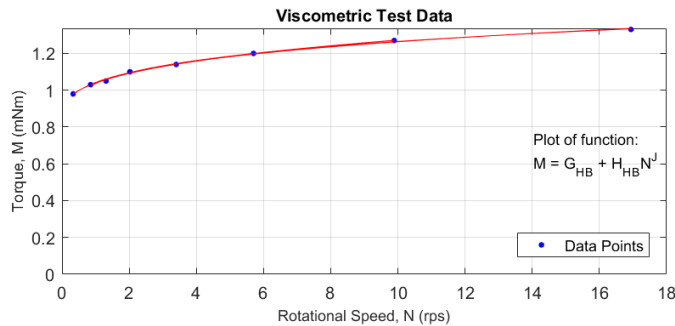


Herschel-Bulkley Parameters - Non-linear regression analysis:

- All 8 points: $\tau_y = -23.93$ Pa $K = 64.10$ Pasⁿ $n = 0.08$ $R^2 = 0.992$
- Last 7 points: $\tau_y = 76.79$ Pa $K = 30.13$ Pasⁿ $n = -0.11$ $R^2 = 0.998$
- First 7 points: $\tau_y = 6.20$ Pa $K = 18.70$ Pasⁿ $n = 0.18$ $R^2 = 0.995$
- First 6 points: $\tau_y = 14.31$ Pa $K = 8.55$ Pasⁿ $n = 0.28$ $R^2 = 0.995$
- First 5 points: $\tau_y = 18.85$ Pa $K = 3.77$ Pasⁿ $n = 0.43$ $R^2 = 0.997$
- Middle 5 points: $\tau_y = -100.80$ Pa $K = 188.31$ Pasⁿ $n = 0.04$ $R^2 = 0.998$
- Middle 6 points: $\tau_y = 315.45$ Pa $K = 151.49$ Pasⁿ $n = -0.02$ $R^2 = 0.999$

NB: Only positive values plotted
 Experiment and analysis performed by: Matthew Adamson

Figure D.5: Viscometer Test Results: Tiller Clay 2 $c_{ur} < 0.1$ kPa

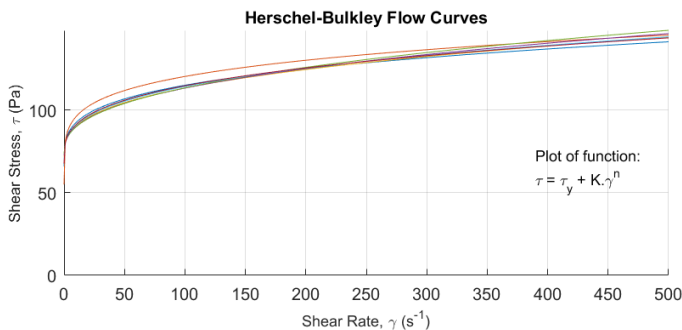


Tiller Clay 2 - Cur = 0.1kPa

Material: Tiller Clay 2
 Test date: 15/03/2017

Remoulded Shear Strength, Cur = 0.1 kPa
 Water Content, w = 66.3%
 Liquidity Index, IL = 3.11
 Salinity, S = 2.30 g/L

Viscometric System: Wide Gap
 Spindle Height, h = 21.1 mm
 Inner Cylinder Radius, Ri = 7.0 mm
 Outer Cylinder Radius, Ro = 13.75 mm

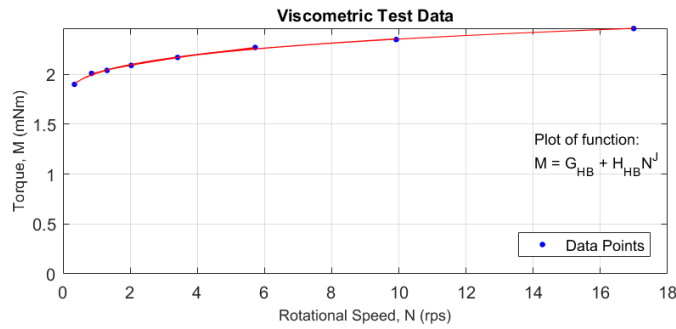


Herschel-Bulkley Parameters - Non-linear regression analysis:

- All 8 points: $\tau_y = 65.94$ Pa $K = 14.37$ Pasⁿ $n = 0.27$ $R^2 = 0.997$
- Last 7 points: $\tau_y = 55.00$ Pa $K = 25.81$ Pasⁿ $n = 0.20$ $R^2 = 0.997$
- First 7 points: $\tau_y = 71.30$ Pa $K = 8.76$ Pasⁿ $n = 0.34$ $R^2 = 0.998$
- First 6 points: $\tau_y = 72.72$ Pa $K = 7.37$ Pasⁿ $n = 0.37$ $R^2 = 0.996$
- First 5 points: $\tau_y = 73.42$ Pa $K = 6.67$ Pasⁿ $n = 0.39$ $R^2 = 0.992$
- Middle 5 points: $\tau_y = 69.20$ Pa $K = 10.43$ Pasⁿ $n = 0.32$ $R^2 = 0.993$
- Middle 6 points: $\tau_y = 67.74$ Pa $K = 11.85$ Pasⁿ $n = 0.30$ $R^2 = 0.997$

NB: Only positive values plotted
 Experiment and analysis performed by: Matthew Adamson

Figure D.6: Viscometer Test Results: Tiller Clay 2 $c_{ur} = 0.1$ kPa

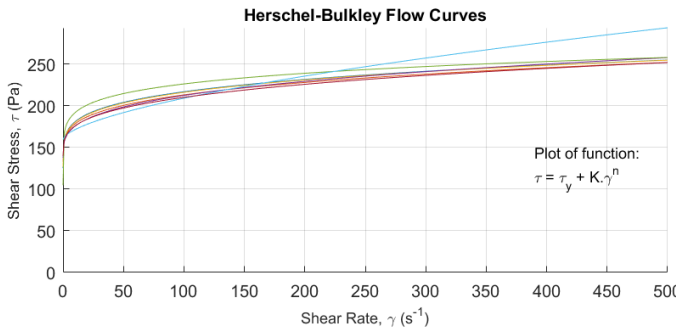


Tiller Clay 2 - Cur = 0.2kPa

Material: Tiller Clay 2
 Test date: 15/03/2017

Remoulded Shear Strength, Cur = 0.2 kPa
 Water Content, w = 57.6%
 Liquidity Index, IL = 2.50
 Salinity, S = 2.30 g/L

Viscometric System: Wide Gap
 Spindle Height, h = 21.1 mm
 Inner Cylinder Radius, Ri = 7.0 mm
 Outer Cylinder Radius, Ro = 13.75 mm

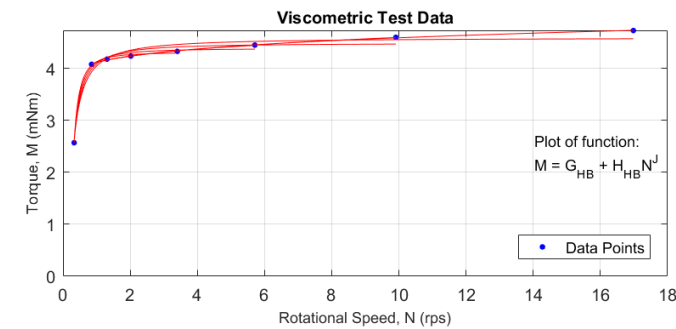


Herschel-Bulkley Parameters - Non-linear regression analysis:

All 8 points:	$\tau_y = 125.25$ Pa	$K = 33.95$ Pas ⁿ	$n = 0.22$	$R^2 = 0.998$
Last 7 points:	$\tau_y = 132.92$ Pa	$K = 25.92$ Pas ⁿ	$n = 0.25$	$R^2 = 0.997$
First 7 points:	$\tau_y = 126.70$ Pa	$K = 32.19$ Pas ⁿ	$n = 0.22$	$R^2 = 0.996$
First 6 points:	$\tau_y = 137.68$ Pa	$K = 19.34$ Pas ⁿ	$n = 0.29$	$R^2 = 0.994$
First 5 points:	$\tau_y = 104.80$ Pa	$K = 62.54$ Pas ⁿ	$n = 0.14$	$R^2 = 0.992$
Middle 5 points:	$\tau_y = 159.67$ Pa	$K = 2.87$ Pas ⁿ	$n = 0.62$	$R^2 = 0.999$
Middle 6 points:	$\tau_y = 140.21$ Pa	$K = 18.35$ Pas ⁿ	$n = 0.29$	$R^2 = 0.994$

NB: Only positive values plotted
 Experiment and analysis performed by: Matthew Adamson

Figure D.7: Viscometer Test Results: Tiller Clay 2 $c_{ur} = 0.2\text{kPa}$

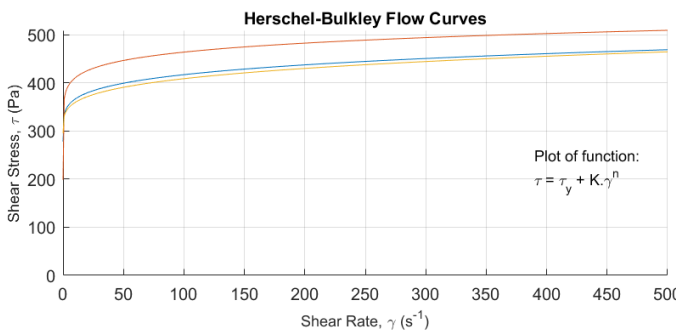


Tiller Clay 2 - Cur = 0.29kPa

Material: Tiller Clay 2
 Test date: 15/03/2017

Remoulded Shear Strength, Cur = 0.29 kPa
 Water Content, w = 52.0%
 Liquidity Index, IL = 2.01
 Salinity, S = 2.30 g/L

Viscometric System: Wide Gap
 Spindle Height, h = 21.1 mm
 Inner Cylinder Radius, Ri = 7.0 mm
 Outer Cylinder Radius, Ro = 13.75 mm



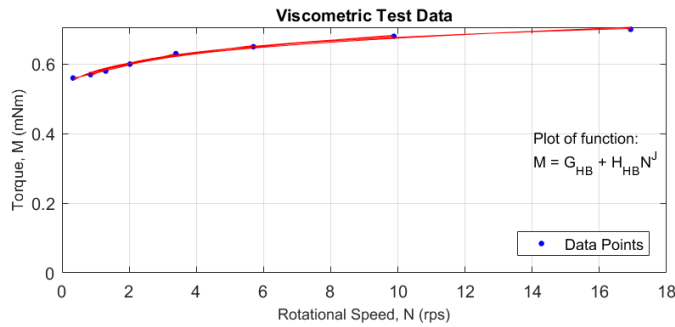
Herschel-Bulkley Parameters - Non-linear regression analysis:

All 8 points:	$\tau_y = 387.78$ Pa	$K = -259.11$ Pas ⁿ	$n = -1.17$	$R^2 = 0.973$
Last 7 points:	$\tau_y = 277.80$ Pa	$K = 56.17$ Pas ⁿ	$n = 0.20$	$R^2 = 0.998$
First 7 points:	$\tau_y = 378.81$ Pa	$K = 583.98$ Pas ⁿ	$n = -1.41$	$R^2 = 0.984$
First 6 points:	$\tau_y = 370.35$ Pa	$K = 157.46$ Pas ⁿ	$n = -1.72$	$R^2 = 0.994$
First 5 points:	$\tau_y = 363.97$ Pa	$K = -1242.66$ Pas ⁿ	$n = -2.05$	$R^2 = 0.999$
Middle 5 points:	$\tau_y = 198.61$ Pa	$K = 168.87$ Pas ⁿ	$n = 0.10$	$R^2 = 0.994$
Middle 6 points:	$\tau_y = 295.31$ Pa	$K = 36.00$ Pas ⁿ	$n = 0.25$	$R^2 = 0.996$

NB: Only positive values plotted
 Experiment and analysis performed by: Matthew Adamson

Figure D.8: Viscometer Test Results: Tiller Clay 2 $c_{ur} = 0.29\text{kPa}$

Perniö Clay

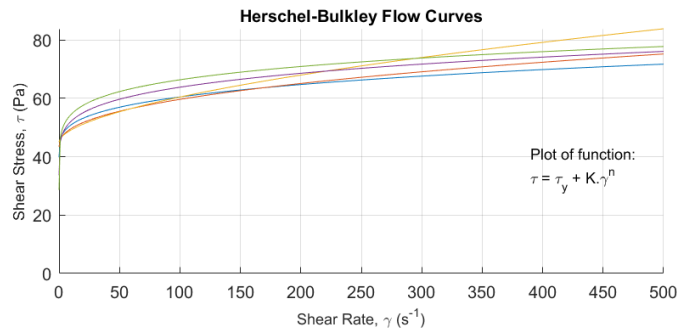


Perniö Clay - Cur < 0.1kPa

Material: Perniö Clay
 Test date: 12/05/2017

Remoulded Shear Strength, Cur < 0.1 kPa
 Water Content, $w = 95.2\%$
 Liquidity Index, IL = 2.23
 Salinity, S = 1.01 g/L

Viscometric System: Wide Gap
 Spindle Height, $h = 21.1$ mm
 Inner Cylinder Radius, Ri = 7.0 mm
 Outer Cylinder Radius, Ro = 13.75 mm

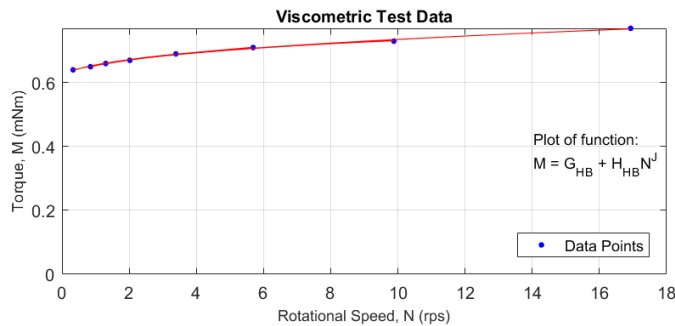


Herschel-Bulkley Parameters - Non-linear regression analysis:

All 8 points: $\tau_y = 39.80$ Pa $K = 5.96$ Pasⁿ $n = 0.27$ $R^2 = 0.984$
 Last 7 points: $\tau_y = 31.03$ Pa $K = 112.03$ Pasⁿ $n = 0.05$ $R^2 = 0.995$
 First 7 points: $\tau_y = 43.42$ Pa $K = 2.36$ Pasⁿ $n = 0.42$ $R^2 = 0.986$
 First 6 points: $\tau_y = 45.02$ Pa $K = 1.10$ Pasⁿ $n = 0.57$ $R^2 = 0.982$
 First 5 points: $\tau_y = 46.65$ Pa $K = 0.18$ Pasⁿ $n = 1.04$ $R^2 = 0.998$
 Middle 5 points: $\tau_y = 33.62$ Pa $K = 11.36$ Pasⁿ $n = 0.21$ $R^2 = 0.990$
 Middle 6 points: $\tau_y = 28.63$ Pa $K = 17.71$ Pasⁿ $n = 0.16$ $R^2 = 0.995$

NB: Only positive values plotted
 Experiment and analysis performed by: Matthew Adamson

Figure D.9: Viscometer Test Results: Perniö Clay $c_{ur} < 0.1kPa$ 1

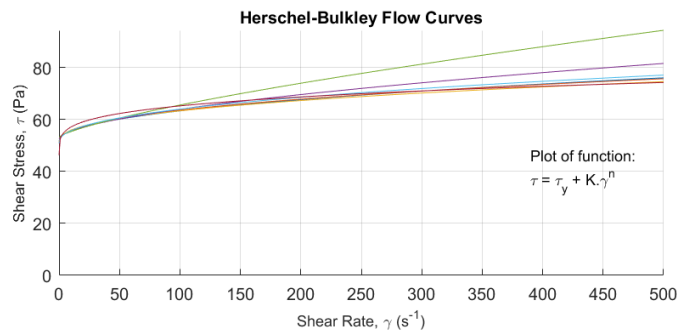


Perniö Clay - Cur < 0.1kPa

Material: Perniö Clay
 Test date: 18/05/2017

Remoulded Shear Strength, Cur < 0.1 kPa
 Water Content, $w = 90.7\%$
 Liquidity Index, IL = 2.08
 Salinity, S = 1.02 g/L

Viscometric System: Wide Gap
 Spindle Height, $h = 21.1$ mm
 Inner Cylinder Radius, Ri = 7.0 mm
 Outer Cylinder Radius, Ro = 13.75 mm

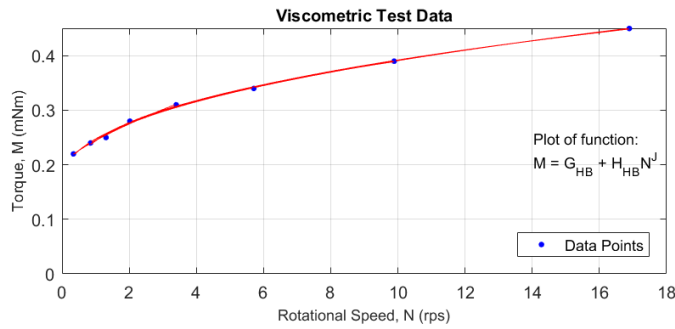


Herschel-Bulkley Parameters - Non-linear regression analysis:

All 8 points: $\tau_y = 51.82$ Pa $K = 1.35$ Pasⁿ $n = 0.46$ $R^2 = 0.997$
 Last 7 points: $\tau_y = 50.94$ Pa $K = 1.86$ Pasⁿ $n = 0.42$ $R^2 = 0.996$
 First 7 points: $\tau_y = 51.19$ Pa $K = 1.86$ Pasⁿ $n = 0.41$ $R^2 = 0.994$
 First 6 points: $\tau_y = 52.54$ Pa $K = 0.79$ Pasⁿ $n = 0.58$ $R^2 = 0.997$
 First 5 points: $\tau_y = 53.13$ Pa $K = 0.40$ Pasⁿ $n = 0.74$ $R^2 = 0.999$
 Middle 5 points: $\tau_y = 50.85$ Pa $K = 1.82$ Pasⁿ $n = 0.43$ $R^2 = 0.998$
 Middle 6 points: $\tau_y = 46.28$ Pa $K = 6.21$ Pasⁿ $n = 0.24$ $R^2 = 0.997$

NB: Only positive values plotted
 Experiment and analysis performed by: Matthew Adamson

Figure D.10: Viscometer Test Results: Perniö Clay $c_{ur} < 0.1kPa$ 2

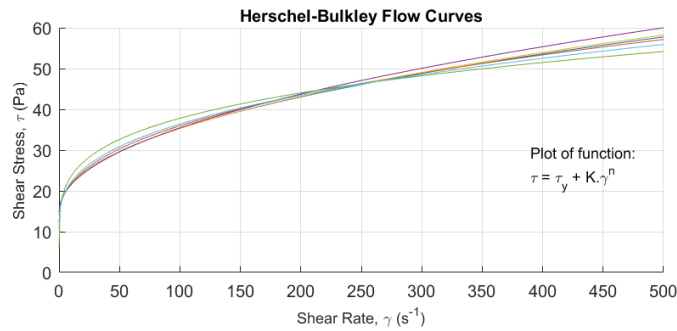


Pernio Clay - Cur = 0.1kPa

Material: Pernio Clay
 Test date: 8/03/2017

Remoulded Shear Strength, Cur = 0.1 kPa
 Water Content, w = 83.1%
 Liquidity Index, IL = 1.84
 Salinity, S = 1.04 g/L

Viscometric System: Wide Gap
 Spindle Height, h = 21.1 mm
 Inner Cylinder Radius, Ri = 7.0 mm
 Outer Cylinder Radius, Ro = 13.75 mm

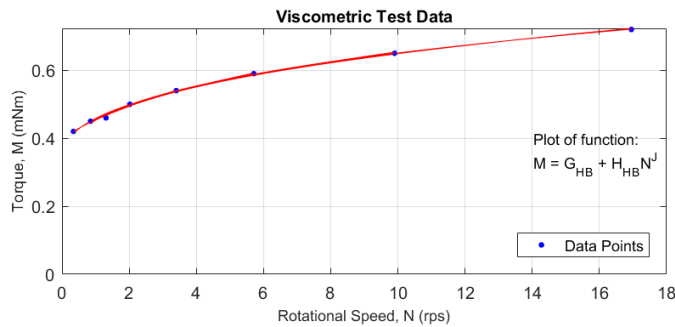


Herschel-Bulkley Parameters - Non-linear regression analysis:

All 8 points: $\tau_y = 14.21$ Pa K = 2.66 Pasⁿ n = 0.45 R² = 0.998
 Last 7 points: $\tau_y = 12.30$ Pa K = 3.82 Pasⁿ n = 0.40 R² = 0.998
 First 7 points: $\tau_y = 14.38$ Pa K = 2.53 Pasⁿ n = 0.46 R² = 0.995
 First 6 points: $\tau_y = 14.78$ Pa K = 2.21 Pasⁿ n = 0.49 R² = 0.990
 First 5 points: $\tau_y = 16.78$ Pa K = 0.77 Pasⁿ n = 0.73 R² = 0.991
 Middle 5 points: $\tau_y = 6.18$ Pa K = 9.60 Pasⁿ n = 0.26 R² = 0.991
 Middle 6 points: $\tau_y = 10.70$ Pa K = 5.11 Pasⁿ n = 0.35 R² = 0.996

NB: Only positive values plotted
 Experiment and analysis performed by: Matthew Adamson

Figure D.11: Viscometer Test Results: Pernio Clay $c_{ur} = 0.1kPa$

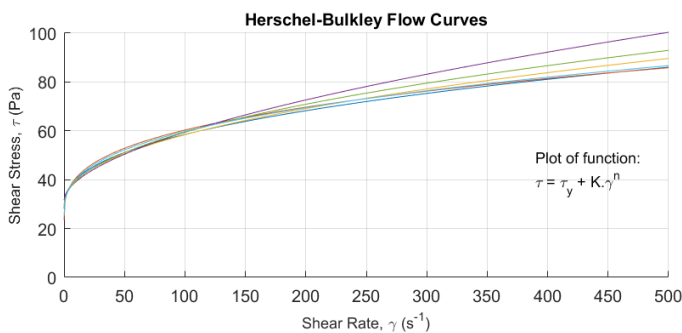


Pernio Clay - Cur = 0.2kPa

Material: Pernio Clay
 Test date: 8/03/2017

Remoulded Shear Strength, Cur = 0.2 kPa
 Water Content, w = 81.1%
 Liquidity Index, IL = 1.70
 Salinity, S = 1.26 g/L

Viscometric System: Wide Gap
 Spindle Height, h = 21.1 mm
 Inner Cylinder Radius, Ri = 7.0 mm
 Outer Cylinder Radius, Ro = 13.75 mm

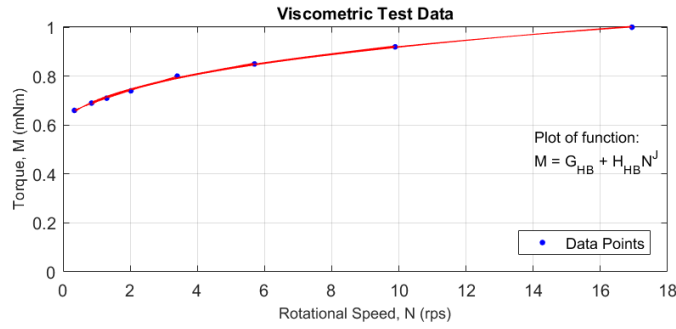


Herschel-Bulkley Parameters - Non-linear regression analysis:

All 8 points: $\tau_y = 28.11$ Pa K = 4.78 Pasⁿ n = 0.40 R² = 0.997
 Last 7 points: $\tau_y = 23.37$ Pa K = 8.20 Pasⁿ n = 0.33 R² = 0.998
 First 7 points: $\tau_y = 29.73$ Pa K = 3.47 Pasⁿ n = 0.46 R² = 0.996
 First 6 points: $\tau_y = 31.58$ Pa K = 2.08 Pasⁿ n = 0.56 R² = 0.994
 First 5 points: $\tau_y = 32.99$ Pa K = 1.13 Pasⁿ n = 0.71 R² = 0.990
 Middle 5 points: $\tau_y = 28.93$ Pa K = 3.63 Pasⁿ n = 0.46 R² = 0.992
 Middle 6 points: $\tau_y = 25.14$ Pa K = 6.66 Pasⁿ n = 0.36 R² = 0.996

NB: Only positive values plotted
 Experiment and analysis performed by: Matthew Adamson

Figure D.12: Viscometer Test Results: Pernio Clay $c_{ur} = 0.2kPa$

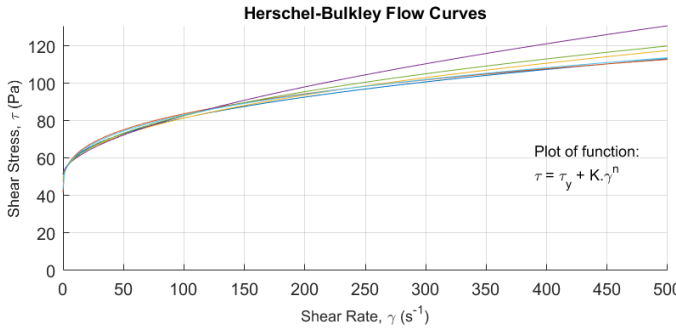


Pernio Clay - Cur = 0.29kPa

Material: Pernio Clay
 Test date: 8/03/2017

Remoulded Shear Strength, Cur = 0.29 kPa
 Water Content, w = 74.3%
 Liquidity Index, IL = 1.56
 Salinity, S = 1.40 g/L

Viscometric System: Wide Gap
 Spindle Height, h = 21.1 mm
 Inner Cylinder Radius, Ri = 7.0 mm
 Outer Cylinder Radius, Ro = 13.75 mm

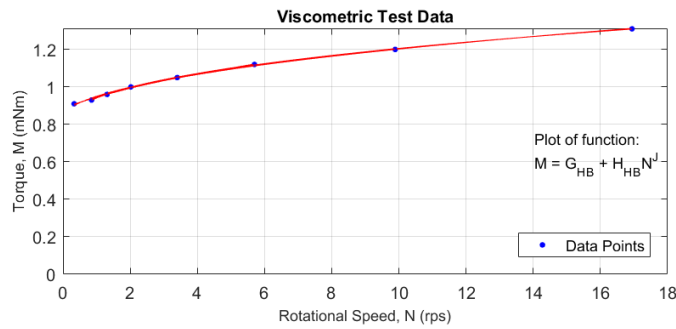


Herschel-Bulkley Parameters - Non-linear regression analysis:

All 8 points:	$\tau_y = 47.60$ Pa	$K = 5.17$ Pas ⁿ	$n = 0.41$	$R^2 = 0.997$
Last 7 points:	$\tau_y = 41.75$ Pa	$K = 9.35$ Pas ⁿ	$n = 0.33$	$R^2 = 0.998$
First 7 points:	$\tau_y = 49.44$ Pa	$K = 3.70$ Pas ⁿ	$n = 0.47$	$R^2 = 0.996$
First 6 points:	$\tau_y = 51.53$ Pa	$K = 2.17$ Pas ⁿ	$n = 0.58$	$R^2 = 0.995$
First 5 points:	$\tau_y = 53.86$ Pa	$K = 0.76$ Pas ⁿ	$n = 0.84$	$R^2 = 0.999$
Middle 5 points:	$\tau_y = 47.69$ Pa	$K = 4.43$ Pas ⁿ	$n = 0.45$	$R^2 = 0.994$
Middle 6 points:	$\tau_y = 43.65$ Pa	$K = 7.69$ Pas ⁿ	$n = 0.36$	$R^2 = 0.997$

NB: Only positive values plotted
 Experiment and analysis performed by: Matthew Adamson

Figure D.13: Viscometer Test Results: Perniö Clay $c_{ur} = 0.29$ kPa

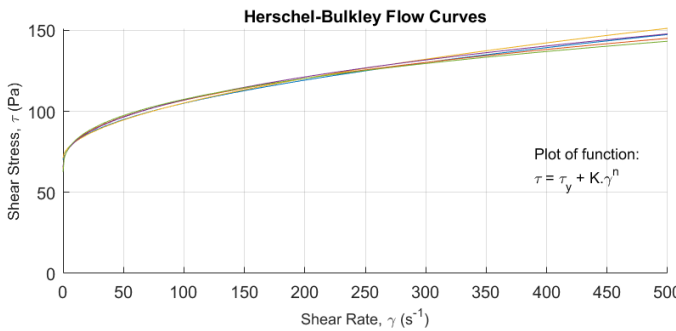


Pernio Clay - Cur = 0.39kPa

Material: Pernio Clay
 Test date: 9/03/2017

Remoulded Shear Strength, Cur = 0.39 kPa
 Water Content, w = 70.8%
 Liquidity Index, IL = 1.45
 Salinity, S = 1.51 g/L

Viscometric System: Wide Gap
 Spindle Height, h = 21.1 mm
 Inner Cylinder Radius, Ri = 7.0 mm
 Outer Cylinder Radius, Ro = 13.75 mm

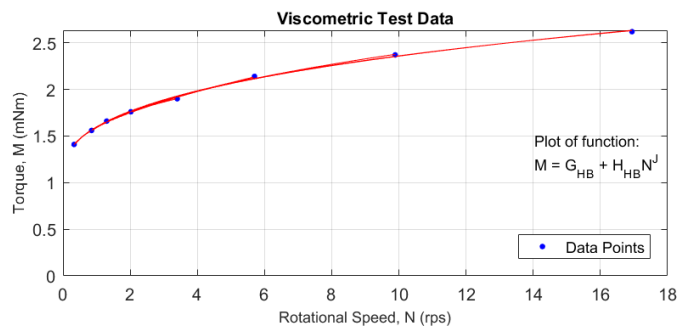


Herschel-Bulkley Parameters - Non-linear regression analysis:

All 8 points:	$\tau_y = 70.21$ Pa	$K = 3.56$ Pas ⁿ	$n = 0.49$	$R^2 = 0.998$
Last 7 points:	$\tau_y = 64.81$ Pa	$K = 6.62$ Pas ⁿ	$n = 0.40$	$R^2 = 1.000$
First 7 points:	$\tau_y = 71.14$ Pa	$K = 2.92$ Pas ⁿ	$n = 0.53$	$R^2 = 0.996$
First 6 points:	$\tau_y = 73.27$ Pa	$K = 1.55$ Pas ⁿ	$n = 0.67$	$R^2 = 0.995$
First 5 points:	$\tau_y = 74.37$ Pa	$K = 0.92$ Pas ⁿ	$n = 0.80$	$R^2 = 0.992$
Middle 5 points:	$\tau_y = 65.83$ Pa	$K = 5.76$ Pas ⁿ	$n = 0.43$	$R^2 = 1.000$
Middle 6 points:	$\tau_y = 62.69$ Pa	$K = 8.30$ Pas ⁿ	$n = 0.37$	$R^2 = 1.000$

NB: Only positive values plotted
 Experiment and analysis performed by: Matthew Adamson

Figure D.14: Viscometer Test Results: Perniö Clay $c_{ur} = 0.39$ kPa

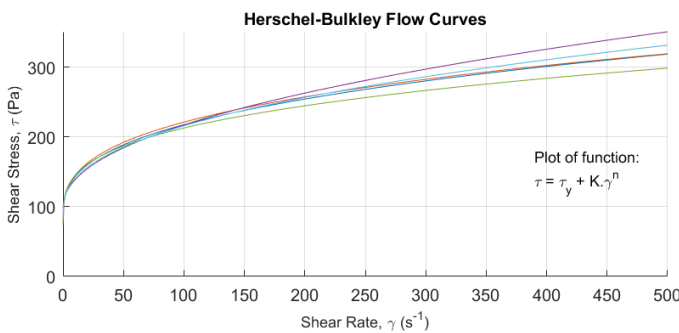


Pernio Clay - Cur = 0.5kPa

Material: Pernio Clay
 Test date: 10/03/2017

Remoulded Shear Strength, Cur = 0.5 kPa
 Water Content, w = 69.1%
 Liquidity Index, IL = 1.39
 Salinity, S = 1.61 g/L

Viscometric System: Wide Gap
 Spindle Height, h = 21.1 mm
 Inner Cylinder Radius, Ri = 7.0 mm
 Outer Cylinder Radius, Ro = 13.75 mm

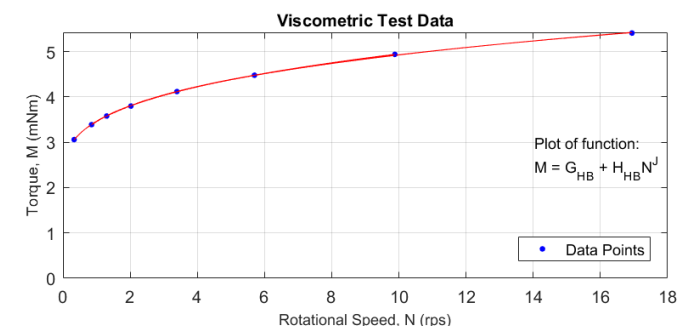


Herschel-Bulkley Parameters - Non-linear regression analysis:

All 8 points:	$\tau_y = 82.88$ Pa	$K = 27.07$ Pas ⁿ	$n = 0.35$	$R^2 = 0.998$
Last 7 points:	$\tau_y = 73.63$ Pa	$K = 34.34$ Pas ⁿ	$n = 0.32$	$R^2 = 0.998$
First 7 points:	$\tau_y = 92.04$ Pa	$K = 18.84$ Pas ⁿ	$n = 0.41$	$R^2 = 0.998$
First 6 points:	$\tau_y = 97.81$ Pa	$K = 13.93$ Pas ⁿ	$n = 0.47$	$R^2 = 0.998$
First 5 points:	$\tau_y = 79.44$ Pa	$K = 32.17$ Pas ⁿ	$n = 0.31$	$R^2 = 0.999$
Middle 5 points:	$\tau_y = 109.21$ Pa	$K = 7.33$ Pas ⁿ	$n = 0.58$	$R^2 = 0.997$
Middle 6 points:	$\tau_y = 92.30$ Pa	$K = 18.66$ Pas ⁿ	$n = 0.41$	$R^2 = 0.998$

NB: Only positive values plotted
 Experiment and analysis performed by: Matthew Adamson

Figure D.15: Viscometer Test Results: Pernio Clay $c_{ur} = 0.5kPa$

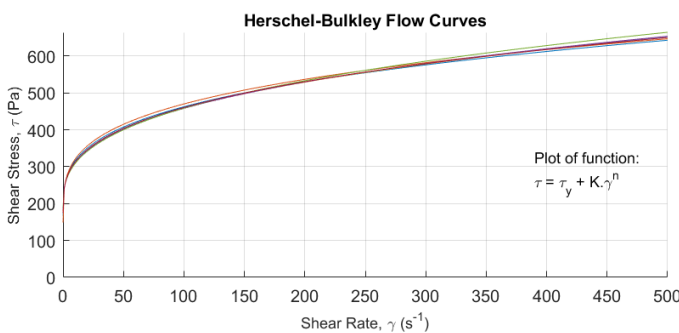


Pernio Clay - Cur = 0.7kPa

Material: Pernio Clay
 Test date: 10/03/2017

Remoulded Shear Strength, Cur = 0.7 kPa
 Water Content, w = 68.4%
 Liquidity Index, IL = 1.28
 Salinity, S = 1.78 g/L

Viscometric System: Wide Gap
 Spindle Height, h = 21.1 mm
 Inner Cylinder Radius, Ri = 7.0 mm
 Outer Cylinder Radius, Ro = 13.75 mm



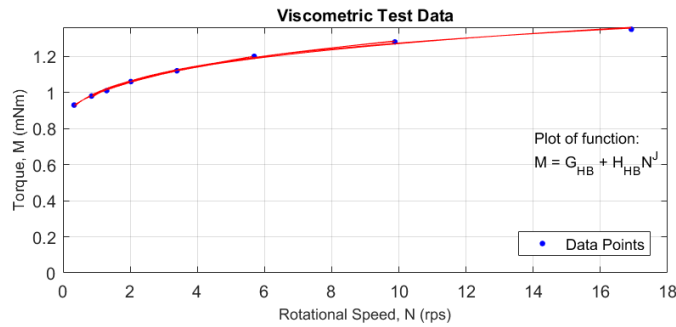
Herschel-Bulkley Parameters - Non-linear regression analysis:

All 8 points:	$\tau_y = 166.27$ Pa	$K = 75.90$ Pas ⁿ	$n = 0.30$	$R^2 = 1.000$
Last 7 points:	$\tau_y = 148.72$ Pa	$K = 91.75$ Pas ⁿ	$n = 0.27$	$R^2 = 1.000$
First 7 points:	$\tau_y = 180.12$ Pa	$K = 61.74$ Pas ⁿ	$n = 0.33$	$R^2 = 1.000$
First 6 points:	$\tau_y = 182.39$ Pa	$K = 59.42$ Pas ⁿ	$n = 0.33$	$R^2 = 1.000$
First 5 points:	$\tau_y = 188.05$ Pa	$K = 53.49$ Pas ⁿ	$n = 0.35$	$R^2 = 1.000$
Middle 5 points:	$\tau_y = 175.94$ Pa	$K = 65.23$ Pas ⁿ	$n = 0.32$	$R^2 = 1.000$
Middle 6 points:	$\tau_y = 174.78$ Pa	$K = 66.34$ Pas ⁿ	$n = 0.32$	$R^2 = 1.000$

NB: Only positive values plotted
 Experiment and analysis performed by: Matthew Adamson

Figure D.16: Viscometer Test Results: Pernio Clay $c_{ur} = 0.7kPa$

Clayey Silt

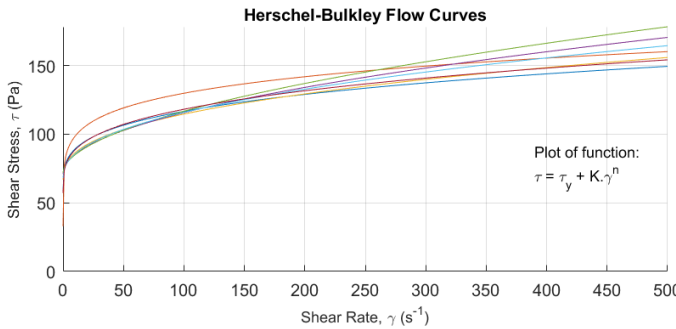


Clayey Silt - Cur < 0.1 kPa

Material: Clayey Silt
 Test date: 16/05/2017

Remoulded Shear Strength, Cur < 0.1 kPa
 Water Content, w = 58.5%
 Liquidity Index, IL = 3.54
 Salinity, S = 1.56 g/L

Viscometric System: Wide Gap
 Spindle Height, h = 21.1 mm
 Inner Cylinder Radius, Ri = 7.0 mm
 Outer Cylinder Radius, Ro = 13.75 mm

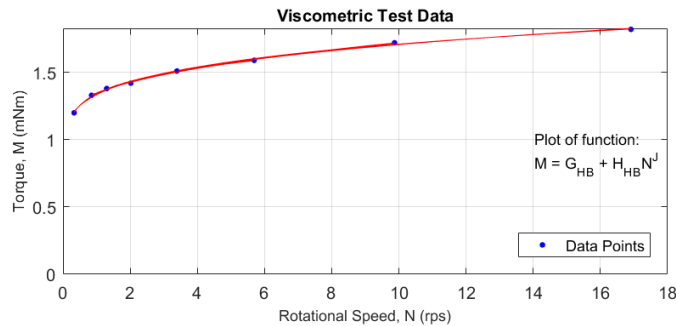


Herschel-Bulkley Parameters - Non-linear regression analysis:

All 8 points: $\tau_y = 59.06$ Pa $K = 15.90$ Pasⁿ $n = 0.28$ $R^2 = 0.995$
 Last 7 points: $\tau_y = 32.95$ Pa $K = 44.46$ Pasⁿ $n = 0.17$ $R^2 = 0.998$
 First 7 points: $\tau_y = 66.94$ Pa $K = 8.05$ Pasⁿ $n = 0.39$ $R^2 = 0.998$
 First 6 points: $\tau_y = 71.09$ Pa $K = 4.51$ Pasⁿ $n = 0.50$ $R^2 = 0.999$
 First 5 points: $\tau_y = 72.00$ Pa $K = 3.77$ Pasⁿ $n = 0.54$ $R^2 = 0.999$
 Middle 5 points: $\tau_y = 68.14$ Pa $K = 6.43$ Pasⁿ $n = 0.44$ $R^2 = 0.999$
 Middle 6 points: $\tau_y = 57.31$ Pa $K = 16.10$ Pasⁿ $n = 0.29$ $R^2 = 0.999$

NB: Only positive values plotted
 Experiment and analysis performed by: Matthew Adamson

Figure D.17: Viscometer Test Results: Clayey Silt $c_{ur} < 0.1$ kPa

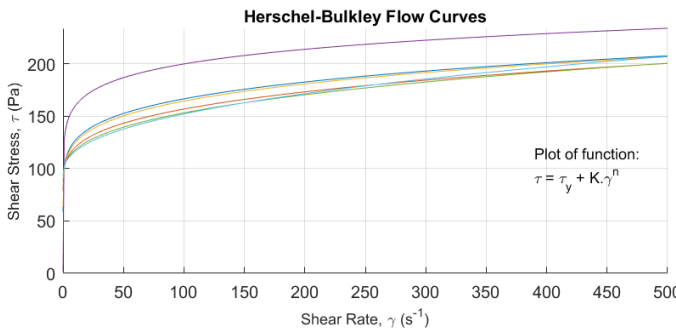


Clayey Silt - Cur = 0.1 kPa

Material: Clayey Silt
 Test date: 10/05/2017

Remoulded Shear Strength, Cur = 0.1 kPa
 Water Content, w = 52.2%
 Liquidity Index, IL = 2.92
 Salinity, S = 1.66 g/L

Viscometric System: Wide Gap
 Spindle Height, h = 21.1 mm
 Inner Cylinder Radius, Ri = 7.0 mm
 Outer Cylinder Radius, Ro = 13.75 mm



Herschel-Bulkley Parameters - Non-linear regression analysis:

All 8 points: $\tau_y = 59.02$ Pa $K = 42.72$ Pasⁿ $n = 0.20$ $R^2 = 0.997$
 Last 7 points: $\tau_y = 79.23$ Pa $K = 21.74$ Pasⁿ $n = 0.28$ $R^2 = 0.997$
 First 7 points: $\tau_y = 63.49$ Pa $K = 37.15$ Pasⁿ $n = 0.22$ $R^2 = 0.995$
 First 6 points: $\tau_y = 1.86$ Pa $K = 125.90$ Pasⁿ $n = 0.10$ $R^2 = 0.996$
 First 5 points: $\tau_y = -245.97$ Pa $K = 545.73$ Pasⁿ $n = 0.03$ $R^2 = 0.994$
 Middle 5 points: $\tau_y = 87.98$ Pa $K = 13.72$ Pasⁿ $n = 0.34$ $R^2 = 0.996$
 Middle 6 points: $\tau_y = 93.67$ Pa $K = 8.88$ Pasⁿ $n = 0.41$ $R^2 = 0.998$

NB: Only positive values plotted
 Experiment and analysis performed by: Matthew Adamson

Figure D.18: Viscometer Test Results: Clayey Silt $c_{ur} = 0.1$ kPa

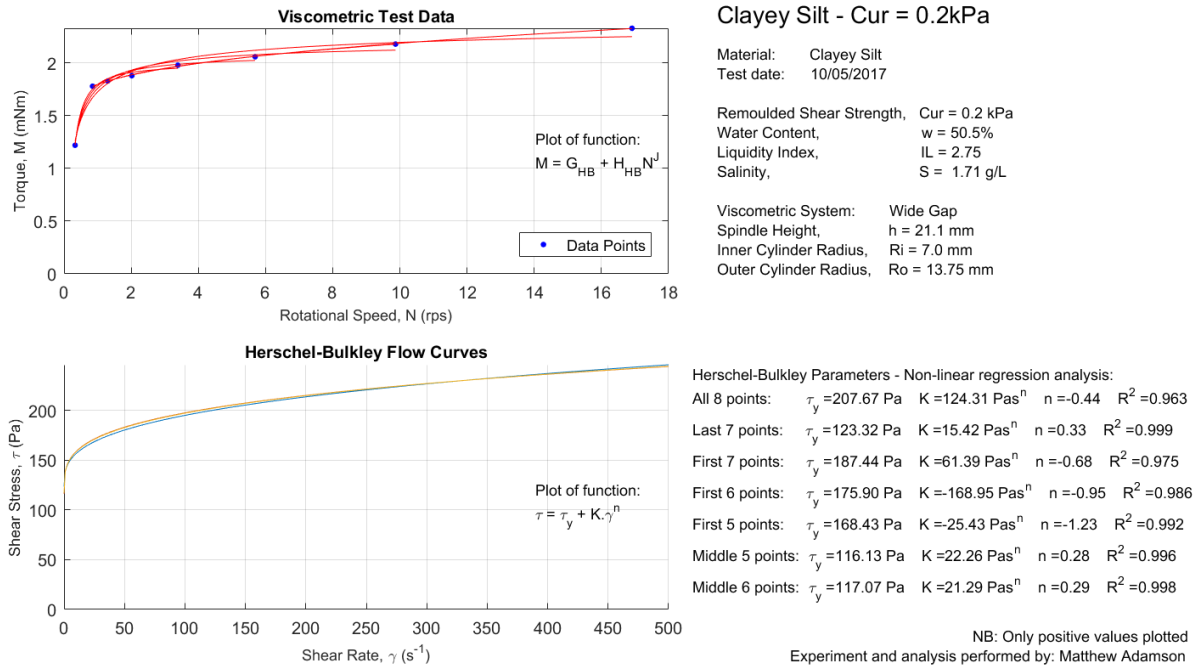


Figure D.19: Viscometer Test Results: Clayey Silt $c_{ur} = 0.2kPa$

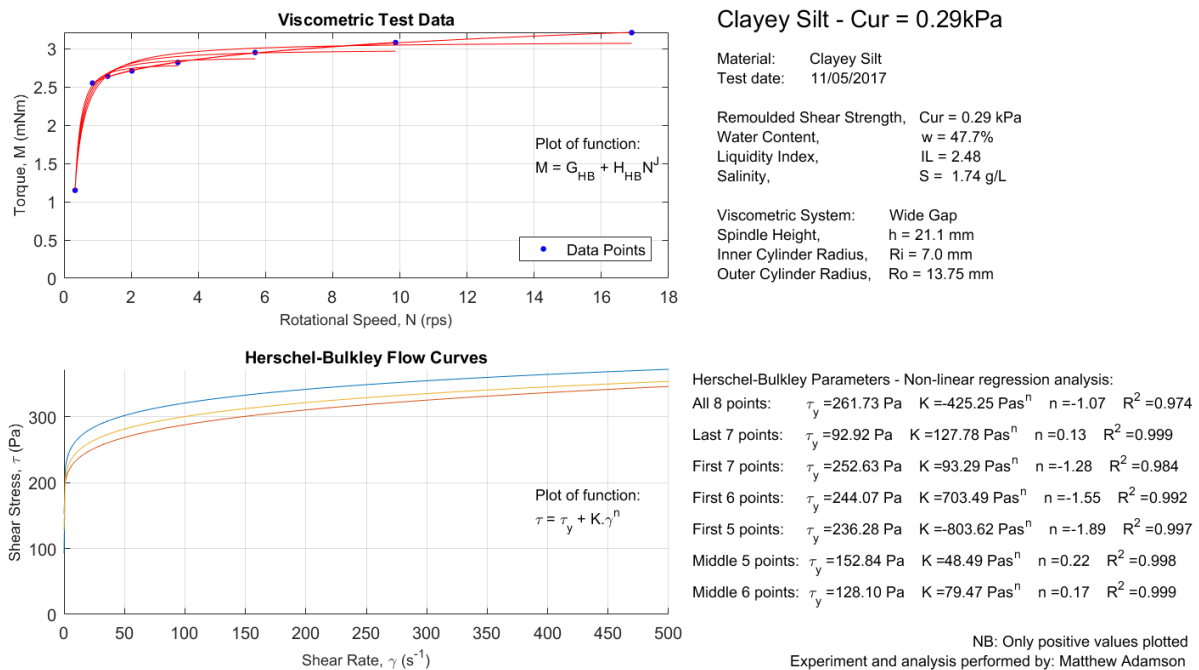


Figure D.20: Viscometer Test Results: Clayey Silt $c_{ur} = 0.29kPa$